# DEHUMIDIFICATION TECHNOLOGY EVALUATION AND MOISTURE BALANCE MODELLING FOR GREENHOUSE HUMIDITY CONTROL

A Thesis Submitted to the

College of Graduate and Postdoctoral Studies

In Partial Fulfillment of the Requirements

For the Degree of Doctor of Philosophy

In the Department of Chemical and Biological Engineering

University of Saskatchewan

Saskatoon, Saskatchewan

By

Jingjing Han

# PERMISSION TO USE

In presenting this thesis in partial fulfillment of the requirements for a Postgraduate degree from the University of Saskatchewan, I agree that the Libraries of this University may make it freely available for inspection. I further agree that permission for copying of this thesis in any manner, in whole or in part, for scholarly purposes may be granted by the professor or professors who supervised my thesis work or, in their absence, by the Head of the Department or the Dean of the College in which my thesis work was done. It is understood that any copying or publication or use of this thesis or parts thereof for financial gain shall not be allowed without my written permission. It is also understood that due recognition shall be given to me and to the University of Saskatchewan in any scholarly use which may be made of any material in my thesis.

Requests for permission to copy or to make other uses of materials in this thesis in whole or part should be addressed to:

Head of the Department of Chemical and Biological Engineering

University of Saskatchewan, 57 Campus Drive

Saskatoon, Saskatchewan, S7N 5A9

Canada

or

Dean of the College of Graduate and Postdoctoral Studies

University of Saskatchewan, 110 Science Place

Saskatoon, Saskatchewan, S7N 5C9

Canada.

# ABSTRACT

Excessively high relative humidity (RH) occurred in the greenhouses almost all year around. Various methods of dehumidification are available for greenhouses. To find a feasible method for greenhouse dehumidification, three methods including air-to-air heat exchangers, exhaust ventilation system, as well as the mechanical refrigeration dehumidification were compared in a tomato greenhouse in the cold region of Canadian Prairies. The experiment results showed that dehumidification by the exhaust fan system was the most cost-effective method with the lowest capital and maintenance cost. However, similar to the heat exchangers, the exhaust fan system is only effective during cold and mild seasons, and not during warm weather conditions. Even though the mechanical refrigeration dehumidifiers consumed the highest amount of electrical energy thus resulting in the highest cost, they were effective in controlling the indoor moisture year-round due to their independence from outside air conditions. Mechanical refrigeration is recommended for summer dehumidification which is only needed at night and early morning before ventilation cooling starts. Both methods could be used during different seasons to achieve good moisture control year-round.

A moisture balance model for simulating the greenhouse indoor RH and air water vapor partial pressure was developed. The model, named HumidMod, takes plant evapotranspiration as the main moisture source of greenhouse air, which is calculated by a modified Penman-Monteith evapotranspiration model. Condensation on the greenhouse inner cover surface as one of the moisture sinks or sources is calculated by two statistical models developed in a Venlo-type plastic greenhouse. Ventilation or infiltration is estimated as a function of the indoor solar radiation. In the model, the indoor RH and water vapor partial pressure can be directly calculated as a function of the indoor and outdoor air conditions, as well as the plant and greenhouse characteristics. The model was validated by comparing predictions with measured data in a tomato greenhouse, which had a commercial-grade refrigeration dehumidifier for humidity control. The mean absolute uncertainty between the predicted and measured results was about 6.9% for both RH and water vapor partial pressure. The coefficient of determinations were 0.59 and 0.75 for RH and water vapor partial pressure, respectively. A good agreement was found between the predicted and measured results with root mean square error of 5.6% for RH and 0.144 kPa for water vapor partial pressure. This model provides a reliable tool for the estimation of dehumidification requirement

inside a greenhouse to achieve a desired humidity level. Sensitivity analysis of this model to several important input parameters was also conducted in three different seasons: cold winter (January), mild season (April), and summer season (July). The results indicate that the input parameters including the indoor air temperature, incoming solar radiation, air exchange rate, as well as plant leaf area index have a significant influence on the model output so should be decided carefully.

# ACKNOWLEDGMENTS

I would like to express my deepest thanks and appreciation to my Supervisor, Prof. Huiqing Guo. Throughout my PhD studies, she always provides me with invaluable encouragement, guidance and support about my research topic and methods. This thesis would not have been completed without her help.

I would also like to extend my appreciation to all the members of my Graduate Advisory Committee: Prof. Oon-Doo Baik, Prof. Warren Helgason, Prof. Bing Si, Prof. David Sumner, Prof. Lope G. Tabil, and Prof. Doug Waterer for their invaluable support and great advice during the PhD program. In addition, I acknowledge Prof. Hong Li for serving as my external examiner.

My special thanks also go to RLee Prokopishyn for his assistance with my experiment setup and data collection. Many thanks should also be given to my current and previous research group members Mohamed Shamim Ahamed, Zhu Gao, Dandan Huang, Shuyao Dong, Shuang Liu, and Ali Motalebi Damuchali for their help in both my life and research work.

Finally, I gratefully acknowledge the Saskatchewan Agricultural Development Fund (ADF), Department of Chemical and Biological Engineering at the University of Saskatchewan, and Russell Haid Memorial Award for the financial supports during my pursuit of the PhD degree.

# DEDICATION

*I dedicate this thesis to my parents, my brother, and my sister-in-law.*

*Thank you very much for your love, encouragement and support throughout my life.*

# TABLE OF CONTENTS

# LIST OF FIGURES

# LIST OF TABLES

# GENERAL INTRODUCTION

An optimum crop growth environment is essential to improve crop yield and quality. However, high humidity can easily occur inside a greenhouse due to plant transpiration, which is the main moisture source in greenhouses (Shrivastava et al., 1994; Wang and Li, 2008). Another main reason is the use of single or double-polyethylene cladding for the last 50 years (Roberts and Mears, 1969), which leads to more moisture captured inside the well-sealed greenhouses causing high relative humidity (RH). The reason to avoid high RH inside a greenhouse is that it can lead to a loss of plants due to fungal diseases, leaf necrosis, and calcium deficiencies thus reducing crop production and produce quality (Bakker, 1991; Campen et al., 2003; Körner and Challa, 2003). Therefore, dehumidification in greenhouses becomes important to ensure successful plant production.

Nowadays, many methods are explored to dehumidify a greenhouse, e.g., traditional ventilation, chilled water condensation, hygroscopic dehumidification, air-to-air heat exchanger, etc. The most competitive method as suggested by Campen (2009) is dehumidification by air-to-air heat exchangers compared to condensation on a cold surface and an absorbing hygroscopic material. However, there is no study to test the existing mechanical refrigeration dehumidifiers for greenhouse humidity control. Besides, limited information exists on how to determine the dehumidification requirement for a greenhouse.

To determine the dehumidification needs of greenhouses, a moisture balance model needs to be developed. Plant evapotranspiration is the main moisture source for greenhouse indoor air. As for moisture sinks, condensation on the greenhouse roof and plant leaves, air exchange by ventilation and infiltration along with dehumidification systems are methods that remove the moisture from the greenhouse air. There has been little research in the literature dealing with the measurement of condensation rates in greenhouses or any other facilities. Montross et al. (2006) designed a low-cost condensation sensing system using a commercially available leaf wetness sensor. The experiment conducted in a greenhouse revealed that the system could accurately predict the occurrence of condensation. However, no further experiments were performed to measure the

amount of condensation. De Freitas and Schmekal (2003) devised a home-made condensation sensor and used it to measure the condensation rate in a cave located in New Zealand. The researchers concluded that the measured condensation rate correlated well with the calculated condensation rate. This physical model can also be used to calculate the condensation rate on the inner surface of the greenhouse covering material. However, to do the calculation, the convective heat transfer coefficient between the indoor air and the cover surface must be known, which is difficult to determine inside a greenhouse.

Hence, the main objectives of this study were to evaluate three dehumidification methods, especially mechanical refrigeration dehumidifiers, for greenhouse humidity control, and to develop and validate a moisture balance model to predict the relative humidity and water vapor partial pressure. To achieve these goals, the following detailed objectives were pursued:

1) to monitor RH profiles of a tomato greenhouse located in a cold region over the growing season of ten months in order to identify high RH periods and dehumidification needs, other indoor environment conditions, including indoor air temperature, solar radiation, $CO_2$ concentration, etc., will be monitored simultaneously;

2) to compare the performance of three different dehumidification methods including air-to-air heat exchanger dehumidification, exhaust ventilation system dehumidification, and mechanical refrigeration (domestic scale) dehumidification in a tomato greenhouse in cold region;

3) to evaluate the dehumidification performance of an air-to-air heat exchanger in another tomato greenhouse, and to explore a method of estimating the dehumidification requirements for greenhouses based on the experimental results;

4) to select a commercial-grade mechanical refrigeration dehumidifier for tomato greenhouse humidity control, and to evaluate the performance of this dehumidifier and conduct an economic analysis on the costs and benefits;

5) to develop a condensation measurement method for greenhouse cover inner surface condensation quantification;

6) to quantify condensation on a greenhouse cover inner surface by applying the measurement method developed by this study, identify the condensation profiles over the growth season, and to

evaluate theoretical condensation models and generate regression models for condensation rate prediction; and

7) to develop a moisture balance model to predict the indoor RH and water vapor partial pressure in a greenhouse, to validate the model using data collected in the condensation measurement tomato greenhouse located in a cold region, and to conduct sensitivity analysis of the model to main important input parameters.

## Organization of the Thesis

This thesis is organized in a manuscript-style. It is presented in the form of published or prepared manuscripts. It is comprised of eight chapters. A brief introduction is added at the beginning of each chapter to elaborate the contribution of the study and to describe the connection of the manuscript to the context of the thesis. A general discussion chapter is also presented at the end of the thesis.

Chapter 1 presents the comparison results of three dehumidification methods – air-to-air heat changer dehumidification, exhaust ventilation system dehumidification, and mechanical refrigeration dehumidification – in a tomato greenhouse based on their effectiveness, capital cost, operating cost, durability, and ease of installation and maintenance. It is published in *Applied Engineering in Agriculture,* 2015, Vol. 31(1), pp. 133-142.

Chapter 2 is the study of the dehumidification performance of an air-to-air heat exchanger in a tomato greenhouse and it also gives the estimation of the dehumidification requirement of the greenhouse. It is published in *Applied Engineering in Agriculture,* 2015, 31(2), pp. 291-300.

Chapter 3 presents the selection of a commercial-grade mechanical refrigeration dehumidifier for a tomato greenhouse and the evaluation of the performance of this dehumidifier and economic analysis on the costs and benefits. It is published in *Transactions of the ASABE,* 2016, Vol. 59(4), pp. 933-941.

Chapter 4 presents the development of a measurement method for condensation rate on a flat surface by using a commercially available leaf wetness sensor, which is calibrated in an environment chamber. It is accepted for publication in *Information Processing in Agriculture* in June 2018.

Chapter 5 presents the results of applying this condensation rate measurement method in a tomato greenhouse. It is submitted to *Biosystems Engineering* in April 2018.

Chapter 6 presents two statistical regression models for condensation rate estimation inside a tomato greenhouse using the experimental data from Chapter 5. It is a prepared manuscript and ready to submit.

Chapter 7 is on the development of a moisture balance model to simulate and predict the greenhouse indoor RH and water vapor partial pressure. Measured data in a tomato greenhouse are used to validate the model. It is a prepared manuscript and ready to submit.

Chapter 8 presents the results of sensitivity analysis of the moisture balance model to several important input parameters to explore their impacts on the model simulation results. It is a prepared manuscript and ready to submit.

The last Chapter provides a general discussions, contributions, and recommendations for future studies of this research topic.

# CHAPTER 1

# COMPARISON OF GREENHOUSE DEHUMIDIFICATION STRATEGIES IN COLD REGIONS

(Published in *Applied Engineering in Agriculture*, 2015, Vol. 31(1), pp. 133-142. DOI: https://doi.org/10.13031/aea.31.10723)

Jingjing Han, Zhu Gao, Huiqing Guo, Robert Brad, Doug Waterer

## Contribution of this paper to over study

The performance of mechanical refrigeration dehumidifiers was first compared to air-to-air heat exchangers and exhaust ventilation systems for greenhouse humidity control. The comparison included capital cost, operating cost, durability, ease of installation and maintenance, and effectiveness for different seasons of the year. Even though the dehumidifiers had the highest operating cost, they were effective for humidity control year-round. Therefore, a commercial-grade mechanical refrigeration dehumidifier was selected and tested in a tomato greenhouse for humidity control in Chapter 3. This chapter fulfills objective 2.

The manuscript presented in this chapter has been published in *Applied Engineering in Agriculture*. The data analyses and manuscript writing were performed by the first author (PhD student – Ms Jingjing Han). The manuscript was critically reviewed by the third author (supervisor – Prof. Huiqing Guo). The experimental testing was conducted by the second author (PhD student – Mrs Zhu Gao) and the fourth author (Mr. Robert Brad). The fifth author (retired Prof. Doug Waterer) provided suggestions on field measurement.

## 1.1 Abstract

Two dehumidification methods, including air-to-air heat exchangers and mechanical refrigeration dehumidifiers, were compared with dehumidification using a conventional exhaust ventilation system. The comparisons included capital cost, operating cost, durability, ease of installation and maintenance, and effectiveness for different seasons of the year. The heat exchangers were more effective for moisture control during cold and mild seasons than during humid and warm periods, while the dehumidifiers were effective in controlling the indoor moisture year-round due to their independence from outside air conditions. While the dehumidifiers consumed the highest amount of electrical energy thus resulting in the highest cost, they consumed the lowest amount of total energy, defined as the sum of the electrical energy consumption and the resultant heat loss from the greenhouse due to dehumidification. Although the heat exchanger method consumed approximately 81% of the total energy consumed by the exhaust fan dehumidification system due to the sensible heat recovered from the exhaust air, the total costs of the two methods were similar due to the lower electrical energy consumption by the latter. Considering a ten-year payback period, dehumidification by the exhaust fan system was the most cost-effective method with the lowest capital and maintenance cost. However, it is only effective during cold and mild seasons, and not during warm weather conditions. Mechanical refrigeration is recommended for summer dehumidification, and both methods could be used during different seasons to achieve good moisture control year-round. After the application of dehumidification, the crop loss rate was reduced by 1.6% to 2.5%, which led to an annual revenue increase of $3,000 per year. Although the average dehumidification cost was approximately 10% of the annual heating cost of the greenhouse, when considering the reduced crop loss and yield increase, dehumidification is strongly recommended.

## 1.2 Nomenclature

| | |
|---|---|
| $A$ | greenhouse cover area, $m^2$ |
| $ach$ | air changes per hour, $h^{-1}$ |
| $b$ | interest rate, % |
| $C_P$ | specific heat capacity of air, J $kg^{-1}$ $°C^{-1}$ |
| $F_p$ | heat loss coefficient per meter of perimeter, W $m^{-1}$ $K^{-1}$ |
| $h_{fg}$ | water heat of condensation, kJ $kg^{-1}$ |
| $h_o$ | enthalpy of the ambient air, kJ $kg^{-1}$ |

$h_1$ enthalpy of the heat exchanger supply air, kJ $kg^{-1}$

$h_2$ enthalpy of the exhaust air entering the heat exchanger, kJ $kg^{-1}$

$M_{ex}$ mass flow rate of the exhaust fans, kg $s^{-1}$

$M_{sup}$ mass flow rate of the heat exchanger supply air, kg $s^{-1}$

$m_{water}$ mass of the condensed water collected by the dehumidifiers, kg

$n$ payback period

$P$ greenhouse perimeter, m

$Q_{eo}$ heat output of the dehumidifiers, kW-h

$Q_{latent}$ latent heat released by condensed water in the dehumidifier, kW-h

$Q_{ld}$ heat released into the greenhouse by the dehumidifiers, kW-h

$Q_{lexf}$ net heat loss through the exhaust fans, kW-h

$Q_{lh}$ net heat loss through the heat exchangers, kW-h

$q_c$ total conduction heat loss, W

$q_{in}$ heat loss due to infiltration, W

$q_{net}$ net heating requirement of the greenhouse, W

$q_s$ thermal radiation heat loss, W

$q_{so}$ sensible heat gain from the sun, W

$q_v$ heat loss due to exhaust ventilation system, W

$t$ running time of the heat exchanger or exhaust fans, h

$t_i$ indoor air temperature, °C

$t_{sky}$ sky temperature, °C

$t_w$ temperature of the condensed water, °C

$U$ conductance of covering materials, W $m^{-2}$ $K^{-1}$

$V$ volume of the greenhouse, $m^3$

$V_{exh}$ exhaust fan ventilation rate, $m^3$ $s^{-1}$

$W$ humidity ratio of the air, $kg_w$ $kg_{air}^{-1}$

$\varepsilon_c$ emissivity coefficient for thermal radiation of the polythene plastic film

$\rho$ air density, kg $m^{-3}$

$\sigma$ Stefan-Boltzmann constant, W $m^{-2}$ $K^{-4}$

***Subscripts***

*i* indoor air

*o* outdoor air

***Abbreviations***

*CRF* capital recovery factor

*EVSD* exhaust ventilation system dehumidification

*HED* heat exchanger dehumidification

*MRD* mechanical refrigeration dehumidification

*RH* relative humidity, %

## 1.3 Introduction

For the last 50 years (Roberts and Mears, 1969), single or double-polyethylene cladding has been used in greenhouses to provide better sealing and insulation, and to reduce air infiltration and heating costs. In these well-sealed greenhouses, high relative humidity (RH) levels are present due to low air exchange rates and low rates of vapor condensation on the inside plastic film surface (Reiersen and Sebesta, 1981; Mortensen, 1986; Rousse et al., 2000; Campen et al., 2003; Campen, 2009). This can lead to dew or water condensation on plant leaf surfaces, which provides an ideal growing condition for fungal diseases. Additionally, high humidity has an impact on plant photosynthesis and pollination, resulting in reduced crop growth and poor produce quality (Bakker, 1991; Kittas and Bartzanas, 2007). Therefore, dehumidification in greenhouses becomes essential to ensure successful plant production.

Today, various methods of dehumidification are available for greenhouses. One method is to reduce the moisture production, which is realized by improving the irrigation system and using plastic film mulch, as well as maintaining a high temperature inside the greenhouse. However, dehumidification methods have limited effect because the main moisture source in greenhouses is plant transpiration (Shrivastava et al., 1994; Wang and Li, 2008). Some research has been carried out on hygroscopic dehumidification for greenhouses, which involves the use of highly concentrated salt solutions (bromides, chlorides, etc.). The installation of the system is complex because a pump system is required between the absorbing surface located inside the greenhouse and the re-conditioning of the salt solution outside of the greenhouse (Campen and Bot, 2001). Additionally, the chemicals involved may lead to environmental problems if leakage occurs (Campen and Bot, 2001). Heat pumps have also been considered as an energy-efficient heating and cooling method (Byun et al., 2006; Tong et al., 2010); however, the experiments conducted by Chasseriaux (1987) and Boulard et al. (1989) both revealed that this method was unable to sufficiently meet greenhouse dehumidification requirements. Ventilation is a very fundamental and effective way to dehumidify a greenhouse; moist inside air is replaced with relatively dry outside air. However, when the ventilation rate for humidity control is greater than that required for temperature control; it also causes energy loss, especially in cold regions with a long heating season (Campen, 2003).

Campen (2009) compared several dehumidification methods for a commercial greenhouse—including air-to-air heat exchangers, ventilation, chilled water condensation—and suggested that the most promising and economical method is to use heat exchangers. Gao (2012) studied four dehumidification methods in a greenhouse located in a cold region in the Canadian Prairies, which included the three methods in Campen's study in addition to mechanical refrigeration for dehumidification. Gao (2012) observed that during winter conditions the indoor RH was high during the daytime and low at night, while under warm and mild weather, indoor conditions were reversed with low indoor RH during the daytime and high during the nighttime. Therefore, the main periods requiring dehumidification are nights and early mornings during the summer and mild weather conditions, and the daytime hours in the winter. Gao (2012) concluded that the air-to-air heat exchanger was effective almost year-round; that is, in cold and mild seasons and even during cool nights during the summer in this region, but ineffective when the outdoor air was warm and humid. However, mechanical dehumidification could be effective year-round, and it was the most energy-efficient dehumidification method (Gao, 2012). Chilled water dehumidification was the most power intensive and costly method and was not recommended (Gao, 2012).

There are also some researches have been done on testing the performance of a liquid desiccant dehumidification system for greenhouse humidity control (Seemann, 2013; Hao, et al., 2015; Ali, et al., 2017); however, most of those studies focuses on the greenhouse environmental conditions, no report or data has been released yet on energy consumption by a liquid desiccant dehumidification system for commercial greenhouse application.

The objective of this study was to explore three different dehumidification methods—air-to-air heat exchanger dehumidification (*HED*), exhaust ventilation system dehumidification (*EVSD*), and mechanical refrigeration dehumidification (*MRD*)—for greenhouses in a cold region based on their effectiveness during different seasons of the year, capital cost, operating cost, durability, and ease of installation and maintenance in order to make recommendations to greenhouse growers for dehumidification strategies.

## 1.4 Materials and Methods

### 1.4.1 Greenhouse specifications

A commercial greenhouse was used in this study, which was located near the city of Prince Albert, Saskatchewan, at 53.22° latitude, 105.68° longitude, and 428 m elevation. The building was a vaulted, steel-framed, single-span greenhouse covered by inflated double layer 6-mil polythene plastic film. It was 9.1 m wide, 29.3 m long, and 4.2 m high at the ridge, as shown in Figures 1.1 and 1.2. Figure 1.2 also illustrates the equipment layout in the greenhouse. Tomatoes were planted in a bag filled with a peat-based medium and planted in six rows for a total of 612 plants, averaging a density of 2.3 plants per square meter. The greenhouse had a north entrance door connected to a head house. Two air inlets were located on the north wall at a height of 0.8 m. The size of the small inlet was 0.9 × 0.9 m and the large inlet was 1.2 × 1.2 m. Two exhaust fans were situated on the south wall at a height of 1.4 m. The small one (EM36 Exhaust Fan, Munters Italy S.p.A., Chiusavecchia, Italy) had a propeller diameter of 0.915 m and a capacity of 4.4 $m^3$ $s^{-1}$ at a static pressure of 20 Pa (Munters, 2014a). The larger exhaust fan (EM50n Exhaust Fan, Munters Italy S.p.A., Chiusavecchia, Italy) had a propeller diameter of 1.27 m and a capacity of 8.8 $m^3$ $s^{-1}$ at a static pressure of 25 Pa (Munters, 2014b). Both units were tested at standard conditions of 20°C and 101.3 kPa. The greenhouse was heated by a hot water heating system and the heat was distributed using two water-to-air heat exchangers and two perforated inflatable plastic air ducts with a diameter of 0.5 m. A drip irrigation system was used for water and nutrient supply.

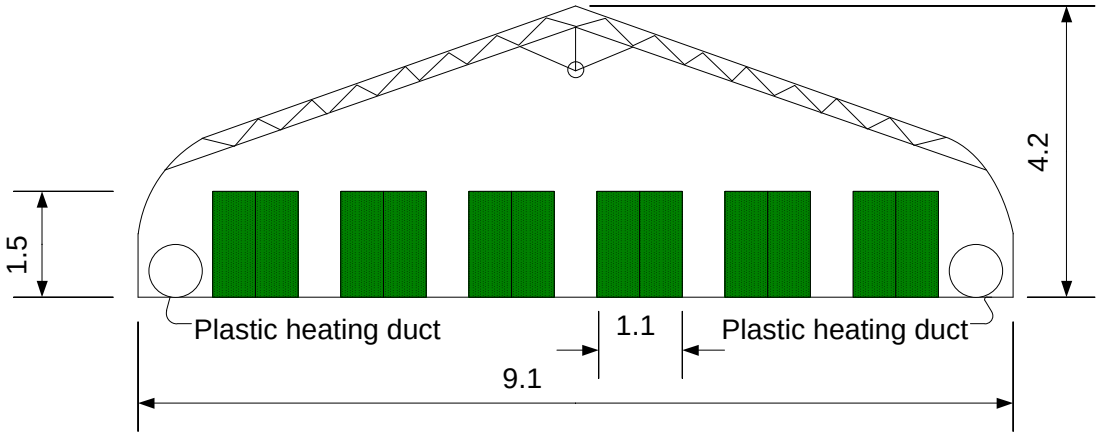


**Figure 1.1. Sketch of the greenhouse cross section (dimensions in m).**

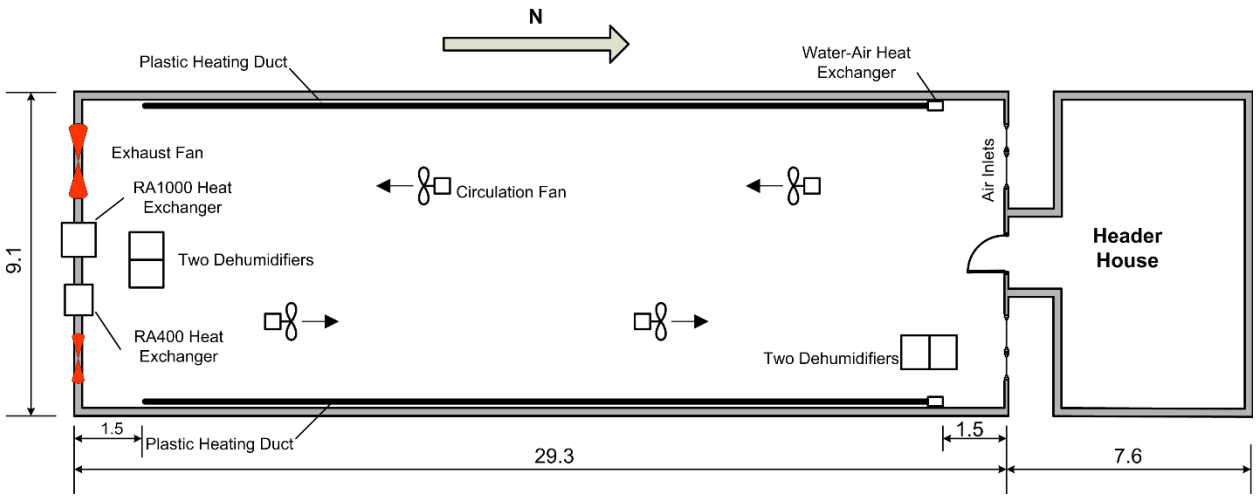


**Figure 1.2. Sketch of the greenhouse layout (dimensions in m).**

## 1.4.2 Dehumidification methods

### *1.4.2.1 Dehumidification requirement determination*

Detailed information about the selection of the dehumidification equipment was described in Gao's thesis (2012). Moisture production during the daytime was due to plant transpiration and water evaporation from the top of the growing media. An estimated 25% of solar radiation entering the greenhouse was converted to latent heat (Albright, 1990). Moisture was removed from the greenhouse primarily through mechanical ventilation. The design temperature was 22°C during the daytime and 18°C at night. The RH set point was 75%. The historical meteorological data for Prince Albert (Gao, 2012) were used to calculate the ventilation rate necessary for greenhouse humidity control. Results showed that the required ventilation rate for greenhouse dehumidification ranged from 0.38 to 1.71 $m^3 s^{-1}$ (Gao, 2012). The main purpose of the field experiment was to test cold and mild season dehumidification since high RH was a more serious problem during these seasons as observed by the greenhouse growers in the region. Thus, equipment was selected to meet this requirement. Warm seasons have high dehumidification needs that were not met by the selected equipment, but the dehumidification methods still contributed to RH control.

### *1.4.2.2 Heat exchanger dehumidification (HED)*

In this study, two Del-Air air-to-air heat exchangers (Model RA400 and RA1000, Del-Air Systems Ltd., Humboldt, SK, Canada) were selected. The total exhaust fan flow rate of the two

heat exchangers was 0.532 $m^3 s^{-1}$, sufficient to meet the dehumidification requirements during cold and mild weather conditions. They were installed in the south wall of the greenhouse approximately 2.5 m above the ground between two exhaust fans (Figure 1.3). Specifications are given in Table 1.1. Each heat exchanger had one supply fan and one exhaust fan. Inside moist air was exhausted from the greenhouse by its exhaust fan, while the outside air entered the greenhouse through the supply fan. The sensible heat of the warm exhaust air was transferred to the incoming cold air through the core of the heat exchangers. This decreased the heat loss while the incoming air was dehumidified. The temperatures of the air entering and leaving the two heat exchangers were monitored by T-type thermocouples (OMEGA Engineering Inc., Laval, QC, Canada). They were calibrated against a thermocouple simulator-calibrator (Model 1100, Ectron Corporation, San Diego, CA, USA). They had a deviation of 0.3°C at 100°C. The RA400 heat exchanger would operate when the inside RH exceeded 75%. When the inside RH exceeded 80%, both heat exchangers would operate.

**Figure 1.3. Heat exchangers (left, visible from the outside; center, visible from the inside) and Model 6510E dehumidifiers setup (right).**

**Table 1.1. Technical parameters of the heat exchangers and dehumidifiers from the manufacturer.**

| Equipment | | Capacity ($m^3 s^{-1}$) | Moisture Removal Rate ($L day^{-1}$) | Energy (W) |
|---|---|---|---|---|
| Del-Air RA400 heat exchanger | Supply air fan<br>Exhaust air fan | 0.147<br>0.183 | 200* | 235 |
| Del-Air RA1000 heat exchanger | Supply air fan<br>Exhaust air fan | 0.242<br>0.349 | 400* | 368 |
| Dandy DDR6510E dehumidifier | Fan speed | 0.076 | 30.8** | 668 |

*Both units were tested at conditions of -30°C and 95% RH outside weather conditions and 20°C and 70% RH indoor conditions at the static pressure of 12 Pa (DEL-AIR SYSTEMS, 2014).
** Unit was tested under unspecified room condition (Danby Dehumidifiers DDR6510E, 2014).

#### *1.4.2.3 Exhaust ventilation system dehumidification (EVSD)*

Even though there were two exhaust fans installed on the south wall, they were sealed during the winter, and only operated for temperature control during spring, summer, and fall when the indoor temperature was above 22°C. During this study, the ventilation rates and electric power consumption of the *EVSD* method were taken to be the same as those of the heat exchanger exhaust fans. In fact, an exhaust fan used in *EVSD* with the same air flow rate as the exhaust fan in *HED* would require slightly less power consumption due to the lower flow resistance, resulting in lowered operating costs; however, this difference was not addressed in the study. The supply air entered the greenhouse by infiltration during our study. It is important to note that, for commercial applications, a designated air inlet should be installed to reduce drafts in the greenhouse. The indoor RH was assumed to be controlled the same as for the *HED* method, which is a reasonable assumption because the humidity of the incoming air was the same for both methods. The only difference was that there was some sensible heat recovered by the incoming supply air with the *HED* method. This amount of recoverable heat contributed little to the air temperature increase. The greenhouse temperature was accurately controlled by the heating system. Therefore, the indoor RH and temperature were the same for both *EVSD* and *HED* methods. For this reason, a separate *EVSD* method was not necessary and was not investigated during our study.

According to the collected data, when the indoor RH exceeded 75%, the temperature controlled ventilation fans were in operation for cooling only 3% of the time. This mainly occurred during the summer and fall seasons. Therefore, the influence of the existing ventilation fans on the greenhouse dehumidification was negligible.

#### *1.4.2.4 Mechanical refrigeration dehumidification (MRD)*

Due to the high capital cost of commercial-grade dehumidifiers, four identical Danby domestic mechanical dehumidifiers (Model DDR6510E, Danby Products Ltd., Guelph, ON, Canada) were used in the greenhouse. The main reason for choosing this model was its low cost-capacity ratio as compared to larger commercial dehumidifiers. Two of the Danby dehumidifiers were set at the south end of the greenhouse, and the other two were located at the north end of the greenhouse (Figures 1.2 and 1.3). The RH set point was 75%. The condensate from the dehumidifiers was collected in containers and the amount was recorded daily. The capacity of each dehumidifier was

about 1.3 L $h^{-1}$ under room conditions unspecified by the manufacturer. The actual water collection record showed a 20% lower capacity since the total capacity of the four dehumidifiers was approximately 4.2 L $h^{-1}$, which was used for the calculation of the latent heat released by the dehumidifiers during our study.

### 1.4.3 Experimental data collection

To compare the performance of these dehumidification systems, a cycle of six days was used: the first three days the heat exchangers operated, and the following three days the dehumidifiers operated. The cycle was repeated during the crop production season from 7 March to 9 December, 2010, with a total of 46 cycles. The greenhouse did not operate during January and February due to low ambient temperature and light conditions. The greenhouse environmental parameters — including the inside air temperature and RH, solar radiation, and $CO_2$ concentration — were measured by a temperature and relative humidity probe (CS500, Campbell Scientific Inc., Edmonton, AB, Canada), which was placed inside a radiation shield, a pyranometer sensor (LI-200, LI-COR Inc., Lincoln, NE, USA), and a $CO_2$ analyzer (Guardian Plus Infrared Gas Monitor, Edinburgh Sensors Ltd., Hingham, MA, USA), respectively. They were all installed at the center of the greenhouse, about 2 m above the ground. A humidity generator (Model 1200 Humidity Generator, Thunder Scientific Corporation, Albuquerque, NM, USA), a LICOR (LI-200, LI-COR Inc., Lincoln, NE, USA), and $CO_2$ calibration gas (0 ppm and 2295 ppm, Bras Air Corporation, USA) were used to calibrate these sensors. Solid state relays were used to activate the heat exchangers and dehumidifiers when the RH set points were reached, and the total operating time of the heat exchangers and dehumidifiers was monitored. All the environmental parameters, as well as equipment operating times, were monitored every minute, and 10-min averages were recorded by a data logger (CR10X, Campbell Scientific Inc., Edmonton, AB, Canada). The outside weather conditions were monitored by a weather station installed 100 m away from the greenhouse in an open field. The same type of sensors as used in the greenhouse were deployed to measure the outside air temperature, RH, solar radiation, as well as wind speed and direction. All meteorological parameters were recorded every 20 min by another data logger (CR1000, Campbell Scientific Inc., Edmonton, AB, Canada) due to its smaller storage capacity.

### 1.4.4 Data analysis

Ten months of data (7 March to 9 December 2010) were collected for analysis. Three criteria were applied to evaluate the performance of the dehumidification methods: RH control, energy consumption, and cost. The operating cost, capital cost, and the payback period were taken into consideration in the economic analysis. The annual heating cost of the greenhouse was also estimated and compared with the cost of dehumidification.

#### *1.4.4.1 Dehumidification energy consumption*

For *HED*, the total energy consumption comprised the electrical energy consumption for the supply and exhaust fans, and the heat loss through the exhaust air and the supply air that had a higher temperature than the outside air due to heat recovery. For *EVSD*, the total energy consumption comprised the electricity consumption of the heat exchanger exhaust fan(s) and the heat loss through ventilation; that is, the heat exchanger exhaust fans exhausting air and supplying ambient air. The heat loss of the *HED* and the *EVSD* are given by:

$$Q_{\mathrm{lh}} = \left[M_{\mathrm{ex}} h_2 - M_{\mathrm{sup}} h_1 - \left(M_{\mathrm{ex}} - M_{\mathrm{sup}}\right) h_{\mathrm{o}}\right] \times t \qquad (1.1),$$

$$Q_{\mathrm{lexf}} = \mathrm{M}_{\mathrm{ex}} (h_2 - h_{\mathrm{o}}) \times t \qquad (1.2),$$

where $Q_{\mathrm{lh}}$ is the net heat loss to the ventilation air of the heat exchangers between the exhaust and incoming air, in kW-h, and the make-up supply outside air coming into the greenhouse through infiltration due to the higher exhaust air mass flow rate compared to the supply air; $Q_{\mathrm{lexf}}$ is the net heat loss through the exhaust fans, in kW-h; $M_{\mathrm{ex}}$ is the mass flow rate of the exhaust air, in kg $s^{-1}$; $M_{\mathrm{sup}}$ is the mass flow rate of the supply air, in kg $s^{-1}$; $h_1$ is the enthalpy of the supply air as it leaves the heat exchanger prior to mixing with the greenhouse air, in kJ $kg^{-1}$; $h_2$ is the enthalpy of the exhaust air entering the heat exchanger, in kJ $kg^{-1}$; $h_{\mathrm{o}}$ is the enthalpy of the ambient air, in kJ $kg^{-1}$; and $t$ is the running time of the heat exchanger or exhaust fan, in h.

For the *MRD* dehumidifiers, the energy consumption was the electricity consumption because there was no heat loss to the outside of the greenhouse due to dehumidification; instead it released heat to the greenhouse. The heat released to the greenhouse included the sensible heat output of the dehumidifier motors and the latent heat released by the condensate (Gao, 2012). The total heat released into the greenhouse by the dehumidifiers was estimated from:

$$Q_{ld} = Q_{eo} + Q_{latent} = Q_{eo} + \frac{h_{fg} \times m_{water}}{3600} \quad (1.3),$$

where $Q_{ld}$ is the heat released into the greenhouse by the dehumidifiers, in kW-h; $Q_{eo}$ is the heat output of the dehumidifiers, which was assumed to be 90% of its electrical energy consumption to prevent overestimation of heat release (ASHRAE, 2009), in kW-h, and is calculated using the power consumption of the dehumidifier multiplied by the running time; $Q_{latent}$ is the latent heat released by condensed water in the dehumidifiers, in kW-h; $h_{fg}$ is water heat of condensation, in kJ $kg^{-1}$, which is calculated by $h_{fg} = 2501 - 2.42 \times t_w$; $t_w$ is the temperature of the condensed water, in °C, and it is assumed equal to the average room air temperature (Albright, 1990); and $m_{water}$ is the mass of the condensed water collected by the dehumidifiers, in kg.

The electrical cost was \$0.097 $kWh^{-1}$ (SaskPower, 2011). Although this greenhouse used coal for heating, most greenhouses in this region use natural gas, so the study calculated heating cost for both fuels. The annual average natural gas price during 2010 was \$5.1 $GJ^{-1}$, which was equivalent to \$0.018 $kWh^{-1}$ (SaskEnergy, 2011). The efficiency of a natural gas heating system was estimated to be 90%. The coal price was \$0.016 $kWh^{-1}$. The heating efficiency for the coal boiler was assumed to be 70%. Heat loss by dehumidification was calculated only when heating was required (i.e., when the heating system was operating and dehumidification was required).

The annual cost of using the three dehumidification methods was also calculated, which included the capital cost, maintenance, interest, and depreciation. The capital recovery factor method (*CRF*) was used to determine the interest and depreciation:

$$CRF = \frac{b(1+b)^n}{(1+b)^n - 1} \quad (1.4),$$

where $b$ is the interest rate, in %, set at 6%; and $n$ is the payback period, chosen as 10 years. The calculated *CRF* equals 0.136 and was used for the interest and depreciation calculations.

#### *1.4.4.2 Annual heating cost*

In order to compare the dehumidification cost with the heating cost, the annual heating cost of the greenhouse was also calculated. For the greenhouse, the heat loss occurred through conduction and convection, radiation heat loss, air infiltration, and ventilation. Heat gain was mainly dependent on solar radiation and supplemental heating. The inside RH was designed to be maintained at 75%,

and the inside temperature was set at 18°C at night and 22°C to 25°C during the daytime, depending on the season. One half of the solar energy penetrating the greenhouse was assumed to be sensible heat (Albright, 1990). The inside solar radiation measured during the experiment was used to calculate heat gain to the greenhouse. The heat loss through the greenhouse envelope, infiltration, and thermal radiation can be expressed as follows (Albright, 1990; ASABE Standards, 2006):

$$q_c = \left(\sum UA + F_p P\right)(t_i - t_o) \quad (1.5),$$

$$q_{in} = \frac{achV\left[C_P\left(\rho_i t_i - \rho_o t_o\right) + h_{fg}(W_i - W_o)\right]}{3600} \quad (1.6),$$

$$q_s = \sigma\varepsilon_c\left(t_i^4 - t_{sky}^4\right)A \quad (1.7),$$

where $q_c$ is the total conduction heat loss through the greenhouse structure including the cover and perimeter, in W; $q_{in}$ is the heat loss due to infiltration, in W; $q_s$ is the thermal radiation heat loss through the greenhouse cover, in W; $U$ is the conductance of covering materials, such as double layer polythene plastic film, and its inside and outside surface resistance to heat transfer, in W $m^{-2}$ $K^{-1}$, where the average calculated value equals 2.5 W $m^{-2}$ $K^{-1}$; $A$ is the area of covering material, in $m^2$; $F_p$ is the heat loss coefficient per meter of perimeter, in W $m^{-1}$ $K^{-1}$, chosen as 1.45 W $m^{-1}$ $K^{-1}$ (ASHRAE, 2009); $P$ is the greenhouse perimeter, in m; $t_i$ is the indoor air temperature, in °C; $t_{sky}$ is sky temperature, in °C, which is calculated by $t_{sky} = 0.0552 \times (t_o + 273.16)^{1.5} - 273.16$ (Berroug et al., 2011); $t_o$ is the outdoor air temperature, in °C; $\rho_i$ is inside air density, in kg $m^{-3}$; $\rho_o$ is outside air density, in kg $m^{-3}$; $ach$ is air changes per hour, in $h^{-1}$, it was 0.5 during the cold seasons of March, November, and December, 0.6 during the mild seasons of April, May, and October, and 0.75 during the warm seasons of June, July, August, and September (ASABE Standards, 2006); $V$ is the volume of the greenhouse, 876 $m^3$; $C_P$ is specific heat capacity of air, in J $kg^{-1}$ $°C^{-1}$; $W_i$ is humidity ratio of the inside air, in $kg_w$ $kg_{air}^{-1}$; $W_o$ is humidity ratio of the outside air, in $kg_w$ $kg_{air}^{-1}$; $\sigma$ is Stefan-Boltzmann constant, $5.67 \times 10^{-8}$ W $m^{-2}$ $K^{-4}$; and $\varepsilon_c$ is emissivity coefficient for thermal radiation of the polythene plastic film, 0.4 (Berroug et al., 2011).

Therefore, the heating requirement for the greenhouse can be determined from:

$$q_{net} = q_{in} + q_c + q_v + q_s - q_{so} \quad (1.8),$$

where $q_{net}$ is the net heating requirement of the greenhouse, in W; $q_v$ is the heat loss due to the exhaust ventilation system, in W, which is calculated by $q_v = \rho_i V_{exh} C_P (t_i - t_o)$; $V_{exh}$ is the exhaust

fan ventilation rate, in $m^3\ s^{-1}$; and $q_{so}$ is the sensible heat gain from the sun, in W. According to Albright (1990), one half of the solar radiation penetrating the greenhouse can be considered sensible heat.

## 1.5 Results and Discussion

### 1.5.1 RH control

The monthly percentages of time when the indoor RH exceeded 75%, 80%, and 85% are presented in Table 1.2. The table also shows the monthly average indoor RH. There were no data recorded due to instrument problems from: 27 August, 11:20 h to 28 August, 05:50 h; 1 September, 07:50 h, 08:20 h, and 08:50 h to 11:50 h; 3 September, 16:20 h to 4 September, 05:50 h. The data analysis is based on all available data collected. The weather conditions were classified into three groups: the cold season or winter season (January, February, March, November, and December), the mild season (April, May, and October), and the summer season (June, July, August, and September).

The percent of time the RH exceeded 75% from April to November for both methods was above 30%, while during June to October, the percentages were greater than 50%. During March and December, the inside RH was much lower than that during other months, which was caused by low plant transpiration rate during March with small plants and high condensation rates on the inner surface of the cladding during December.

Although an RH of 75% was the set point for the dehumidifiers and the small heat exchanger, the set point allowed dehumidification to start earlier to prevent higher levels of RH. Hence, effectiveness of the dehumidification system for RH control should be evaluated using the amount of time the RH exceeded 80%. As presented in Table 1.2, both methods controlled the RH level satisfactorily most of the time during the winter and mild seasons with the RH exceeding 80% from 0% to 18.8% of the time for *HED*, and from 0% to 27.6% for *MRD*. The former system outperformed the latter most of the time. For both methods, during the summer period, an RH exceeding 80% occurred 26.6% to 52.6% of the time. The selection of the dehumidification capacity was originally based on moisture removal rates during the cold and mild periods, not during the summer. The methods were observed to meet the original objective satisfactorily during

the winter and mild seasons; however, higher dehumidification capacity was required during the summer months.

**Table 1.2. Percent of time (%) of high RH in the greenhouse with the two dehumidification methods.**

| *Month* | *Ave $RH_i$ (%)* | | *$RH_i \geq 75\%$* | | *$RH_i \geq 80\%$* | | *$RH_i \geq 85\%$* | |
|---|---|---|---|---|---|---|---|---|
| | *HED* | *MRD* | *HED* | *MRD* | *HED* | *MRD* | *HED* | *MRD* |
| Mar | 65.2 | 66.1 | 6.7 | 3.2 | 0 | 0 | 0 | 0 |
| Apr | 71.4 | 70.6 | 33.4 | 35.3 | 12.3 | 8.8 | 1.3 | 1.3 |
| May | 68.8 | 69.7 | 31.9 | 35.1 | 15.0 | 13.1 | 1.7 | 2.7 |
| Jun | 72.8 | 72.1 | 50.0 | 56.1 | 36.7 | 35.6 | 21.5 | 15.4 |
| Jul | 75.5 | 74.7 | 60.7 | 59.5 | 52.6 | 52.5 | 38.4 | 26.6 |
| Aug | 78.5 | 76.4 | 71.8 | 61.7 | 50.1 | 51.1 | 35.1 | 32.0 |
| Sep | 76.4 | 77.2 | 56.2 | 62.8 | 26.6 | 37.2 | 5.9 | 10.1 |
| Oct | 76.7 | 76.9 | 65.4 | 63.2 | 18.8 | 27.6 | 1.1 | 4.9 |
| Nov | 74.0 | 75.0 | 42.2 | 54.5 | 11.2 | 19.6 | 0.6 | 1.9 |
| Dec | 70.5 | 71.0 | 17.6 | 31.0 | 0.5 | 14.4 | 0 | 0 |
| Average | 73.0 | 73.0 | 43.6 | 46.2 | 22.4 | 26.0 | 10.6 | 9.5 |

Achieving performance that meets the 75% RH at all times during the cold and mild seasons would require a significant increase in the dehumidification capacity, which would be costly and unnecessary. This is because most of the peak RH periods occurred during late morning to afternoon during the cold season when transpiration moisture had accumulated, yet the ventilation was at a minimum because the inside temperature was lower than the set point for cooling. During this period, the inner surface temperature of the greenhouse cover was likely higher than the dew point due to the solar radiation so little condensation occurred. Once the ventilation operated to cool, the RH would reduce rapidly. During the mild season, most of the peak RH periods occurred during the night and early morning due to the lower ventilation rate. However, there was less condensation on the inner surface of the greenhouse cover because of the relatively high outside air temperature. Since the main purpose of greenhouse dehumidification is to reduce the occurrence of surface condensation, it may not be necessary to increase the dehumidification capacity to prevent all of these high RH occurrences.

The heat exchangers worked effectively during the cold and mild seasons with the RH exceeding 80% for up to 18.8% of the time; however, it was not effective during the summer. When only the small heat exchanger was working, it would only meet winter dehumidification requirement with an RH set point of 75%.

Table 1.2 indicates that the percentages of the time the RH exceeded 75% and 80% was lower when using *HED* than when using *MRD*, while it was the opposite for an RH exceeding 85% during the summer; that is, the occurrence of an RH exceeding 85% under *MRD* control was lower than that under *HED* control. Figure 1.4 shows the percent of the time that the RH exceeded 80% and 85% with the *HED* and *MRD* methods. The dehumidifiers were more effective for high RH control than the heat exchangers during summer conditions. In comparison, the heat exchangers performed better during the colder months because of the dry and cold outside air, while they were not as effective during summer months due to the lower humidity ratio difference with the outside air. In fact, the dehumidifiers' performance was not affected by the outdoor weather condition and only depended on the inside air condition.

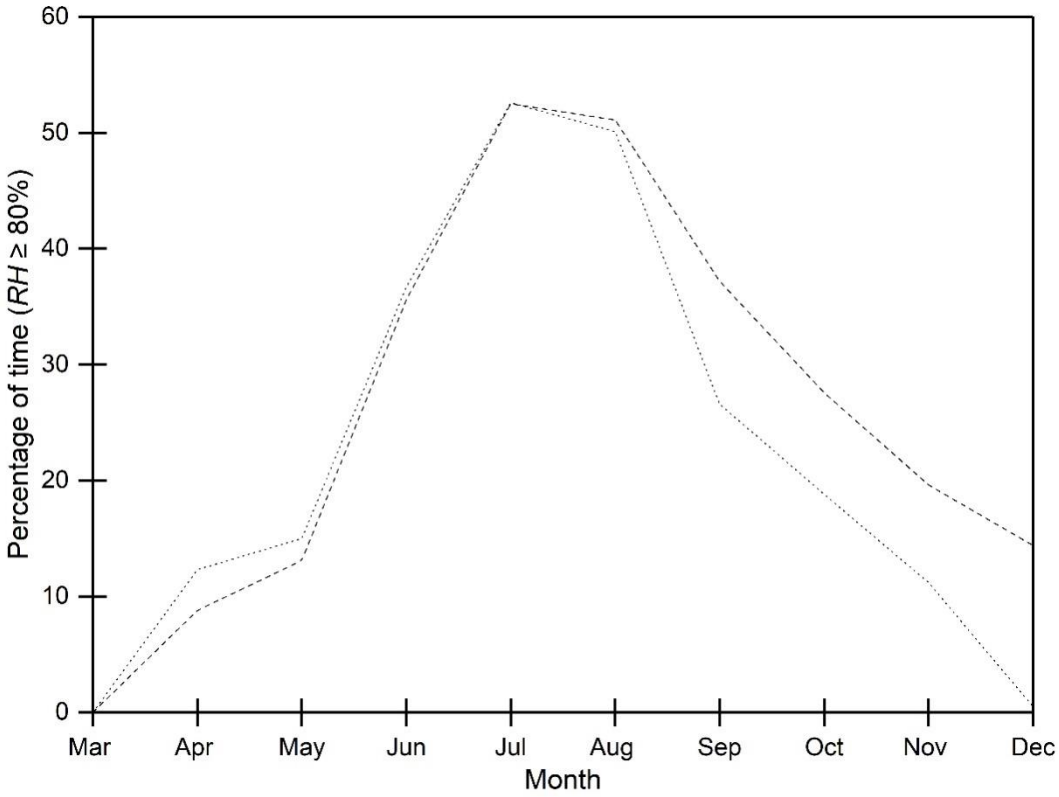

(a)

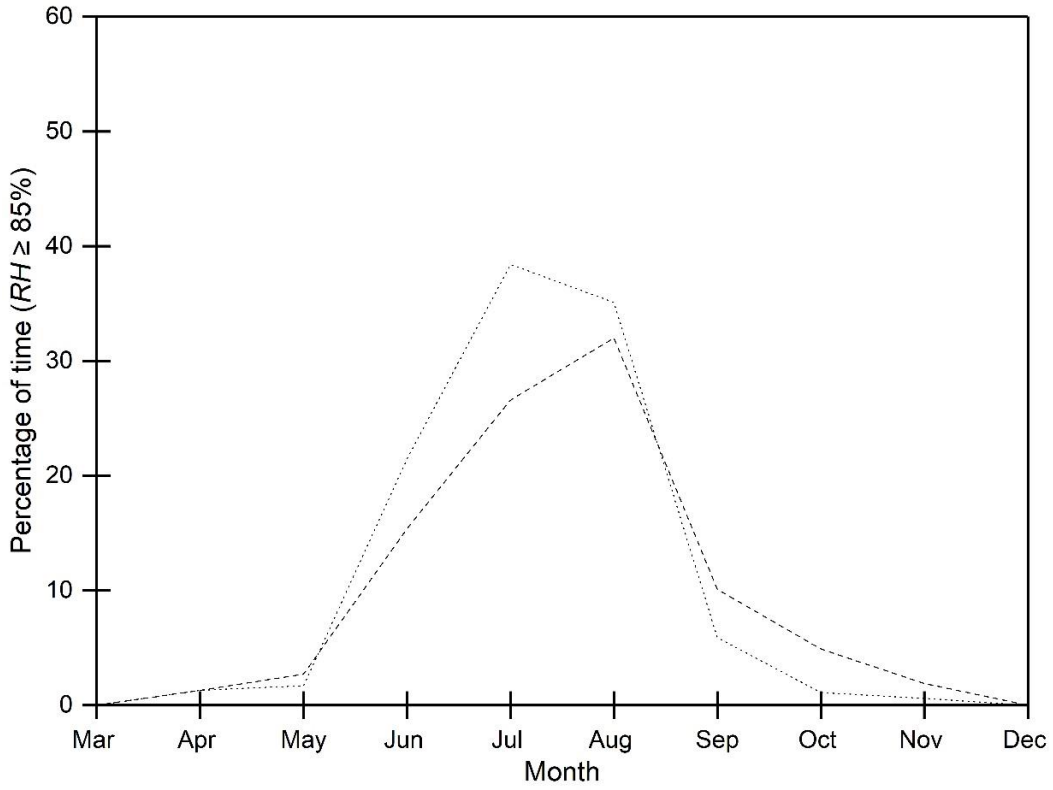


(b)

**Figure 1.4. Monthly average indoor high *RH* occurrence percentages with the use of the heat exchangers and dehumidifiers: (a) percentage of the time the *RH* exceeded 80%; (b) percent of the time the RH exceeded 85%; ·····, heat exchanger; -----, dehumidifier.**

### 1.5.2 Economic analysis of the dehumidification system

Table 1.3 shows the energy consumption of the three dehumidification methods. The heat loss caused by the *MRD* was negative (i.e., providing heat instead of losing heat) due to the heat released to the greenhouse by the motors and the condensate. Because of the low heating requirement during the summer months, the calculated heat loss due to the dehumidification system was assumed to be zero. Two reasons can account for the low values for March and December: one reason was that the indoor RH was very low, and the second reason was that the data was only collected for 14 days and 9 days during March and December, respectively.

The electrical energy consumed by the *EVSD* and *HED* were $0.80 \times 10^{-3}$ GWh and $1.41 \times 10^{-3}$ GWh, respectively. The *MRD* method consumed the most electrical energy of 0.010 GWh, which was 7.3 times that of the *HED*, and 12.9 times that of the *EVSD*. However, the total energy consumption of $4.39 \times 10^{-3}$ GWh by using the *MRD* method was the lowest because of the latent heat of the condensate released to the greenhouse, compared with 0.014 GWh by the *EVSD* and

0.011 GWh by the *HED*. As well, most of the electrical energy used by the dehumidifiers was converted to sensible heat released to the greenhouse. The *EVSD* method had the highest energy consumption due to high heat loss but lowest power consumption. The *HED* method consumed 81% of the total energy consumption of the *EVSD* method due to the sensible heat recovered from the exhaust air.

As for the total cost, although the *HED* method consumed less energy than the *EVSD* method, its electricity consumption was much higher, which resulted in a slightly higher total cost of $298 for the *HED* compared to $292 for the *EVSD.* Due to the high electrical energy consumption of the dehumidifier, the annual cost by the *MRD* was around $908 if coal was using as the heating source, which was about three times the cost of the other two methods. If natural gas was used as the heating fuel, which was more expensive than coal, the annual cost using *MRD* was reduced to $882, which was 2.5 and 2.6 times of those of the *EVSD* and *HED* methods, respectively. Table 1.3 illustrates how the *HED* method is slightly more economical than the *EVSD* method when the heating fuel is more costly.

**Table 1.3. Dehumidification energy consumption using coal (or natural gas as given in the brackets in the last row) as the heating fuel.**

| *Month* | *EVSD* | | | | *HED* | | | | *MRD* | | | |
|---|---|---|---|---|---|---|---|---|---|---|---|---|
| | *Elec ($\times 10^{-3}$ GWh)* | *Heat Loss ($\times 10^{-3}$ GWh)* | *Total Energy ($\times 10^{-3}$ GWh)* | *Cost (Coal, $)* | *Elec ($\times 10^{-3}$ GWh)* | *Heat Loss ($\times 10^{-3}$ GWh)* | *Total Energy ($\times 10^{-3}$ GWh)* | *Cost (Coal, $)* | *Elec ($\times 10^{-3}$ GWh)* | *Heat Loss ($\times 10^{-3}$ GWh)* | *Total Energy ($\times 10^{-3}$ GWh)* | *Cost (Coal, $)* |
| Mar | 0.01 | 0.26 | 0.27 | 4.9 | 0.01 | 0.19 | 0.20 | 4.4 | 0.09 | -0.09 | 0.00 | 7.3 |
| Apr | 0.06 | 1.81 | 1.87 | 34.6 | 0.10 | 1.36 | 1.46 | 31.7 | 0.91 | -0.43 | 0.47 | 81.3 |
| May | 0.06 | 1.82 | 1.88 | 34.6 | 0.10 | 1.37 | 1.47 | 31.5 | 0.99 | -0.48 | 0.52 | 88.6 |
| Jun | 0.12 | 0.00 | 0.12 | 11.2 | 0.20 | 0.00 | 0.20 | 19.5 | 1.18 | 0.00 | 1.18 | 115.0 |
| Jul | 0.15 | 0.00 | 0.15 | 14.1 | 0.25 | 0.00 | 0.25 | 24.5 | 1.14 | 0.00 | 1.14 | 110.7 |
| Aug | 0.15 | 0.00 | 0.15 | 14.3 | 0.26 | 0.00 | 0.26 | 24.9 | 1.23 | 0.00 | 1.23 | 119.2 |
| Sep | 0.10 | 1.57 | 1.67 | 35.0 | 0.18 | 1.31 | 1.49 | 38.3 | 1.37 | -0.64 | 0.72 | 122.5 |
| Oct | 0.09 | 2.93 | 3.02 | 55.8 | 0.16 | 2.28 | 2.44 | 52.3 | 1.43 | -1.51 | -0.08 | 114.7 |
| Nov | 0.06 | 3.20 | 3.26 | 57.0 | 0.11 | 2.29 | 2.40 | 47.1 | 1.33 | -1.48 | -0.15 | 105.7 |
| Dec | 0.02 | 1.81 | 1.83 | 30.8 | 0.035 | 1.30 | 1.33 | 24.1 | 0.66 | -1.30 | -0.64 | 43.2 |
| Total | 0.80 | 13.40 | 14.21 | 292* (353**) | 1.41 | 10.08 | 11.49 | 298* (343**) | 10.32 | -5.93 | 4.34 | 908* (882**) |

*using coal heating, **using natural gas heating

Figure 1.5 summarizes the percentage of heat exchanger and dehumidifier operating time when heating was required in the greenhouse. About one quarter of the dehumidifier's operating time contributed to the greenhouse heating in April, May, and September, while it was over half of its operating time in March, October, November, and December. However, during the remaining time when the greenhouse was in cooling mode, the heat released by the dehumidifiers increased the greenhouse cooling load. Most of the heat exchanger operating time (except September) occurred when heating was required, so it recovered some of the heat as compared to the *EVSD* method, but lost more heat as compared to that of the *MRD* method. There was still about 28% to 60% of the heat exchanger operating time when heating was not required from March to November (i.e., the greenhouse was in cooling mode and heat recovery was unnecessary).

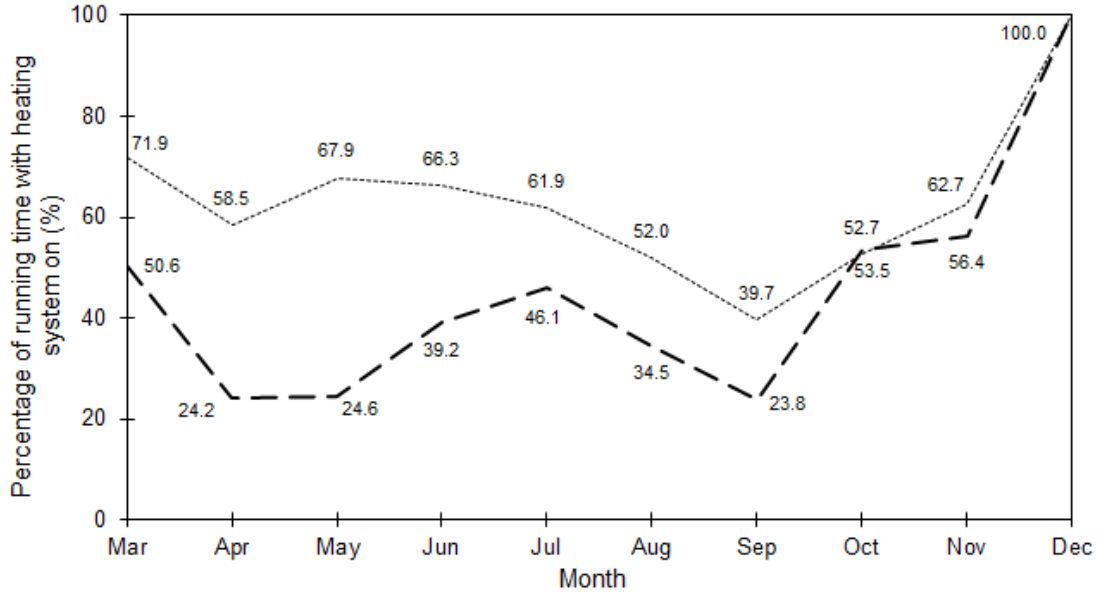


**Figure 1.5. Percentage of heat exchanger and dehumidifier operating time when heating was required; ·····, heat exchanger; - - -, dehumidifier.**

Table 1.4 summarizes the annual cost results for the three dehumidification methods, taking into account the capital cost of the equipment, the depreciation and interest, and the cost for maintenance. Natural gas is used for heating in this analysis and the large heat exchanger was used in this calculation since it would meet the dehumidification requirements during the cold and mild seasons. The cost of repair and maintenance for the *HED* was assumed to be \$50 year$^{-1}$ and \$200 year$^{-1}$ for the *MRD*. The maintenance cost was estimated to be \$20 year$^{-1}$ for the *EVSD*.

**Table 1.4. Annual costs of the three dehumidification methods.**

| | *EVSD* | *HED* | *MRD (four units)* |
|---|---|---|---|
| Capital cost ($) | 750 | 3000 | 1200 |
| Annual fixed and operating costs | | | |
| Depreciation & interest | 102 | 408 | 163 |
| Repair and maintenance | 20 | 50 | 200 |
| Energy cost | 353 | 343 | 882 |
| Total annual cost ($) | 475 | 801 | 1245 |

The total annual cost by the *EVSD* and *HED* were $475 and $801, respectively. It was $1245 by the *MRD* method, which was the most costly dehumidification method mainly due to its highest electricity consumption. The *EVSD* was the most economical method due to its low capital and maintenance cost; thus, it is the recommended method for greenhouse dehumidification. However, similar to *HED*, it is not effective during warm and humid weather. During such conditions, the *MRD* method is recommended.

### 1.5.3 Greenhouse annual heating cost

The greenhouse annual heating requirement without any dehumidification was estimated in order to compare the heat loss and cost increase due to dehumidification with the regular greenhouse heating energy requirement. Details are given in Table 1.5.

As shown in Table 1.5, the total greenhouse net heating requirement was 0.31 GWh. The heat loss using the *EVSD* and *HED* methods were 0.013 GWh and 0.010 kWh, which was only 4.3% and 3.2% of the total greenhouse net heating requirement, respectively. In fact, the dehumidifier released $5.9 \times 10^{-3}$ GWh sensible heat into the greenhouse. Hence, even though there may be some heat loss through dehumidification, it has no significant influence on the greenhouse total net heating requirement. If coal is used as the heating fuel, the heating cost for ten months (March to December) is approximately $4,029. The dehumidification cost would only be 7.2%, 7.4%, and 22.5% of the annual heating cost for the *EVSD*, *HED*, and *MRD* methods, respectively. If using natural gas, it would only cost 6.9%, 6.7%, and 17.2% for the *EVSD*, *HED* and *MRD* methods, respectively.

**Table 1.5. Comparison of dehumidification heat loss and greenhouse annual heating requirement without dehumidification.**

| *Month (2010)* | *$T_i$ (°C)* | *$RH_i$ (%)* | *Heat Loss ($\times 10^{-3}$ GWh)* | *Solar Gain ($\times 10^{-3}$ GWh)* | *Net Heat Requirement ($\times 10^{-3}$ GWh)* | *Dehumidification Heat Loss ($\times 10^{-3}$ GWh)* | | |
|---|---|---|---|---|---|---|---|---|
| | | | | | | *EVSD* | *HED* | *MRD* |
| Mar | 22 | 75 | 49.22 | 7.26 | 33.71 | 0.26 | 0.19 | -0.09 |
| Apr | 24 | 75 | 60.11 | 9.42 | 19.68 | 1.81 | 1.36 | -0.43 |
| May | 24 | 75 | 62.77 | 12.08 | 16.08 | 1.82 | 1.37 | -0.48 |
| Jun | 25 | 75 | 57.07 | 14.00 | 7.14 | 0.00 | 0.00 | 0.00 |
| Jul | 25 | 75 | 45.57 | 15.37 | 7.50 | 0.00 | 0.00 | 0.00 |
| Aug | 25 | 75 | 54.52 | 11.38 | 9.47 | 0.00 | 0.00 | 0.00 |
| Sep | 24 | 75 | 61.96 | 6.42 | 15.75 | 1.57 | 1.31 | -0.64 |
| Oct | 24 | 75 | 59.35 | 5.03 | 22.79 | 2.93 | 2.28 | -1.51 |
| Nov | 22 | 75 | 59.05 | 1.95 | 50.58 | 3.20 | 2.29 | -1.48 |
| Dec | 22 | 75 | 70.04 | 1.49 | 68.55 | 1.81 | 1.30 | -1.30 |
| Total | | | 720.39 | 115.26 | 311.83 | 13.40 | 10.08 | -5.93 |

There was no dehumidification in place before this study was conducted; and 10 to 15 tomato plants were lost each year due to high RH, around 1.6% to 2.5% of the total plants. After the heat exchangers and dehumidifiers were installed, no plant loss occurred. The average sale price of the tomatoes was approximately $6.6/kg, and the average yield was 30 kg per plant; therefore, the annual revenue increases by $3,000. This is approximately 3.4 to 8.7 times the total annual cost of the three different dehumidification methods. Hence, dehumidification is strongly recommended for greenhouse humidity control.

## 1.6 Conclusions

From the study the following conclusions were drawn.

1) The experimental results showed that the heat exchangers controlled RH satisfactorily during the cold and mild seasons, but were not effective during humid and warm weather conditions. Mechanical refrigeration dehumidification was effective for controlling indoor moisture year-round.

2) Mechanical refrigeration dehumidifiers had the lowest energy consumption, followed by the heat exchangers and the exhaust ventilation system dehumidification. However, regarding total

cost, mechanical refrigeration dehumidification was the most costly method due to high electricity consumption, while the exhaust ventilation system dehumidification was the cheapest way of dehumidifying.

3) From the annual cost analysis considering a 10-year payback period - including the capital cost of the equipment, the depreciation and interest, and the cost for repair and maintenance - the exhaust ventilation system dehumidification is the most economical method due to its low capital and maintenance cost; hence, it is recommended for greenhouse dehumidification in cold and mild seasons.

4) During the summer season, mechanical refrigeration dehumidification is recommended for humidity control. A combination of the exhaust ventilation system dehumidification and the mechanical refrigeration dehumidification would provide the most effective and economical way of humidity control year-round. A low-cost, high-efficiency, high-capacity and durable dehumidification method should be explored for the summer weather conditions in the future.

5) After the application of dehumidification, the crop loss rate was reduced by 1.6% to 2.5%. The annual revenue was also increased by $3,000 per year. Although the average dehumidification cost was approximately 10% of the annual heating cost of the greenhouse, when considering the reduced crop loss and yield increase, dehumidification is strongly recommended.

# CHAPTER 2

# DEHUMIDIFICATION REQUIREMENT FOR A GREENHOUSE LOCATED IN A COLD REGION

(Published in *Applied Engineering in Agriculture*, 2015, Vol. 31(2), pp. 291-300. DOI: https://doi.org/10.13031/aea.31.10844)

Jingjing Han, Huiqing Guo, Robert Brad, Zhu Gao, Doug Waterer

## Contribution of this paper to overall study

This paper presented an experimental method for greenhouse dehumidification requirement determination based on the performance of an air-to-air heat exchanger. The greenhouse experienced high RH even though there was an air-to-air heat exchanger installed inside for dehumidification. That was because the heat exchanger was less effective and insufficient for humidity control during the nights and early mornings in warm season. The estimated dehumidification requirement of the greenhouse was used to determine the capacity of a commercial-grade mechanical refrigeration dehumidifier in Chapter 3. This chapter fulfills objective 3.

The manuscript presented in this chapter has been published in *Applied Engineering in Agriculture*. The first author (PhD student – Ms Jingjing Han) conducted the experiment, collected and analyzed the experimental data and wrote the manuscript. The second author (Prof. Huiqing Guo) reviewed the manuscript. The third author (PhD student – Mrs Zhu Gao) and the fourth author (Mr. Robert Brad) helped with the experimental setup. The fifth author (retired Prof. Doug Waterer) provided suggestions on field measurements.

## 2.1 Abstract

High levels of relative humidity (RH) commonly occur inside greenhouses, which lead to condensation on plant leaf surfaces. In addition, condensation on interior building surfaces occurs, resulting in water dripping on plants, providing an ideal growing condition for fungal diseases, and also contributing to the deterioration of equipment and building materials. Limited information exists on how to determine dehumidification requirements within greenhouses. In this study, an air-to-air heat exchanger was used to provide dehumidification for a commercial greenhouse under cold weather conditions, and the data were used to estimate the dehumidification requirements of the greenhouse. The experiment was conducted over a seven-month period during which the greenhouse environmental parameters were monitored. The results showed that the heat exchanger controlled the RH well during cold and mild seasons, although it did not meet the peak capacity requirement. It was found to be less effective and insufficient during the nights and early mornings of summer. Based on the experimental data, the dehumidification requirement for satisfactory control of humidity was estimated to be 14.8 L $h^{-1}$ or 0.018 L $h^{-1}$ per square meter of greenhouse floor area; this dehumidification capacity could control RH at 75% during nights and early mornings in cold and mild weather conditions but can result in higher RH during the daytime. This dehumidification level could also reduce the occurrence of high RH during the summer season early in the morning and at night. The percentage of time the RH exceeded 75% could be reduced to 26% during the warm season, and 12% during the cold and mild seasons. Meeting the peak requirement would require a 58.8% increase of dehumidification capacity, which would be expensive.

## 2.2 Nomenclature

| | |
|---|---|
| *ExtraRate* | extra moisture removal rate for the greenhouse, L $h^{-1}$ |
| $M_{exh}$ | volumetric flow rate of the heat exchanger exhaust air, $m^3$ $s^{-1}$ |
| *MRA* | actual amount of moisture removed by the heat exchanger, L $h^{-1}$ |
| *t* | time, h |
| *V* | volume of the greenhouse, $m^3$ |
| $W_d$ | design air humidity ratio at 75% RH set point and the actual inside air temperature, $kg_w$ $kg_{air}^{-1}$ |
| $W_i$ | inside air humidity ratio, $kg_w$ $kg_{air}^{-1}$ |

| | | | |
|---|---|---|---|
| $W_o$ | outside air humidity ratio, $kg_w\ kg_{air}^{-1}$ | $\rho$ | inside air density, kg $m^{-3}$ |

## 2.3 Introduction

High relative humidity (RH) in greenhouses results in condensation on plant leaf surfaces. Additionally, condensation on interior building surfaces can cause dripping onto plants, floors, and workers. Moisture on building or plant surfaces can lead to increased occurrences of fungal diseases and may also create a hazard to workers. Additionally, high humidity can impact plant photosynthesis and pollination, resulting in crop growth reduction and poor produce quality (Bakker, 1991; Campen et al., 2003; Kittas and Bartzanas, 2007). Hence, dehumidification is crucial for the greenhouse plant environment.

Generally, the inner surface of a building removes a significant amount of water vapor and can play an important role in reducing RH. During the last 50 years, there has been an increase in double polyethylene cladding in greenhouse compared to the traditional single-pane glass in an effort to reduce heating costs (Roberts and Mears, 1969). However, higher levels were the result, because less condensation occurred on the greenhouse glazing and lower air exchange (Reiersen and Sebesta, 1981; Mortensen, 1986; Rousse et al., 2000), thereby requiring additional dehumidification requirement.

Although there are a number of studies related to greenhouse dehumidification, limited information exists on how to determine the dehumidification requirement of a greenhouse. Chasseriaux (1987) and Boulard et al. (1989) pointed out that systems using heat pumps for greenhouse dehumidification cannot meet dehumidification requirements or sufficiently improve greenhouse humidity conditions. An experiment carried out by Seginer and Zlochin (1997) showed that lower wind speed and high ambient humidity ratios lead to high dehumidification requirements. Campen et al. (2003) compared several dehumidification methods, including condensation on a cold surface, forced ventilation combined with an air-to-air heat exchanger, and an absorbing hygroscopic dehumidifier with the use of a traditional exhaust ventilation system to dehumidify the greenhouse. They suggest that a heat exchanger is the most promising and economical method for greenhouse humidity control. HORTITRANS, developed by Jolliet (1994), is a mathematical model for estimating condensation, ventilation, as well as plant transpiration. The model is able to predict water and heat production within a greenhouse and the resultant humidity; however, there

is no research or experimental data to validate this model, thus limiting its application for quantifying dehumidification requirements. Even though Campen et al. (2003) applied the simulation model KASPRO as developed by De Zwart (1996) to calculate dehumidification needs, soil evaporation, assumed to be one of the main moisture sources in a greenhouse, was not considered.

Greenhouses on the Canadian Prairies, a cold region, can experience conditions of excessive RH almost year-round, especially from April to November; thus, some degree of dehumidification is required for most of the year (Gao et al., 2010). Dehumidification through the use of the traditional exhaust ventilation would result in significant heat loss. Therefore, the air-to-air heat exchanger is a promising dehumidification method for this cold region.

The objective of this study was to evaluate the dehumidification performance of an air-to-air heat exchanger in a tomato greenhouse in Saskatchewan, Canada, and to explore a method of estimating the dehumidification requirements for greenhouses based on the experimental results. The energy savings and the heating cost data related to the use of the heat exchanger are not included in this paper.

## 2.4 Materials and Methods

### 2.4.1 Greenhouse specifications

A commercial greenhouse was used in this study. It is located in Grandora, Saskatchewan, 23 km west of Saskatoon, at 52.09° latitude, -107.03° longitude, and 504 m elevation. It is a three-span greenhouse covered by a double layer 6-mil polyethylene plastic film on the roof and polycarbonate panels on the side walls, except for the north wall, which was an insulated wood-frame wall. The greenhouse is 19.2 m wide and 43.9 m long. The eave height is 4.3 m and the ridge height is 6.7 m (Figure 2.1). Tomato plants were planted in peat-based growing medium bags in 11 rows with a total of 2,125 plants, averaging 2.5 plants per square meter. The greenhouse was heated with hot water pipes located above ground between the rows of plants. Three natural gas boilers were used to heat the hot water, which were all put in the headhouse. The greenhouse had three exhaust fans (FC050-4E exhaust fan, ZIEHL-ABEGG, Sainte-Claire, QC, Canada) placed in the east wall at a height of 3.8 m and roof vents for cooling. These fans were turned on only when

the indoor temperature was above 24°C and turned off when the temperature was reduced to 22°C during the spring, summer, and fall seasons, and they were sealed during the winter period. Each exhaust fan had a diameter of 0.548 m and a capacity of 2.1 $m^3$ $s^{-1}$ at a static pressure of 20 Pa (Axial Fans, 2012). A drip irrigation system was used to supply water and nutrients. The floor was covered by landscaping fabric, with soil underneath.

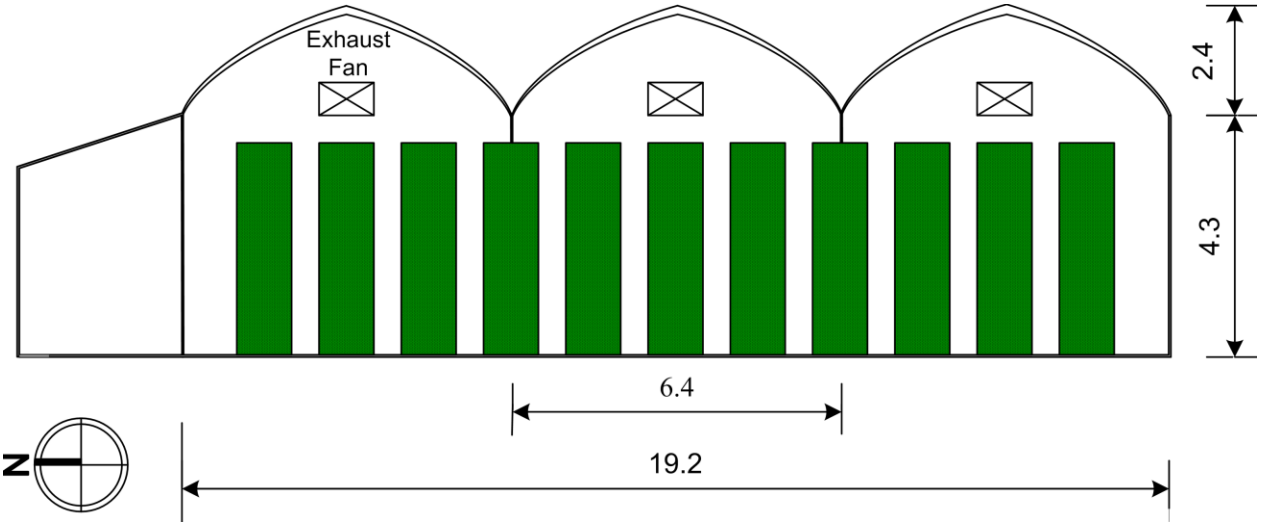


**Figure 2.1. Sketch of the greenhouse cross section (dimensions in m).**

### 2.4.2 Dehumidification method

An air-to-air heat exchanger (vanEE HRV12LC, Venmar Ventilation Inc., Drummondville, Quebec, Canada) was installed in the east wall of the greenhouse at a height of 3.5 m, as shown in Figure 2.2. The heat exchanger had one supply fan and one exhaust fan. It operated at two speeds. At the high speed setting, the ambient air entered the greenhouse through the supply fan at a speed of 0.40 $m^3$ $s^{-1}$, and the inside air is discharged from the greenhouse through the exhaust fan at a speed of 0.58 $m^3$ $s^{-1}$. At the low speed setting, the flow rates of the supply and exhaust fans were 0.32 $m^3$ $s^{-1}$ and 0.50 $m^3$ $s^{-1}$, respectively. The recommended RH range for tomatoes is 60% to 70% (Snyder, 2001). However, since the main purpose of greenhouse dehumidification was to reduce the occurrence of condensation on plant surfaces or on the greenhouse's interior surface, an RH of 70% was chosen as the set point for the low speed of the heat exchanger and 75% RH for the high speed. Even though the set point for the high speed represents a 5% higher setting than the optimum range, it was still considered an acceptable level for tomato plants. It must be pointed out that the size of the heat exchanger was selected to control humidity during the fall, winter, and spring

seasons, which was from September to May, but not necessarily during the summer months from June to August.

**Figure 2.2. Heat exchanger installation.**

A type T thermocouple (OMEGA Engineering Inc., QC, Canada) was used to measure the air temperature leaving the supply fan before it entered the greenhouse. Another one was used to measure the exhaust air temperature existing through the exhaust fan, as shown in Figure 2.3. The incoming air temperature of the exhaust stream was assumed to be the same as the inside greenhouse air temperature, while the incoming air from the intake fan was assumed to be the same as the outdoor ambient air temperature. The thermocouples had an accuracy of 0.3°C at 100°C and were calibrated against a thermocouple simulator-calibrator (Model 1100, Ectron Corporation, San Diego, CA, USA.) before the experiment. There were six horizontal airflow fans with two at each span, and they were running continuously.

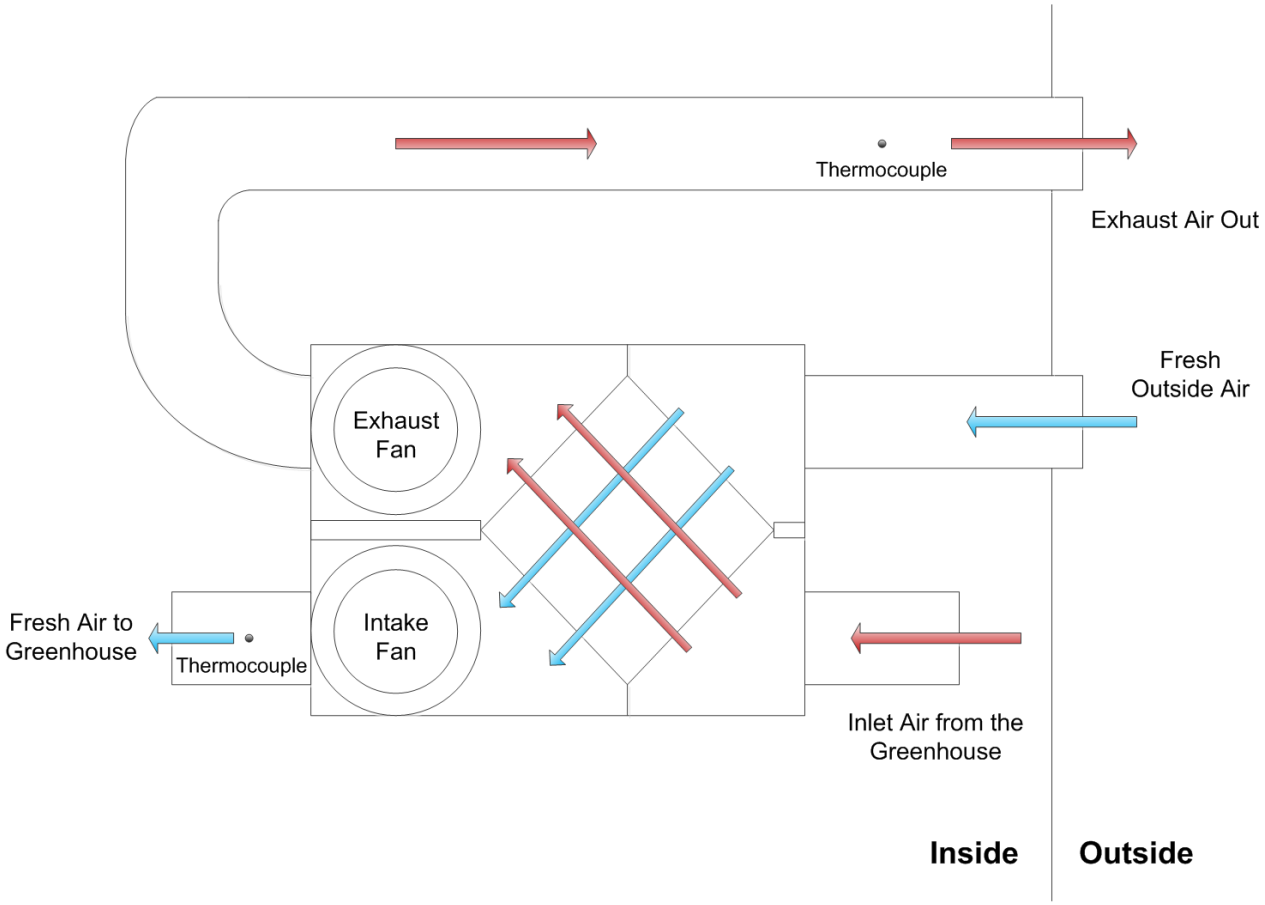


**Figure 2.3. Heat exchanger air flow diagram.**

### 2.4.3 Experimental data collection

The greenhouse was shut down during the coldest months of December, January, and February. The tomato plants are transplanted in the greenhouse in early March, and pulled out in early December 2011. During the early part of the growing season from March to April, the plants were very small, resulting in low transpiration rates and an acceptable RH. Therefore, the heat exchanger was not operated until May. Hence, data collected from May to November 2011 were used to evaluate the performance of the heat exchanger for humidity control and to estimate the dehumidification requirements of the greenhouse. The indoor air temperature and RH were measured with a CS500 temperature and relative humidity probe (Campbell Scientific Inc., Edmonton, AB, Canada) that was placed inside a radiation shield and installed in the center of the greenhouse, 1.8 m above the ground. The probe had an accuracy of ±0.2 to ±1.4°C over the temperature measurement range of -40°C to 60°C, and ±3% over the range of 10% to 90% and ±6% in the range of 90% to 100% with RH measurement. The humidity measurements were calibrated

using a humidity generator (Model 1200 Humidity Generator, Thunder Scientific Corporation, Albuquerque, NM, USA) before the experiment.

A CR 10X data logger (Campbell Scientific Inc., Edmonton, AB, Canada) was installed near the east wall of the greenhouse. The inside temperature and RH values, the heat exchanger operation (on/off), and the incoming and outgoing air temperatures of the heat exchanger were all monitored every minute with 10-min averages recorded. The ventilation and heating equipment were all controlled by the greenhouse ventilation control system based on temperature, and the sensor was installed in the middle of the greenhouse at a height of 1.5 m. The ambient weather conditions (temperature and RH) were obtained from the Environment Canada website for Saskatoon (Environment Canada, 2011), because the distance between the weather station and the experimental greenhouse was only 23 km. The equipment locations and sensor placements are illustrated in Figure 2.4.

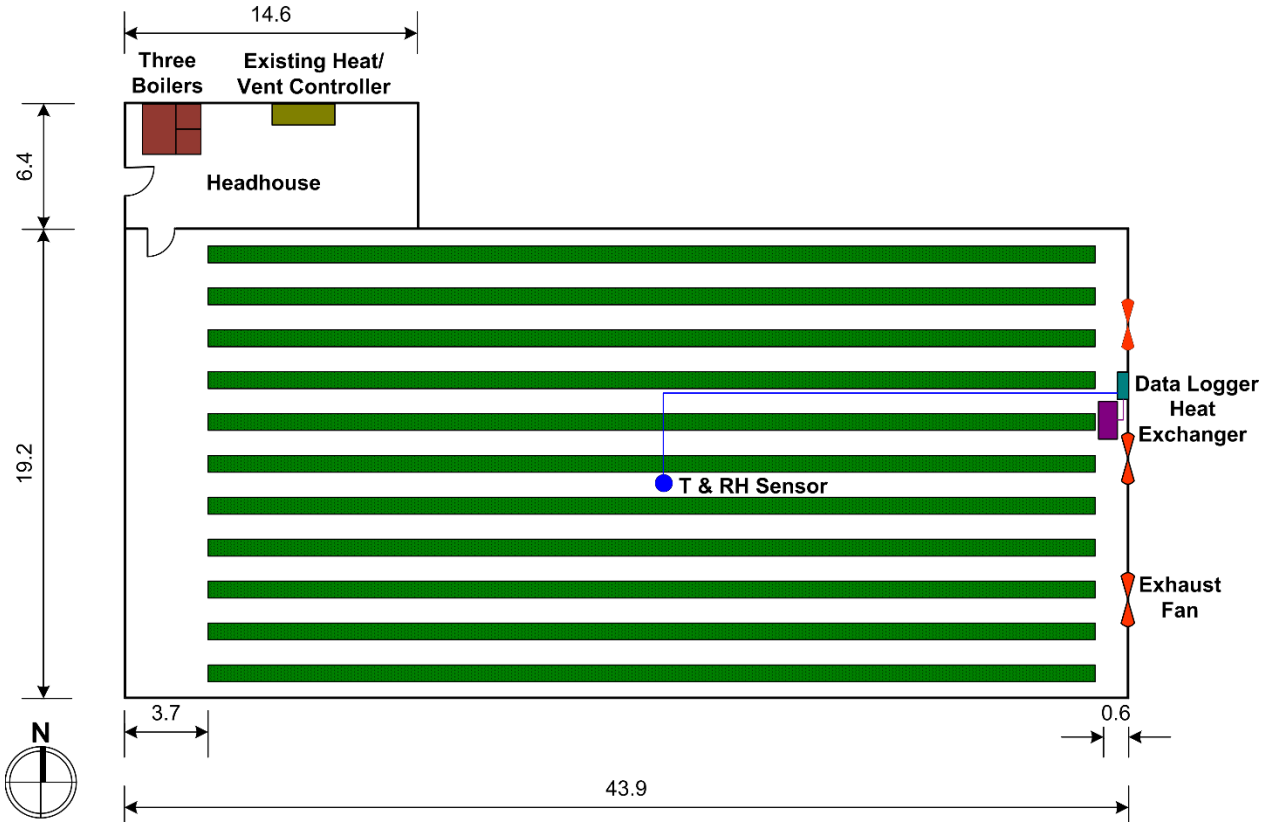


**Figure 2.4. Sketch of the greenhouse layout and measurement position (dimensions in m).**

### 2.4.4 Data analysis

In order to evaluate the performance of the heat exchanger, the actual amount of moisture removed per hour from the greenhouse by the heat exchanger, which is the net difference of the moisture vented from the greenhouse by the exhaust fan and the moisture gain from the incoming ambient air through the intake fan of the heat exchanger and infiltration (the sum of the total ambient supply air mass flow rate equals the exhaust air mass flow rate when the ventilation system is not in operation during cold and mild seasons), can be calculated from:

$$MRA = 3600\rho M_{exh}(W_i - W_o) \qquad (2.1),$$

where $MRA$ is the actual amount of moisture removed by the heat exchanger, in L $h^{-1}$; $M_{exh}$ is volumetric flow rate of the exhaust air of the heat exchanger, in $m^3$ $s^{-1}$; $\rho$ is inside air density, in kg $m^{-3}$; $W_i$ is inside air humidity ratio, in $kg_w$ $kg_{air}^{-1}$; and $W_o$ is outside air humidity ratio, in $kg_w$ $kg_{air}^{-1}$.

Since the heat exchanger could not maintain the RH at or below its set point at all times, there were some periods when the indoor RH was higher than 75%, especially during nights and early mornings during the warm season, and during the daytime for mild and cold weather conditions. During these periods, the heat exchanger could not meet the greenhouse dehumidification requirement and additional moisture needed to be removed to keep the inside RH at or below the set point. This additional removal rate, when the inside RH was higher than 75%, can be estimated as follows:

$$ExtraRate = \frac{V\rho(W_i - W_d)}{t} \qquad (2.2),$$

where $ExtraRate$ is extra moisture removal rate for the greenhouse, in L $h^{-1}$; $V$ is volume of the greenhouse, in $m^3$; $W_d$ is design air humidity ratio at 75% RH set point and the actual inside air temperature, in $kg_w$ $kg_{air}^{-1}$; and $t$ is time that it takes for the dehumidification device to remove the extra amount of moisture from the greenhouse, in h.

## 2.5 Results and Discussion

### 2.5.1 RH control

The percentages of total time when the indoor RH exceeded 75%, 80%, and 85% during each month are shown in Figure 2.5. Figure 2.6 gives the monthly average indoor and outdoor environmental conditions.

As shown in Figure 2.5, the percentages of the time the RH exceeded 75% were all above 55% from May to August. This resulted from the warm and humid outdoor weather conditions. A total of 48% of the time, the inside RH was greater than 80% during May, June, and July. However, the situation was much better from September to November, as there was less than 5% of the time that the inside RH was higher than 85%, which means that the heat exchanger controlled the indoor RH very well during mild and cold seasons, while it was less effective under warm weather conditions. As mentioned previously, the heat exchanger was selected to control RH for cold and mild seasons rather than summer conditions. Therefore, the high RH during the summer months was not unexpected, especially since the summer in which the experiment was conducted was more humid than average (average RH for June to August of 70.1% compared to the historical average of 67.5% in the years 1981-2010 (Environment Canada, 2014)).

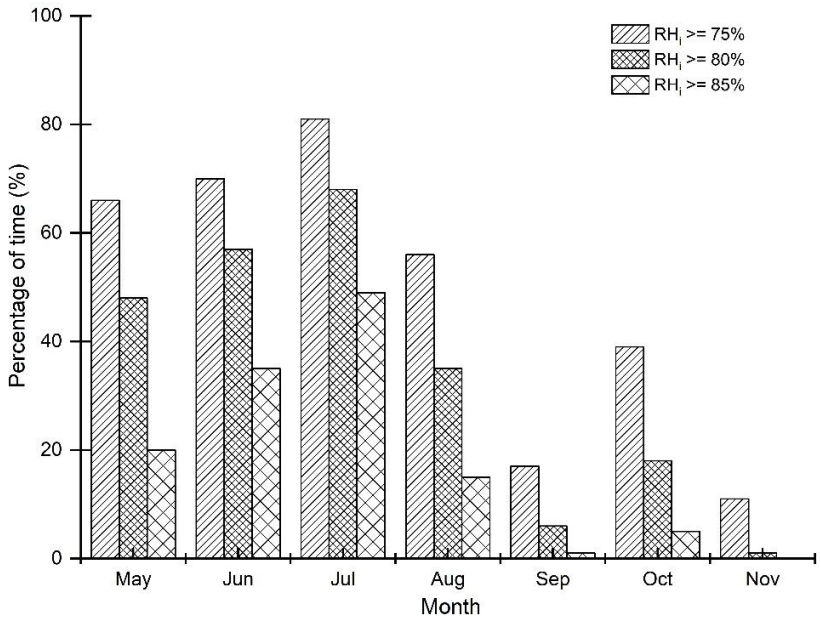


**Figure 2.5. Monthly average indoor high RH occurrence percentages.**

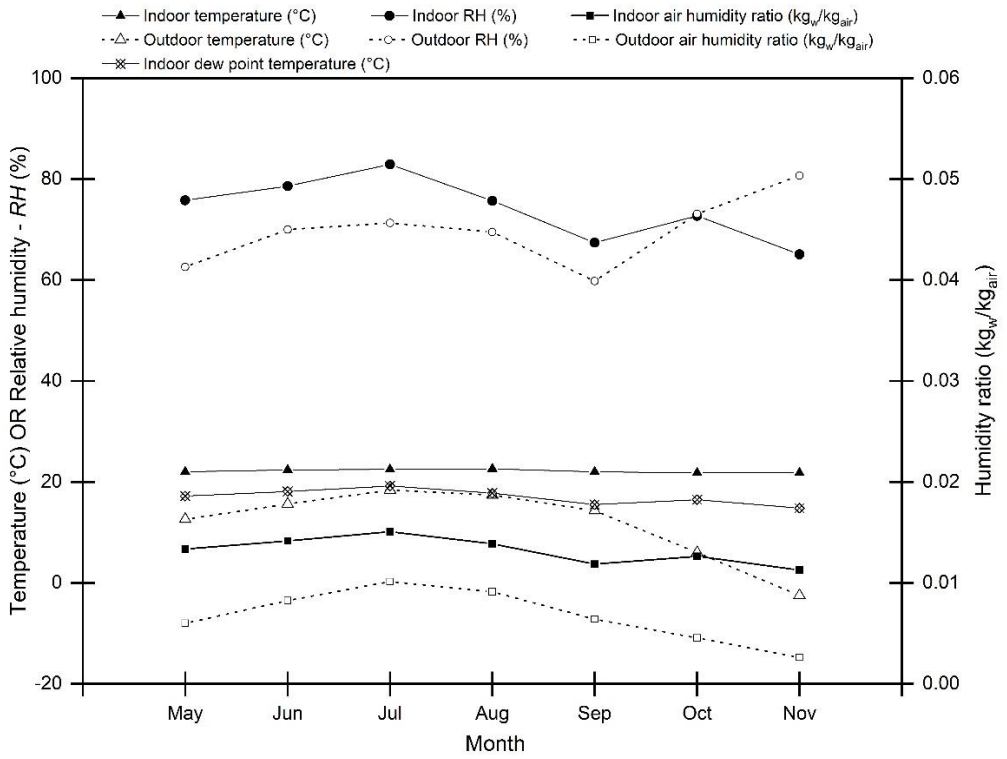


**Figure 2.6. Monthly average climatic conditions.**

The general trend of the RH diurnal profile during October and November was the indoor RH being higher during daytime and lower during nighttime, while just the opposite occurred from May to September with the inside RH being lower during the daytime and higher during the nighttime. The reason for this is that, during the cold season, the ventilation system is shut down and the air exchange relies on infiltration, which is assumed to be very low for this type of well-sealed greenhouse, yet the high rate of transpiration and evaporation during daytime releases high amounts of moisture into the air causing a high RH. During the night period, the outside air temperature drops, causing low temperatures on the interior surface of the cladding material, which is lower than the dew point temperature of the indoor air; furthermore, the indoor set point temperature also decreases from 22°C to 19°C, thus reducing the air's moisture-holding capacity. These two factors cause high condensation rates on the internal surfaces of covering materials and also on the floor surface, removing moisture from the air and causing indoor RH reduction. Figure 2.7 displays such typical indoor climatic conditions during the cold season. The last diurnal RH peak was caused by the indoor temperature switching from day to night; that is from 22°C to 19°C. The heat exchanger only needed to run during the daytime and was able to control the RH during the cold season.

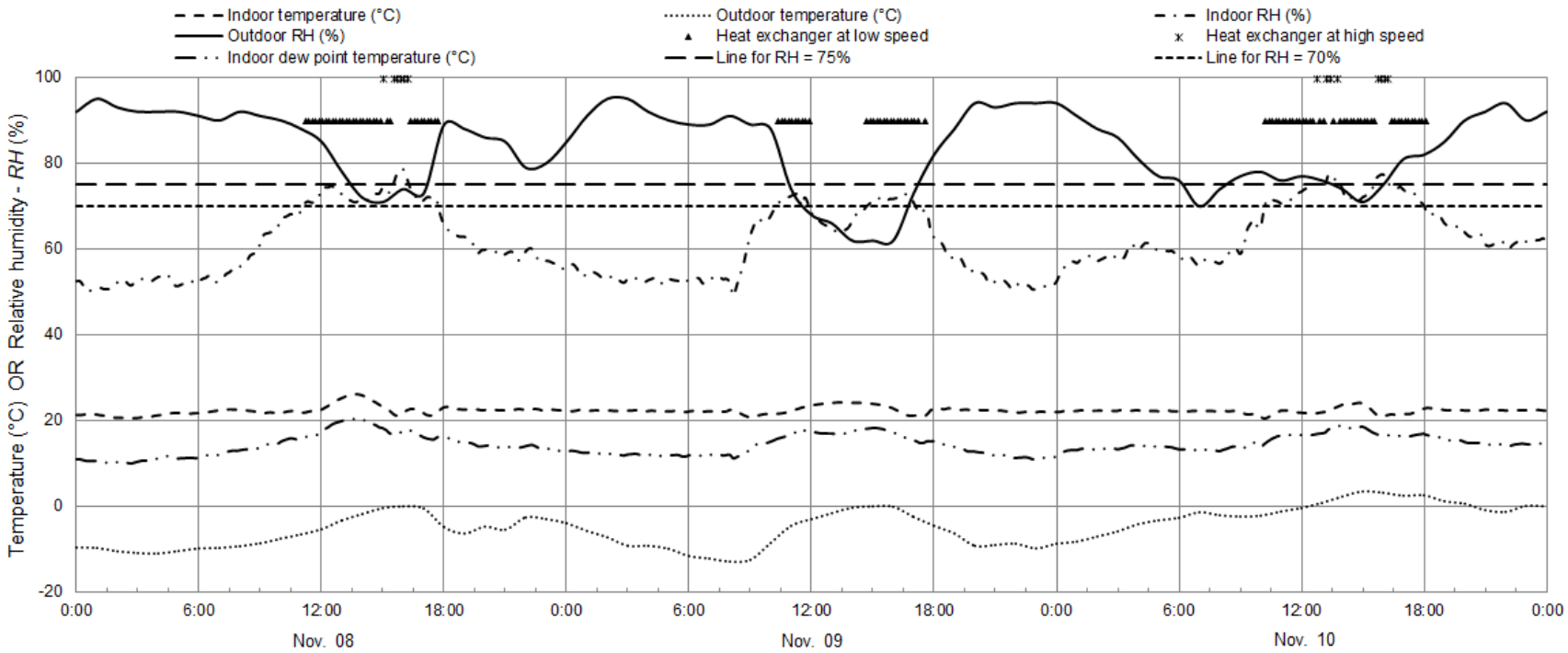


**Figure 2.7. Indoor conditions and the heat exchanger operating frequency on November 8-10, 2012.**

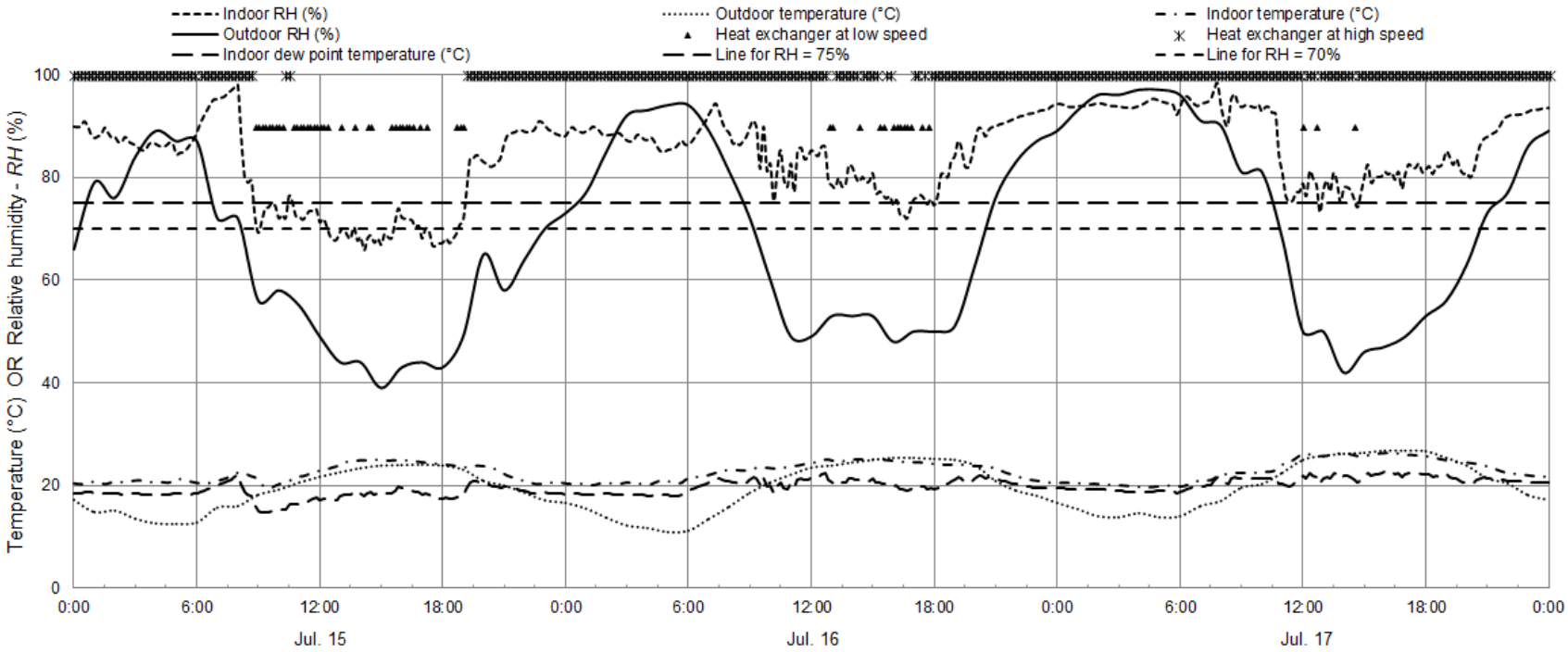


**Figure 2.8. Indoor conditions and the heat exchanger operating frequency on July 15-17, 2012.**

During the mild and warm seasons, the high ventilation rate required by temperature control brought drier air from outside to replace the moist indoor air during the daytime, causing a lower RH during the daytime as shown in Figure 2.8. The heat exchanger was operating at high speed for most of the time during the warm season, yet it was not effective in controlling the RH during the night due to high ambient RH. The peak RH occurred between 07:00 and 10:00h before the temperature exceeded the set point for temperature control with the cooling fans. Once the ventilation system was in operation, the RH in the greenhouse reduced quickly unless the outside air was humid, which is infrequent in this region (semi-arid region with a hot and dry summer). During the nighttime, the exhaust fans were operating at low speed or shut down due to the low outside temperature, but the outside temperature was not always low enough to cause the interior surface of the cladding material's temperature to be below the dew point, so most of the moisture in the air was kept inside, causing high RH. The experimental results indicate that the heat exchanger was not effective for humidity control during warm humid weather conditions as expected. The persistently high RH also indicates that the soil moisture evaporation is another contribution for greenhouse moisture, considering the relatively low plant transpiration rate at night and the moisture removed by the heat exchanger, the ventilation system, and the condensation. Additionally, the drip irrigation system did not operate during the nighttime and the growing medium evaporation was considered part of soil evaporation.

### 2.5.2 Heat exchanger moisture removal rate

Using the indoor and outdoor air temperature and RH values, the monthly average amount of moisture removed by the heat exchanger, (i.e., moisture removal rate over the periods when the RH was at or above the RH set point) is shown in Figure 2.9. The heat exchanger had higher removal rates during cold and mild weather conditions than during the warm season, confirming that the performance of the heat exchanger depends on the differential humidity ratio between inside and outside.

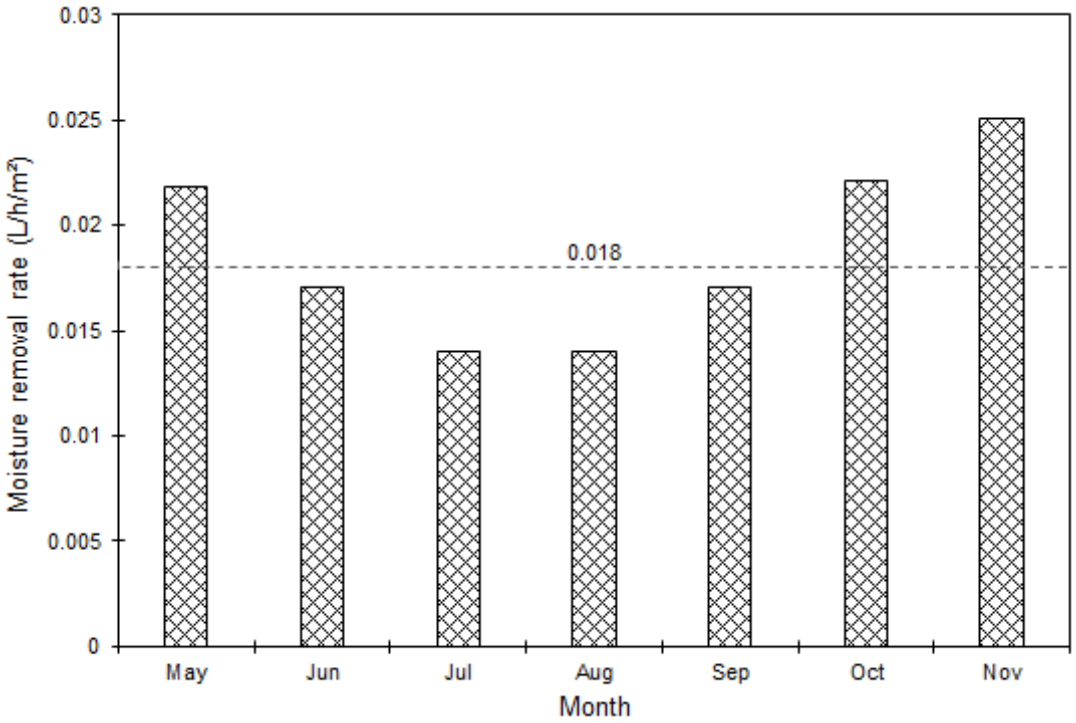


**Figure 2.9. Average hourly moisture removal rate (L $h^{-1}$ $m^{-2}$) by the heat exchanger in each month from May to November.**

To determine the peak dehumidification requirement, the experimental period was separated into two sub-periods according to ambient temperature. May to August is the warm summer period with average ambient temperatures above 12.6°C, while September to November is a cool period with average monthly ambient temperatures below 12.6°C. Figure 2.10 gives the comparison of these two periods regarding diurnal hourly average moisture removal rates of the heat exchanger, as well as the indoor RH and indoor and ambient humidity ratio. During the warm period, the heat exchanger had a higher hourly average moisture removal rate during the daytime from 07:00 to 18:00h. The maximum value was 0.019 L $h^{-1}$ per square meter of greenhouse floor area or 16.1 L $h^{-1}$ for the whole greenhouse. During the cool period, the values were 0.002 to 0.009 L $h^{-1}$ $m^{-2}$ higher than that during the warm season, when the maximum rate was 0.025 L $h^{-1}$ $m^{-2}$ (greenhouse total volume of 20.7 L $h^{-1}$). The hourly average moisture removal rates of the heat exchanger during the warm and cool periods were 0.016 and 0.020 L $h^{-1}$ $m^{-2}$, respectively. The total amount of moisture removed from the greenhouse by the heat exchanger was 13.6 and 16.9 L $h^{-1}$ during the warm and cool periods, respectively. This indicates better performance during the cool period. During the warm period, the indoor humidity ratio typically peaked at 14:00h, while during the cool period it peaked at 13:00h. The difference between the RH peak period and the humidity ratio

peak period was because during the humidity ratio peak period, the indoor temperature was high due to high solar radiation combined with high crop transpiration, thereby resulting in a high humidity ratio. The average humidity ratio differences between the inside and outside air were 0.006 and 0.008 $kg_w\ kg_{air}^{-1}$ during the warm and cool periods, respectively. The diurnal RH values indicated that the indoor RH was high from 22:00h and peaked at 08:00h during warm weather conditions, while during the cool period the RH values began to increase from 08:00h and peaked at 09:00h. This level was maintained until the peak at 17:00h, which was due to the set point temperature switching from day to night, and consequently started decreasing. The mean RH values during the warm and cool periods were 82.6% and 75.1%, respectively. The highest RH value during the warm period was 87.7%, which was 10% higher than that during the cool period.

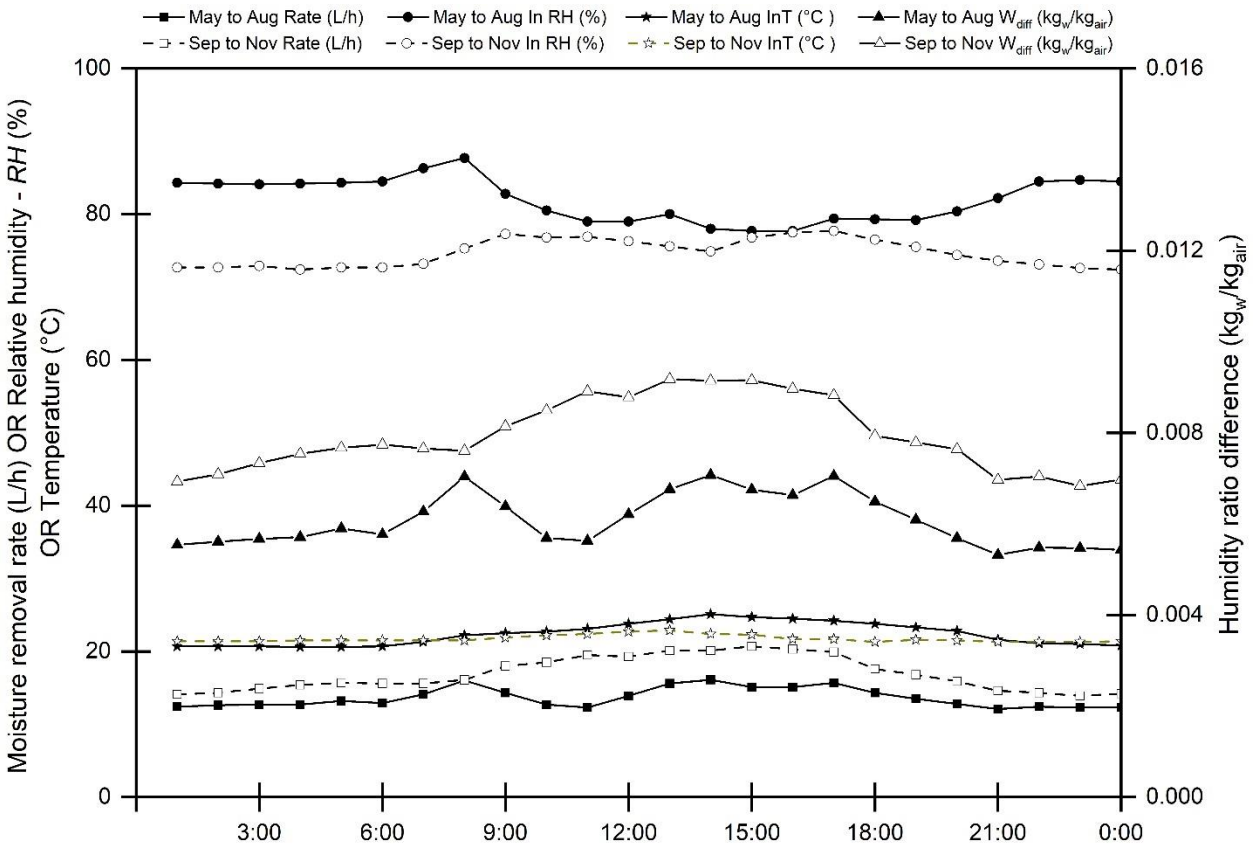


**Figure 2.10. Diurnal hourly average relative humidity (*RH*), temperature (*T*), humidity ratio difference ($W_{diff}$) and heat exchanger moisture removal rates.**

The mean moisture removal rate of the heat exchanger during the seven-month period is approximately 14.8 L $h^{-1}$ or 0.018 L $h^{-1}$ per square meter of greenhouse floor area. Overall, the heat exchanger controlled the indoor RH very well during cold and mild seasons, but it was not effective for humidity control and not economic efficient during the summer time.

### 2.5.3 Additional moisture removal rate

The additional moisture removal rate is the difference between that required to control RH at 75% and the amount that the heat exchanger removed. Table 2.1 shows moisture removal rates in addition to that removed by the heat exchanger based on a set point RH of 75%. Negative values of additional moisture removal rates indicate that the actual moisture removal rate of the heat exchanger was greater than the dehumidification requirement (for an RH target of 75%). The three distinct diurnal periods were grouped based on a similar moisture removal rate within each period. During the warm period, 22:00 to 06:00h is the nighttime period, 07:00 to 09:00h is the morning peak period, and 10:00 to 21:00h is the daytime period. For the cool period, 18:00 to 08:00h is the nighttime period, 09:00 to 14:00h is the daytime with stable RH and moisture removal requirement, and then it peaked from 15:00 to 17:00h.

**Table 2.1. Heat exchanger and additional moisture removal rate.[a]**

| *Time (h)* | *Warm Period (May – Aug)* | | | *Time (h)* | *Cool Period (Sep – Nov)* | | |
|---|---|---|---|---|---|---|---|
| | *Removal Rate ($L\ h^{-1}\ m^{-2}$)* | *Additional ($L\ h^{-1}\ m^{-2}$)* | *Total ($L\ h^{-1}\ m^{-2}$)* | | *Removal Rate ($L\ h^{-1}\ m^{-2}$)* | *Additional ($L\ h^{-1}\ m^{-2}$)* | *Total ($L\ h^{-1} m^{-2}$)* |
| 7 - 9 | 0.018 (0.006) ($n$ = 295) | 0.012 (0.006) | 0.029 (0.010) | 9 - 14 | 0.023 (0.006) ($n$ = 325) | 0.006 (0.004) | 0.024 (0.010) |
| 10 - 21 | 0.017 (0.006) ($n$ = 808) | 0.005 (0.003) | 0.022 (0.011) | 15 - 17 | 0.024 (0.006) ($n$ = 157) | 0.006 (0.004) | 0.027 (0.000) |
| 22 - 6 | 0.015 (0.004) ($n$ = 835) | 0.010 (0.005) | 0.025 (0.007) | 18 - 8 | 0.018 (0.006) ($n$ = 1133) | -0.002 (0.003) | 0.017 (0.008) |
| Average | 0.016 (0.006) | 0.009 (0.006) | 0.025 (0.001) | | 0.022 (0.006) | 0.001 (0.004) | 0.023 (0.005) |

[a]Numbers in the parentheses are the standard deviations and n is the number of measurements.

The general trend of the rate of additional moisture removal was that, during the warm season, it was high during nighttime and early morning, and low during daytime, which followed the same trend as the indoor RH. During the cool period, the opposite trend occurred with high values during the daytime and low values during the nighttime. The additional moisture removal rate during the warm season was quite stable from 10:00 to 21:00h with an average value of 0.005 L $h^{-1}$ $m^{-2}$. It started to increase to an average value of 0.010 L $h^{-1}$ $m^{-2}$ from 22:00h and peaked at 08:00h, with the peak value of 0.014 L $h^{-1}$ $m^{-2}$. The lowest value was 0.003 L $h^{-1}$ $m^{-2}$, which occurred at 16:00h.

During the cool period, there was no need for additional moisture removal from 20:00 to 07:00h. The only period that required additional moisture removal was during the daytime from 08:00 until 19:00h. The peak value was only 0.003 L $h^{-1}$ $m^{-2}$, which was much less than during the warm season. From 10:00 to 17:00h, the total moisture removal rate required during the cool period was greater than 0.024 L $h^{-1}$ $m^{-2}$ and higher than during the warm period. From 18:00 until 9:00h, the value was less than 0.023 L $h^{-1}$ $m^{-2}$ and it was lower than during the warm season. Under warm weather conditions, the total moisture removal rate was higher than 0.024 L $h^{-1}$ $m^{-2}$ from 22:00 until 09:00h, with a peak value of 0.033 L $h^{-1}$ $m^{-2}$. Both the hourly average of additional moisture removal rate and total moisture removal rate were higher during the warm period than during the cool period.

### 2.5.4 Dehumidification requirements

The main purpose of greenhouse dehumidification in this study is to control the indoor RH at an acceptable level during the cool seasons from September to November and from March to April. Considering the actual moisture removal rates of the heat exchanger and its humidity control performance, the average moisture removal rate during the seven-month period (i.e., 14.8 L $h^{-1}$ or 0.018 L $h^{-1}$ $m^{-2}$) could be considered the greenhouse dehumidification requirement. There are two reasons for using this value.

The first reason is that the indoor RH must be maintained at an acceptable level to decrease the occurrence of condensation on the inner surfaces of the building, which is one of the main sinks for greenhouse moisture removal, especially during the nighttime of the cool period. Compared with the total moisture removal requirement as shown in Table 2.1, the moisture removal rate of 0.018 L $h^{-1}$ $m^{-2}$ is equal to or higher than that of the total rate required for nighttime and early morning, which means the heat exchanger can meet the dehumidification requirement during the nights and early mornings of the cool period. Although this rate may be less than that of the total rate required for daytime in both the cool and warm periods, solar radiation becomes a significant contributor for the temperature of the inside surface of the building to be high enough to prevent that high RH, thereby not allowing much condensation on the indoor surfaces. The second reason is that, during the cooling period in warm and mild seasons when the cooling exhaust fans are in operation and the indoor temperature is above the set point, the indoor RH drops rapidly; thus, the cooling exhaust fans are the main moisture removal equipment for these periods.

Table 2.2 shows the theoretical time that the inside RH exceeds 75% when 0.018 L $h^{-1}$ $m^{-2}$ of moisture removal rate is provided. In this table, "Required Removal Rate" is the total moisture removal rate calculated in Table 2.1. "Occurrence frequency" is the ratio of the moisture removal difference of "Required Removal Rate" and the provided rate of 0.018 L $h^{-1}$ $m^{-2}$ to the "Required Removal Rate." The time with the inside RH exceeding 75% in each hour is also given. The results indicate that, during the warm period, there would be around 6 hours per day where the inside RH would be greater than 75%, relative to the previous 16 hours experienced in the greenhouse. The period with an RH exceeding 75% would mainly occur during nights and early mornings. During the cool period, it would be only 12.2% of the time per hour where the inside RH would exceed 75%, which only occurs during the daytime. RH would not exceed 75% during the nighttime or early morning. For 2.9 hours per day, the inside RH would be higher than 75%. With the 0.018 L $h^{-1}$ $m^{-2}$ of moisture removal rate, the situation of high RH occurrences during nights and early mornings in the summertime, and during the daytime in the mild and cold seasons, would be greatly reduced. The occurrence of high RH during the nighttime in the cool period would also be prevented.

**Table 2.2. Occurrence frequency of inside RH exceeding 75% under dehumidification capacity of 0.018 L $h^{-1}$ $m^{-2}$.**

| | *Warm Period* | | | | *Cool Period* | | |
|---|---|---|---|---|---|---|---|
| *Time (h)* | *Required Removal Rate (L $h^{-1}$ $m^{-2}$)* | *Percentage of the time (RH ≥ 75%) (%)* | *Time when RH over 75% (min $h^{-1}$)* | *Time (h)* | *Required Removal Rate (L $h^{-1}$ $m^{-2}$)* | *Percentage of the Time (RH ≥ 75%) (%)* | *Time when RH over 75% (min $h^{-1}$)* |
| 7-9 | 0.029 | 36.1 | 21.7 | 9-14 | 0.024 | 25.4 | 15.2 |
| 10-21 | 0.022 | 21.6 | 13.0 | 15-17 | 0.027 | 29.7 | 17.8 |
| 22-6 | 0.025 | 27.7 | 16.6 | 18-8 | 0.017 | 0.0 | 0.0 |
| Average/ Sum | 0.025 | 25.7 | 6 (h $day^{-1}$) | | 0.023 | 12.2 | 2.9 (h $day^{-1}$) |

Overall, as shown in Table 2.2, with the capacity of 0.018 L $h^{-1}$ $m^{-2}$ or so, the greenhouse dehumidification requirement during cold and mild seasons can be met if combined with the greenhouse exhaust ventilation system. Additionally, this would help control the indoor RH better during the summer time. There would be less than 25.7% and 12.2% of the time in the warm period and cold and mild periods where the inside RH exceeds 75%, respectively.

## 2.6 Conclusions

During the experimental period, the heat exchanger controlled the indoor RH well with less than 20% of the time that an RH of 80% was exceeded from September to November; however, it was less effective during the summertime. The moisture removal rate of the heat exchanger is high with cool outside air. The greenhouse dehumidification requirement is estimated to be 14.8 L $h^{-1}$ or 0.018 L $h^{-1}$ per square meter of greenhouse floor area for the cool period when combined with the exhaust ventilation system. With this removal rate, there would theoretically be less than 12.2% of the time where the inside RH is greater than 75% during the cool period. A high RH would mainly occur during the daytime, and the RH would be well controlled during nights and early mornings. During the summertime, with this removal rate, the percentage of RH exceeding 75% would be reduced from the previous 68% to 25.7%; that is, reduced from 16 hours to 6 hours per day with the RH exceeding 75%. The percentages of RH over 80% or more would be much less. Meeting the peak requirement would require a 58.8% increase of dehumidification capacity, which is expensive and unnecessary. Further research and experimental data are required to verify the results.

# CHAPTER 3

# MECHANICAL REFRIGERATION DEHUMIDIFIER PERFORMANCE EVALUATION IN A TOMATO GREENHOUSE IN COLD REGIONS

(Published in *Transactions of the ASABE*, 2016, Vol. 59(4), pp. 933-941. DOI: https://doi.org/10.13031/trans.59.11662)

Jingjing Han, Huiqing Guo, Robert Brad, Doug Waterer

## Contribution of this paper to overall study

Based on the experimental results in Chapter 2, a commercial-grade mechanical refrigeration dehumidifier was selected for greenhouse dehumidification. The performance of the unit including humidity control effectiveness, the operating cost, as well as the plant loss rate and the greenhouse annual revenue, were analyzed in this chapter. Besides the normal electricity energy factor, a heat energy factor was also used to evaluate the unit performance considering the condensation process also contributes to greenhouse heating. This chapter fulfills the objectives 1 and 4.

The manuscript included in this chapter has been published in *Transactions of the ASABE*. The experimental setup, data collection and analyses, and manuscript writing were performed by the first author (PhD student – Ms Jingjing Han). The manuscript was critically reviewed by the second author (supervisor – Prof. Huiqing Guo). The third author (Mr. Robert Brad) helped with the experimental setup. The fourth author (Prof. Doug Waterer) provided suggestions on field measurement.

## 3.1 Abstract

A commercial-grade mechanical refrigeration dehumidifier was installed in a tomato greenhouse for humidity control, and relative humidity was monitored for one year. The results indicated that the indoor RH condition was controlled much better by the dehumidifier than by the previous air-to-air heat exchanger. Considering a 10-year payback period, the annual cost of the dehumidifier was about $4,000 in 2013. Even though the capital cost and annual cost of the dehumidifier were high, the plant loss rate due to high relative humidity was dramatically reduced from 43.3% prior to 2012 without dehumidification to 0.9% in 2013. The annual revenue was also increased by about 10% in 2012, compared with that in 2009 to 2011. The increased revenue indicated that the equipment payback period was within one year. Considering all the benefits, dehumidification is strongly recommended for greenhouse humidity control in cold regions.

## 3.2 Nomenclature

| | |
|---|---|
| $b$ | interest rate, % |
| $CRF$ | capital recovery factor |
| $EF_e$ | electricity energy factor, L kWh$^{-1}$ |
| $EF_h$ | heat energy factor, L kWh$^{-1}$ |
| $h_{fg}$ | water heat of condensation, kJ kg$^{-1}$ |
| $m_{water}$ | mass of the condensed water collected by the dehumidifiers, kg |
| $n$ | payback period |
| $Q_e$ | electrical energy consumption by the dehumidifier, kW-h |
| $Q_{eo}$ | heat output of the dehumidifiers, kW-h |
| $Q_{latent}$ | latent heat released by condensed water in the dehumidifier, kW-h |
| $Q_{ld}$ | heat released into the greenhouse by the dehumidifiers, kW-h |
| $RH$ | relative humidity, % |

## 3.3 Introduction

Nowadays, humidity control draws more and more attention from greenhouse producers. The main reason is that high relative humidity (RH) causes fungal diseases, which reduce yields and impair produce quality (Campen et al., 2003). The methods used for greenhouse dehumidification include improving the irrigation system, exhaust ventilation based on humidity control, chilled water condensation dehumidification, chemical dehumidification, air-to-air heat exchangers, mechanical refrigeration dehumidifiers, etc. For commercial greenhouses in cold regions, the most suitable and economical methods for dehumidification are ventilation with heat recovery and

condensation on a cold surface, as suggested by Campen (2009). Gao (2012) and Han et al. (2011) found that chilled water dehumidification was the most energy-intensive and costly method. An air-to-air heat exchanger could control the humidity well in cold and mild seasons but was not effective in humid and warm weather conditions. Mechanical dehumidification was recommended for year-round humidity control.

Han et al. (2015b) used an air-to-air heat exchanger in a commercial greenhouse for humidity control. The results revealed that the capacity of the heat exchanger could not meet the dehumidification requirement of the greenhouse, especially during summer. The dehumidification requirement of the greenhouse was estimated to be about 14.8 L $h^{-1}$ based on analysis of the amount of water removed by the heat exchanger. Based on this calculation, a commercial-grade mechanical dehumidifier was selected and installed inside the same greenhouse in September 2012.

The objective of this study was to evaluate the performance of a commercial-grade dehumidifier in a greenhouse and conduct an economic analysis on the costs and benefits.

## 3.4 Materials and Methods

### 3.4.1 Greenhouse specifications

A commercial greenhouse was used in this study, which was located in Grandora, Saskatchewan, 25 km west of Saskatoon, at 52.11° N latitude, 106.98° W longitude, and 504 m elevation. It was a three-span greenhouse covered by inflated double-layer 6-mil polythene plastic film on the roof and polyethylene panels on the sidewalls, except the north wall, which was an insulated wooden wall. The thickness of the north wall was 11.4 cm, and its thermal conductivity was 0.23 W $m^{-2}$ $K^{-1}$. The greenhouse was 19.2 m wide and 43.9 m long. The eave height was 4.3 m, and the ridge height was 6.7 m. Tomato plants were planted in bags filled with general-purpose peat-based growing medium and planted in 11 rows with a total of 2,125 plants, averaging a density of 2.5 plants $m^{-2}$. The greenhouse was heated by black iron hot water pipes located above ground between the rows of tomato plants. Four natural gas boilers were used to heat the hot water. The greenhouse had three exhaust fans (FC050-4E, Ziehl-Abegg, Sainte-Claire, QC, Canada) on the east wall at a height of 3.8 m and roof vents for cooling. The exhaust fans, with an impeller diameter of 0.548 m, had a capacity of 2.1 $m^3$ $s^{-1}$ at a static pressure of 20 Pa (Ziehl-Abegg, 2012). A drip

irrigation system was used for water and nutrient supply. In March 2013, the grower started to build a fourth span, which was attached to the third span. By the end of May 2013, small cucumber plants were planted in the fourth span. There was only a small opening between the fourth span and the third span. The sidewall between them was not removed until the end of the year.

### 3.4.2 Dehumidification method

Before 30 August 2012, an air-to-air heat exchanger (vanEE HRV12LC, Venmar Ventilation, Inc., Drummondville, QC, Canada) was used inside the greenhouse for dehumidification. The RH set points were 70% for the low speed of the heat exchanger and 75% for the high speed. The average moisture removal rate of the heat exchanger from May to November in 2011 was 14.8 L $h^{-1}$, or 0.018 L $h^{-1}$ $m^{-2}$ of greenhouse ground area (Han et al., 2015b). However, its effectiveness was influenced by the indoor and outdoor air conditions, and it was not effective in RH control, especially during the humid and warm season. In addition, it required frequent maintenance. Therefore, the air-to-air heat exchanger was shut down, and a commercial dehumidifier (DCA3000T, Dehumidifier Corporation of America, Cedarburg, WI, USA) was installed inside the greenhouse, as shown in Figure 3.1. This unit was selected for its large dehumidification capacity (14.7 L $h^{-1}$ at 75% relative humidity and 21°C air temperature). The airflow rate of the dehumidifier was 1.42 $m^3$ $s^{-1}$. A small room was built at the east end of the greenhouse to house the dehumidifier. To distribute the drier and warmer exhaust air from the dehumidifier, a metal discharge duct was installed along the east wall of the greenhouse, and multiple perforated plastic film ducts running east-west along the tomato rows above ground were installed to distribute air evenly inside the greenhouse. A tank with the total volume of 670 L was placed inside the small room to collect the water condensed by the dehumidifier. To monitor the power consumption of the dehumidifier, a current sensor (AT50 B10, LEM, Inc., Milwaukee, WI, USA) was used. The accuracy of the sensor was less than ±1.5% of its measurement range. A type-T thermocouple (Omega Engineering, Inc., QC, Canada) and a humidity sensor (HM1500LF, Measurement Specialties, Inc., Toulouse, France) were used to measure the temperature and RH of the exhaust air from the dehumidifier. The thermocouples had an accuracy of 0.3°C at 100°C and were calibrated against a thermocouple simulator-calibrator (model 1100, Ectron Corp., San Diego, CA, USA). The humidity sensor had an accuracy of ±3% in the RH measurement range of 10% to 90%. A humidity generator (model 1200, Thunder Scientific Corp., Albuquerque, NM, USA) was used to calibrate the sensor. Both

sensors were placed inside the metal duct near the outlet of the dehumidifier. The dehumidifier had its own humidity control sensor, which was located at the center of the greenhouse with the other environmental monitoring sensors.


(a)

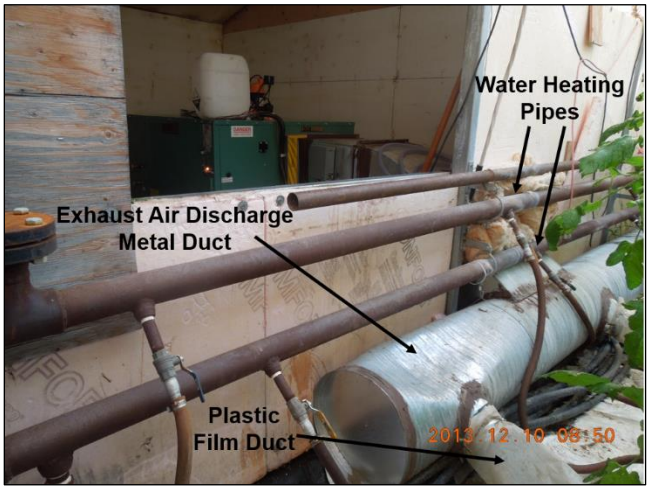


(b)

**Figure 3.1. (a) Dehumidifier and water tank and (b) discharge duct.**

Initially, the RH set point of the dehumidifier was set at 63% to determine if the equipment was working appropriately. The set point was then changed to 68% on 6 September 2012 to control the indoor RH at about 75%. However, the indoor RH was greater than 75% for more than 45% of the time in September and October 2012. Therefore, the RH set point of the dehumidifier was set to 63% in 2013. The unit started running on 15 April and was used until the greenhouse was shut down on 10 December 2013.

### 3.4.3 Experimental data collection

The indoor air temperature and RH were measured with a temperature and relative humidity probe (CS500, Campbell Scientific, Edmonton, Alberta, Canada) that was placed inside a radiation shield and installed at the center of the greenhouse, 1.8 m above the ground. The probe had a temperature accuracy of ±0.2°C to ±1.4°C over a measurement range of -40°C to 60°C and RH accuracies of ±3% over a range of 10% to 90% RH and ±6% over a range of 90% to 100% RH. The same humidity generator (model 1200, Thunder Scientific Corp., Albuquerque, NM, USA) was used to calibrate the sensor. A pyranometer sensor (LI-200, Li-Cor, Lincoln, NE, USA) was installed inside the greenhouse at the ridge height to measure the inside solar radiation. The sensor was calibrated by the manufacturer against an Eppley precision spectral pyranometer (PSP) (Li-Cor, 2012). The indoor $CO_2$ concentration was measured with a K-30 sensor (CO2Meter, Inc., Ormond Beach, Fla.) that was installed inside the greenhouse above the plants. The sensor had an accuracy of ±30 ppm plus ±3% of the measured value. It was calibrated per the manufacturer's instructions (CO2Meter, 2012).

A data logger (CR10X, Campbell Scientific, Edmonton, AB, Canada) was installed near the east wall of the greenhouse. All the environmental parameters as well as the operating times of the exhaust fans and dehumidifier and their power consumption were monitored every minute, with 10 min averages recorded by the data logger. The other pieces of ventilation and heating equipment were controlled based on temperature by the greenhouse ventilation control system, which was installed in the header house north of the greenhouse. Ambient weather conditions (temperature and RH) were obtained from Environment Canada. The equipment locations and sensor placement are shown in Figure 3.2.

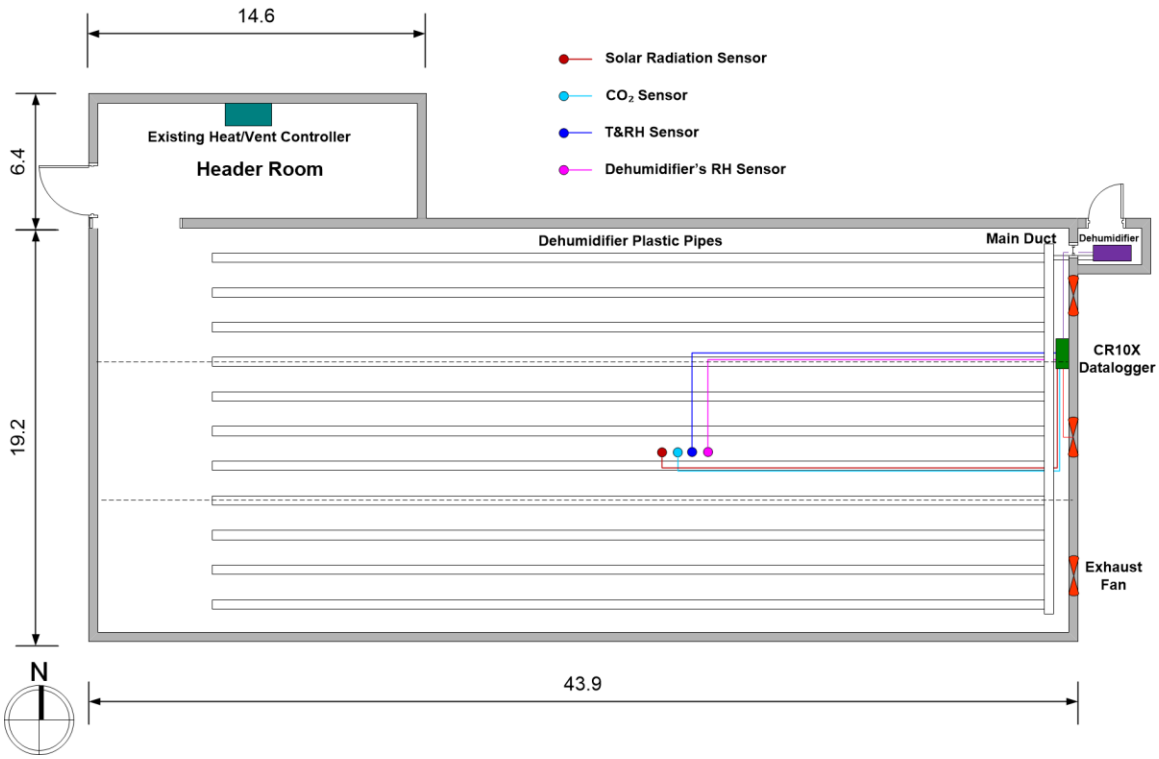


**Figure 3.2. Greenhouse layout and sensor locations (dimensions in m).**

### 3.4.4 Data analysis

In 2012, experimental data were collected for seven months from 3 May to 23 November, when the greenhouse was shut down. In 2013, the greenhouse started in February, and data were collected for nine months from 14 March to 30 November. Before August 2012, the heat exchanger was used for dehumidification; the dehumidifier was used after that. All data collected in 2012 and 2013 were used for data analysis. The performance of the dehumidifier was evaluated based on the indoor RH, energy consumption, energy factor, and greenhouse revenue increase.

#### *3.4.4.1 Dehumidifier energy consumption*

For the dehumidifier, the total energy consumption was the sum of the electrical energy consumption and the heat released to the greenhouse. The heat released to the greenhouse included the sensible heat output of the dehumidifier motor and the latent heat released by the condensate. The total heat released into the greenhouse by the dehumidifier was given by (Han et al., 2015a):

$$Q_{\mathrm{ld}} = Q_{\mathrm{eo}} + Q_{\mathrm{latent}} = Q_{\mathrm{eo}} + \frac{h_{\mathrm{fg}} \times m_{\mathrm{water}}}{3600} \qquad (3.1),$$

where $Q_{ld}$ is heat released into the greenhouse by the dehumidifier, in kW-h; $Q_{eo}$ is heat output of the dehumidifier, which was assumed to be 90% of its electrical energy consumption to prevent overestimation of heat release (ASHRAE, 2009), in kW-h, and is calculated using the power consumption of the dehumidifier multiplied by the operating time; $Q_{latent}$ is latent heat released by condensate from the dehumidifier, in kW-h; $h_{fg}$ is vaporization heat of water, in kJ kg$^{-1}$, which is calculated by $h_{fg} = 2501 - 2.42 \times t_w$; $t_w$ is the temperature of the condensed water, in °C, and it is assumed equal to the room air temperature (Albright, 1990); $m_{water}$ is mass of the condensate collected by the dehumidifiers, in kg.

The electricity cost was \$0.1108 kWh$^{-1}$ in 2012 and \$0.1162 kWh$^{-1}$ in 2013 (Saskatoon, 2013). The greenhouse used natural gas for heating. The annual average natural gas price during 2012 and 2013 was \$5.28 GJ$^{-1}$, which was equivalent to \$0.0211 kWh$^{-1}$ (SaskEnergy, 2013). The efficiency of the natural gas heating system was estimated to be 90%.

#### *3.4.4.2 Dehumidifier energy factor*

An important factor that is normally used to evaluate the performance of dehumidifiers is the energy factor (*EF*), which is defined as the total amount of water (in L) removed per kWh of electricity consumed by the dehumidifier at standard test conditions of 26.7°C air temperature and 60% RH at sea level (Hong Kong, 2008). In this study, the energy factor was called the electricity energy factor ($EF_e$) and was determined from:

$$EF_e = \frac{m_{water}}{Q_e} \qquad (3.2),$$

where $EF_e$ is electricity energy factor, in L kWh$^{-1}$; and $Q_e$ is electrical energy consumption by the dehumidifier, in kW-h.

According to Canada's energy efficiency regulations for household appliances, the minimum $EF_e$ for dehumidifiers is 2.5 L kWh$^{-1}$ if the water removal capacity of the unit is greater than 35.5 L d$^{-1}$ (NRC, 2015). However, there is no such standard for commercial dehumidifiers, which might be due to their high water removal capacity and power consumption.

Considering the weather conditions in cold regions, where the heating season is long, the sensible heat output of the dehumidifier and the latent heat released during the condensation process also contribute to greenhouse heating. Therefore, another energy factor, the heat energy

factor ($EF_h$), was used in this study to evaluate the heating contribution of the dehumidifier. $EF_h$ is defined as the ratio between the amount of water condensed by the dehumidifier and the total heat released into the greenhouse by the unit. Because the water removal capacity and power consumption of commercial dehumidifiers are greater than those of domestic dehumidifiers, the heat released into the greenhouse cannot be ignored due to its contribution to the heating of the greenhouse. Equation 3.3 was used to calculate $EF_h$:

$$EF_h = \frac{m_{water}}{Q_{ld}} \quad (3.3),$$

where $EF_h$ is the heat energy factor, in L $kWh^{-1}$.

$EF_h$ should be considered only during the heating season, not during cooling periods. In cold regions such as the Canadian Prairies, the heating season is long and includes some summer nights and even days. During cooling periods, the heat released to the greenhouse would increase the cooling load and is therefore undesirable. However, the amount of heat released should be negligible compared to the total cooling requirement of the greenhouse and thus was not considered in the energy and cost analysis.

#### *3.4.4.3 Dehumidifier annual cost*

The annual cost of using the dehumidifier was also calculated, which included the capital cost, maintenance, interest, and depreciation. The capital recovery factor (*CRF*) (Lindeburg, 1992) was used to calculate the interest and depreciation, given as follows:

$$CRF = \frac{b(1+b)^n}{(1+b)^n - 1} \quad (3.4),$$

where *b* is the interest rate, in %, set at 6%; and *n* is the payback period, chosen as 10 years. The calculated *CRF* was 0.136 and was used for the interest and depreciation calculation.

## 3.5 Results and Discussion

### 3.5.1 RH control effect

Table 3.1 lists the monthly percentages of time when the indoor RH exceeded 75%, 80%, and 85% in 2012 and 2013. It also shows the monthly average indoor RH. The weather is classified

into three groups: cold season (January, February, March, November, and December), mild season (April and October), and warm season (May, June, July, August, and September). As shown in Table 3.1, the percentages of time when the inside RH exceeded 75%, 80%, and 85% were all lower in 2013 than in 2012, especially when the size of the greenhouse was increased by 33% in 2013. They were reduced by more than 30% from June to September in 2013 compared with that period in 2012. The monthly average indoor RH was lower than 75% all the time in 2013, while it was above 75% during the summer in 2012. There were two reasons for the lower RH in 2013 than 2012. One reason was that the weather in 2013 was slightly drier and colder than in 2012, as shown in Figure 3.3. The other reason, which should be the main reason, was that the heat exchanger was ineffective in humid and warm weather, while the dehumidifier's performance was not affected by these weather conditions. The dehumidification capacity of the dehumidifier was much larger than that of the heat exchanger during the warm season. Even though the dehumidifier was not operating at the capacity stated by the manufacturer, all the data reveal that the dehumidifier controlled the indoor RH very well year-round, compared with the heat exchanger, especially during summer and fall nights, meeting most of the dehumidification requirement for the greenhouse.

**Table 3.1. Percentages of time of high *RH* in the greenhouse.**

| *Month* | *Average RH (%)* | | *RH ≥ 75%* | | *RH ≥ 80%* | | *RH ≥ 85%* | |
|---|---|---|---|---|---|---|---|---|
| | *2012* | *2013* | *2012* | *2013* | *2012* | *2013* | *2012* | *2013* |
| Mar | - | 71.5 | - | 32.9 | - | 9.4 | - | 0.2 |
| Apr | - | 76.2 | - | 59.0 | - | 26.9 | - | 6.8 |
| May | 73.8[a] | 70.3 | 57.5[a] | 40.4 | 33.6[a] | 24.4 | 7.7[a] | 14.3 |
| Jun | 76.9[a] | 70.7 | 70.9[a] | 38.2 | 56.3[a] | 11.3 | 29.9[a] | 0.8 |
| Jul | 82.4[a] | 73.6 | 78.1[a] | 47.9 | 68.4[a] | 23.7 | 50.5[a] | 5.7 |
| Aug | 83.5[a] | 71.7 | 81.5[a] | 38.6 | 69.3[a] | 11.0 | 55.3[a] | 2.4 |
| Sep | 76.0 | 67.7 | 63.9 | 16.3 | 42.9 | 1.3 | 17.9 | 0.0 |
| Oct | 74.3 | 71.5 | 45.7 | 26.2 | 18.4 | 6.7 | 3.2 | 0.6 |
| Nov | 62.3 | 65.0 | 8.8 | 9.9 | 1.2 | 2.0 | 0.0 | 0.3 |

[a] Heat exchanger dehumidification was applied from May to August in 2012, and the dehumidifier was used after that.

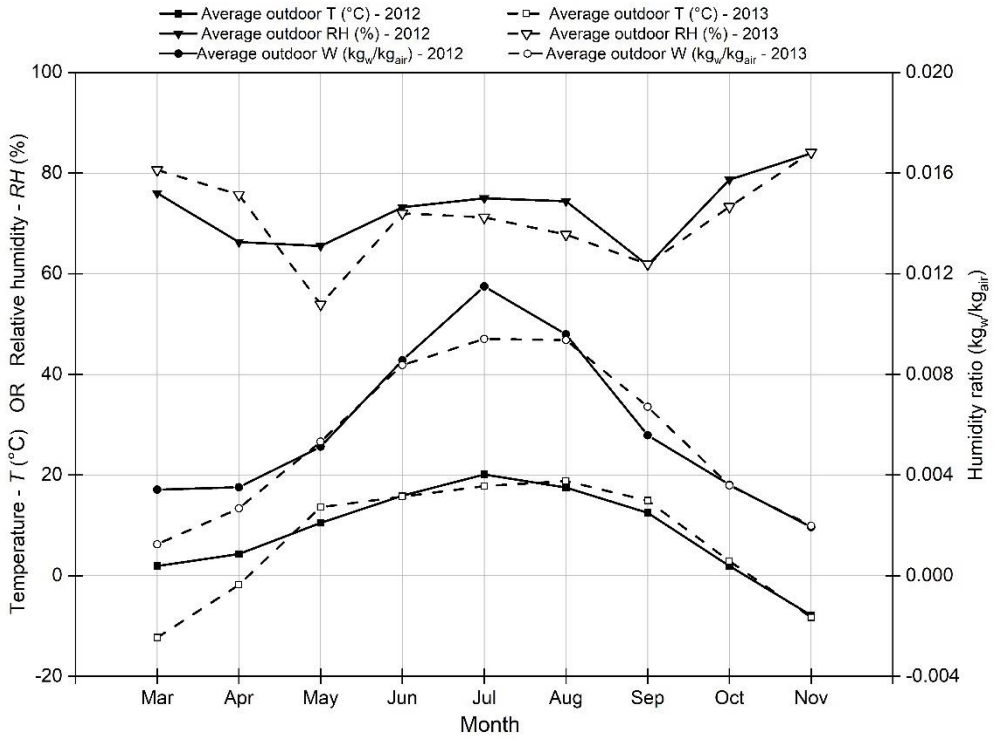


(a)

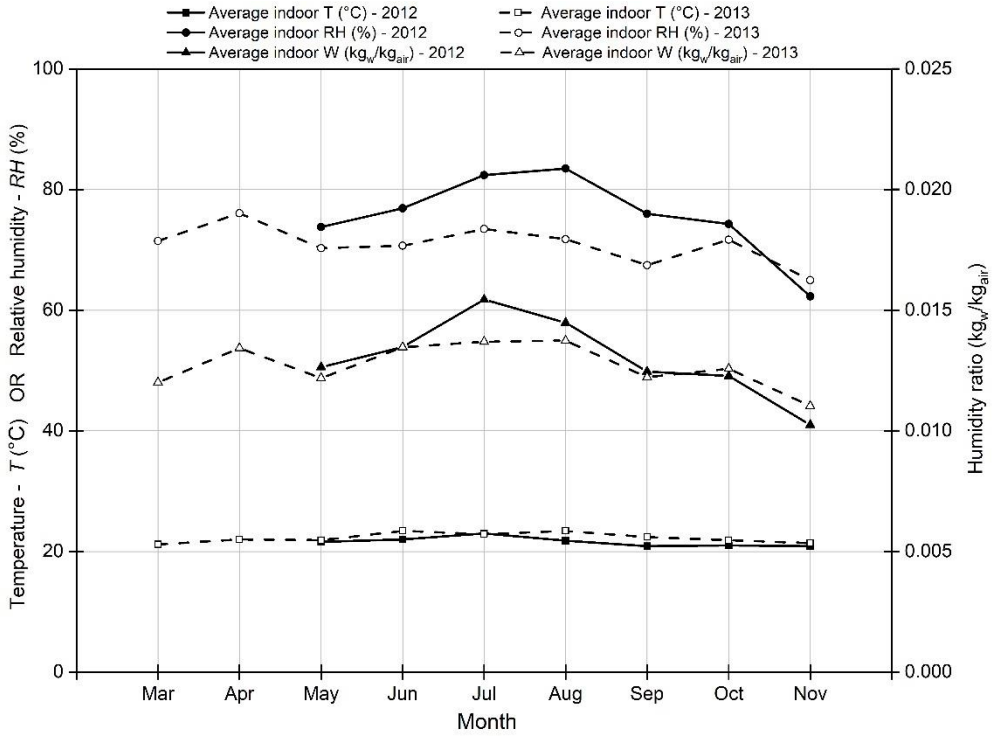


(b)

**Figure 3.3. Monthly average temperature (*T*), relative humidity (*RH*), and humidity ratio (*W*) in 2012 and 2013: (a) ambient and (b) inside.**

### 3.5.2 Dehumidifier performance

#### *3.5.2.1 Dehumidifier operation condition*

Generally, in mild and summer seasons, the dehumidifier was running most of the time during the night due to the high indoor RH. During the day, the indoor RH was lower than the set point due to ventilation by the exhaust fans and roof vents. Ventilation brought cooler and drier outside air into the greenhouse and replaced the hot and humid indoor air. During the winter, the indoor RH was high during the day due to plant transpiration and limited ventilation (mostly by infiltration) and low at night due to low moisture production and condensation. Hence, the dehumidifier was in operation mostly during the day and stopped during the night.

Figure 3.4 shows typical greenhouse indoor RH conditions in the summer of 2013 with operation of the dehumidifier. When the dehumidifier started running, the indoor RH started to drop. Although the dehumidifier was not able to control the RH to 63%, setting the set point at such a low value delayed and shortened the high RH (>80%) periods. As shown in Figure 3.4, during the day from 15 to 16 August, the dehumidifier did not run even though the indoor RH was above the set point. The unit may have been shut down by the grower due to the high indoor air temperature, which also occurred during other warm periods. The dehumidifier was effective for humidity control, as the RH was above 80% only 11% to 23.7% of the time in summer. The high RH (>80%) periods occurred mainly after sunrise due to high transpiration and low ventilation and did not last long. Higher temperature of the plastic film after sunrise limited or prevented condensation on the inner surface of the plastic film; therefore, little or no adverse effect was observed on the plants. Figure 3.4 also shows the daily amount of water collected by the dehumidifier. The dehumidifier collected more water during the night than during the day because the dehumidifier was in operation longer at night due to the high RH.

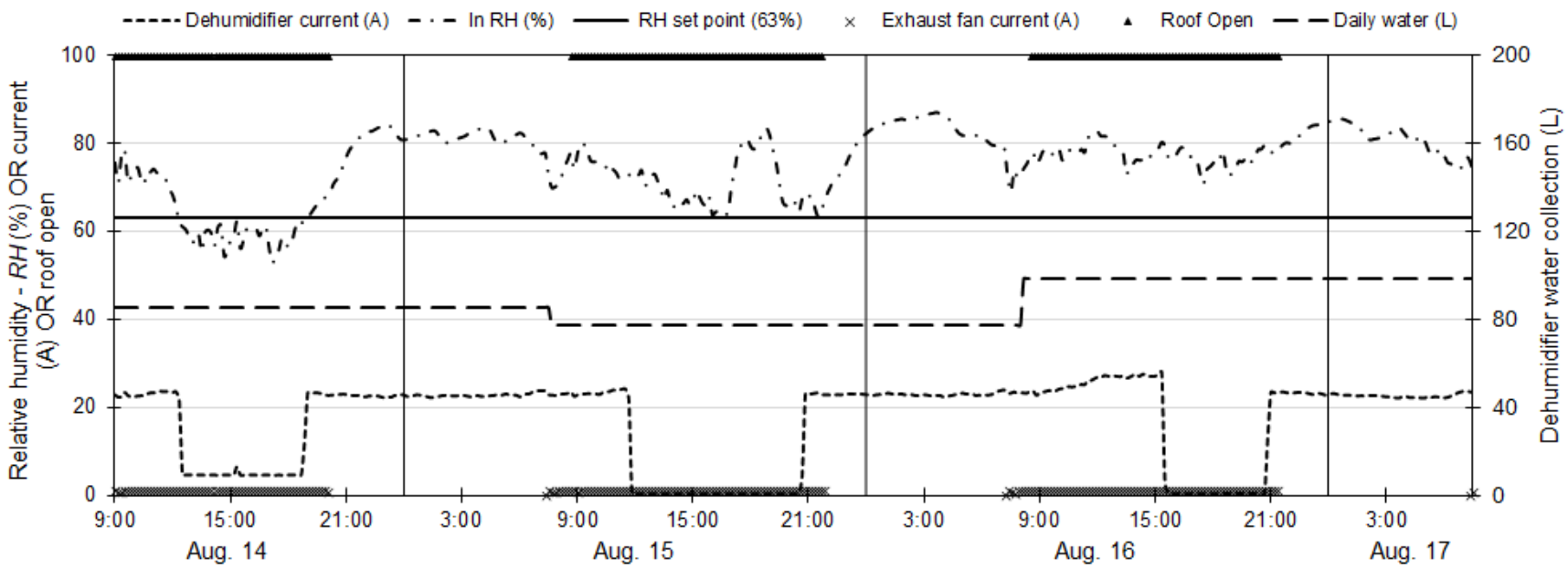


**Figure 3.4. Greenhouse indoor relative humidity (*RH*) conditions on August 14-17, 2013.**

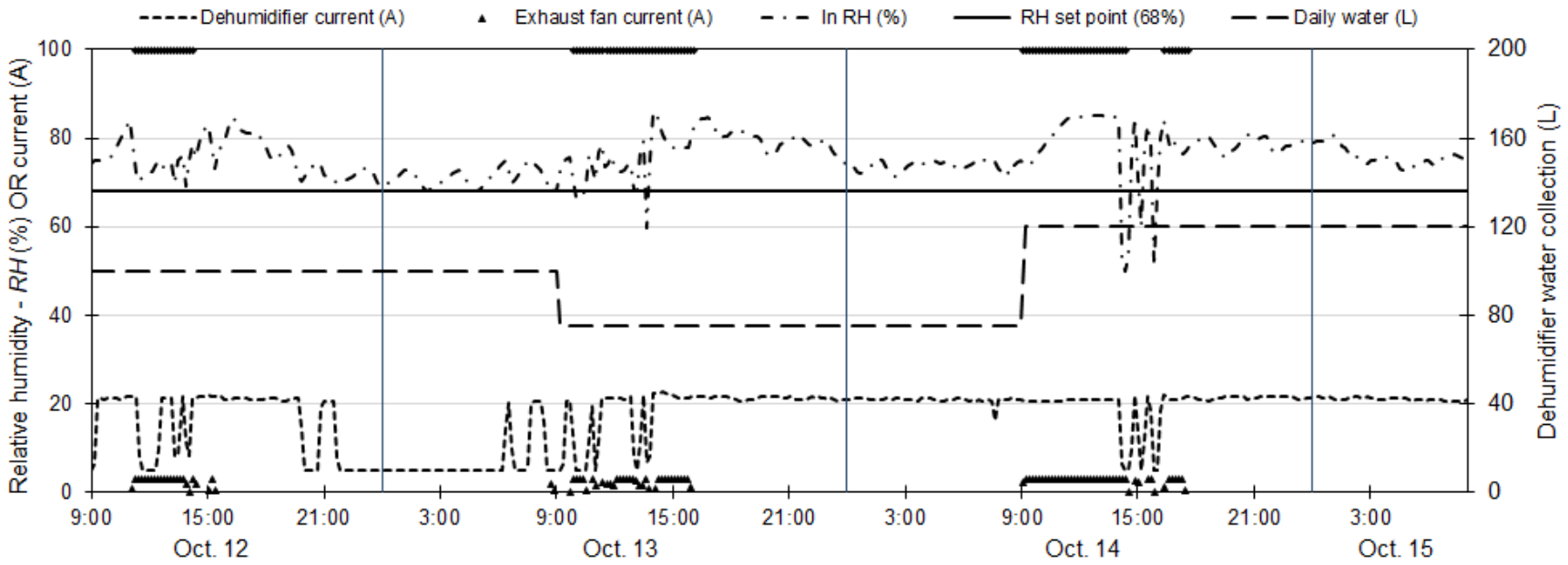


**Figure 3.5. Greenhouse indoor relative humidity (*RH*) conditions and dehumidifier performance on October 12-15, 2012.**

Figure 3.5 shows the greenhouse indoor RH conditions in the mild season from 12 to 15 October 2012. During this period, the roof was not open for long periods during the day due to the cool ambient weather conditions. The indoor RH was higher than the dehumidifier RH set point; therefore, the dehumidifier was running most of the time and collected more water than during the warm season. However, higher condensation on the greenhouse cover material played an important role in reducing the indoor RH, resulting in lower inside RH than during summer.

Overall, the commercial dehumidifier showed effective control of the indoor RH and could maintain the indoor RH at an acceptable level year-round, not only during the cold and mild seasons but also in summer. High RH periods occurred at night or early morning in summer and during the day in mild and cold seasons when the dehumidifier's capacity was not large enough to keep the RH below 80%. If two hours were needed to remove the extra moisture from the greenhouse to keep the indoor RH at or below 80%, then this would require an increase in the dehumidifier's capacity of as much as 88% from April to August and about 10% from September to November. The capital cost of the dehumidification system would almost double, and the power consumption and operating cost would also double. Therefore, this increase in capacity would not be cost-effective. Instead, it is recommended that the ventilation system should be activated for short periods to remove the excess moisture, or an exhaust fan should be installed to control RH when the RH is greater than 80% during mild and cold seasons.

#### *3.5.2.2 Energy consumption and cost*

Table 3.2 lists the estimated total energy consumption and energy cost of the dehumidifier. The dehumidifier was started on 15 April 2013. However, there was no water collection record due to freezing of the pump and the ground in the room that housed the dehumidifier. The underground electrical cable to the greenhouse failed on 6 May, and the dehumidifier stopped running for ten days until 16 May. Therefore, the amount of water condensed by the dehumidifier in April and May in 2013 is only an estimate based on observations by the grower.

**Table 3.2. Dehumidifier energy consumption and energy cost (heat release was calculated only when greenhouse heating was on).**

| *Year* | *Month* | *Collected Water (L)* | *Energy Consumption ($\times 10^{-3}$ GW-h)* | | | *Dehumidification Cost ($)* | | |
|---|---|---|---|---|---|---|---|---|
| | | | *Electricity* | *Heat Release* | *Total Energy* | *Electricity* | *Heat Release* | *Total Cost* |
| 2012 | Sep | 2353 | 1.52 | 0.73 | 0.79 | 161 | -11 | 150 |
| | Oct | 2679 | 1.94 | 1.34 | 0.59 | 205 | -21 | 184 |
| | Nov | 305 | 0.68 | 0.28 | 0.35 | 72 | -4 | 63 |
| | Total | 5337 | 4.13 | 2.35 | 1.73 | 438 | --36 | 402 |
| 2013 | Apr | 400 | 1.53 | 0.33 | 1.20 | 178 | -7 | 171 |
| | May | 700 | 1.41 | 0.48 | 0.92 | 163 | -10 | 153 |
| | Jun | 1610 | 3.03 | 0.09 | 2.94 | 353 | -2 | 351 |
| | Jul | 1409 | 2.72 | 0.41 | 2.32 | 317 | -9 | 308 |
| | Aug | 1937 | 2.90 | 0.12 | 2.78 | 337 | -2 | 335 |
| | Sep | 2083 | 2.82 | 0.36 | 2.46 | 328 | -8 | 320 |
| | Oct | 1719 | 3.26 | 0.86 | 2.40 | 378 | -18 | 360 |
| | Nov | 1040 | 1.85 | 0.57 | 1.28 | 215 | -12 | 203 |
| | Total | 10898 | 19.52 | 3.22 | 16.31 | 2269 | -68 | 2201 |

The electricity consumption by the dehumidifier, as shown in Table 3.2, was the total power consumption of the unit. The dehumidifier's exhaust fan was designed to run all the time, even when dehumidification was not needed, resulting in higher power consumption. In 2012, when dehumidification was not used, the power consumption by the dehumidifier's exhaust fan was 10%, 17%, and 76% of the total power consumption of the dehumidifier in September, October, and November, respectively. In 2013, the power consumption of the exhaust fan was about 3.5% of the total power consumption from June to October, while it was 19.5% of the total power consumption in November. The heat release, as shown in Table 3.2, was calculated only when the greenhouse heating system was on. The inside air temperature set point for the heating system was 20°C at night and 22°C during the day. A negative value of heat release indicates that the heat release by dehumidification was higher than the power consumption of the dehumidifier; thus, the dehumidifier released energy as heat into the greenhouse.

As shown in Table 3.2, the dehumidifier condensed more water during mild and cold seasons than during warm seasons, when the dehumidifier was running for shorter periods due to operation of the ventilation fans and roof vents. The dehumidifier ran mostly during the night in warm seasons. In cold seasons, the dehumidifier ran mostly during the day because of the high RH levels during the day and low RH levels at night. During mild seasons, even though the indoor RH was not very high, it was higher than the dehumidifier RH set point; therefore, the dehumidifier ran almost all day long and condensed more water.

The capital cost of the DCA3000T dehumidifier is $11,365. The estimated annual energy cost of the unit is $2,201, as shown in Table 3.2. The cost of repair and maintenance of the dehumidifier is estimated as $250 year$^{-1}$. Considering a 10-year payback period, the interest and depreciation are $1,545 year$^{-1}$. Therefore, the total annual cost is about $3,996. The annual cost of dehumidification was $4.7 m$^{-2}$, while the energy cost was $2.6 m$^{-2}$.

#### *3.5.2.3 Energy factors*

Table 3.3 lists the electricity energy factor ($EF_e$) and heat energy factor ($EF_h$) for the dehumidifier. The $EF_e$ and $EF_h$ were calculated only when dehumidification was used. The power consumed by the dehumidifier's exhaust fan when dehumidification was not used was excluded from the total power consumption. As shown in Table 3.3, the average energy factors of $EF_e$ and $EF_h$ were 2.06 and 0.82 in 2012, which were higher than in 2013. This means that the dehumidifier performed more efficiently in 2012 compared with its performance in 2013, which is also reflected in Table 3.2, as the dehumidifier collected more water in 2012 than in 2013. The main reason was that the performance of the dehumidifier was influenced by the indoor RH level: the higher the indoor RH level, the higher the water removal capacity. According to Table 3.1, the monthly average indoor RH was higher in 2012 than in 2013. As a result, the values of $EF_e$ and $EF_h$ were larger at night than during the day, and therefore more water was collected during the night.

**Table 3.3. Dehumidifier energy factors during the day and at night.**

| *Year (RH set point)* | *Season* | $EF_e$ | | | $EF_h$ | | |
|---|---|---|---|---|---|---|---|
| | | *Day* | *Night* | *Average* | *Day* | *Night* | *Average* |
| 2012 (68%) | Cold | 1.16 | 0.00[a] | 1.16 | 0.67 | 1.32 | 0.80 |
| | Mild | 1.01 | 3.22 | 2.02 | 0.59 | 0.98 | 0.77 |
| | Warm | 2.28 | 2.27 | 2.27 | 0.86 | 0.92 | 0.89 |
| | Average | 1.47 | 2.81 | 2.06 | 0.70 | 0.97 | 0.82 |
| 2013 (63%) | Cold | 0.83 | 1.75 | 1.26 | 0.53 | 0.72 | 0.62 |
| | Mild | 0.49 | 0.92 | 0.68 | 0.37 | 0.59 | 0.47 |
| | Warm | 0.91 | 1.00 | 0.97 | 0.57 | 0.61 | 0.60 |
| | Average | 0.78 | 1.08 | 0.95 | 0.51 | 0.62 | 0.57 |

[a] There was no water collection by the dehumidifier at night in November 2012; hence, $EF_e$ at night was zero.

Figure 3.6 shows the diurnal profiles of $EF_e$, $EF_h$, and indoor RH for the dehumidifier over a three-day period in 2013. The general trend of $EF_e$ and $EF_h$ was that they were high at night and low during the day, which followed the same trend as indoor RH. Overall, the DCA3000T

dehumidifier has higher water removal capacity and higher efficiency with higher indoor RH levels. This is also correlated with its higher energy factor at high RH. As shown in Table 3.3 and Figure 3.6, $EF_e$ and $EF_h$ had the same trend. In other words, they had a positive relationship with each other.

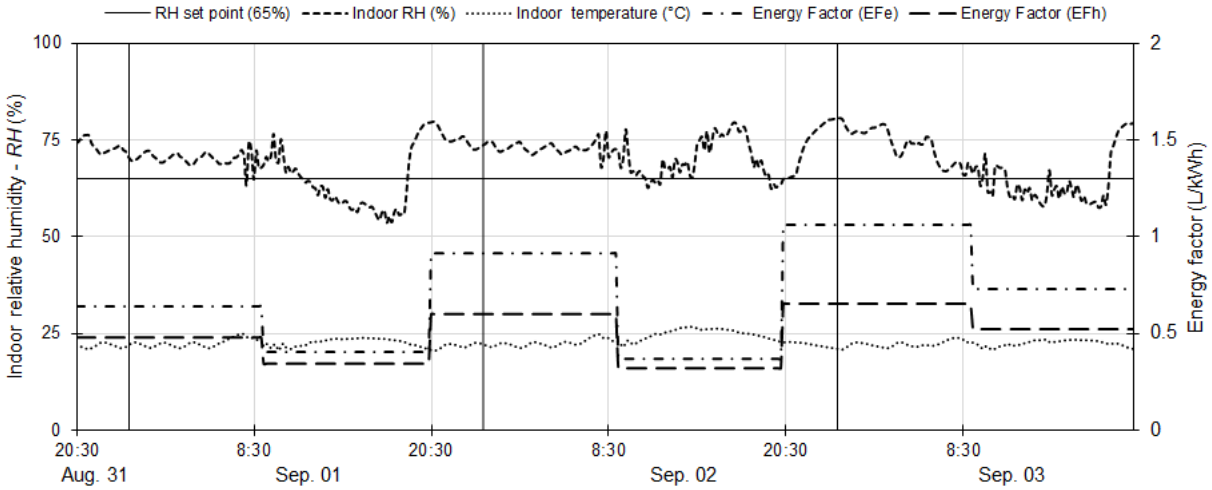


**Figure 3.6. Dehumidifier energy factors during August 31 to September 03, 2013.**

The cost of removing 1 L of water from the greenhouse was calculated based on the energy factors. Table 3.4 lists the electricity cost per liter of water removed from the greenhouse and the amount of heating cost saved due to the dehumidification heat release to the greenhouse when natural gas is used as the heating fuel. The last column in Table 3.4 is the ratio of the heating savings to the total electricity cost. In another word, 47.8% and 30.3% of the electricity cost in 2012 and 2013, respectively, were recovered by the heat released to the greenhouse.

**Table 3.4. Energy cost and savings during the dehumidifying process.**

| *Year (RH set point)* | *Season* | *$EF_e$* | | *$EF_h$* | | *Saving (%)* |
|---|---|---|---|---|---|---|
| | | *Average* | *Cost ($/L)* | *Average* | *Savings ($/L)* | |
| 2012 (68%) | Cold | 1.16 | 0.096 | 0.80 | 0.026 | 27.6 |
| | Mild | 2.02 | 0.055 | 0.77 | 0.027 | 50.0 |
| | Warm | 2.27 | 0.049 | 0.89 | 0.024 | 48.6 |
| | Average | 2.06 | 0.054 | 0.82 | 0.026 | 47.8 |
| 2013 (63%) | Cold | 1.26 | 0.092 | 0.62 | 0.034 | 36.9 |
| | Mild | 0.68 | 0.171 | 0.47 | 0.045 | 26.3 |
| | Warm | 0.97 | 0.119 | 0.60 | 0.035 | 29.7 |
| | Average | 0.95 | 0.122 | 0.57 | 0.037 | 30.3 |

### 3.5.3 Dehumidification benefits

As observed by the grower, before using the heat exchanger for dehumidification in 2011, more than 20% of the plants died each year due to high humidity, and this loss was as high as 45.1% in 2010. After the heat exchanger was installed in 2011, the loss rate was reduced to 7.2% in 2011. After installation of the DCA3000T dehumidifier in August 2012, only 0.9% and 3.2% of the plants died in 2012 and 2013, respectively.

Due to the low plant loss, the annual revenue in 2012 was increased by 12.5%, 14.6%, and 8.5% compared with that in 2009, 2010, and 2011, respectively. Even though the estimated annual cost of the dehumidifier is as high as $3,996, it was only about 2.6% of the total annual revenue in 2012. Compared with the annual revenue in 2009 to 2011, the increased revenue in 2012 was higher than the capital cost of the dehumidifier, which means that growers could achieve payback within one year. Therefore, commercial-grade dehumidifiers are recommended for humidity control in large greenhouses.

## 3.6 Conclusions

A commercial-grade dehumidifier was selected and installed in a northern greenhouse for humidity control. The experimental results showed that the dehumidifier controlled the indoor RH better than the previous heat exchanger due to its larger water removal capacity and year-round effectiveness, whereas the heat exchanger was not effective during warm seasons. The heating cost savings due to heat released by the dehumidifier accounted for 30.3% to 47.8% of the electricity cost of the dehumidifier; thus, the net electricity cost due to the implementation of the dehumidifier was significantly reduced. Considering a 10-year payback period, the annual cost of the dehumidifier is estimated at about $4,000. Even though the capital cost and annual cost of the dehumidifier were high, the plant loss rate was dramatically reduced from 43.3% in 2007 to 0.9% in 2013. The annual revenue in 2012 was also increased by 12.5%, 14.6%, and 8.5% compared with that in the previous three years when there was no dehumidification. The grower achieved equipment payback within one year.

The commercial dehumidifier controlled the greenhouse RH very well. The capital cost is one of the concerns when selecting an appropriate commercial dehumidifier for greenhouse humidity

control. High values of the electricity energy factor and heat energy factor are two critical factors, especially in cold regions where the heating season is long and the heating cost is high. Geared dehumidifiers or geared heat pump driers have higher moisture removal capacity. However, no geared commercial dehumidifier is available in the market yet. The application of a geared dehumidification system in greenhouses could be studied in the future.

# CHAPTER 4

# DEVELOPMENT OF A METHOD FOR CONDENSATION RATE MEASUREMENT ON FLAT SURFACES

(Accepted in *Information Processing in Agriculture* in June 2018).

Jingjing Han, Huiqing Guo

## Contribution of this paper to overall study

A method was developed for measurement of condensation rate on flat surfaces such as the inner surface of greenhouse covers. A commercially available leaf wetness sensor was calibrated in an environment chamber under different room temperature and RH conditions. A linear regression relationship was found between the sensor voltage output and the amount of condensate on the sensor surface, so this regression model can be used to convert the sensor voltage to condensation rate. This method was used to measure condensation rate on a greenhouse inner cover surface in Chapter 5. This chapter fulfills objective 5.

The manuscript presented in this chapter was accepted to publish in *Information Processing in Agriculture*. The experimental method development, lab measurement, data analyses, and manuscript writing were performed by the first author (PhD student - Ms Jingjing Han), and the manuscript was reviewed by the second author (supervisor – Prof. Huiqing Guo).

## 4.1 Abstract

Condensation on greenhouse interior surfaces plays an important role in reducing indoor air humidity. There is no standard method to measure condensation rate in greenhouses or in any other buildings. In this study, a commercially available leaf wetness sensor was calibrated in an environment chamber under different room temperature and RH conditions, which included five temperatures of 18, 20, 22, 24, and 26°C, and five RH levels of 40, 55, 65, 75, and 85%. The sensor surface temperature was maintained the same as the room temperature. Room temperature water was sprayed on the sensor surface, simulating condensate. The voltage output of the sensor changed due to varying amounts of condensate on the sensor surface. The amount of condensate on the sensor surface was divided into five groups from 0 to 0.5 g (or 0 to 0.015 g $cm^{-2}$ of sensor surface area) with an interval of 0.1 g. The statistical analysis showed that both sensor temperature and indoor RH had no significant effect on the sensor voltage output. The voltage output was positively correlated to the amount of condensate. A linear regression model was developed between the voltage output and the amount of condensate. This tool is considered as a breakthrough of technology for condensation rate measurement on greenhouse interior surfaces, or on any other surfaces with condensation. Anyone can use this sensor and the development relationship for measuring condensation rate as the sensor is not pricy and the method is easy to use, thus the method should be widely used as a standard method.

## 4.2 Nomenclature

| | | | |
|---|---|---|---|
| $C$ | amount of condensate, g | $T$ | temperature, °C |
| $CR$ | condensation rate, mg $cm^{-2}$ | $T_s$ | sensor surface temperature, °C |
| $LWS$ | leaf wetness sensor | $V$ | voltage output, mV |
| $R^2$ | coefficient of determination | **Subscripts** | |
| $RH$ | relative humidity, % | i | indoor |
| $RH_i$ | room relative humidity, % | s | sensor surface |
| $S.D.$ | standard deviation | | |

## 4.3 Introduction

Greenhouses provide a suitable environment to ensure crop yield and quality. However, relative humidity (RH) can easily reach a high level due to high plant transpiration and evaporation rates (Pieters et al., 1994). Dehumidification is often needed to keep the RH level in a suitable range. In order to determine dehumidification needs of greenhouses, we need to identify the two major moisture sinks. The first is condensation on the interior surface of a greenhouse, especially during the cold season, while the second is moisture removed by ventilation. The rate of moisture removal by condensation needs to be quantified in order to quantify requirements for mechanical dehumidifiers or other forced dehumidification measures.

There has been little research in the literature dealing with the measurement of condensation rates in greenhouses or any other facilities. Most of the relevant literature discussed the measurement of dew occurrence on plant surfaces and used devices such as mini-lysimeters (Richards, 1999), absorbent paper (Richards, 1999), and filter paper (Barradas and Glez-Medellín, 1999). However, there does not appear to be any information relating to estimating condensation rate.

Mini-gutter is a widely used method for condensation rate measurement in a greenhouse, which is located at the lower part of the greenhouse. However, the experiments conducted by Granados et al. (2011), and Seginer and Kantz (1986) reveal that too much work is involved in this method if accurate condensation rate measurement is required, which includes collecting roof water as well as wiping off the thin water film attached to the cover surface. The study conducted by Cemek and Demir (2005) had a similar problem, which used a stereobinoculer microscope to take photographs of the greenhouse sidewall and roof to determine the condensate characteristics, including area, volume, diameters, and the number of drops. Besides, the subject error exists when calculating the volume and counting the number of drops, which limits its application in greenhouses.

Besides the methods mentioned above, an electrical impedance grid was first introduced to measure dew duration in a study conducted by Pedro and Gillespie (1981). A very similar condensation sensor was made by placing parallel copper tracks on a horizontal plastic support as used by Rodríguez et al. (2008). The sensor was only used to predict the occurrence of condensation.

Montross et al. (2006) designed a low-cost condensation sensing system using a commercially available leaf wetness sensor. The experiment conducted in a greenhouse revealed that the system could accurately predict the occurrence of condensation. However, no further experiments were performed to measure the amount of condensation. De Freitas and Schmekal (2003) devised a home-made condensation sensor and used it to measure the condensation rate in a cave located in New Zealand. The sensor was made on a circuit board that consisted of copper wires. The action of the sensors considered the resistance changes when condensation occurred on the sensor surface, and then the relationship between the signal output and the weight of water on the board was then obtained to estimate the condensation rate. The researchers concluded that the measured condensation rate correlated well with the calculated condensation rate, which was defined as the humidity ratio difference between the cave air and the condensation surface multiplied by the combined convective water vapor transfer coefficient. This physical model can also be used to calculate the condensation rate on the inner surface of the greenhouse covering material. However, to do the calculation, the convection heat transfer coefficient between the indoor air and the cover surface must be known, which is difficult to determine inside a greenhouse. Due to the difficulty of determining the convection heat transfer coefficient in the physical model, this study focuses on the experiment measurement.

Inspired by De Freitas and Schmekal (2003) and Montross et al. (2006), the objective of this study was to find an easy way to measure the condensation rate on a surface by using a commercially available leaf wetness sensor (*LWS*). This sensor was calibrated in an environment chamber to establish the relationship between the sensor voltage output and the amount of condensate on the sensor surface, which can then be used to measure the condensation rate on any surface, including the target use in greenhouses.

## 4.4 Condensation Measurement

### 4.4.1 Leaf wetness sensor and experiment setup

An electronic leaf wetness sensor (Decagon Devices Inc., Pullman, WA, USA) has recently been widely used to detect dew duration on plant leaf surfaces. This sensor is 11.2 cm long, 5.8 cm wide, 0.65 mm thick, and is leaf-shaped, as illustrated in Figure 4.1. The surface area is 34 $cm^2$. The sensor has a wide operating temperature range between -20 to 60℃ and requires very little

power (2.5 V @ 2mA to 5.0 V @7 mA). It is made of fiberglass and can detect tiny amounts of water/ice on the sensor surface. It is covered in a white coating with a hydrophobic, waxy cuticle. In this way, moisture is detected once there is any present on the sensor surface.

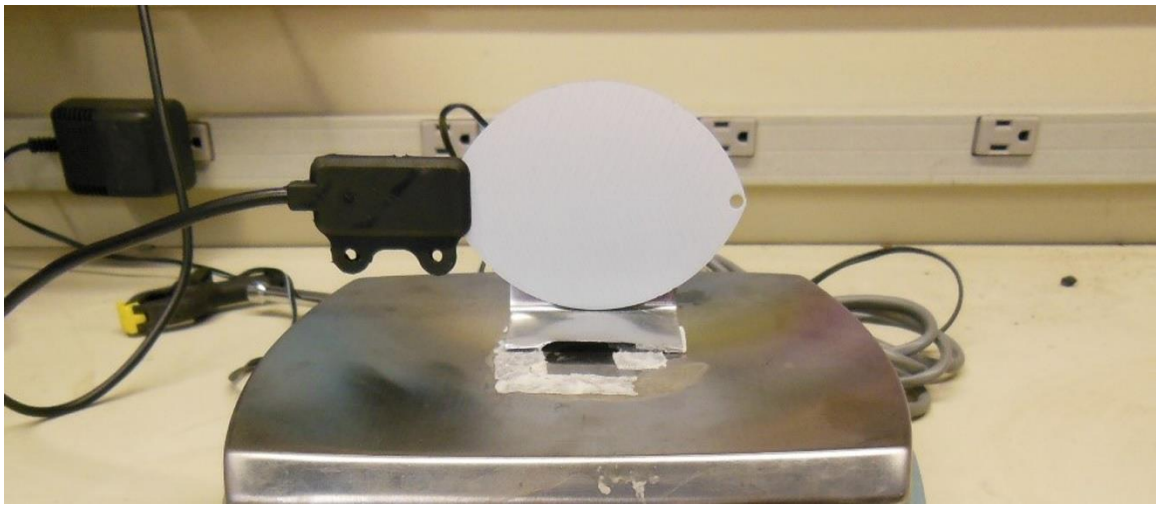

**Figure 4.1. Leaf wetness sensor.**

This sensor was calibrated in an environment control chamber. The initially chilled sensor surface was considered to simulate a lower surface temperature than the room temperature. It was abandoned due to two reasons. One was that it was very difficult to achieve and maintain a specific low sensor surface temperature for the test. The other reason was that the sensor voltage output at a specific time should be only determined by the amount of water on the sensor surface and the temperature of the water on the sensor surface. Over a period of time, the impact of heat and moisture exchange between the sensor and water with the surrounding environment such as air velocity, thermal radiation, the evaporation of water on the sensor surface will be reflected on the variation of the voltage output. Thus, in application in a greenhouse or any other places, the condensate and sensor surface temperature should determine the sensor voltage output,whereas the other factors' impact on the condensation and sensor voltage will be reflected by varying sensor temperature and voltage output measured. Because of these reasons, a simplified method was adopted by maintaining the sensor and a bottle of distilled water in the chamber to achieve the room temperature. The water sprayed on the sensor surface to mimic condensate, the sensor voltage output and the amount of condensate were then measured, and the relationship of these two parameters was finally analyzed. The impact of sensor surface temperature and indoor RH on the sensor voltage output were tested.

In the laboratory, the sensor was connected to a multimeter to measure the voltage output in millivolts (mV) (Figure 4.2). A scale (Adventurer Pro AV812, Chaus Corporation, Pine Brook, NJ, USA) with a resolution of 0.01 g and an accuracy of ±0.02 g was used to measure the mass of the sensor before and after water was sprayed on its surface. To begin, the sensor was dry. Very fine drops of water were sprayed on the sensor surface with an atomizer. When the water was sprayed on the sensor surface, the voltage output changed. Both the net mass of the water and the voltage output were recorded. Before spraying water again for the next measurement, the sensor surface was wiped dry. This process was repeated several times. Each time, more water was sprayed on the sensor until there were water droplets dripping from its surface.

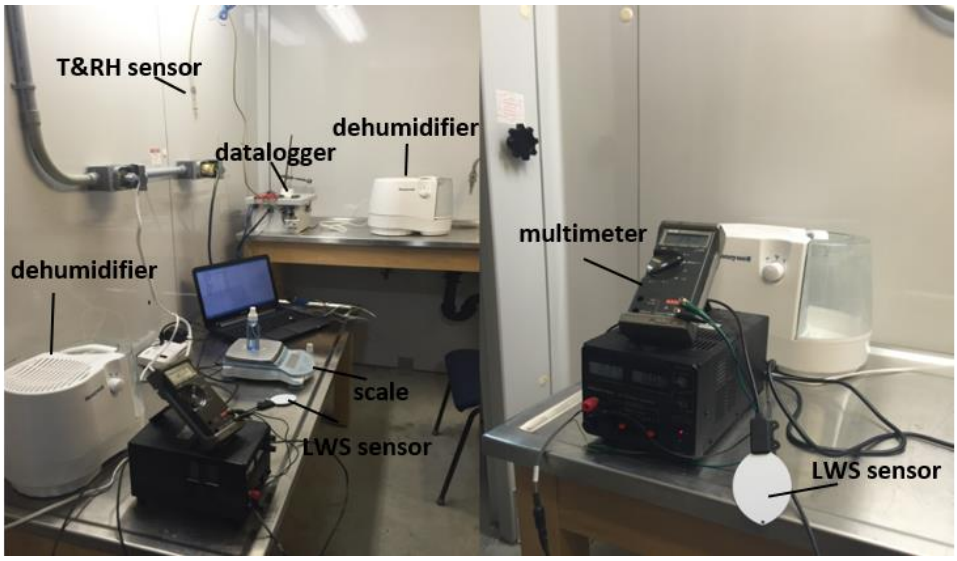


**Figure 4.2. Equipment setup for the leaf wetness sensor calibration.**

The sensor surface temperature and the temperature of the water used to spray on the sensor surface were the same as the chamber room temperature as they were placed in the chamber till they reach the room temperature. The amount of water sprayed on the surface was considered to have no effect on the sensor surface temperature as the measurement after each spray was taken place immediately so the evaporation could be neglected as well as the evaporation caused cooling.

Besides room temperature and RH, there are other factors may affect condensation and sensor reading such as thermal radiation, air movement, and dust on the sensor surface. There was no thermal radiation source other than the fluorescent lights and their impact on the sensor surface was negligible. There was no active air movement in the chamber during the measurement, therefore, the influence of the air velocity on the sensor surface was also negligible. This applies

to most residential and commercial buildings where indoor thermal radiation and air velocity are both low; however, if the sensor is used in rooms with significant thermal radiation or air movement, the effects of air velocity and solar radiation on condensation rates should be taken into consideration. For example, in greenhouses during cold seasons when condensation occurs, the greenhouse cover surface air speed is very low thus the results of this study can be used. Once the greenhouse is in ventilation cooling mode, then the indoor air velocity impact may not be negligible. Including air velocity impact on condensation will be future research work.

Preliminary testing was conducted to see the effects of dust on the sensor surface in the laboratory, which showed that voltage output would decrease if there was any dust on the sensor surface. The sensor surface was cleaned to make sure there was no dust before each test so the sensitivity of the sensor to surface dust accumulation was excluded in this study. However, when applying the sensor in field measurement, the sensor surface may need to be cleaned periodically to make sure no visible dust on the surface.

### 4.4.2 Experiment design

#### *4.4.2.1 Angle impact test*

To simplify the experiment, the impact of the sensor angle was first tested inside the environment control chamber with the room temperature varying from 18 to 28°C and RH varying from 35 to 85%. The air temperature and RH inside the chamber were measured with a CS500 temperature and relative humidity probe (Campbell Scientific Inc., Edmonton, AB, Canada). The probe had an accuracy of ±0.2 to ±1.4°C with the temperature measurement range of -40 to 60°C, and ±3% over the range of 10% to 90% and ±6% in the range of 90% to 100% with RH measurement.

Three different angles between the sensor and the horizontal surface of 30°, 60°, and 90° were tested. To do so, the sensor was glued on a metal plate to form the desired angle with the sensor surface facing down (Figure 4.3). The sensor was tested under four room temperatures of 18, 21.5, 25, and 28.5 °C, and four levels of room RH of 40%, 55%, 65% and 80%. For each angle, the condensate amount was ranged from 0 to 0.50 g before dripping occurred. The condensate amount was grouped into 5 levels, with an interval of 0.1 g. For each condensate amount group under each angle, the measurement was repeated at least twice. Based on the measurement results, the software

SPSS 22 (Statistical Package for the Social Sciences, SPSS Inc. and IBM Company, Chicago, IL, USA) was used to do the statistical analysis.

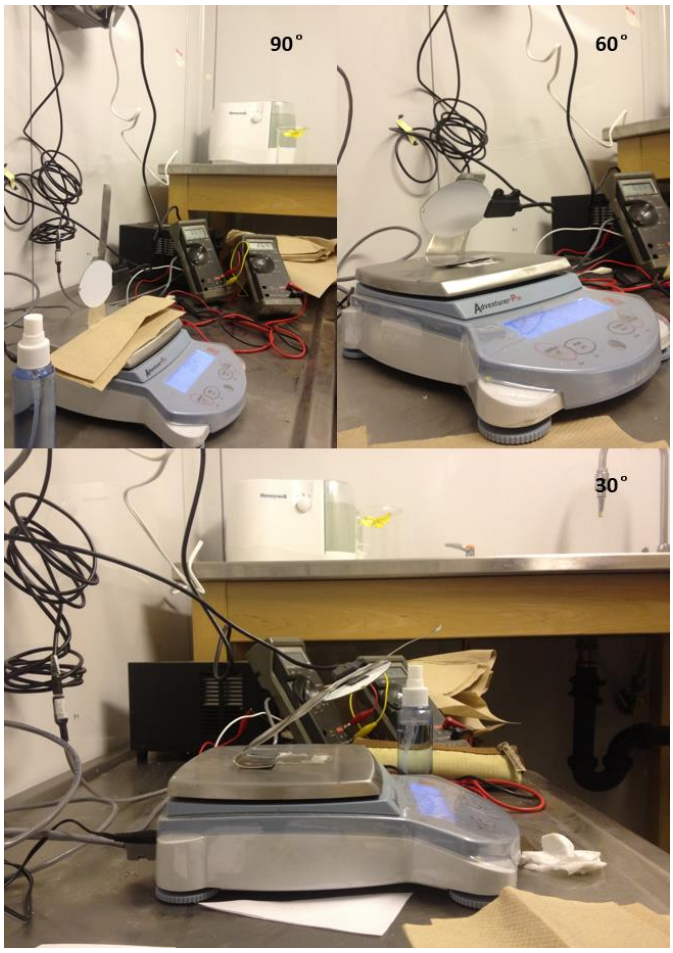


**Figure 4.3. Test of the leaf wetness sensor at different angles.**

As shown in Figure 4.4, the relationship between the voltage output and the amount of condensate on the sensor surface were plotted under different angles. The voltage output had a significant linear relationship with the amount of condensate on the sensor surface with high $R^2$ values (greater than 0.87) under all three sensor angles.

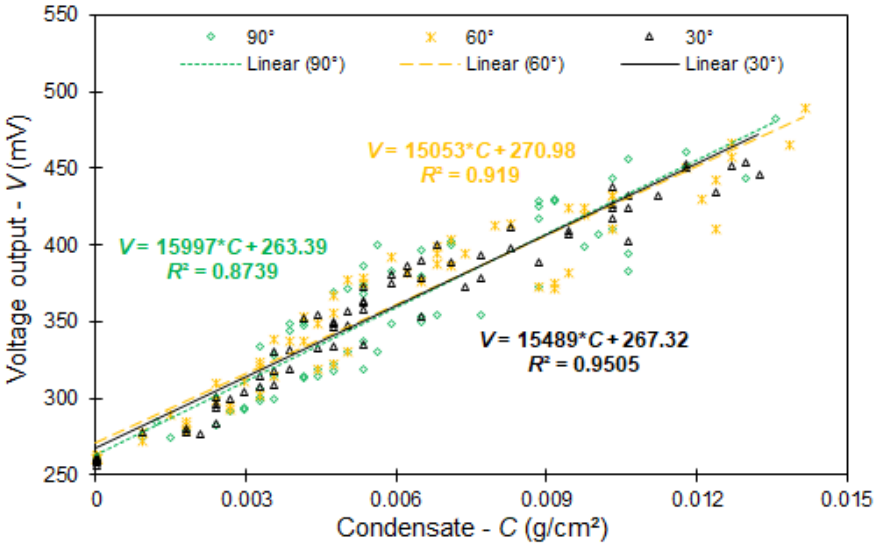


**Figure 4.4. Condensate results at different room temperature and relative humidity (the sensor surface facing down with angles of 90°, 60°, and 30°).**

Table 4.1 also compares voltage outputs and the amount of condensate at the angles. As the sensor angle was increased from 30° to 60°, there was no significant difference in voltage output or in condensate ($P > 0.05$). Figure 4.4 also shows the same results with the three plotted lines almost overlapping. There was also no significant difference in voltage output or in the amount of condensate when the sensor angle was increased from 30° to 90° or 60° to 90° ($P > 0.05$).

**Table 4.1. Multiple comparisons for voltage output (*V*) at three different sensor angles (30°, 60°, and 90°).**

| *Dependent* | *(I) Angle* | *(J) Angle* | *Mean Difference (I-J)* | *Std. Error* | *P* |
|---|---|---|---|---|---|
| Voltage (*V*) | 30 | 60 | -2.4 | 10.4 | 0.972 |
| | | 90 | 6.8 | 10.2 | 0.781 |
| | 60 | 90 | 9.2 | 10.4 | 0.652 |
| Condensate (*C*) | 30 | 60 | -0.09 | 0.21 | 0.907 |
| | | 90 | 0.12 | 0.21 | 0.819 |
| | 60 | 90 | 0.21 | 0.21 | 0.572 |

Table 4.2 shows the one-way ANOVA analysis results when the sensor angle was set as the only independent factor. The voltage output and the amount of condensate on the sensor surface were both set as dependent variables. As shown in Table 4.2, the sensor angle had no significant impact either on the voltage output or on the amount of condensate (both $P > 0.05$).

**Table 4.2. One-way ANOVA results of voltage output (*V*) and amount of condensate (*C*) as affected by the sensor angles.**

| *Dependent* | | *Sum of Squares* | *df* | *Mean Square* | *F* | *P* |
|---|---|---|---|---|---|---|
| Voltage (*V*) | Between group | 3060 | 2 | 1530 | 0.426 | 0.654 |
| | Within group | 718685 | 200 | 3593 | | |
| | Total | 721745 | 202 | | | |
| Condensate (*C*) | Between group | 1.5 | 2 | 0.76 | 0.517 | 0.597 |
| | Within group | 294.2 | 200 | 1.47 | | |
| | Total | 295.7 | 202 | | | |

In summary, the sensor angle had no significant influence either on voltage output or on the amount of condensate on the sensor surface if no dripping occurred; therefore, the following calibration procedure of the *LWS* only considers the variables of indoor air temperature (i.e. sensor surface temperature) and RH.

#### *4.4.2.2 Calibration design*

Considering the main application of this sensor will be in greenhouses to measure the condensation rate on the inner cover surface, even though the sensor surface temperature would reach up to higher than 30°C, there would be no condensation occurrence at such high temperature. Considering the normal temperature and RH ranges of greenhouses, the sensor was calibrated under five different surface temperature levels of 18, 20, 22, 24, and 26°C, which was taken the same as the room air temperature, and five different RH levels of 40, 55, 65, 75, and 85%. The amount of water manually sprayed on the sensor surface was not easy to control, although efforts were made to try to spray the same amount of water on the sensor surface for replication purpose at a specific condensation rate, the amount of water sprayed still varied around the target level. Additionally, the interaction effect among the variables on the voltage output needed to be tested via the ANOVA analysis. Therefore, the amount of condensate on the sensor surface was divided into five groups or levels from 0 to 0.5 g (i.e. 0 to 0.015 g per square centimeter of sensor surface area), with an interval of 0.1 g. All tests were conducted in the same environment control chamber and each treatment was repeated three to five times.

## 4.5 Results and Discussion

### 4.5.1 Calibration results

Figure 4.5 shows the results of the voltage output under each condition. Each data point in the graph represents the mean value for each condensation group under the test temperature and RH condition. The more condensate on the sensor surface, the higher the voltage output at the same surface temperature and RH. The relationship between the voltage output and the amount of condensate on the sensor surface was positively correlated. With the same indoor RH and condensate level, the voltage output as affected by room temperature did not show any pattern as shown in Figure 4.5, but it had the highest values at the sensor temperature of 20°C for most of the conditions.

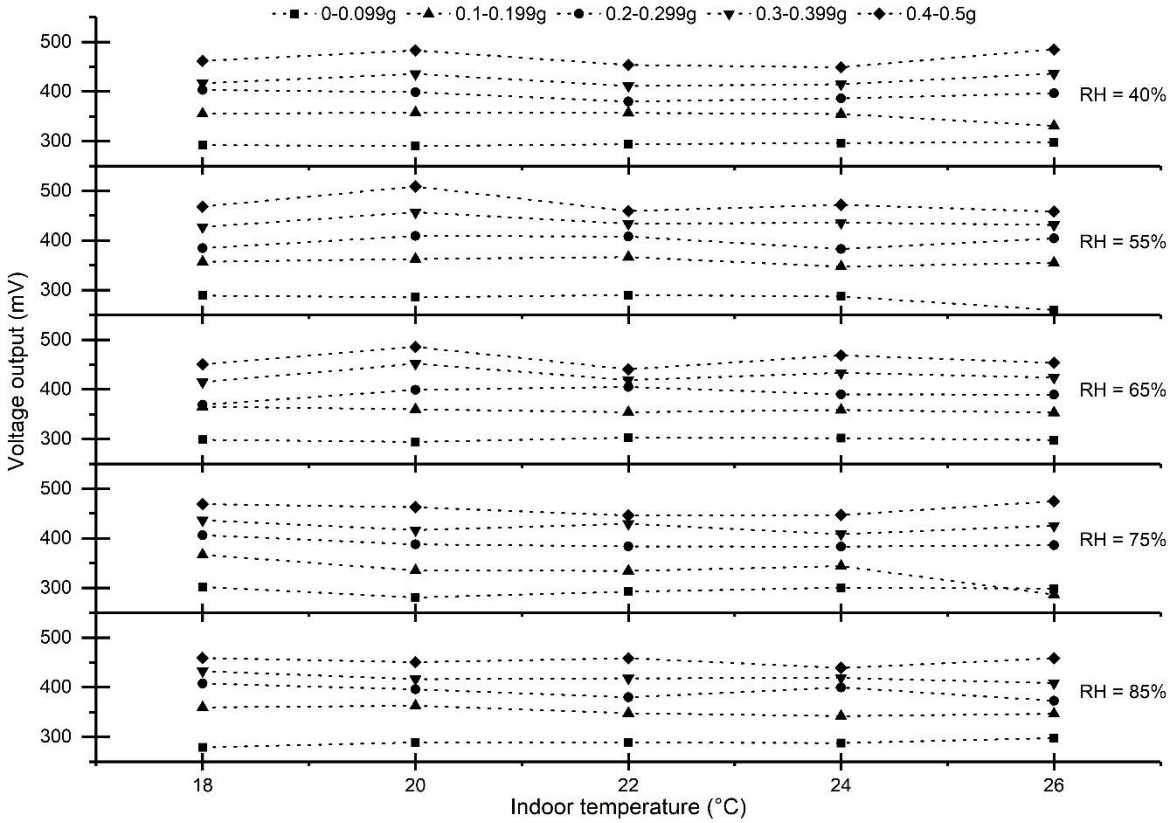


**Figure 4.5. Voltage outputs under different room conditions and condensate levels.**

Figure 4.6 gives the average voltage output for each condensate level under the same sensor temperature (Figure 4.6.a) and indoor RH (Figure 4.6.b), respectively. The voltage output increased as the amount of condensate on the sensor surface increased either at the same sensor temperature

or at the same indoor RH. When the sensor temperature was at 20°C, the voltage output had the highest value for each condensate level amongst all other temperatures if the condensate was greater than 0.2 g as shown in Figure 4.6.a. Besides 20°C, there was no pattern of voltage change affected by temperature. Figure 4.6.b illustrates that the voltage output was the highest at 55% RH when the amount of condensate was greater than 0.1 g, while the lowest voltage output occurred at higher RH levels of 75% and 85%.

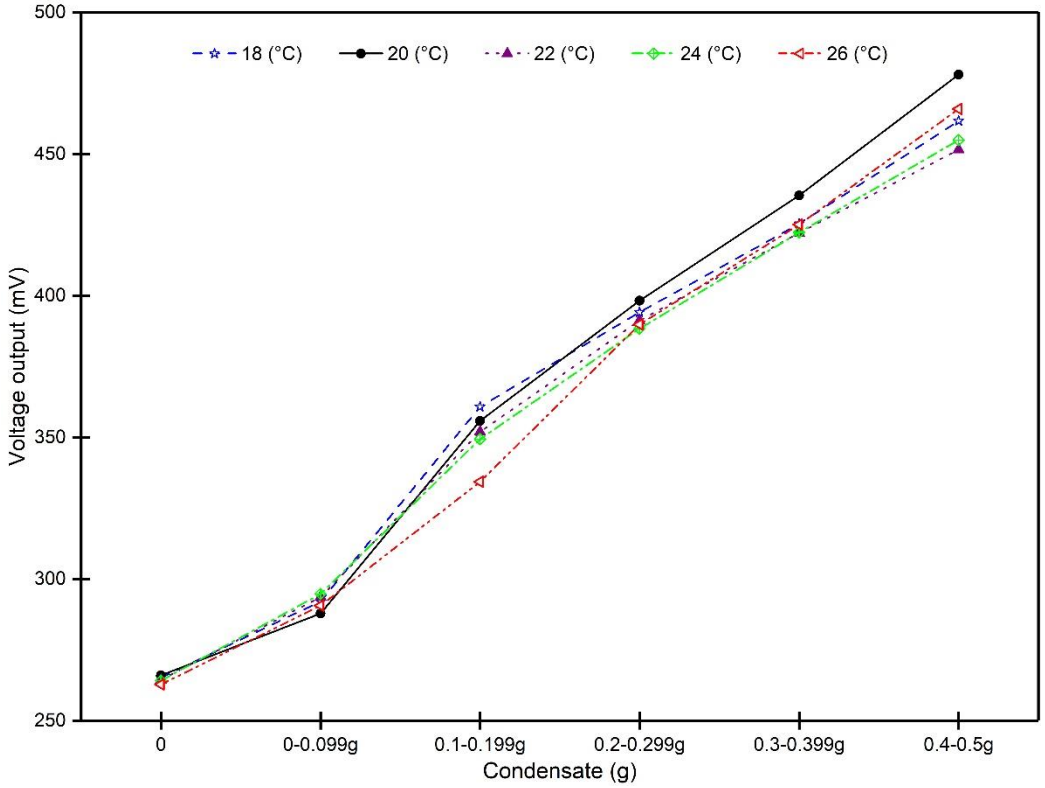


(a)

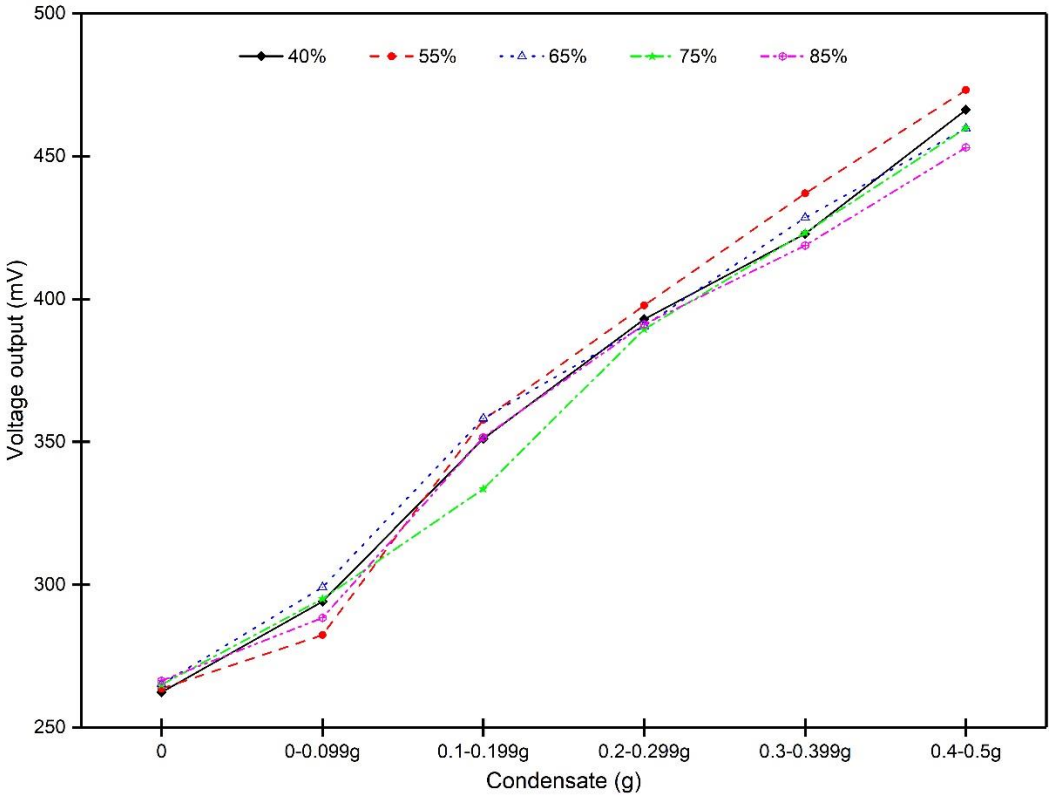


(b)

**Figure 4.6. Average voltage output values: (a) at the same temperature (°C); (b) at the same relative humidity (%).**

Table 4.3 shows the average voltage output and standard deviation at each condensate level under all testing temperatures or RH levels. There was not a substantial fluctuation among the voltage outputs at different temperature and RH levels; the standard deviation values were very low compared with the average voltage output values.

**Table 4.3. Average voltage output (*V*) and standard deviation.**

| *Condensate Group (g)* | *Temperature* | | *RH* | |
|---|---|---|---|---|
| | *V (mV)* | *S.D. (mV)* | *V (mV)* | *S.D. (mV)* |
| 0 – 0.099 | 291.8 | 2.7 | 291.8 | 6.5 |
| 0.1 – 0.199 | 350.4 | 10.0 | 350.4 | 10.0 |
| 0.2 – 0.299 | 392.4 | 3.9 | 392.4 | 3.3 |
| 0.3 – 0.399 | 426.1 | 5.4 | 426.1 | 7.0 |
| 0.4 – 0.5 | 462.4 | 10.4 | 462.4 | 7.6 |

Note: S.D. means standard deviation.

### 4.5.2 Statistical analysis and modeling

Three parameters (i.e., sensor temperature, room RH, and the amount of condensate on the sensor surface) were tested in the lab and a three-way ANOVA was used to determine whether there was any interaction effect among the three variables on voltage output. Table 4.4 shows the ANOVA results. Only the amount of condensate on the sensor surface had a significant effect on sensor voltage output ($P < 0.05$). Room RH and sensor temperature did not have significant impact on sensor voltage output ($P > 0.05$) and there was no significant interaction effect among the three variables on voltage output ($P > 0.05$). This result means the voltage is solely determined by the condensate mass on the sensor surface while the condensate mass is determined by the sensor surface temperature and air RH.

**Table 4.4. Three-way ANOVA results for voltage as affected by the three variables (temperature - $T_s$, $RH$, and condensate mass - $C$).**

| *Source of Variation* | *df* | *MS* | *F* | *P* |
|---|---|---|---|---|
| Sensor temperature ($T_s$) | 4 | 500 | 1.189 | 0.315 |
| Room RH ($RH_i$) | 4 | 772 | 1.834 | 0.122 |
| Condensate ($C$) | 4 | 263457 | 625.683 | 0.000 |
| $T_s \times C$ | 16 | 332 | 0.789 | 0.698 |
| $RH_i \times C$ | 15 | 219 | 0.520 | 0.930 |
| $T_s \times RH_i$ | 16 | 496 | 1.179 | 0.283 |
| $T_s \times RH_i \times C$ | 52 | 301 | 0.715 | 0.929 |
| Error | 326 | 421 | | |
| Total | 438 | | | |

Both a multiple linear regression and second-order polynomial regression were conducted to model the relationship between the independent variables and the voltage output. Even though the $R^2$ value of the polynomial regression model of 0.926 was slightly higher than that for the linear regression model of 0.908 (voltage vs. condensate), to reduce the complexity of the model, the linear regression model was selected for statistical modeling. Table 4.5 gives the regression results, which used all the original data. Future data can be used to verify this model.

**Table 4.5. Linear regression results for statistical modeling (*P* values in brackets).**

| *Dependent Variable* | *Model* | $R^2$ | *Constant* | *Coefficients (P value)* | |
|---|---|---|---|---|---|
| | | | | *C (g)* | $T_s$ *(°C)* |
| Voltage Output (mV) | 1 | 0.910 | 301.4 (0.000) | 403.3 (0.000) | -0.794 (0.005) |
| | 2 | 0.908 | 283.8 (0.000) | 402.9 (0.000) | N/A |

The room RH was excluded from the regression models due to its insignificant effect on voltage output. Model 1 includes both sensor temperature and condensate and the $R^2$ value for the prediction model is 0.910. Model 2 only includes the variable of condensate with $R^2$ being 0.908, almost the same as in Model 1. Thus, Model 2 was selected for use in application of this method. As discussed previously, this final model does not directly include surface temperature and room RH but their effects are indirectly involved as the quantity of the condensate is determined by the surface temperature and room RH. Hence, only voltage needs to be measured and there is no need to use these two parameters and other parameters in calculating *CR*. The coefficient value indicates that the amount of condensate on the sensor surface positively correlates to voltage output. Model 2 for the voltage output *V* (mV) can be calculated by condensate *C* (g) as:

$$V = 283.8 + 402.9 \times C \qquad (4.1).$$

The data recorded inside the greenhouse is the *LWS* sensor voltage output. As the amount of water condensing on the sensor is what the experiment tried to measure, Equation 4.2 was obtained from Equation 4.1 to predict the amount of water condensing on the sensor surface with a known voltage output. Equation 4.3 was obtained from Equation 4.2 to predict condensation rate (*CR*) in mg $cm^{-2}$ of the sensor surface.

$$C = 0.0025 \times V - 0.70 \qquad (4.2),$$

$$CR = 0.073 \times V - 20.72 \qquad (4.3).$$

Equations 4.2 and 4.3 will be used in the field experiment to measure the amount of condensate on the greenhouse inner covering materials and can be used for any other applications or similar experiments as well.

## 4.6 Conclusions

A commercial leaf wetness sensor was calibrated in an environment chamber in order to measure the condensation rate inside a greenhouse. Three different angles between the sensor and a horizontal surface of 30°, 60°, and 90° were tested. It was concluded that the sensor angle had no significant effect on the voltage; therefore, it was removed from the list of variables impacting voltage. The sensor was then tested under various conditions, which included: five different surface temperatures of 18, 20, 22, 24, and 26°C (which was taken the same as the air temperature), and five different RH levels of 40, 55, 65, 75, and 85%. The amount of condensate on the sensor surface was also divided into five groups from 0 to 0.5 g (0 to 0.015 g $cm^{-2}$) with an interval of 0.1 g.

The measured results showed that the voltage output was positively correlated to the amount of condensate no matter what the room RH or the sensor temperature was. Based on the statistical analysis, there was no significant effect of sensor temperature or RH on sensor voltage, and there were no interaction effects from the sensor temperature, RH, and the amount of condensate on the voltage. Only the amount of condensate proved to have a significant influence on voltage output. A positive relationship exists between the voltage output and the amount of condensate on the sensor surface. A linear regression model to predict the condensation rate using only sensor voltage was developed ($R^2$ = 0.908). This calibrated leaf wetness sensor can be used to measure any surface condensation rate. For future work, a wider sensor surface temperature and room conditions should be explored to mimic a cold surface condensation in a room conditions as the greenhouse cover surface temperature may go much lower than the room temperature. In future studies, the leaf wetness sensor will be installed inside a tomato greenhouse and the linear regression model will be applied to estimate the condensation rate on the inner covering surface.

This study is considered as a breakthrough of technology for quantifying condensate, providing a critical tool in quantifying condensation rate on greenhouse inner surface cover which is the major moisture sink in greenhouse. With this tool, the development of greenhouse air moisture balance model and water balance model will be possible. This will allow accurate calculation of dehumidification capacity determination for greenhouse moisture control. Anyone can use this sensor and the development relationship for measuring condensation rate as the sensor is not pricy and the method is easy to use, thus the method should be widely used as a standard method.

# CHAPTER 5

# MEASUREMENT AND MODELLING OF CONDENSATION ON GREENHOUSE COVER: PART I CONDENSATION MEASUREMENT

(Submitted to *Biosystems Engineering* in April 2018)

Jingjing Han, Huiqing Guo, Robert Brad

## Contribution of this paper to overall study

Very little research has been reported on quantifying condensation rate on greenhouse inner covers. In this Chapter, the method developed in Chapter 4 for measuring condensation rates in a building like a greenhouse was applied to measure condensation rate in a tomato greenhouse for one growing season of eight months. Three leaf wetness sensors were installed in the greenhouse. By monitoring the voltage output of the sensors, the condensation rate was calculated based on the linear regression model developed in Chapter 4. The results indicated that condensation mainly occurred during the nighttime and early morning. The cover surface mainly acted as a moisture sink during the nighttime and a moisture source during the daytime to the moisture balance of the greenhouse air. This chapter fulfills objective 6.

The manuscript included in this chapter was submitted to *Biosystems Engineering*. The first author (PhD student – Ms Jingjing Han) conducted the experiment, analyzed the experimental data and wrote the manuscript. The second author (supervisor - Prof. Huiqing Guo) reviewed the manuscript. The third author (Mr. Robert Brad) helped with the experimental setup.

## 5.1 Abstract

Understanding the moisture sources and sinks is essential to manage the indoor relative humidity for the plants. This study focuses on applying a new method that uses a calibrated leaf wetness sensor to measure the condensation rate on the greenhouse inner cover surface. Three sensors were installed in a tomato greenhouse to measure the condensation rate on the interior surface of air-inflated double layer plastic film. The experiment was conducted for eight months from April to November. The results revealed that condensation mainly occurred during the nighttime and early morning when there was weak or no solar radiation. The plastic film mainly acted as a moisture sink during the nighttime and a moisture source during the daytime to the moisture balance of the greenhouse air. The hourly average condensation rate during the nighttime in each month varied from the lowest of 0.5 g $h^{-1}$ per square meter of greenhouse floor area in November to the highest of 19.0 g $h^{-1}$ per square meter of greenhouse floor area in May. The average condensation rate during the nighttime in the eight months was around 9.5 g $m^{-2}$ $h^{-1}$ or 88.6 g $m^{-2}$ $d^{-1}$. As measured in the greenhouse, there was around 21,362 liters of water or 25.3 L $m^{-2}$ of greenhouse floor area condensed on the greenhouse inner cover surface over the eight months period at night. A statistical model will be developed in the future to predict condensation rate based on the greenhouse plant condition and indoor and outdoor environment conditions.

## 5.2 Nomenclature

| | | | |
|---|---|---|---|
| $C$ | amount of condensate, g | $T_c$ | cover inner surface temperature, °C |
| $CR$ | condensation rate, g $m^{-2}$ $h^{-1}$ | $T_{dp}$ | indoor air dew point temperature, °C |
| $LWS$ | leaf wetness sensor | $\Delta T$ | temperature correct factor, °C |
| $RH$ | relative humidity, % | $V$ | leaf wetness sensor voltage output, mV |
| $S_i$ | solar radiation getting into the greenhouse, W $m^{-2}$ | | |

## 5.3 Introduction

Condensation on the inner surface of the greenhouse cover has long been a serious problem in greenhouses. Not only can the condensation lead to plant disease or discomfort for greenhouse workers, it can also contribute up to 20% of the total nighttime heat loss in a double-layer plastic

film greenhouse during cold weather conditions when supplemental heating is needed (Silveston et al., 1980; Pieters et al., 1994). In addition, it limits light transmittance and solar radiation. Therefore, avoiding condensation is important, especially in a cold region like Canada, where the heating season is very long and even during summer nights heating is required in greenhouses.

There is no well-accepted method for measuring condensation rates in a building like a greenhouse. In Cemek and Demir's research (2005), the sidewall and roof of a greenhouse were photographed, then the characteristics of condensation on the sidewall and roof, including area, volume, diameter, and the number of the condensation drops, were determined by a stereobinocular microscope. Nevertheless, it was a rough way to measure condensation rate on a greenhouse roof and sidewall. In addition, the water condensation on the inner surface of the covering materials is greatly affected by the solar radiation which changes with time. Not only this method is complicated and time-consuming, yet subject to large uncertainty. The potentially subjective error when counting the number of the drops and calculating their volume also limits the application in greenhouses.

A mini-gutter that is usually attached to the lower part of the greenhouse is the most common method used for collecting the condensate water from the greenhouse roof. Granados et al. (2011) applied this method to measure condensation flux in a glasshouse. Hourly value of condensation flux measured was from 0 to 15.6 g $m^{-2}$ $h^{-1}$, with the average value of 1.8 g $m^{-2}$ $h^{-1}$, while the daily value could reach up to 147 g $m^{-2}$ $d^{-1}$ in February inside the glasshouse. However, the problem with this study is that the water dripping off from the inner surface of the covering material and the thin film of water left attached to the inside cover surface were not taken into consideration. Therefore, the condensation rate measured was underestimated compared with the actual rate. Seginer and Kantz (1986) took both conditions into consideration. They measured condensation flux using mini-gutter in a very small greenhouse (4 × 5 m) covered by a single polyethylene sheet in Israel which varied from 3.6 to 25.2 g $m^{-2}$ $h^{-1}$; however, too much work was involved in this method, including collecting the water dripping off from the roof and wiping off the thin water film left attached to the inside cover surface, making it impractical in a large commercial greenhouse. Another problem with this method is the mini-gutter causing light interception. Therefore, a more simple and practical method should be developed for condensation flux measurement inside a greenhouse.

To solve the problems mentioned above, the researchers of this study developed a simple and reliable method by using a commercially available leaf wetness sensor (*LWS*) to measure condensation rate (Chapter 4). The sensor is leaf-shaped and made of fiberglass. Its surface is very sensitive to moisture. Tiny amounts of water/ice on the surface can be detected with different amounts of voltage output. Considering the greenhouse indoor environment condition, the sensor was calibrated in a climate-controlled chamber with five temperature levels of 18, 20, 22, 24, and 26°C, and five RH levels of 40, 55, 65, 75, and 85%. The amount of water sprayed on the sensor surface was recorded as well as the voltage output. Three different angles between the sensor and a horizontal surface of 30°, 60°, and 90° were tested as well. The results showed that sensor angle has no influence on the voltage. There are also no significant effect of room temperature or RH on the sensor voltage. The voltage output (mV) has a positively linear relationship with the amount of condensate (g) on the sensor surface ($R^2$ = 0.908). Compared with the home-made condensation sensor developed by De Freitas and Schmekal (2003), this method saves both time and effort.

Equipped with this method, the objective of this research was to apply this calibrated leaf wetness sensor to measure the condensation rate on a greenhouse inner cover surface in order to quantify the condensation rate and occurrence profiles in a cold region in Canada.

## 5.4 Materials and Methods

### 5.4.1 Experimental greenhouse

The experimental greenhouse was located in Grandora, Saskatchewan, 23 km west of Saskatoon, at 52.09$^o$ latitude, -107.03$^o$ longitude and 504 m elevation. It was a three-span commercial greenhouse covered by air-inflated double layer 6-mil polyethylene plastic film on the roof and polycarbonate panels on the side walls, except for the north wall, which was an insulated wood-frame wall. The greenhouse was 19.2 m wide and 43.9 m long. The eave height was 4.3 m and the ridge height was 6.7 m (Figure 5.1). Tomato plants were planted in peat-based growing medium bags in 11 rows with a total of 2,100 plants, averaging 2.5 plants per square meter. The greenhouse was heated with hydronic heating system and the water pipes were located above the ground between rows of tomato plants. Four natural gas boilers were used to heat the water. The greenhouse had three exhaust fans (FC050-4E exhaust fan, ZIEHL-ABEGG, Sainte-Claire, QC, Canada) placed in the east wall at a height of 3.8 m. Each exhaust fan had a diameter of 0.548 m

and a capacity of 2.1 $m^3$ $s^{-1}$ at a static pressure of 20 Pa (Axial Fans, 2012). There were also roof vents for cooling. These fans were turned on only when the indoor temperature was above 24°C and turned off when the temperature was reduced to 22°C during the spring, summer, and fall seasons, and they were sealed during the winter season to minimize infiltration. A drip irrigation system was used to supply water and nutrients. The floor was covered by landscaping fabric, with soil underneath.

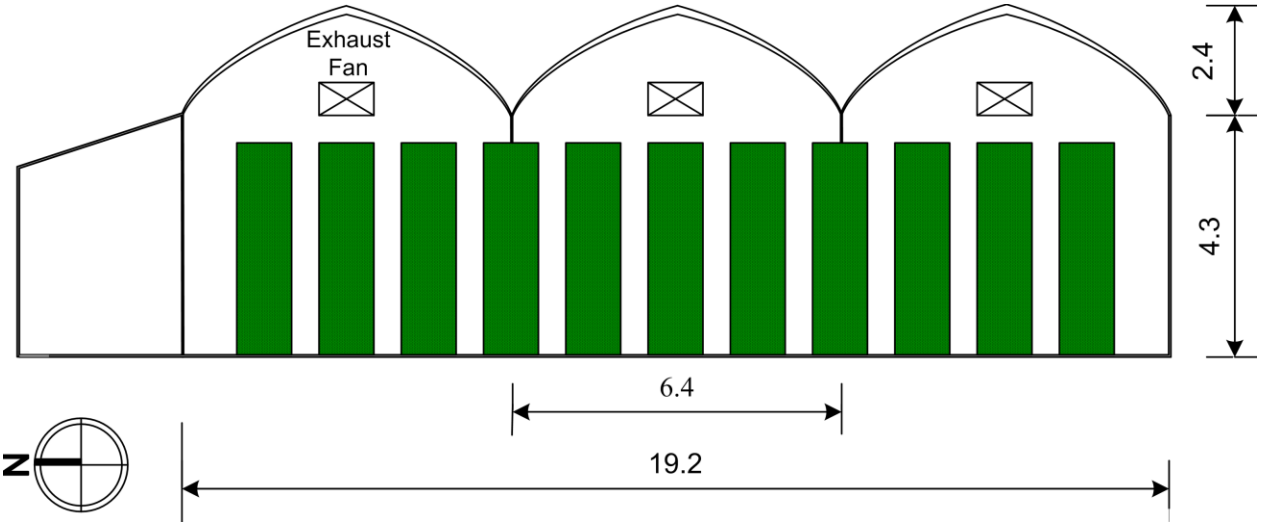


**Figure 5.1. Sketch of the greenhouse cross section (unit: m).**

### 5.4.2 Experimental instrument setup

In this experiment, three leaf wetness sensors (Decagon Devices Inc., Pullman, WA, USA) were installed in the greenhouse with one placed on the first span and two located on the second span (Figure 5.2). There were no sensors installed on the third span as at the time of instrument installation, its roof cover was being replaced. The sensors were installed close to the eave at the east end of the greenhouse. Two air velocity transducers (TSI Model 8475, Minneapolis, MN, USA) with the measuring range of 0 to 0.5 m $s^{-1}$ were installed at the same locations as the leaf wetness sensors: one at the first span and the other one at the second span. T-type thermocouples were used to measure the sensor and greenhouse cover surface temperatures, which were adhered directly to the sensor and greenhouse cover surface. Because the thermocouple was exposed to the sunlight directly, a temperature correction factor ($\Delta T$) for 0.3 mm in diameter is used, which is calculated from (Abdel-Ghany et al., 2006):

$$\Delta T = -0.22 + 5.11 \times (1.0 - \exp(-0.0024 \times S_i)) \quad R^2 = 0.94 \qquad (5.1),$$

where $\Delta T$ is the correct factor for the temperature measuring by exposing the thermocouple directly to the sunlight, in °C; $S_i$ is the solar radiation getting into the greenhouse which was measured in this study, in W $m^{-2}$. The actual cover temperature is obtained by subtracting $\Delta T$ from the value of the temperature measured directly by the thermocouple exposed to the solar radiation flux.

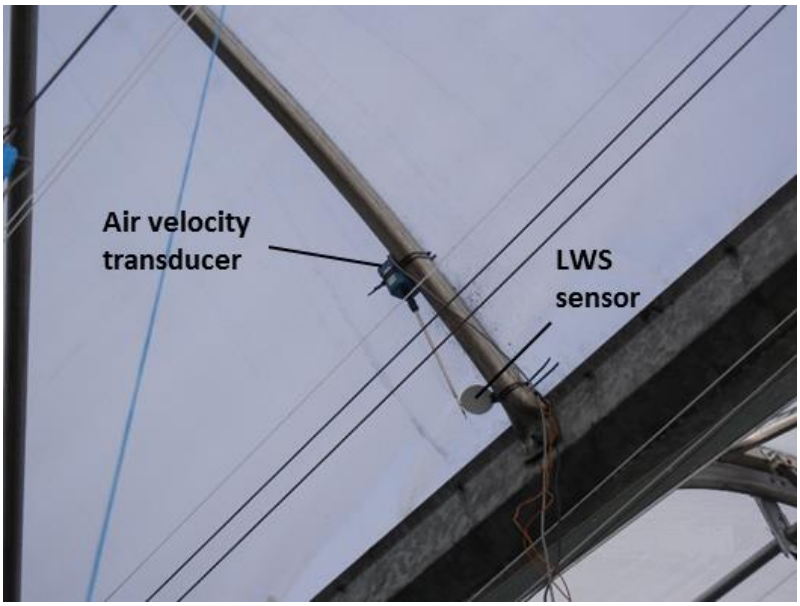


**Figure 5.2. Leaf wetness sensor setup.**

The greenhouse indoor climatic environment was also monitored. A CS500 temperature and RH probe (Campbell Scientific Inc., Edmonton, AB, Canada) was placed inside a radiation shield and installed in the center of the greenhouse 1.8 m above the ground to monitor the inside air temperature and RH. The indoor solar radiation was monitored with a LI-200 Pyranometer (LI-COR Inc., Lincoln, NE, USA), which was installed in the center of the greenhouse over the eave, about 4.3 m above the ground to avoid any obstructions. During the experiment, a DCA 3000T dehumidifier (DCA Inc., Cedarburg, WI, USA) was installed and located at the east end of the greenhouse for humidity control. A FTB8000B flow meter (OMEGA Inc., Laval, QC, Canada) was also installed in the headhouse to monitor the amount of water irrigated into the greenhouse.

A CR 10X datalogger (Campbell Scientific Inc., Edmonton, AB, Canada) was installed against the east wall of the greenhouse. The inside temperature and RH data, solar radiation, the leaf wetness sensor reading, the air velocities, the thermocouples and the pulse from the flow meter were all monitored every minute, and ten-min averages and the total amount of irrigating water were recorded by the datalogger. The ventilation and heating equipment were all controlled by the greenhouse ventilation control system based on temperature, and the temperature sensor was

installed in the middle of the greenhouse at a height of 1.5 m. The ambient weather conditions (temperature and RH) were obtained from Environment Canada website for Saskatoon as the distance between the weather station and the experimental greenhouse was only 23 km. The equipment locations and sensor locations are illustrated in Figure 5.3.

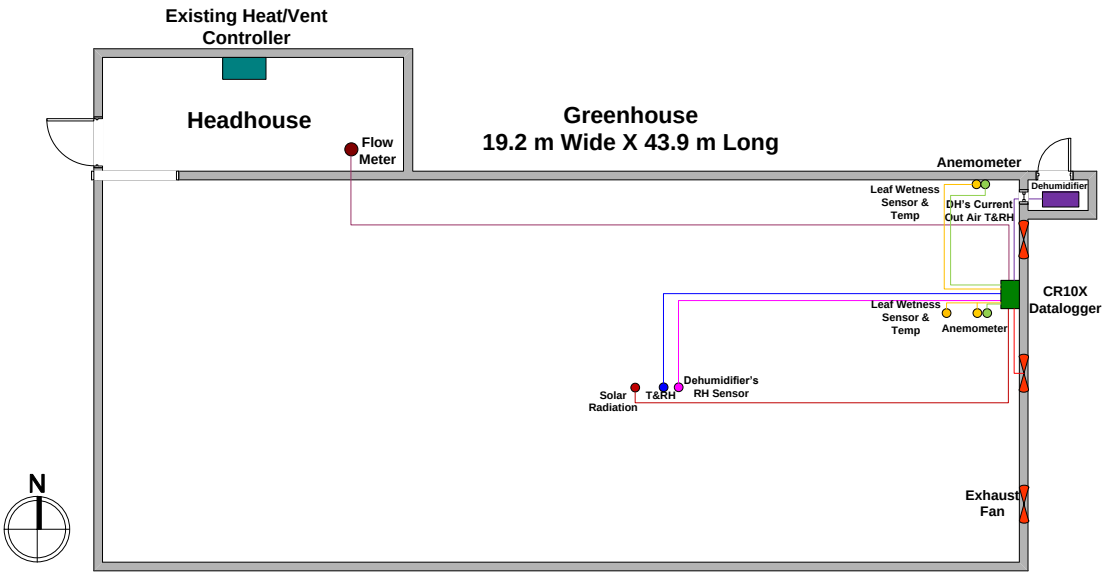


**Figure 5.3. Sketch of the greenhouse layout and measurement position (unit: m).**

## 5.5 Results and Discussion

The experiment was conducted inside the greenhouse for almost eight months from early 04 April until 30 November 2013.

### 5.5.1 Indoor temperature and RH conditions

Condensation occurs on the building surface when the surface temperature is lower than the air dew point temperature. Table 5.1 shows the average values of the greenhouse cover interior surface temperature ($T_c$) and the indoor air dew point temperature ($T_{dp}$) during different periods of time from April to November. The day was categorized into four periods, each period had similar $T_c$ and condensation rate. They are night (20:00-7:00), morning (7:00-10:00), noon to afternoon (10:00-15:00), and late afternoon to evening (15:00-20:00). The table also gives the percentages of the time when $T_c$ was lower than $T_{dp}$ in each period, i.e. the percentage of the time when condensation would occur on the interior cover surface during each period of time. The indoor and outdoor air conditions were similar in June, July, and August; therefore, Table 5.1 gives the average

values of the three months. Figure 5.4 gives the minimum, maximum, and average values of $T_c$ and $T_{dp}$ in each month.

**Table 5.1. Average air dew point temperature ($T_{dp}$) and cover temperature ($T_c$) and the percentages of the time when $T_c$ was lower than $T_{dp}$.**

| *Time Period* | *Temperature* | *Apr* | *May* | *Jun - Aug* | *Sep* | *Oct* | *Nov* |
|---|---|---|---|---|---|---|---|
| 20:00 – 7:00 | $T_c$ | 5.8 | 13.8 | 16.6 | 14.2 | 7.7 | 1.9 |
| | $T_{dp}$ | 16.4 | 16.4 | 17.8 | 16.3 | 16.0 | 12.9 |
| | $T_c < T_{dp}$ (%) | 78.3 | 83.6 | 80.4 | 87.6 | 100 | 100 |
| 7:00 – 10:00 | $T_c$ | 12.2 | 25.5 | 26.5 | 20.0 | 12.2 | 5.0 |
| | $T_{dp}$ | 18.3 | 17.9 | 18.0 | 17.2 | 17.4 | 13.8 |
| | $T_c < T_{dp}$ (%) | 21.3 | 3.3 | 4.7 | 24.4 | 91.4 | 100 |
| 10:00 – 15:00 | $T_c$ | 21.6 | 32.6 | 33.6 | 26.1 | 19.7 | 14.6 |
| | $T_{dp}$ | 19.2 | 15.9 | 17.5 | 14.8 | 16.3 | 16.8 |
| | $T_c < T_{dp}$ (%) | 9.6 | 0.0 | 1.7 | 2.0 | 25.2 | 86.0 |
| 15:00 – 20:00 | $T_c$ | 14.7 | 29.5 | 30.2 | 23.0 | 15.2 | 8.6 |
| | $T_{dp}$ | 18.1 | 12.9 | 17.0 | 15.5 | 16.6 | 15.2 |
| | $T_c < T_{dp}$ (%) | 25.8 | 2.6 | 0.9 | 20.0 | 71.0 | 98.7 |
| Average/Total Percentage | $T_c$ | 10.0 | 22.4 | 24.2 | 19.2 | 12.3 | 6.3 |
| | $T_{dp}$ | 17.3 | 15.8 | 17.6 | 15.9 | 16.4 | 14.3 |
| | $T_c < T_{dp}$ (%) | 45.9 | 39.5 | 38.0 | 47.8 | 77.3 | 96.8 |

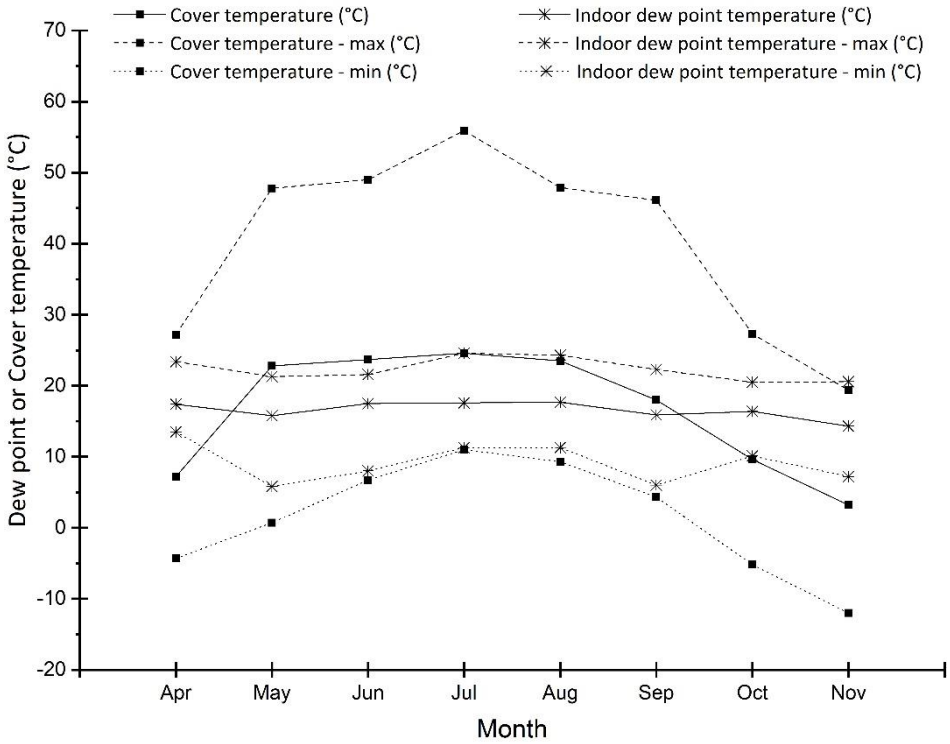


**Figure 5.4. Monthly indoor dew point temperature and cover interior temperature (mean, max, min).**

As shown in Figure 5.4, $T_{dp}$ fluctuation was not very large during the eight months, which is due to the controlled indoor air temperature and RH. The monthly average $T_{dp}$ varied from 14.3°C in November to 17.6°C in the summer month. The lowest $T_{dp}$ of 12.9°C occurred in November in 20:00-07:00 due to the relatively dry indoor air condition, and again in 15:00-20:00 in May due to the relatively lower indoor RH.

In April, although the plants were not fully grown and transpiration was not high, the ventilation rate was low due to the cold outside air temperature, and condensation would occur 45.9% of the time when $T_c$ was lower than $T_{dp}$. At night condensation occurrence would reach up to 78.3% of the time. From May to September, the crops were fully grown and evapotranspiration was high, and the ventilation rate was also high due to high ambient temperature; so there was about 38% to 39.5% of the time from May to August, and 47.8% of the time in September, when condensation could occur, mainly at night. During the daytime, $T_c$ was higher than $T_{dp}$ most of the time, therefore, low or no condensation was observed from 7:00 until 20:00. Condensation mainly occurred during the nighttime and early morning from 20:00 to 7:00 for 80.4% to 87.6% of the time in the 11 hours of nighttime. In October and November, $T_c$ was lower than $T_{dp}$ almost all day except a few hours in the noon time due to the cold ambient weather condition in addition to high evapotranspiration from mature plants.

As seen from Figure 5.4, the monthly average $T_c$ was higher than 22°C from May to August. There was three months (April, October, and November) that the average $T_c$ was close to or even lower than 10°C but still above 0°C. The maximum temperature of the inner cover could reach up to 59.1°C due to the strong incoming solar radiation in the summer season. $T_c$ could be below zero at night in November due to the cold outside weather. The difference of the monthly average $T_c$ between the daytime and nighttime was greater than 10°C from May to September, while it was between 6°C and 10°C during the cooler months.

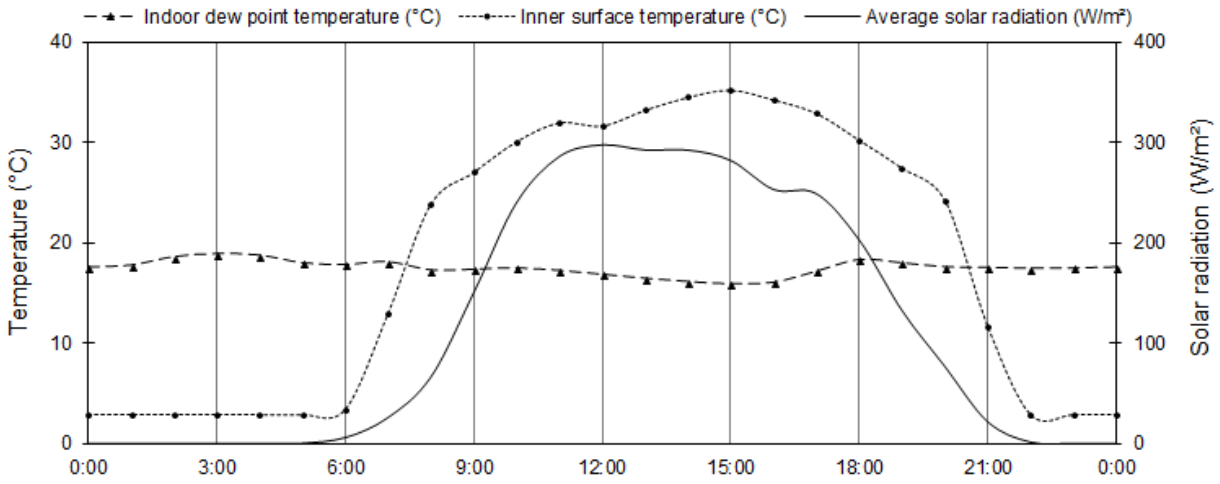


**Figure 5.5. Daily average indoor air dew point temperature and plastic film inner surface temperature in June.**

Figure 5.5 shows the daily average $T_{dp}$ and $T_c$ in June. Between 8:00 and 20:00, $T_c$ was higher than $T_{dp}$ due to the solar radiation. During the nighttime and early morning, $T_c$ was lower than $T_{dp}$, causing condensation. It is also clearly shown that cover temperature was greatly depending on solar radiation.

The monthly average indoor RH was around 70% from May to October with the highest of 76% in April and the lowest 65% in November. The percentile when the indoor RH exceeded 75% was the highest in April with 59%, while it was between 38% and 48% from May to August and only 9.9% in November. This indicates in cold weather although the RH is low, condensation can still occur on the cover; therefore, condensation control could not be successful just by controlling indoor RH, the other factors determining condensation occurrence such as inner surface temperature and air velocity should also be considered.

The general trend of the RH diurnal profile during the mild and summer season was that the indoor RH was lower during the daytime due to the ventilation cooling by the exhaust fans and roof vent and higher during nighttime and early morning due to low ventilation. In winter, the roof vent and the exhaust fans were not in operation, the indoor RH was low at night due to high condensation and high during the daytime due to plant transpiration and low infiltration. More details about the indoor RH conditions can be found in the research by Han et al. (2016).

### 5.5.2 Measured condensation rate

The linear relationship between the leaf wetness sensor voltage output and the amount of condensate on the sensor surface is determined by (Chapter 4):

$$C = 0.0025 \times V - 0.70 \qquad (5.2),$$

where $C$ is the amount of water condensate on the sensor surface, in g; $V$ is the leaf wetness sensor voltage output, in mV.

In Equation 5.2, $C$ gives the true condensation condition on the inner plastic film surface at any time of a day. As the inner surface is one of the main moisture sources or sinks in the greenhouses, the main purpose of quantifying condensation on the inner surface is to provide information to the moisture balance model to estimate the dehumidification needs of the greenhouse for humidity control. For this purpose, the required information is the condensate change in a certain period of time instead of the absolute condensate on the cover surface. By analyzing the variation of the condensation rate (*CR*) change in a certain period of time, e.g. 1 hour, the moisture removed by the inner cover surface from the greenhouse air or the moisture regain by the greenhouse air from the evaporation of the condensate can be estimated. Therefore, the hourly *CR* (i.e., the hourly net amount of water condensed on the cover surface) was obtained by subtracting the previous hourly *C* value from the current hourly *C* value and it was given in condensate per square meter of floor area. The positive hourly *CR* means that more moisture is removed from the greenhouse air and the inner surface acts as a moisture sink of the greenhouse air. In case of negative hourly *CR*, it means the evaporation of the condensate from the inner cover surface is greater than the amount of condensation. The condensate is regained by the greenhouse air so the cover surface acts as a moisture source to the air. In case of unchanging *CR*, it indicates equilibrium state of condensation and evaporation. If there is no water on the cover surface, especially during the daytime, there should be neither condensation nor evaporation occurring. Among all the above analysis, dripping of the condensate from the cover surface is not taken into consideration due to the difficulty of quantifying the amount of drip.

The general daily pattern of condensation occurrence from April to November was that condensation mainly occurred right after the sunset until shortly after the sunrise when the indoor RH was high. During warm season from May to October daytime *CR* was low due to ventilation

cooling system, combined with the high indoor air and cover surface temperature, but in April and November, daytime *CR* could be higher than that of the night due to low air exchange and high transpiration. The total percentage of the time when condensation occurred during the eight months was 39%, which were mainly detected during the nighttime. There was around 34% of the time neither condensation nor evaporation occurred on the cover surface due to the dry cover surface. This phenomenon mainly occurred during the daytime from May to September due to strong incoming solar radiation and high cover inner surface temperature. Evaporation occurred on the cover surface for the rest of the time. The hourly average positive *CR* during the eight months was 13.2 g $m^{-2}$ $h^{-1}$. The total hourly *CR* during the eight months was close to zero.

Table 5.2 shows the hourly average *CR* in each month during the daytime and nighttime, respectively. As mentioned before, the hourly *CR* should be positive (condensation is greater than evaporation), negative (condensation is less than evaporation), or equal to zero (condensation is the same as evaporation). When the film inner surface is dry, especially during the daytime, there is no condensation or evaporation occurs. Those situations are not included in the calculation. No matter during the daytime or the nighttime, the highest hourly *CR* occurred in April due to low ambient temperature and low ventilation rate. During the daytime, hourly average *CR* were almost all negative values except in November, which indicated that evaporation was greater than condensation on the cover surface during the daytime. The cover surface acted as a moisture source of the greenhouse air. The opposite situation occurred at night from 20:00 pm to 7:00 am as more moisture condensed on the film inner surface from the greenhouse air. The cover surface acted as a moisture sink of the greenhouse air. In November, *CR* were positive values both during the daytime and the nighttime. Condensation was greater than evaporation all day long, even though the nighttime *CR* was lower than that of the other months, which was caused by the lower indoor air humidity ratio.

**Table 5.2. Hourly average condensation rate (g $m^{-2}$ $h^{-1}$) in each month during the daytime and nighttime.**

| *Month* | *Daytime (7:00 - 20:00)* | *Nighttime (20:00 - 7:00)* | *Average* |
|---|---|---|---|
| Apr | -17.5 | 16.4 | 0.4 |
| May | -36.8 | 19.0 | -0.5 |
| Jun | -27.3 | 11.8 | 0.0 |
| Jul | -26.7 | 8.7 | 0.1 |
| Aug | -20.6 | 9.4 | 0.0 |
| Sep | -16.6 | 9.8 | 0.1 |
| Oct | -6.4 | 5.8 | 0.0 |
| Nov | 0.4 | 0.5 | 0.0 |
| Average | -13.8 | 9.5 | 0.0 |

Figure 5.6 shows a typical diurnal pattern of the hourly *CR* in three consecutive days in May. It also shows the absolute amount of condensate on the film inner surface. The amount of condensate on the cover surface started to accumulate right after the sunset and peaked before the sunrise. After the sunrise, the plant transpiration started, and the indoor RH started to increase and $T_{dp}$ increase. Due to the solar radiation, the cover temperature increased faster than $T_{dp}$ and soon was higher than $T_{dp}$, leading to the evaporation of condensate on the inner plastic film surface so the measured condensation rate was negative and dropped rapidly. After the noon time and before the sunset, the cover surface became dry. There was neither condensation nor evaporation occurred on the cover surface for a few hours until the sunset. After the sunset, the ventilation rate was low, the indoor RH began to increase, and the cover temperature reduced to lower than $T_{dp}$ and then moisture started to condense on the cover surface. High *CR* occurred until the early morning after sunrise and before ventilation cooling started.

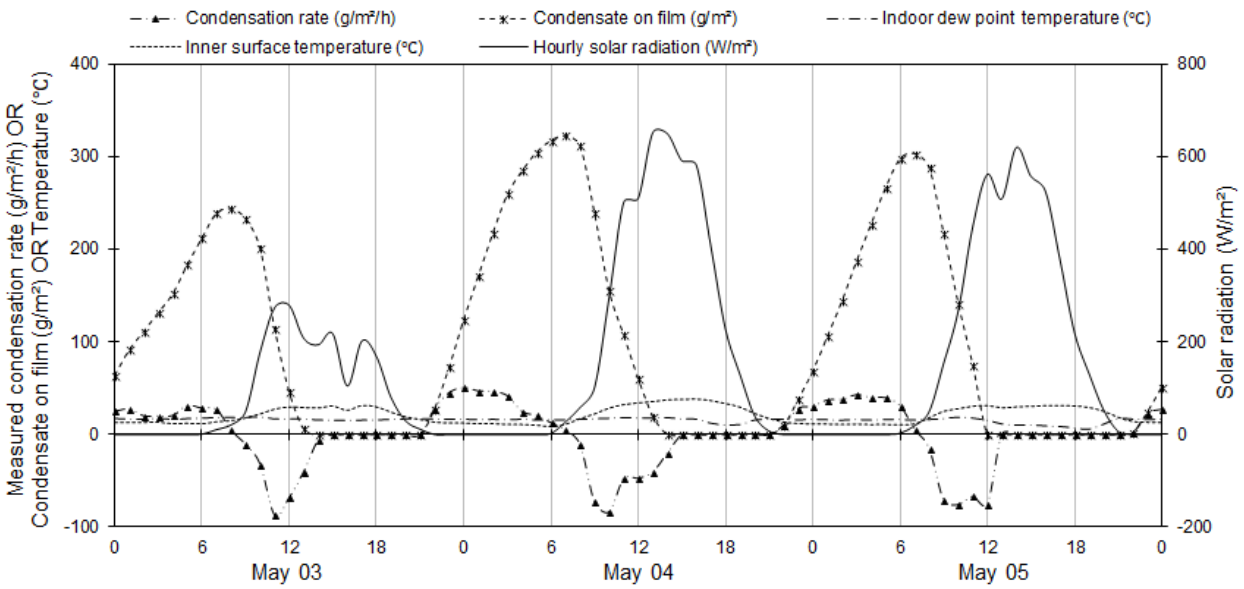


**Figure 5.6. Condensation rate in a three-day period in May.**

During October and November, the condensation was mainly detected a few hours before the sunset, overnight, until after the sunrise. Figure 5.7 shows the diurnal pattern of condensation occurrence in three days in October. There were two peaks in a day, once in the morning after sunrise when high transpiration had started but ventilation cooling had not started due to the low ambient temperature, moisture produced was trapped inside causing high RH and high condensation on the cover. The second peak occurred in the evening after sunset, when the ambient temperature dropped so the cover temperature dropped quickly, ventilation cooling ceased, indoor temperature reduced to night set point; all these reasons caused RH increase and condensation increase. In addition, the condensation rate was less than the other months mainly because the moisture production rate and the indoor humidity ratio were at much lower levels comparing with the other months. During the daytime, when the solar radiation was strong, evaporation was greater than condensation, and there was little, or no condensation occurred.

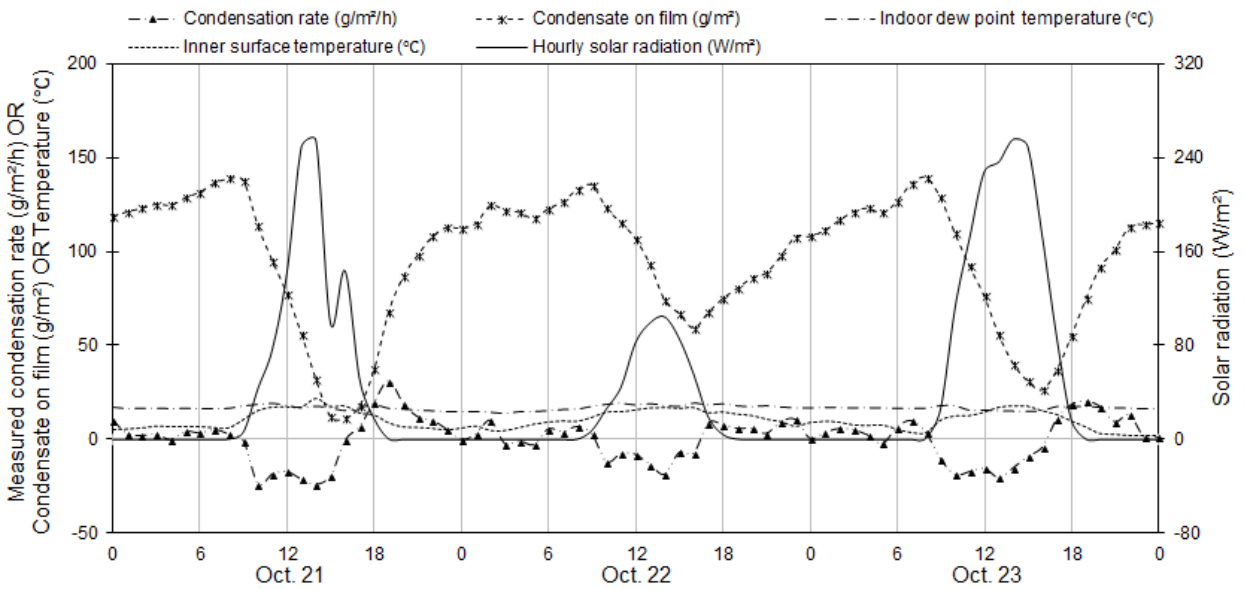


**Figure 5.7. Condensation rate in a three-day period in October.**

Figure 5.8 displays the monthly average of daily *CR* during the daytime and nighttime and also the indoor and outdoor air conditions. During the daytime from 7:00 am until 20:00 pm, evaporation was greater than condensation, therefore, the daily sum of *CR* was negative, except in November. Condensate on the cover surface was evaporated into the greenhouse air. The cover surface acted as a moisture sink to the moisture balance model of the greenhouse air. During the nighttime from 20:00 pm until the early morning 7:00 am, the daily sum of *CR* was all positive during the eight months, indicating that condensation was greater than evaporation. More condensate was observed on the cover surface. The cover surface acted as an important moisture sink for the greenhouse dehumidification.

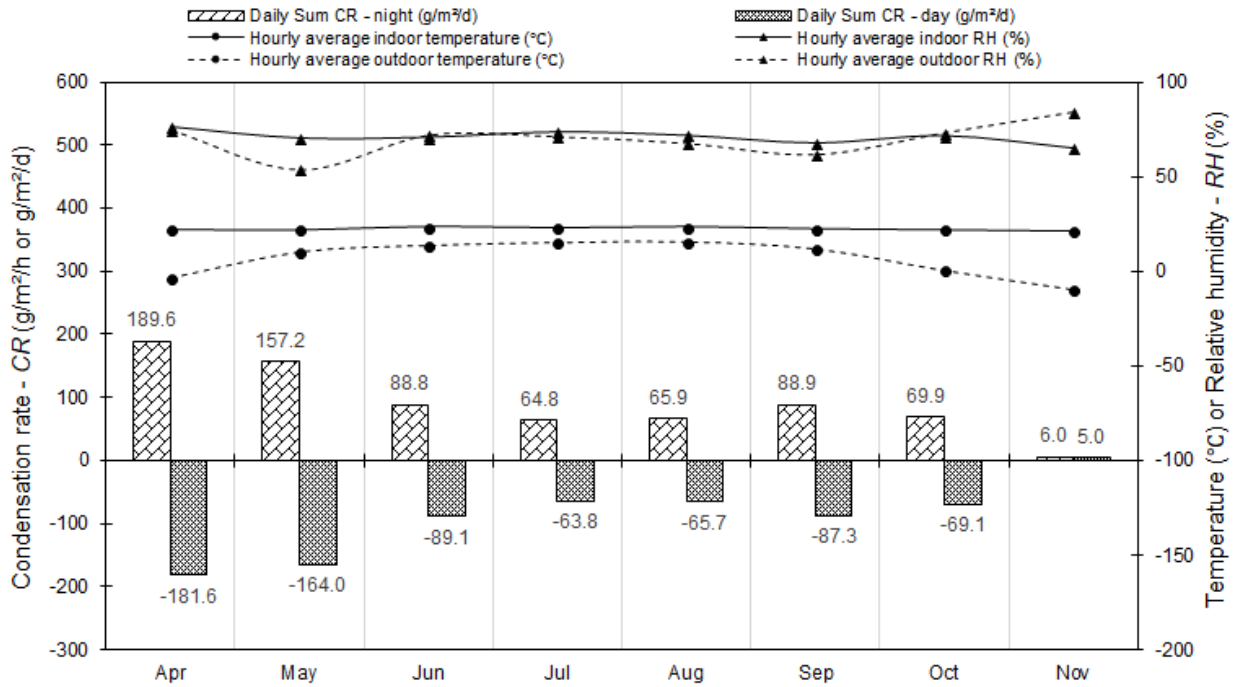


**Figure 5.8. Monthly average of daily condensation rate values and environment conditions.**

The maximum daily sum of *CR* occurred during the nighttime was 374.6 g $m^{-2}$ $d^{-1}$ which was in April. The average hourly condensation rate during the nighttime in the eight months was around 9.5 g $m^{-2}$ $h^{-1}$; while the daily average value at night was 88.6 g $m^{-2}$ $d^{-1}$. The monthly average of daily *CR* was greater than 150 g $m^{-2}$ $d^{-1}$ in April and May at night. Even though that the condensation rate was low during the summer months from June to August, the least daily *CR* occurred in November. The same pattern was found for the hourly average *CR*. The main reason was that during April, May, September and October, the plants were still in the stage of high yield, high transpiration resulted in the high indoor RH, the ventilation cooling was not in full capacity, causing the high rate of condensation during the nighttime. While during November, the plant was in the last growing stage and transpiration was not strong compared with the other months, the indoor humidity ratio was low leading to low condensation on the plastic film surface. As to the daily sum of *CR* during the daytime, evaporation was greater than condensation from April until October, as the negative values shown in Figure 5.8. More condensate evaporated into the greenhouse air in April and May. Only in November, condensation occurred all day during both the daytime and nighttime. The daily average evaporation rate was 88.3 g $m^{-2}$ $d^{-1}$ during the daytime. As shown in Figure 5.8, the condensation rate during the nighttime was close to the evaporation rate during the daytime.

As discussed before, there was over 77% and 97% of the time that the plastic film inner surface temperature was lower than the indoor air dew point temperature in October and November, respectively, which means condensation should occur on the inner cover surface. However, based on the experiment results, only around 48% and 61% of the time that condensation was detected. The percentage of the time when condensation occurred from June until September was around 10% lower than the percentage of the time when the plastic film inner surface temperature was lower than the indoor air dew point temperature. In April and May, it was close to the period of the time when the film inner surface temperature was lower than the indoor air dew point temperature. The reason might be that the indoor RH and humidity ratio was lower in October and November, even there might be condensation, it was hard to detect due to the low condensation rate. Not only the outdoor and indoor air temperatures have influence on condensation rate, the indoor RH and humidity ratio also have an effect on the condensation rate. Based on the data collected from this experiment, a statistical model to predict condensation rate based on the indoor and outdoor environment conditions could be developed, which will be reported later.

Accumulating the hourly condensation rate measured over the eight months period at night, there was a total of around 21,362 liters of water or 25.3 L $m^{-2}$ of floor area, or 9.5 g $m^{-2}$ $h^{-1}$condensed on the greenhouse cover surface. Compared with the condensation rate measured in the glass greenhouses, which was with an average value of 1.8 g $m^{-2}$ $h^{-1}$ (Granados et al., 2011) or 9.43 g $m^{-2}$ $h^{-1}$ (Feuilloley and Guillaume, 1990), the condensation rate on the double layer plastic film greenhouse was higher.

## 5.6 Conclusions

In this study, a commercially available leaf wetness sensor was calibrated to measure the condensation rate. Tests conducted in the laboratory indicated that the sensor voltage output had a significant linear relationship with the amount of condensate on the sensor surface; therefore, the sensor can be used to measure condensation rate. The sensor was installed in a tomato greenhouse to measure the condensate rate on the inflated double layer plastic film cover inner surface from April to November in a northern climate. The results indicated that condensation mainly occurred during the nighttime and early morning. During warm season from May to October daytime condensation rate was low due to ventilation cooling, but in April and November, daytime

condensation rate could be higher than that of the night due to low air exchange and high transpiration. The maximum condensation occurred in April and May. During the summer time from June to September, there was much less condensate, while the least condensation was observed in November due to the lowest indoor RH and humidity ratio. During the daytime from 7:00 am to 20:00 pm, evaporation was greater than condensation and the cover surface acted as a moisture source of the greenhouse air. The opposite situation occurred at night from 20:00 pm until 7:00 am as the cover surface acted as a moisture sink of the greenhouse air. The hourly average condensation rate during the nighttime in a month varied from 0.5 g $m^{-2}$ $h^{-1}$ of floor area in November to 19.0 g $m^{-2}$ $h^{-1}$ in May. The highest hourly condensation rate measured was 95.1 g $m^{-2}$ $h^{-1}$ which occurred on April 10$^{th}$. The maximum daily sum of condensation rate during the nighttime was 374.6 g $m^{-2}$ $d^{-1}$ which occurred on April 17$^{th}$. The average hourly condensation rate during the nighttime in the eight months was around 9.5 g $m^{-2}$ $h^{-1}$ or 88.6 g $m^{-2}$ $d^{-1}$. As measured in the experiment, there was around 21,362 liters of water or 25.3 L $m^{-2}$ of floor area condensed on the greenhouse cover surface during the nighttime in the whole eight months.

Overall, the leaf wetness sensor can be used to measure the amount of condensate on the inner cover surface in the greenhouse so the total moisture on the inner cover surface at any time can be obtained. For the purpose of estimating the dehumidification needs of the greenhouse for humidity control, the amount of condensate change (i.e. condensation rate) can also be obtained. This method provides a very simple and cost-effective device to measure the condensation rate on the greenhouse interior cover surface. Future work is needed to develop a statistic model to predict condensation rate based on the indoor and outdoor environment conditions.

# CHAPTER 6

# MEASUREMENT AND MODELLING OF CONDENSATION ON GREENHOUSE COVER: PART II THEORETICAL AND REGRESSION MODELS

(This is a prepared manuscript and will be submitted soon)

Jingjing Han, Huiqing Guo

## Contribution of this paper to overall study

Analytical models for predicting condensation rate can be found in literature, however, it is difficult to accurately determine the convective heat transfer coefficient used in the models thereby the application of these models for condensation quantification is rare. In Chapter 5, the condensation rate on a greenhouse inner cover surface was measured by leaf wetness sensors for eight months. The data collected in Chapter 5 were used in three theoretical models to predict condensation rate in the greenhouse. Results showed that the theoretically calculated condensation rate was much higher than the measured data. The relationship between condensation rate and the greenhouse indoor and outdoor environment conditions was explored using the data collected in Chapter 5. Two statistical models for predicting condensation rate were developed and validated by using the measured data. These two models were also used for predicting condensation rate in the moisture balance model in Chapter 7. This chapter fulfills objective 6.

The manuscript presented in this chapter will be submitted soon. The first author (PhD student – Ms Jingjing Han) analyzed the data and wrote the manuscript, and the second author (supervisor – Prof. Huiqing Guo) reviewed the manuscript.

## 6.1 Abstract

The condensation rate measured on a greenhouse cover inner surface from April to November was compared with the results obtained from three different convective heat transfer coefficient models. Results showed that the theoretically calculated condensation rate was much higher than the measured data. This study presents two regression models to predict condensation rate occurred on the greenhouse inner cover surface, one for the daytime and another for the nighttime. Statistical parameters of $R^2$, mean absolute error (*MAE*) and the root mean square error (*RMSE*) between predicted and measured condensation rates were used to measure the models consistency. Both models can fit the measured data well during May, July, and September, except during November. The nighttime condensation rate model had better performance at explaining the measured condensation rate from April to October. Both models can be used for condensation rate estimation inside the greenhouse from April to October, except during the cold winter in November when the greenhouse moisture production rate and the indoor humidity ratio were at much lower levels comparing with the other months.

## 6.2 Nomenclature

| | |
|---|---|
| $A$ | area, $m^2$ |
| $C_P$ | specific heat of air at constant pressure, kJ $kg^{-1}$ $K^{-1}$ |
| $CR$ | condensation rate, g $m^{-2}$ $s^{-1}$ |
| $CR_{mi}$ | ith component of the measured value, g $m^{-2}$ $s^{-1}$ |
| $CR_{pi}$ | ith component of the predicted value, g $m^{-2}$ $s^{-1}$ |
| $h_{ci}$ | greenhouse cover inside convective heat transfer coefficient, W $m^{-2}$ $K^{-1}$ |
| $k_v$ | combined convective water vapor transfer coefficient, g $m^{-2}$ $s^{-1}$ |
| $n$ | total number of data points |
| $P$ | atmospheric pressure, kPa |
| $P_w$ | air water vapor partial pressure, kPa |
| $q_c$ | convective heat transfer, W $m^{-2}$ |
| *Solar* | solar radiation getting into the greenhouse, W $m^{-2}$ |
| $T$ | air temperature, °C |
| $\Delta T$ | temperature difference between indoor air and cover inner surface, °C |
| *VPD* | vapor pressure deficit, kPa |
| $w$ | humidity ratio, $kg_w$ $kg_{air}^{-1}$ |
| $\lambda$ | latent of condensation (or vaporization) of water at the air temperature, kJ $kg^{-1}$ |

***Subscripts***

| | |
|---|---|
| $c$ | cover inner surface |
| $d$ | daytime |
| $g$ | ground |
| $i$ | inside air |

| | |
|---|---|
| *n* | nighttime |
| *o* | outside air |
| *sc* | saturation at cover inner surface |

***Abbreviations***

| | |
|---|---|
| *AirSpeed* | air speed near cover surface, m $s^{-1}$ |
| *LWS* | leaf wetness sensor |
| *MAE* | mean absolute error |
| *RH* | relative humidity, % |
| *RMSE* | root mean square error |
| $R^2$ | coefficient of determination |
| *Stdev* | standard deviation |
| *VIF* | variance inflation factor |

## 6.3 Introduction

Condensation is a complex process coupling both heat and mass transfer. Studies have been conducted to investigate the relationship between condensation and heat transfer or light transmission of a greenhouse cover (Delwiche and Willits, 1984; Feuilloley and Issanchou, 1996; Von Elsner et al., 2000; Pollet and Pieters, 2002; Cemek and Demir, 2005; Šinkūnas and Kiela, 2011). Han and Guo (Chapter 4) first developed a condensation measurement method to allow continuous condensation rate measurement on the greenhouse inner cover surface. A commercially available leaf wetness sensor was calibrated in an environment chamber under different room temperature and RH conditions. Water was sprayed on the sensor surface to mimic condensate. The statistical analysis showed that both sensor temperature and room RH had no significant effect on the sensor voltage output. A linear regression model was developed between the voltage output and the amount of condensate on the sensor surface. This method was applied to measure the condensation rate on the inner surface of a tomato greenhouse for eight months (Chapter 5). The results revealed that this was a feasible and reliable method to measure the amount of water condensed on the greenhouse cover surface. However, no further work was conducted on condensation rate prediction model (Chapter 5).

High relative humidity (RH) in greenhouses can cause fungal diseases, reduce yields and impair produce quality (Bakker, 1991; Kittas and Bartzanas, 2007). To control humidity, the dehumidification loads of greenhouses need to be known to allow selection of the dehumidifiers for the greenhouses. As condensation is a major sink of moisture in the air, prediction of condensation rate is required to allow accurate determination of dehumidification needs of the greenhouses.

The objective of this study was to develop two empirical models to predict the condensation rate on the inner surface of a tomato greenhouse cover during the daytime and at night, respectively.

## 6.4 Theoretical Models of Condensation Rate

Condensation occurs on the inner surface of a greenhouse cover when the cladding inside surface temperature is lower than the greenhouse air dew point temperature. The amount of condensate on the inner surface of a greenhouse cover is proportional to the humidity ratio difference between the inside air humidity ratio and the saturation humidity ratio at the cover inner surface temperature. It can be estimated from (De Freitas and Schmekal, 2003):

$$CR = (w_i - w_{sc})k_v \quad (6.1),$$

where $CR$ is the condensation rate on the inner surface of a greenhouse cover, in g $m^{-2}$ $s^{-1}$; $w_i$ is the humidity ratio of the inside air, in $kg_w$ $kg_{air}^{-1}$; $w_{sc}$ is the saturation humidity ratio at the cover inner surface temperature, in $kg_w$ $kg_{air}^{-1}$; $k_v$ is the combined convective water vapor transfer coefficient, in g $m^{-2}$ $s^{-1}$ (De Freitas and Schmekal, 2003).

The latent heat given to the cover during the condensation process is expressed by:

$$q_c = k_v \lambda \quad (6.2),$$

where $q_c$ is the convective heat transfer, in W $m^{-2}$; and $\lambda$ is the latent heat of condensation (or vaporization) of water at the air temperature, in kJ $kg^{-1}$.

The convective water vapor heat transfer can be calculated as follows (De Freitas and Schmekal, 2003):

$$q_c = \frac{1.07 h_{ci} \lambda}{C_P} \quad (6.3),$$

where $h_{ci}$ is the inside convective heat transfer coefficient of the greenhouse cover, in W $m^{-2}$ $K^{-1}$; $C_P$ is the specific heat of air at constant pressure, in kJ $kg^{-1}$ $K^{-1}$.

The humidity ratio is a function of vapor pressure, which can be determined from (Albright, 1990).

$$w = \frac{0.622 P_w}{P - P_w} \quad (6.4),$$

where $w$ is the humidity ratio, in $kg_w\ kg_{air}^{-1}$; $P_w$ is the air water vapor partial pressure, in kPa; and $P$ is the atmospheric pressure, in kPa.

Hence, the condensation rate can be calculated as follows by Equation 6.5 when introducing Equations 6.2 to 6.4 into Equation 6.1:

$$CR = \frac{0.666 h_{ci} (P_{wi} - P_{wsc})}{C_P P} \qquad (6.5),$$

where $P_{wi}$ is the inside air water vapor partial pressure, in kPa; $P_{wsc}$ is the saturation water vapor pressure at the cover inner surface temperature, in kPa.

The calculation is very simple; however, the difficult part is how to determine the convective heat transfer coefficient. As suggested by Papadakis et al. (1992), in situ measurements can be used for the determination of the outside convective heat transfer coefficient of the greenhouse cover, which vary due to the geometries of the greenhouses. The experiment conducted in a semi-cylindrical greenhouse with PVC cover material by Kittas (1986) obtained the following Equation 6.6 to determine the inside convective heat transfer coefficient, $h_{ci}$, for the inside of the greenhouse cover,

$$h_{ci} = 4.3 \times (T_i - T_c)^{0.25} \quad (T_i > T_c) \qquad (6.6),$$

where $T_i$ and $T_c$ are the temperatures of the inside air and the cover inner surface, respectively, in °C. As reported by Kittas (1986), the inside convective heat transfer coefficient ranged from 5 to around 10 $W\ m^{-2}\ K^{-1}$ when the indoor air temperature was 2°C higher than the cover inner surface temperature. However, Cemek and Demir (2005) stated that the chemical structures of covering materials affect the condensation. Hence, these experimental results could not be applied in the greenhouses covered by the polyethylene (PE) film. In addition, Kittas (1986) only took the natural convection conditions into account to get the convective heat transfer coefficient value.

From in situ experiment in a twin-span greenhouse covered with polyethylene film with no plants inside, Papadakis et al. (1992) gave the following Equations 6.7 and 6.8 to calculate the convective heat transfer coefficient during the daytime and nighttime, respectively.

$$\text{Daytime} \quad h_{ci} = 1.95 \times (T_i - T_c)^{0.3} \quad (T_c - T_i \leq 11.1°C) \qquad (6.7),$$

$$\text{Nighttime} \quad h_{ci} = 2.21 \times (T_i - T_c)^{0.33} \quad (0.3 < T_i - T_c \leq 13.8°C) \qquad (6.8).$$

However, as measured in the experimental greenhouse of this study, the temperature difference between the inside air and the cover surface could reach as high as 22°C during the daytime. Hence, the application of the above two equations is limited by the given temperature differences.

Jolliet (1994) suggested that this coefficient could be estimated as $3.5A_c/A_g$ W m$^{-2}$ K$^{-1}$, where $A_c/A_g$ is the ratio of the covering area to the ground area; however, the researcher did not state which type of material this estimation could be applied for. In the research by Garzoli and Blackwell (1981), the calculated heat loss using the convective heat transfer coefficient value suggested by ASHRAE was overestimated as compared with the actual value. In another study, the $h_{ci}$ value recommended by McAdams (1954) was turned out underestimate of the actual heat loss; the best fit of the value was found to be 7.2 W m$^{-2}$ K$^{-1}$ by this study.

The recommended values or models of the convective heat transfer coefficient mentioned above were applied to calculate the theoretical *CR* (condensation rate) using Equation 6.5. One objective of this study was to compare the measured *CR* in a tomato greenhouse with the calculated theoretical *CR*. Another objective was to develop two statistical models for predicting *CR* on the greenhouse cover inner surface and validate the models by using the measured data.

## 6.5 Materials and Methods

### 6.5.1 Greenhouse specifications

The experimental greenhouse was located in Grandora, Saskatchewan, 23 km west of Saskatoon, at 52.09º latitude, -107.03º longitude and 504 m elevation. It was a three-span greenhouse covered by a double layer 6-mil polyethylene plastic film on the roof and polycarbonate panels on the side walls, except for the north wall, which was an insulated wood-frame wall. The greenhouse was 19.2 m wide and 43.9 m long. The eave height was 4.3 m and the ridge height was 6.7 m (Figure 6.1). Tomato plants were planted in peat-based growing medium bags in 11 rows with a total of 2,100 plants, averaging 2.5 plants per square meter. The greenhouse was heated with hot water pipes located above ground between rows of tomato plants. Four natural gas boilers were used to heat the hot water. The greenhouse had three exhaust fans (FC050-4E exhaust fan, ZIEHL-ABEGG, Saint e-Claire, QC, Canada) placed in the east wall at a height of 3.8 m and roof vents for cooling. These fans were in operation only when the indoor temperature was above 22°C during

the spring, summer, and fall seasons, and were sealed during the winter period. Each exhaust fan had a diameter of 0.548 m and a capacity of 2.1 $m^3$ $s^{-1}$ at a static pressure of 20 Pa (Axial Fans, 2012). A drip irrigation system was used to supply water and nutrients. The floor was covered by landscaping fabric, with soil underneath.

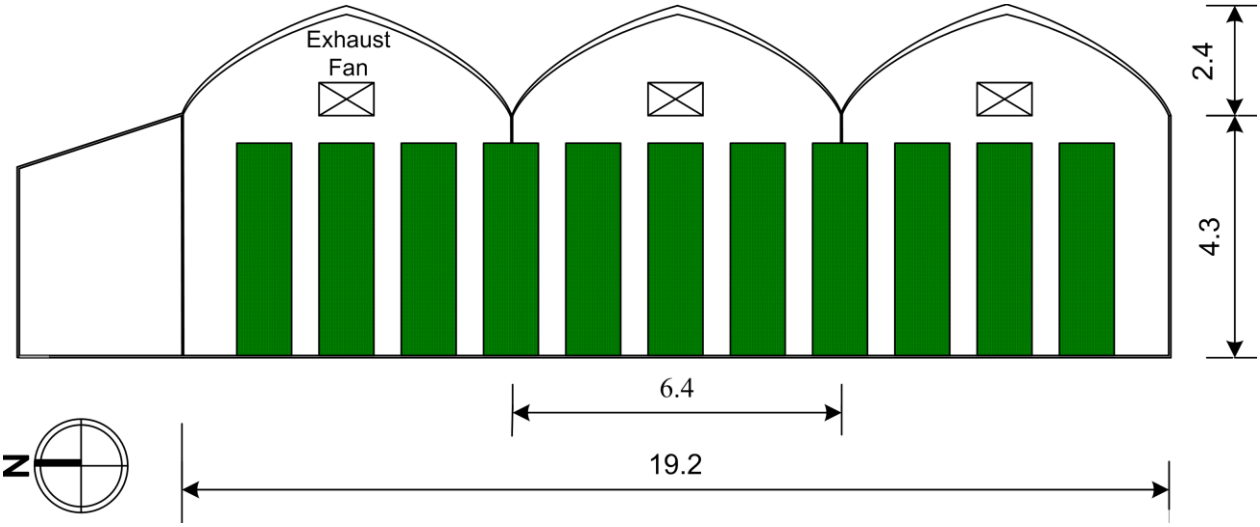


**Figure 6.1. Sketch of the greenhouse cross section (unit: m).**

### 6.5.2 Condensation rate measurement and data collection

A method developed by Han and Guo (Chapter 4) is used to measure condensation rate of the inner surface of the greenhouse cover. Three leaf wetness sensors (Decagon Devices Inc., Pullman, WA, USA) were installed inside the greenhouse to measure the cover inner surface condensation rate. Details about the sensor calibration procedure can be found in the paper "Development of a method for condensation rate measurement on flat surfaces" (Chapter 4); details on the installation of the sensors and the measurement results can be found in the paper "Measurement and modeling of condensation on greenhouse cover - part I condensation measurement" (Chapter 5).

Besides the voltage output of the leaf wetness sensor (*LWS*), the greenhouse indoor environmental conditions, including the indoor air temperature and RH, were all monitored and recorded by a data logger acquisition system. The greenhouse outdoor weather conditions, including the air temperature and RH, were got from Environment Canada website for Saskatoon (Environment Canada, 2013). More detailed information about the acquisition system and the experimental setup can be found in Han et al. (Chapter 5).

### 6.5.3 Statistical analysis

Statistical analyses were performed using Proc Reg of SAS 9.3 (SAS Institute Inc., Cary, NC, USA). Normality of the data was assessed using the Shapiro-Wilk's Statistic ($W > 0.05$). If the data did not follow a normal distribution, transformation was used to achieve normality of the data. Significance was declared at $P < 0.05$.

## 6.6 Results and Discussion

The experiment was conducted inside the greenhouse from early 04 April until 30 November 2013. The data collected during April, June, August, and October were used to develop the regression model of *CR*. The data collected during May, July, September, and November were used to evaluate and validate the regression models.

Based on the measured *CR* and the recorded indoor and outdoor environmental condition, both the daytime and nighttime *CR* had a negative correlation with the variables including the indoor and outdoor air temperature, the plastic cover inner surface temperature, and vapor pressure deficit (*VPD*, which defines as the difference between the water vapor saturation partial pressure and the air water vapor partial pressure) as well, while *CR* had a positive correlation with the other variables. The only exception was that the indoor RH had no correlation with the nighttime *CR* and the outdoor RH had a negative correlation with the nighttime *CR*.

### 6.6.1 Comparison between measured and calculated condensation rates

Three different models or values of the inner cover surface convective heat transfer coefficient as recommended from the literature were applied to calculate the theoretical *CR* including 1) 7.2 W $m^{-2}$ $K^{-1}$ (McAdams, 1954), 2) 3.5 $A_c/A_g$ W $m^{-2}$ $K^{-1}$ (Jolliet, 1994), and 3) the models as expressed by Equations 6.7 and 6.8 from the study of Papadakis et al. (1992). The corresponding calculated results were named as theoretical *CR*1, *CR*2, and *CR*3, respectively.

Table 6.1 shows the model and measured average hourly condensation rate during the whole growing season. They were calculated only considering the periods when condensation occurred in the greenhouse inner cover surface. The general trend of the theoretical *CR* results reveals that the condensation process mainly occurred during early mornings and nights from 17:00 to 07:00h,

which depicted the measured *CR* phenomenon as experienced in the greenhouse, especially during May to September. No or low condensation occurred during the daytime in the whole experimental term. During April, October, and November, condensation occurred almost all day long due to the cold outside weather conditions. Compared with the measured *CR*, the calculated theoretical values were much higher, which means the recommended values or models of the convective heat transfer coefficient were higher than the actual values therefore not applicable for this double-layer plastic film greenhouse. The actual values of the convective heat transfer coefficient calculated by using Equation 6.5 was between 0 to 4 W $m^{-2}$ $K^{-1}$.

**Table 6.1. Average hourly condensation rate (*CR*) values on the greenhouse inner cover surface during eight months from April to November.**

| *Time* | *Theoretical CR (g $m^{-2}$ $h^{-1}$)* | | | *Measured CR (g $m^{-2}$ $h^{-1}$)* |
|---|---|---|---|---|
| | *CR1* | *CR2* | *CR3* | |
| 0-6:00 | 109.5 | 66.5 | 80.9 | 7.7 |
| 6-7:00 | 79.6 | 48.4 | 64.2 | 0.7 |
| 7-8:00 | 0.0 | 0.0 | 25.3 | 0.0 |
| 8-16:00 | 0.0 | 0.0 | 0.0 | 0.0 |
| 16-20:00 | 0.0 | 0.0 | 0.0 | 3.1 |
| 20-21:00 | 45.5 | 27.6 | 45.8 | 7.2 |
| 21-24:00 | 98.1 | 59.6 | 72.5 | 9.6 |
| Average | 111.0 | 67.4 | 82.5 | 9.2 |

Figure 6.2 shows the measured daily average condensation rate from April to November. It can also tell from the graph that the theoretical *CR* was higher than the measured *CR* during the whole growing season. The highest theoretical condensation rate occurred during the cold and mild seasons of April, May, October, and November. However, the measured *CR* reveals that the lowest condensation rate occurred during November, which was caused by the lower indoor humidity ratio and moisture production rate.

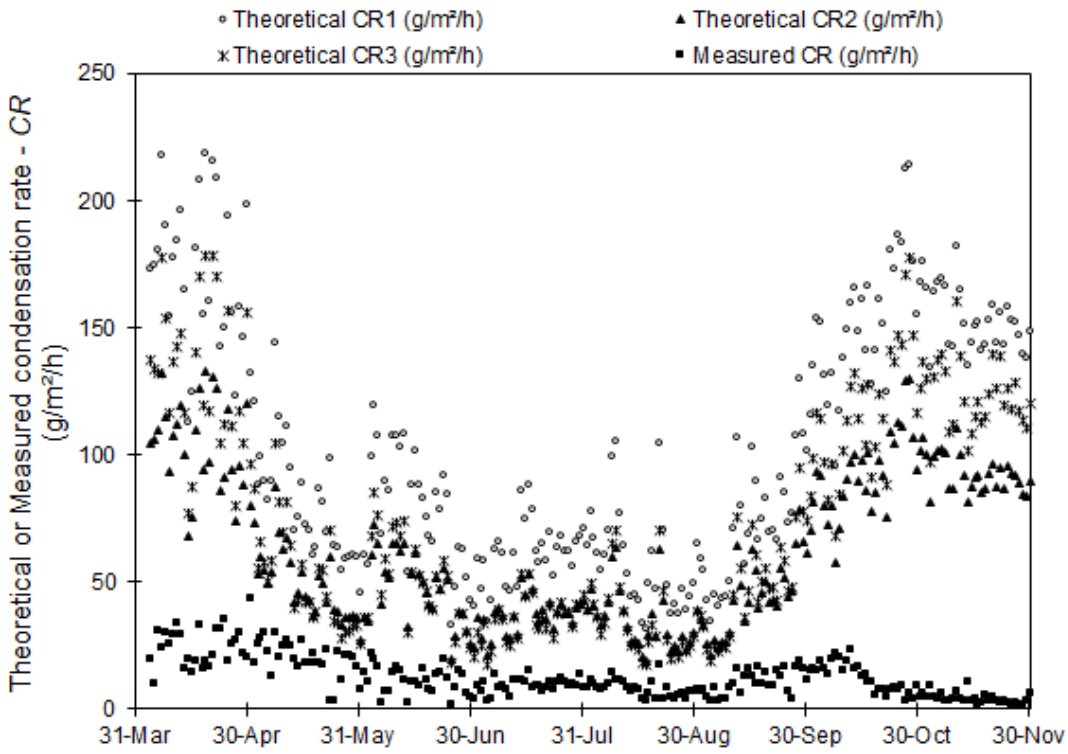


**Figure 6.2. Scatter of daily average measured and theoretical condensation rate from April to November.**

### 6.6.2 Computer modeling simulation results of condensation rate

As the existing *CR* models cannot satisfactorily predict the tomato greenhouse indoor condensation rate, new regression models were developed by this study to estimate the condensation rate with the known plants and the indoor and outdoor environment conditions. As the influencing variables for *CR* are different during the daytime and night, two models should be developed, daytime *CR* model and nighttime *CR* model.

First, a full linear regression model was explored to include all variables in the model so the impact of each variable on *CR* was evaluated. Data collected in April, June, August, and October were used. These variables include temperature difference between the indoor and the cover inner surface temperature ($\Delta T$), incoming solar radiation, indoor air speed near the cover surface, indoor air temperature and RH, outdoor air temperature and RH, *VPD*, and cover inner surface temperature. The results including *P*-values and variance inflation factor (*VIF*) are given in Tables 6.2 and 6.3. *VIF* is a parameter to illustrate the collinearity between the variables, the higher the *VIF* value is, the stronger the collinearity exists between the variables.

**Table 6.2. *P*-values of the *t*-statistic for the condensation rate (*CR*) linear regression models and variance inflation factor (*VIF*) values for the full model and reduced model during the daytime.**

| *Source of Variation* | *P-value (full model)* | *VIF* | *P-value (collinearity removed)* | *P-value (reduced model)* |
|---|---|---|---|---|
| Temperature difference ($\Delta T$) | 0.169 | 1918.4 | <0.0001 | <0.0001 |
| Solar radiation (*Solar*) | 0.557 | 3.2 | 0.003 | <0.0001 |
| Indoor air speed near cover surface (*AirSpeed*) | 0.424 | 2.7 | 0.667 | |
| Room temperature ($T_i$) | 0.012 | 123.7 | 0.177 | |
| Room RH ($RH_i$) | 0.093 | 136.8 | 0.773 | |
| Outside RH ($RH_o$) | 0.045 | 2.0 | 0.760 | |
| Outside temperature ($T_o$) | <0.0001 | 14.3 | | |
| Vapor pressure deficit (*VPD*) | 0.119 | 173.6 | | |
| Film inner temperature ($T_c$) | 0.119 | 173.6 | | |

**Table 6.3. *P*-values of the *t*-statistic for the condensation rate (*CR*) linear regression models and variance inflation factor (*VIF*) values for the full model and reduced model during the nighttime.**

| *Source of Variation* | *P-value (full model)* | *VIF* | *P-value (collinearity removed)* | *P-value (reduced model)* |
|---|---|---|---|---|
| Indoor air speed near cover surface (*AirSpeed*) | 0.057 | 6.8 | <0.0001 | <0.0001 |
| Temperature difference ($\Delta T$) | 0.003 | 918.2 | 0.160 | 0.002 |
| Outside RH ($RH_o$) | 0.027 | 2.0 | 0.014 | |
| Room temperature ($T_i$) | 0.009 | 46.3 | 0.170 | |
| Room RH ($RH_i$) | 0.696 | 466.1 | 0.576 | |
| Outside temperature ($T_o$) | 0.101 | 25.1 | | |
| Vapor pressure deficit (*VPD*) | 0.666 | 484.0 | | |
| Film inner temperature ($T_c$) | 0.003 | 1025.5 | | |

The second and third columns in Tables 6.2 and 6.3 show the *P*-values and *VIF* values for the full linear regression model (with all variables). In the fourth column, *P*-values are presented for the model after removing the variables with the highest *VIF* value sequentially until all *VIF*s are less than 10, which is a threshold value recommended by Montgomery et al. (2012). In the last column, only the variables with significant *P*-values remain. The results indicate only $\Delta T$ and solar

radiation have significant effect on the measured *CR* during the daytime, while during nighttime, the measured *CR* has significant relationship with indoor air speed near the cover surface and $\Delta T$.

Table 6.4 gives the coefficients of the variables in the reduced *CR* models during the daytime and nighttime. The $R^2$ value of 0.61 of the daytime model is slightly higher than that of the nighttime model, which is 0.55, indicating the condensation rate occurred during the daytime can be explained better with the regression model than the nighttime condensation rate. In the daytime model, the *CR* has a linear correlation with the temperature difference. The incoming solar radiation also has significant effect on *CR*. The nighttime *CR* model has a relationship with both the indoor air speed near the cover surface and the temperature difference. The indoor air temperature is not included in both models, because the impact of temperature on *CR* is already reflected by solar radiation and the temperature difference between the indoor and the cover inner surface. It is the same reason for the outdoor temperature and the cover surface temperature not included in both models. *VPD* is also eliminated from both models due to the collinearity with the indoor RH and air temperature. The indoor RH has no significant influence on both models as well according to the statistical analysis results, which means condensation occurrence has little or no relationship with the indoor RH. The other variables are more crucial to condensation occurrence.

**Table 6.4. SAS results of daytime and nighttime condensation rate models.**

| *Model* | *Dependent Variable* | $R^2$ | *Constant* | *Coefficients (P value)* | |
|---|---|---|---|---|---|
| Daytime | $CR_d$ (g m$^{-2}$ h$^{-1}$) | 0.61 | 0.87 (0.056) | $\Delta T$ (°C) | *Solar* (W m$^{-2}$) |
| | | | | 0.43 (0.000) | 0.02 (0.000) |
| Nighttime | $CR_n$ (g m$^{-2}$ h$^{-1}$) | 0.55 | -0.29 (0.818) | *AirSpeed* (m s$^{-1}$) | $\Delta T$ (°C) |
| | | | | 85.51 (0.000) | 0.45 (0.002) |

The statistical models to predict *CR* can be expressed as follows according to Table 6.4:

$$CR_d = 0.87 + 0.43\Delta T + 0.02Solar \quad (6.9),$$

$$CR_n = -0.29 + 85.51AirSpeed + 0.45\Delta T \quad (6.10),$$

where $CR_d$ and $CR_n$ represent the daytime and nighttime condensation rate, respectively, in g $m^{-2}$ $h^{-1}$.

### 6.6.3 Evaluation and validation of the models

To evaluate and valid the above two regression models, the rest of the data set, i.e. data collected during May, July, September, and November were used. The $R^2$, *MAE* (mean absolute error), *RMSE* (root-mean-square error) were used to evaluate the consistency of the models. *MAE* and *RMSE* are defined by Equations 6.11 and 6.12 (Piscia et al., 2012; Yu et al., 2011):

$$MAE = \sum_{i=1}^{n} \left| \frac{CR_{mi} - CR_{pi}}{n} \right| \quad (6.11),$$

$$RMSE = \left( \frac{\sum_{i=1}^{n} \left( CR_{mi} - CR_{pi} \right)^2}{n} \right)^{1/2} \quad (6.12),$$

where $CR_{mi}$ and $CR_{pi}$ are the measured and predicted condensation rate, respectively, and $n$ is the total number of the data points.

Figures 6.3 and 6.4 show the comparison between the measured and predicted daily average *CR* during the daytime and nighttime, respectively. During the day, the predicted *CR* were very close to the measured values from May until the middle of September. During the night, the measured *CR* in July fit the model better than the other months' data, followed by September and May. During May, July, and September, the measured *CR* were much larger than the predicted ones when the condensation rate was greater than 2 or 10 g $m^{-2}$ $h^{-1}$ during the day and night, respectively. The predicted *CR* in November were much higher than the measured data in November. Both models cannot predict the *CR* in November very well due to the special situation when the moisture production rate and indoor humidity ratio were at much lower levels comparing with the other months.

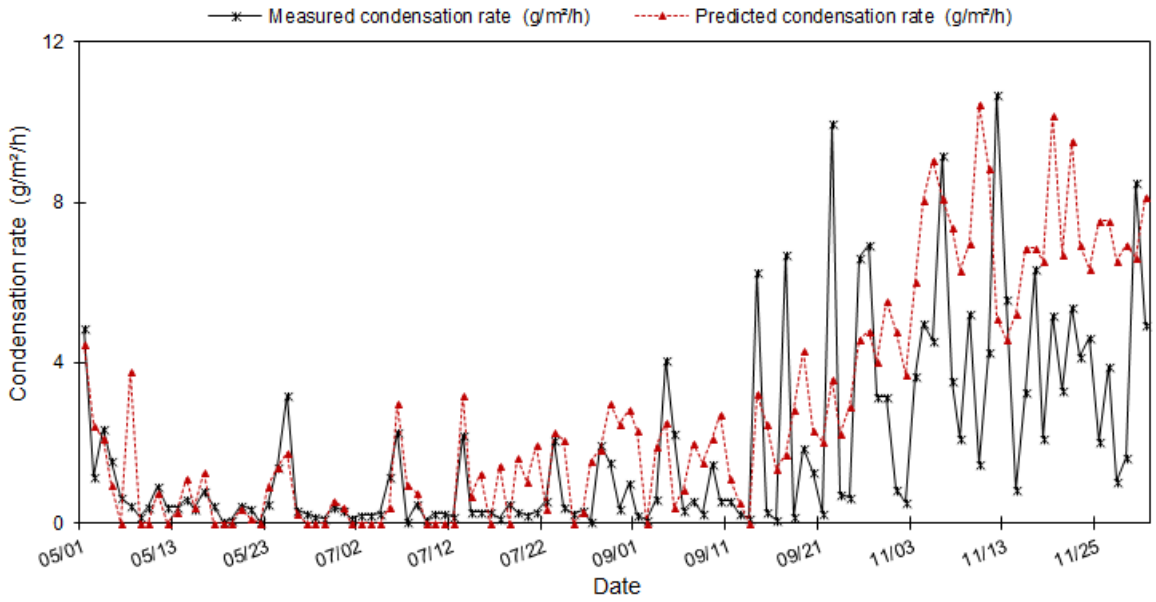


**Figure 6.3. Comparison of the daily average condensation rate between the measured and predicted values during the daytime.**

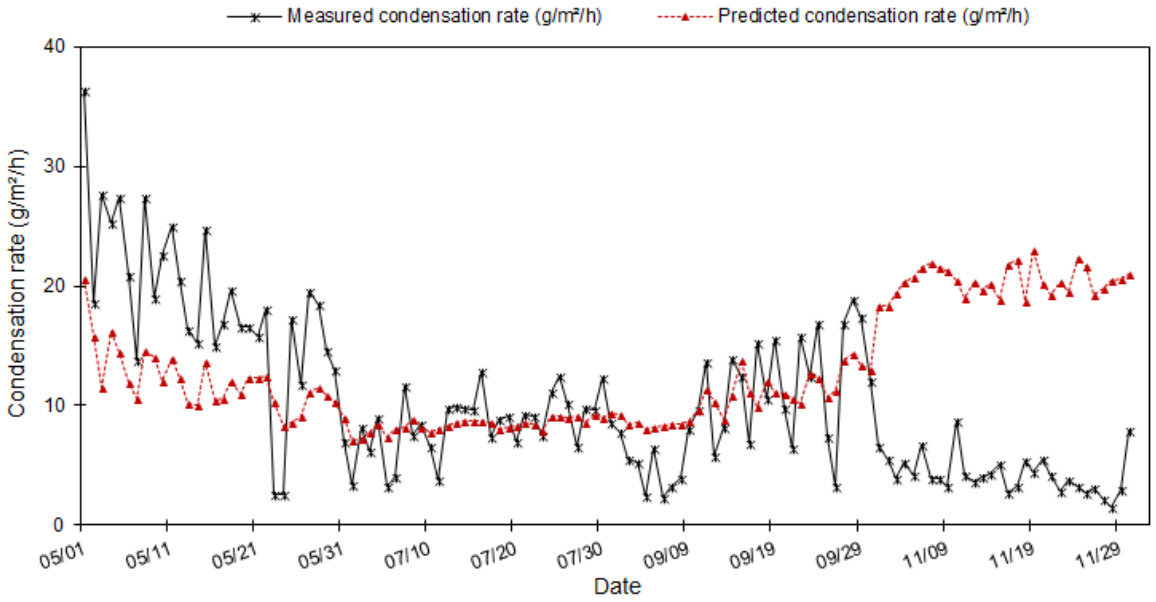


**Figure 6.4. Comparison of the daily average condensation rate between the measured and predicted values during the nighttime.**

Tables 6.5 and 6.6 give the average measured *CR* values, and the $R^2$, *MAE*, and *RMSE* of the two models in each month during the daytime and nighttime, respectively. It also gives the ratios between *MAE* and the average measured *CR* value. The ratios between *RMSE* and the range of the measured *CR* value are also given in the tables.

**Table 6.5. $R^2$, *MAE* and *RMSE* of the daytime model in each month.**

| | *Condensation rate (g $m^{-2}$ $h^{-1}$)* | | | $R^2$ | *MAE* | *MAE/Ave (%)* | *RMSE* | *RMSE/(Max-Min) (%)* |
|---|---|---|---|---|---|---|---|---|
| | *Average (Stdev)* | *Max* | *Min* | | | | | |
| May | 0.81 (1.07) | 4.89 | 0.03 | 0.77 | 0.50 | 61.4 | 0.63 | 13.0 |
| Jul | 0.60 (0.68) | 2.29 | 0.03 | 0.29 | 1.53 | 256.5 | 1.96 | 86.8 |
| Sep | 2.03 (2.66) | 10.00 | 0.07 | 0.21 | 1.97 | 97.2 | 2.38 | 24.0 |
| Nov | 4.33 (2.43) | 10.70 | 0.84 | 0.00 | 3.69 | 85.2 | 4.10 | 41.6 |

Note: Numbers in the parentheses are the standard deviations.

**Table 6.6. $R^2$, *MAE* and *RMSE* of the nighttime model in each month.**

| | *Condensation rate (g $m^{-2}$ $h^{-1}$)* | | | $R^2$ | *MAE* | *MAE/Ave (%)* | *RMSE* | *RMSE/(Max-Min) (%)* |
|---|---|---|---|---|---|---|---|---|
| | *Average (Stdev)* | *Max* | *Min* | | | | | |
| May | 17.68 (6.38) | 27.76 | 2.53 | 0.51 | 7.00 | 40.0 | 7.81 | 30.9 |
| Jul | 8.48 (2.54) | 12.86 | 3.28 | 0.40 | 1.77 | 20.9 | 2.19 | 22.9 |
| Sep | 9.80 (4.99) | 18.82 | 2.32 | 0.56 | 3.28 | 33.5 | 3.82 | 23.1 |
| Nov | 4.56 (1.64) | 12.00 | 1.45 | 0.05 | 15.85 | 347.4 | 16.08 | 152.5 |

Note: Numbers in the parentheses are the standard deviations.

The daytime model could explain around 77% of the measured data during May, which is higher than that during July and September. Also, the ratios are smaller during May than that during July and September. The nighttime model could explain almost more than half of the measured data from May to September. The nighttime model performs more consistency during May, July and September compared with the daytime model. Lower $R^2$ values in November means that both models cannot explain the measured condensation rate very well. The high values of *MAE* and *RMSE* compared with the mean data and the measured range in November also show the same conclusion. The models have poor performance at predicting *CR* in cold season; however, condensation is a very complex process, especially in a greenhouse, which can be influenced not only by the greenhouse characteristics, the environment conditions, but also by the plant characteristics, etc. It is impossible to monitor all the factors. Hence, it is difficult to model *CR*

taking all the circumstances into consideration. However, as compared with the models in the literature, the developed models should be considered acceptable.

Overall, both models can be applied to estimate the condensation rate year-round from April to October, except during the cold winter season when the plant is at the final stage and the greenhouse moisture production rate is at a low level, such as during November. The nighttime model has better performance at explaining the measured *CR* compared with the daytime model.

## 6.7 Conclusions

In this study, the relationship between the measured condensation rate on the greenhouse cover inner surface and the indoor and outdoor environment conditions were investigated. The general trend was that the condensation rate had a negative relationship with the indoor and outdoor air temperature, and with the cover material inner surface temperature. Positive relationship was found between the condensation rate and the indoor air speed near the cover surface which was measured close to the cover surface, and the temperature difference between the indoor and the cover inner surface temperature. In addition, the daytime condensation rate also had a positive correlation with the indoor and outdoor RH and the incoming solar radiation. The indoor RH had no effect on the nighttime condensation rate. The outdoor RH had a negative correlation with the nighttime condensation rate.

Three different convective heat transfer coefficient values or models for calculating the condensation rate were applied. The calculated results were compared with the measured data. They predicted the same trends as heavy condensation occurred during the early morning and at night and high condensation occurred in the cold and mild seasons. However, the calculated condensation rates were at least 7 to 10 times higher than the measured rates. Hence, they cannot be used to predict the condensation rate inside this tomato greenhouse. Two statistical models based on the indoor and outdoor environment conditions were developed to predict the condensation rate occurred during the daytime and nighttime, respectively, using the data measured in April, June, August, and October. Both models were validated by using the measured data in May, July, September, and November. All influencing variables were evaluated on their impact on the *CR*. It turns out that during the daytime only solar radiation and the indoor and cover inner surface temperature difference have significant impact on the measured *CR*, while during the nighttime,

the measured *CR* has significant relationship with indoor air speed near the cover surface and the temperature difference between the indoor and cover inner surface. The results reveal that the nighttime model has better performance at explaining the measured *CR* ($R^2$ = 0.61) compared with the daytime model ($R^2$ = 0.55). Although the $R^2$ values are low, comparing with existing models, the predicted values were in the same range as the measured values. Hence, both models can be used to predict the condensation rate inside the greenhouse from April to October. However, they are not suitable for the cold winter season when the plant is at the final stage and the greenhouse indoor moisture production rate is at a lower level, especially during November or maybe even December.

# CHAPTER 7

# GREENHOUSE MOISTURE BALANCE MODELLING FOR PREDICTING INDOOR HUMIDITY

(This is a prepared manuscript and will be submitted soon)

Jingjing Han, Mohamed S. Ahamed, Huiqing Guo

## Contribution of this paper to overall study

A moisture balance model was developed in this chapter to predict the greenhouse indoor RH and water vapor partial pressure. The dehumidification methods can be selected as discussed in Chapters 1 to 3. The condensation rate was estimated by using the two regression models developed in Chapter 6. The model was validated using data measured in a tomato greenhouse. The model could also be used to quantify and adjust the dehumidification requirement to maintain predetermined RH conditions within a greenhouse. This chapter fulfills objective 7.

The manuscript included in this chapter will be submitted soon. The development of the model, experimental testing, data analysis and manuscript writing were performed by the first author (PhD student – Ms Jingjing Han). The second author (Dr. Mohamed S. Ahamed) helped with the Matlab programming and manuscript review. The third author (supervisor – Prof. Huiqing Guo) reviewed the manuscript.

## 7.1 Abstract

The study presents a moisture balance model (HumidMod) for simulating greenhouse indoor air water vapor partial pressure and relative humidity. The HumidMod model takes evapotranspiration as the main moisture source of the greenhouse air, which is calculated by a modified Penman-Monteith evapotranspiration model. Condensation on the greenhouse inner cover surface as a moisture sink or source is calculated by a statistical model developed in a Venlo-type plastic greenhouse. Ventilation or infiltration is estimated as a function of the indoor solar radiation, which is based on a regression model. In the model, the indoor RH and water vapor partial pressure can be directly calculated as a function of the indoor and outdoor air conditions, as well as the plant and greenhouse characteristics. The model was validated with experimental data from a commercial tomato greenhouse, which had a commercial-grade dehumidifier for humidity control. The mean absolute uncertainty between the predicted and measured results was about 6.9% for both RH and water vapor partial pressure. The coefficients of determination were found 0.59 and 0.75 for RH and water vapor partial pressure, respectively. A good agreement was found between the predicted and measured results with root mean square error of 5.6% for RH and 0.144 kPa for water vapor partial pressure. Based on these results, HumidMod model would be a reliable tool for estimation of dehumidification requirement inside a greenhouse to achieve the desired humidity level.

## 7.2 Nomenclature

| | |
|---|---|
| $A_g$ | greenhouse floor area, $m^2$ |
| $A_l$ | leaf area, $m^2$ |
| $C_P$ | specific heat of water, J $kg^{-1}$ $K^{-1}$ |
| $CR$ | condensation rate, g $m^{-2}$ $h^{-1}$ |
| $E$ | moisture added, extracted, transpired, condensed, exchanged by ventilation or infiltration, kg $m^{-2}$ $h^{-1}$ |
| $e$ | air water vapor partial pressure, kPa |
| $e_s$ | air water vapor pressure at saturation, kPa |
| $e_{sc}$ | saturation water vapor pressure at the cover inner surface temperature, in kPa |
| $h_{ci}$ | convective heat transfer coefficient at the greenhouse cover inner surface, W $m^{-2}$ $K^{-1}$ |
| $I_s$ | incoming shortwave radiation above the canopy, W $m^{-2}$ |
| $LAI$ | leaf area index |
| $l$ | leaf length, m |
| $l_f$ | characteristic dimension of a leaf, m |

| | |
|---|---|
| $M_{water}$ | amount of water extracted by dehumidification, kg |
| $n$ | number of data point |
| $O_i$ | $i^{th}$ component of the measured value |
| $\overline{O}$ | average of the measured value |
| $P$ | atmospheric pressure, kPa |
| $P_i$ | $i^{th}$ component of the predicted value |
| $\overline{P}$ | average of the predicted value |
| $q$ | air flow rate due to ventilation or infiltration, $m^3\ h^{-1}$ |
| $R_n$ | net radiation above canopy, $W\ m^{-2}$ |
| $r_a$ | canopy external, or aerodynamic resistance, $s\ m^{-1}$ |
| $r_c$ | internal canopy resistance to the transfer of water vapor, $s\ m^{-1}$ |
| $r_s$ | stomatal resistance of the leaf, $s\ m^{-1}$ |
| $t$ | time, s |
| $\Delta T$ | temperature difference between the indoor air and the cover inner surface, K |
| $\Delta T_R$ | temperature correct factor, K |
| $\Delta t$ | time difference, s |
| $u$ | mean air speed, $m\ s^{-1}$ |
| $V_g$ | greenhouse volume, $m^3$ |
| $wd$ | leaf width, m |
| $w_i$ | indoor air humidity ratio, $kg_w\ kg_{air}^{-1}$ |
| $w_o$ | outdoor air humidity ratio, $kg_w\ kg_{air}^{-1}$ |
| $\gamma$ | psychrometric constant, $kPa\ K^{-1}$ |
| $\Delta$ | slope of water saturation vapor pressure curve, $kPa\ K^{-1}$ |
| $\lambda$ | latent heat of water vaporization, $kJ\ kg^{-1}$ |
| $\rho$ | air density, $kg\ m^{-3}$ |

***Subscripts***

| | |
|---|---|
| *add* | added to the greenhouse air |
| *c* | condensation or cover |
| *d* | daytime |
| *dh* | dehumidification |
| *i* | indoor air |
| *n* | nighttime |
| *o* | outside air |
| *p* | plant transpiration |
| *v* | ventilation or infiltration |

***Abbreviations***

| | |
|---|---|
| *ACH* | air exchange per hour, $h^{-1}$ |
| *AER* | air exchange rate, $m^3\ s^{-1}$ |
| *ET* | evapotranspiration, $kg\ m^{-2}\ h^{-1}$ |
| *MAPE* | mean absolute percentage error, % |
| $R^2$ | coefficient of determination |
| *RH* | relative humidity, % |
| *RMSE* | root mean square error |
| *VPD* | vapor pressure deficit, kPa |

## 7.3 Introduction

Humidity control inside a greenhouse draws more and more attention from greenhouse growers. Under northern latitudes, an airtight greenhouse is desired for reducing heat loss and energy consumption (Campen et al., 2003, De Halleux and Gauthier, 1998); however, moisture is captured inside the greenhouse causing high relative humidity (RH), which could lead to a loss of

plants due to fungal diseases, leaf necrosis and calcium deficiencies thus reducing crop production and produce quality (Bakker, 1991; Campen et al., 2003; Körner and Challa, 2003). According to Han et al. (2016), loss of plants due to high humidity could reach up to 45% in a commercial greenhouse if there were no dehumidification measures taken.

Han et al. (2015b) used an air-to-air heat exchanger to provide dehumidification for a commercial greenhouse in Saskatchewan, Canada. However, the study was based solely on experimentation, which lacked a theoretical model for dehumidification need prediction. López Mosquera and Martínez Cortizas (1993) analyzed water balance in a tunnel greenhouse, which focused only on the irrigation water balance and did not study the air moisture balance that is directly related to humidity control. De Halleux and Gauthier (1998) developed a greenhouse water balance model, which took evapotranspiration, condensation on the cladding and infiltration and ventilation into account. They applied this model to simulate and predict the energy consumption for dehumidification by ventilation. However, no further discussions were included as to the indoor RH conditions as well as the dehumidification requirements. A similar issue was found in a study conducted by Chandra et al. (1981), who applied a heat and moisture balance model to predict the canopy and greenhouse floor surface temperature, but no information was stated as to the greenhouse dehumidification requirements.

HORTITRANS, a model for estimating the inside humidity as a function of the incoming solar radiation, indoor air temperature, ventilation rate, outdoor air temperature and the RH was presented by Jolliet (1994). The indoor water vapor partial pressure was estimated for a greenhouse by a linearized vapor balance equation, but its application was restricted to the study greenhouse due to the time constant of the system. Stanghellini and De Jong (1995) firstly brought up to solve the moisture balance model by a first order differential equation; however, many parameters were included in their model for the estimation of plant transpiration, condensation, and ventilation. In addition, instead of using the parameter of vapor concentration (kg $m^{-3}$) in their research, relative humidity (RH) or *VPD* (vapor pressure deficit, which is defined as the difference between the saturation water vapor pressure and the actual air water vapor pressure) is used most often as an indicator of the current humidity conditions (Castilla, 2012a).

In modern commercial greenhouses, especially in cold regions, exhaust fan dehumidification is not economical due to significant heat loss during the long heating season extending from

September to April. Also, exhaust fan dehumidification is not effective during humid and warm periods (Han et al., 2015a). Other dehumidification methods should be taken into consideration, such as air-to-air heat exchangers, mechanical refrigeration dehumidifiers, chemical desiccant dehumidifiers, etc. The critical information needed for selecting a dehumidifier for a greenhouse is how to estimate the dehumidifying requirements as greenhouse moisture sources and sinks, such as evapotranspiration, condensation, and ventilation, are all dynamic and difficult to predict. Hence, efforts should be made to explore a method of estimating the dehumidification requirements for greenhouses.

The objective of this study was to develop and validate a moisture balance model named HumidMod to estimate the indoor relative humidity and water vapor partial pressure of greenhouses. This model was also aimed at quantifying and adjusting the dehumidification requirements to maintain a predetermined RH level in a greenhouse.

## 7.4 Theoretical Principle of Moisture Balance Model HumidMod

Evapotranspiration (*ET*) is the main moisture source of greenhouse indoor air. It is the combination of two separate processes whereby water is lost on one hand by plant transpiration and on the other hand from soil face by evaporation. Compared to plant transpiration, evaporation from soil surface is much smaller. Other than that, a fogging system or evaporative cooling is another source if applied in the greenhouse for cooling or humidification purposes. The moisture sinks in greenhouses include the condensation on the greenhouse roof and plant leaves, air exchange by ventilation and infiltration and the dehumidification systems used for moisture removal from greenhouses. Condensation may also be a moisture source during the daytime. Air exchange may also be a moisture source when the ambient humidity ratio is higher than the indoor air humidity ratio. The following are some assumptions of the moisture balance model.

1. The indoor temperature and RH are uniformly distributed because the mechanical air-circulation system is used to avoid air stratification in modern commercial greenhouses.

2. No additional water or moisture is introduced into the greenhouse at night because no irrigation or fogging system is used at that time.

3. Plant leaf surface temperature is considered the same as the indoor air temperature because of negligible temperature differences would occur when the indoor temperature is maintained at the set point.

4. Condensation on the plant leaves is considered negligible due to the surface temperature of plant leaves which is the same as the indoor air temperature that is much higher than the indoor air dew point temperature.

5. Condensation on the side walls is considered negligible as the modern greenhouse in cold regions is well-insulated.

Based on the assumptions, the transient moisture balance model of a greenhouse can be described by the following Equation 7.1:

$$\frac{0.62 \cdot \rho_i \cdot V_g}{A_g \cdot P} \frac{de_i}{dt} = E_P(t) + E_{add}(t) - E_c(t) - E_v(t) - E_{dh}(t) \qquad (7.1),$$

where $\rho_i$ is the indoor air density, in kg $m^{-3}$; $V_g$ is the volume of the greenhouse, in $m^3$; $A_g$ is the greenhouse floor area, in $m^2$; $P$ is the atmospheric pressure, in kPa; $e_i$ is the air water vapor partial pressure, in kPa; $t$ is time, in s; and 0.62 is the ratio of molecular mass of water vapor and air. The term on the left side of Equation 7.1 represents the variation of humidity ratio of the greenhouse air with time $t$. The first term $E_p(t)$ on the right side of Equation 7.1 is evapotranspiration, in kg $m^{-2}$ $h^{-1}$; the second term $E_{add}(t)$ is the moisture added to or extracted from the greenhouse air, in in kg $m^{-2}$ $h^{-1}$; the third term $E_c(t)$ is condensation on the greenhouse inner cover surface, in in kg $m^{-2}$ $h^{-1}$; the fourth term $E_v(t)$ is moisture exchange between the inside and outside air by air exchange (ventilation or infiltration), in in kg $m^{-2}$ $h^{-1}$; the last term $E_{dh}(t)$ is moisture removed from the greenhouse air by dehumidification, in in kg $m^{-2}$ $h^{-1}$.

### 7.4.1 Evapotranspiration

Sufficient evidence illustrates that plant transpiration is the main source of moisture in greenhouses, even when the leaf stomata are closed at night (Seginer et al., 1990). According to Rosengerg et al. (1983), most of the water taken by plants through its roots are transpired into the air with only 1% involved in metabolic activities. To maintain a desired level of RH in greenhouses, accurate estimation of plant transpiration rate becomes crucial.

There are a few models reported to calculate evapotranspiration (Villarreal-Guerrero et al. 2012). A rather well-known model is the Penman-Monteith ET model (P-M model), which is modified by Monteith (1965) based on the model developed by Penman (1948); however, it is mainly applicable for field crops. Takakura et al. (2005) developed another model (Takakura Model) based on the heat balance of the plant canopy to predict the crop evapotranspiration. Although simpler than the P-M model and providing good evapotranspiration predictions for tomato crops, the net solar radiation on the canopy for the Takakura Model needs to be measured by a special crop solarimeter as well as the canopy surface temperature (Takakura et al., 2009), which limits the application of this model. Stanghellini (1987) included leaf area index (*LAI*) into the P-M model and it was proved to have high accuracy for crop evapotranspiration prediction (Jolliet and Bailey, 1992, López-Cruz et al., 2008, Prenger et al., 2002, Villarreal-Guerrero et al. 2012). Hence, the Stanghellini model has been selected in the present study for predicting crop evapotranspiration, as shown in Equation 7.2.

$$E_P\lambda = \frac{\Delta \cdot R_n + \left(\frac{2 \cdot LAI \cdot \rho_i \cdot C_P}{r_a}\right)(e_s - e_i)}{\Delta + \gamma \cdot \left(1 + \frac{r_c}{r_a}\right)} \qquad (7.2),$$

where $E_p$ is evapotranspiration rate, in kg $m^{-2}$ $h^{-1}$; $\lambda$ is the latent heat of water vaporization, in kJ $kg^{-1}$; $\Delta$ is the slope of water saturation vapor pressure curve, in kPa $K^{-1}$; $R_n$ is the net solar radiation getting into the greenhouse, in W $m^{-2}$; *LAI* is plant leaf area index; $C_P$ is the specific heat of water, in J $kg^{-1}$ $K^{-1}$; $e_s$ is air water vapor pressure at saturation, in kPa; $\gamma$ is psychrometric constant, in kPa $K^{-1}$; and $r_c$ is the internal canopy resistance to the transfer of water vapor, in s $m^{-1}$.

The net solar radiation at the crop surface is calculated as follows (Stanghellini, 1987; Villarreal-Guerrero, et al., 2012):

$$R_n = 0.86 \times (1 - \exp(1 - 0.7 \cdot LAI)) \cdot I_s \qquad (7.3),$$

where $I_s$ is the incoming solar shortwave radiation above the canopy, in W $m^{-2}$.

The internal canopy resistance can be calculated from the following relationship (Bailey et al., 1993; Montero et al., 2001):

$$r_c = \frac{r_s}{LAI} \qquad (7.4),$$

where $r_s$ is the stomatal resistance of the leaf, which can be estimated from (Boulard et al., 1991; Boulard and Wang, 2000):

$$r_s = 200 \times \left(1 + \frac{1}{\exp\left(0.05 \times (I_s - 50)\right)}\right) \qquad (7.5).$$

The aerodynamic resistance is given by (Boulard and Wang, 2000):

$$r_a = 220 \times \frac{l_f^{0.2}}{u_i^{0.8}} \qquad (7.6),$$

where $l_f$ is the characteristic dimension of a leaf, in m, and $u_i$ the greenhouse indoor air speed, in m $s^{-1}$.

This HumidMod model can be applied for any kind of greenhouse crops. The characteristic length of the tomato leaf was calculated using the following Equation 7.7 (Montero et al., 2001; Rouphael and Colla, 2004).

$$l_f = \frac{2}{\left(\frac{1}{l}\right) + \left(\frac{1}{wd}\right)} \qquad (7.7),$$

where $l$ is the leaf length, in m; and $wd$ is the leaf width, in m.

### 7.4.2 Condensation on the greenhouse cover

Water condensation on the greenhouse inner cover surface when the inner cover surface temperature is lower than the indoor air dew point temperature is one of the most important moisture sink. Although condensation most likely is a moisture sink for greenhouses as the most condensate will flow or drip down to the ground; however, it can also be a moisture source during the morning when the cover inner surface temperature increases to higher than the dew point temperature of the indoor air due to the incoming solar radiation. The amount of condensate is proportional to the difference between the inside air vapor pressure and the saturation vapor pressure at the cover inner surface temperature. It is calculated using the following Equation 7.8 (De Freitas and Schmekal, 2003).

$$E_c = 3600 \times \frac{0.67 \cdot h_{ci} \cdot (e_i - e_{sc})}{C_p \cdot P} = \frac{2.4 \times 10^3 \cdot h_{ci} \cdot (e_i - e_{sc})}{C_p \cdot P} \qquad (7.8),$$

where $E_c$ is condensation rate on the greenhouse inner cover surface, in kg $m^{-2}$ $h^{-1}$; $h_{ci}$ is the convective heat transfer coefficient at the greenhouse cover inner surface, in W $m^{-2}$ $K^{-1}$; and $e_{sc}$ is the saturation air water vapor pressure at the greenhouse inner cover surface temperature, kPa.

The equation is not complicated; however, it is difficult to determine the convective heat transfer coefficient. Han and Guo (Chapter 6) explored the relationship between the measured condensation rate on the greenhouse inner cover surface and the indoor and outdoor environment conditions experimentally. The research was conducted in a Venlo-type greenhouse covered by a double layer of polyethylene plastic film. From in situ measurements, they obtained the following Equations 7.9 and 7.10 for condensation rate calculations during the daytime and nighttime (Chapter 6):

$$\text{Daytime} \quad CR_d = 0.74 + 0.43 \cdot \Delta T + 0.02 \cdot I_s \qquad (7.9),$$

$$\text{Nighttime} \quad CR_n = -0.29 + 85.51 \cdot u_c + 0.45 \cdot \Delta T \qquad (7.10),$$

where $CR_d$ and $CR_n$ represent the daytime and nighttime condensation rate, which are both scaled to the ground area, in g $m^{-2}$ $h^{-1}$; $\Delta T$ is the temperature difference between the indoor air and the cover inner surface, in K; and $u_c$ is the air speed near the greenhouse inner cover surface, in m $s^{-1}$. The calculated values are the net condensate change on the inner cover surface within one hour. More detailed information about the measured condensation rate and the two equations can be found in the manuscripts by Han et al. (Chapter 5) and Han and Guo (Chapter 6).

### 7.4.3 Air exchange by ventilation and infiltration

Although the exhaust fan ventilation system is designed for temperature control during the spring, summer and fall seasons when the indoor temperature is high, it also helps to remove the moisture from the greenhouse, especially during the daytime. At nighttime, the ventilation system would be shut down, meanwhile, infiltration becomes the only way for air exchange. The moisture removed from the greenhouse by air exchange including ventilation and infiltration can be calculated as follows.

$$E_v = \frac{\rho_i \cdot q_v \cdot (w_i - w_o)}{A_g} = \frac{0.62 \cdot \rho_i \cdot q_v \cdot (e_i - e_o)}{A_g \cdot P} \qquad (7.11),$$

where $E_v$ is the moisture removal rate by ventilation or through infiltration, in kg $m^{-2}$ $h^{-1}$; $q_v$ is the air flow rate due to ventilation or infiltration, in $m^3$ $h^{-1}$; $w_i$ is the humidity ratio of the inside air, in $kg_w$ $kg_{air}^{-1}$; $w_o$ is the humidity ratio of the outdoor air, in $kg_w$ $kg_{air}^{-1}$; and $e_o$ is the outdoor air water vapor partial pressure, in kPa.

### 7.4.4 Dehumidification

If any dehumidification measure is applied in the greenhouse, such as mechanical refrigeration dehumidifier, then the moisture removal rate by the dehumidification method can be expressed by:

$$E_{dh} = \frac{M_{water}}{A_g \cdot \Delta t} \qquad (7.12),$$

where $E_{dh}$ is the moisture removal rate by the dehumidification method, in kg $m^{-2}$ $h^{-1}$; $M_{water}$ is the amount of water extracted by the dehumidification method, in kg; and $\Delta t$ is time difference, in s.

### 7.4.5 Prediction of inside water vapor partial pressure and RH

By introducing Equations 7.2 and 7.11 into the moisture balance model of Equation 7.1, Equation 7.1 becomes:

$$\frac{0.62 \cdot \rho_i \cdot V_g}{A_g \cdot P}\frac{de_i}{dt} = 3.6 \times \frac{\Delta \cdot R_n}{\lambda \cdot \left(\Delta + \gamma \cdot \left(1 + \frac{r_c}{r_a}\right)\right)} + 3.6 \times \frac{(2 \cdot LAI \cdot \rho_i \cdot \frac{C_P}{r_a})}{\lambda \cdot \left(\Delta + \gamma \cdot \left(1 + \frac{r_c}{r_a}\right)\right)} \times e_s - 3.6 \times \frac{\left(2 \cdot LAI \cdot \rho_i \cdot \frac{C_P}{r_a}\right)}{\lambda \cdot \left(\Delta + \gamma \cdot \left(1 + \frac{r_c}{r_a}\right)\right)} \times$$

$$e_i - \frac{0.62 \cdot \rho_i \cdot q_v}{A_g \cdot P} \times e_i + \frac{0.62 \cdot \rho_i \cdot q_v}{A_g \cdot P} \times e_o - E_c - E_{dh} \qquad (7.13).$$

Then Equation 7.13 can be simplified as:

$$\frac{de_i}{dt} + \frac{A_g \cdot P}{0.62 \cdot \rho_i \cdot V_g} \times (b + f) \times e_i = \frac{A_g \cdot P}{0.62 \cdot \rho_i \cdot V_g} \times (a + b \cdot e_s + f \cdot e_o - E_c - E_{dh}) \qquad (7.14).$$

The above equation can be written in the following form:

$$\frac{de_i}{dt} + A \cdot e_i = B \qquad (7.15),$$

where $A$ and $B$ are given by:

$$A = \frac{A_g \cdot P}{0.62 \cdot \rho_i \cdot V_g} \times (b + f), \qquad B = \frac{A_g \cdot P}{0.62 \cdot \rho_i \cdot V_g} \times (a + b \cdot e_s + f \cdot e_o - E_c - E_{dh}).$$

The terms of *a*, *b*, and *f* in the above two equations are defined as:

$$a = \frac{3.6 \cdot \Delta \cdot R_n}{\lambda \cdot (\Delta + \gamma \cdot (1 + \frac{r_c}{r_a})}, \qquad b = \frac{7.2 \cdot LAI \cdot \rho_i \cdot \frac{C_P}{r_a}}{\lambda \cdot (\Delta + \gamma \cdot (1 + \frac{r_c}{r_a})}, \qquad f = \frac{0.62 \cdot \rho_i \cdot q_v}{A_g \cdot P}.$$

Differential Equation 7.15 is solved following linear ordinary differential equation of the first order method. The solution of Equation 7.15 can be given by:

$$e_i = \frac{B}{A} \pm C \cdot e^{-At} \qquad (7.16),$$

where *C* is the constant value when $t = 0$.

The indoor air water vapor partial pressure can be estimated as a function of the indoor and outdoor environment conditions by using Equation 7.16. Then, the indoor RH can be calculated for a given air temperature and humidity ratio as follows:

$$RH = \frac{e_i}{e_s} \times 100\% \qquad (7.17).$$

### 7.4.6 Program design

MATLAB software (MATLAB 2014a, The MathWorks Inc., Natick, MA, USA) was used to solve the mathematical equations and simulate the indoor RH and water vapor partial pressure conditions of a greenhouse. The program is named HumidMod. A programming flow chart for the HumidMod model is shown in Figure 7.1. The input parameters of the HumidMod model include constant values of greenhouse characteristics, air thermal properties and others ($\Delta$, $\gamma$, $\lambda$). The input parameters include the experimentally measured data inside and outside of the greenhouse. The RH of indoor air and air water vapor partial pressure are the output of the HumidMod model. The input measured variables can be hourly averaged data or average data at any length of time, so the outputs depend on the inputs, either hourly data or data at other time intervals. Therefore, the HumidMod model can do either hourly, daily, monthly or yearly simulation.

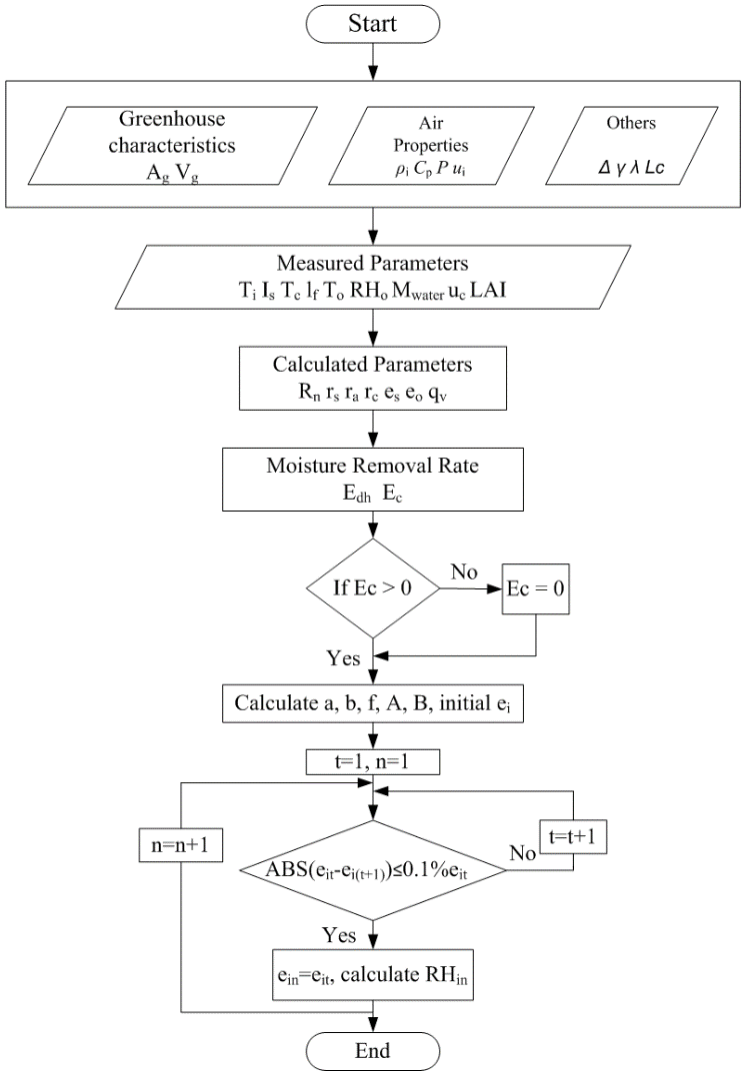


**Figure 7.1. Programming flow chart.**

## 7.5 Model Validation

An experiment was conducted in a Venlo-type plastic greenhouse from March to November 2014 to collect data for the moisture balance model validation. A commercial refrigeration dehumidifier inside the greenhouse was used for humidity control. The measured data from the greenhouse were used to validate the moisture balance model.

### 7.5.1 Experimental greenhouse

Tomato plants were grown in the four-span greenhouse located in Grandora, Saskatchewan, 25 km west of Saskatoon, with 52.11º latitude, 106.98º longitude and 504 m elevation.

The greenhouse was covered by an inflated double layer 6-mil polythene plastic film on the roof and the polyethylene panel on the side walls except the north wall which was an insulated wooden wall. The thickness of the north wall was 11.4 cm with thermal conductivity of 0.23 W $m^{-2}$ $K^{-1}$. The greenhouse was 25.6 m wide and 43.9 m long. The eave height was 4.3 m and the ridge height was 6.7 m. Each tomato plant was planted in a peat-based growing medium bag, and the plants were planted in 15 rows with a total of 2,850 plants, averaging 2.5 plants per square meter. The greenhouse was heated by black iron hot water pipes located above ground between rows of tomato plants. Four natural gas boilers were used to heat the hot water. It had four exhaust fans (FC050-4E exhaust fan, ZIEHL-ABEGG, Saint e-Claire, QC, Canada) placed on the east wall at a height of 3.8 m with roof vents for cooling. The exhaust fans with a propeller diameter of 0.548 m had the capacity of 2.1 $m^3$ $s^{-1}$ at the static pressure of 20 Pa (Axial Fans Main Catalogue FC, 2012). A drip irrigation system was used for water and nutrient supply. Table 7.1 summarizes the greenhouse information as well as constant variables and corresponding units used in the models.

**Table 7.1. Constant variables adopted for the greenhouse moisture balance model.**

| Greenhouse characteristics | |
|---|---|
| Length (m) | 43.9 |
| Width (m) | 25.6 |
| Floor Area $A_g$ ($m^2$) | 1123.8 |
| Volume $V_g$ ($m^3$) | 6182.1 |
| Air velocity $u_i$ (m $s^{-1}$) | 0.15 |
| Air thermal properties (at 20°C) | |
| Density $\rho_i$ (kg $m^{-3}$) | 1.205 |
| Pressure $P$ (Pa) | 101.3 |
| Specific heat $C_P$ (J $kg^{-1}$ $K^{-1}$) | 1005 |
| Others | |
| Slope of water saturation vapor pressure curve $\Delta$ (kPa $K^{-1}$) | 0.145 (at 20°C) |
| Psychrometric constant $\gamma$ (kPa $K^{-1}$) | 0.0668 |
| Latent heat of water vaporization $\lambda$ (kJ $kg^{-1}$) | 2450 |

### 7.5.2 Refrigeration dehumidifier

A commercial mechanical refrigeration dehumidifier (DCA3000T, Dehumidifier Corporation of America, Cedarburg, WI, USA) was installed in the greenhouse, as shown in Figure 7.2. The

unit had a moisture removal capacity of 14.7 L $h^{-1}$ under 75% RH and 21°C. It was housed in a small room attached to the east end of the greenhouse. A discharge metal-duct along the east end of wall along with perforated plastic film duct branches which run east-west along the tomato rows above the ground was used to distribute the drier and warmer exhaust air from the dehumidifier evenly into the greenhouse. A tank with a total volume of 670 L was used to collect the water condensed from the dehumidifier. The dehumidifier had its own humidity control sensor, which was at the center of the greenhouse together with the other environmental monitoring sensors. As the required dehumidifying capacity for the greenhouse was higher than the dehumidifier capacity, the RH set point of the dehumidifier was set at 60% to control the indoor RH at around 75% to shorten high humidity period. The exhaust air temperature and RH from the dehumidifier were measured by a type-T thermocouple (Omega Engineering, Inc., Quebec, Canada) and a humidity sensor (HM1500LF, Measurement Specialties, Inc., Toulouse, France). The thermocouples had an accuracy of 0.3°C at 100°C and were calibrated against a thermocouple simulator-calibrator (model 1100, Ectron Corp., San Diego, Cal.). The humidity sensor had an accuracy of ±3% in the RH measurement range of 10% to 90%. A humidity generator (model 1200, Thunder Scientific Corp., Albuquerque, N.M.) was used to calibrate the sensor. Both sensors were placed inside the metal duct near the outlet of the dehumidifier. The power consumption of the dehumidifier was monitored by a current sensor (AT50 B10, LEM, Inc., Milwaukee, Wisc).


(a) (b)

**Figure 7.2. (a) Dehumidifier setup and the water tank; (b) the discharge metal-duct.**

### 7.5.3 Data collection

Figure 7.3 illustrates the locations of all the sensors used to measure the greenhouse and plant related variables. The greenhouse indoor air temperature and RH were measured by a temperature and relative humidity probe (CS500, Campbell Scientific Inc., Edmonton, AB, Canada), which was placed inside a radiation shield and installed at the center of the greenhouse, 1.8 m above the ground. The probe had an accuracy of ±0.2 to ±1.4°C over a temperature measurement range of -40 to 60°C, and ±3% over the range of 10 to 90% and ±6% in the range of 90 to 100% with RH measurement. A pyranometer sensor (LI-200, LI-COR Inc., Lincoln, NE, USA) was installed inside the greenhouse at the ridge height to measure the inside solar radiation. Two air velocity transducers (TSI Model 8475, Minneapolis, MN, USA) with the measuring range of 0 to 1.0 m/s were installed in the greenhouse. Both had the minimum resolution of 0.07% over the measuring full scales. One was placed on the first span and the other one was put at the second span. Both were put close to the eave at the east end of the greenhouse. A current sensor (AT50 B10, LEM, Inc., Milwaukee, WI, USA) was used for monitoring the power consumption of the exhaust fan. The indoor $CO_2$ concentration was measured with a K-30 sensor (CO2Meter, Inc., Ormond Beach, FL, USA) that was installed inside the greenhouse above the plants. Three T-type thermocouples were used to measure the greenhouse cover surface temperatures, which were adhered directly to the greenhouse cover surface near the air velocity transducers. A correction factor ($\Delta T_R$) for the cover temperature measured by the thermocouples with 0.3 mm in diameter is used, which is calculated using Equation 7.18 as suggested by Abdel-Ghany et al. (2006):

$$\Delta T_R = -0.22 + 5.11 \times (1.0 - \exp(-0.0024 \times I_s)) \quad R^2 = 0.94 \quad (7.18).$$

The actual cover temperature is obtained by subtracting $\Delta T_R$ from the measured temperature.

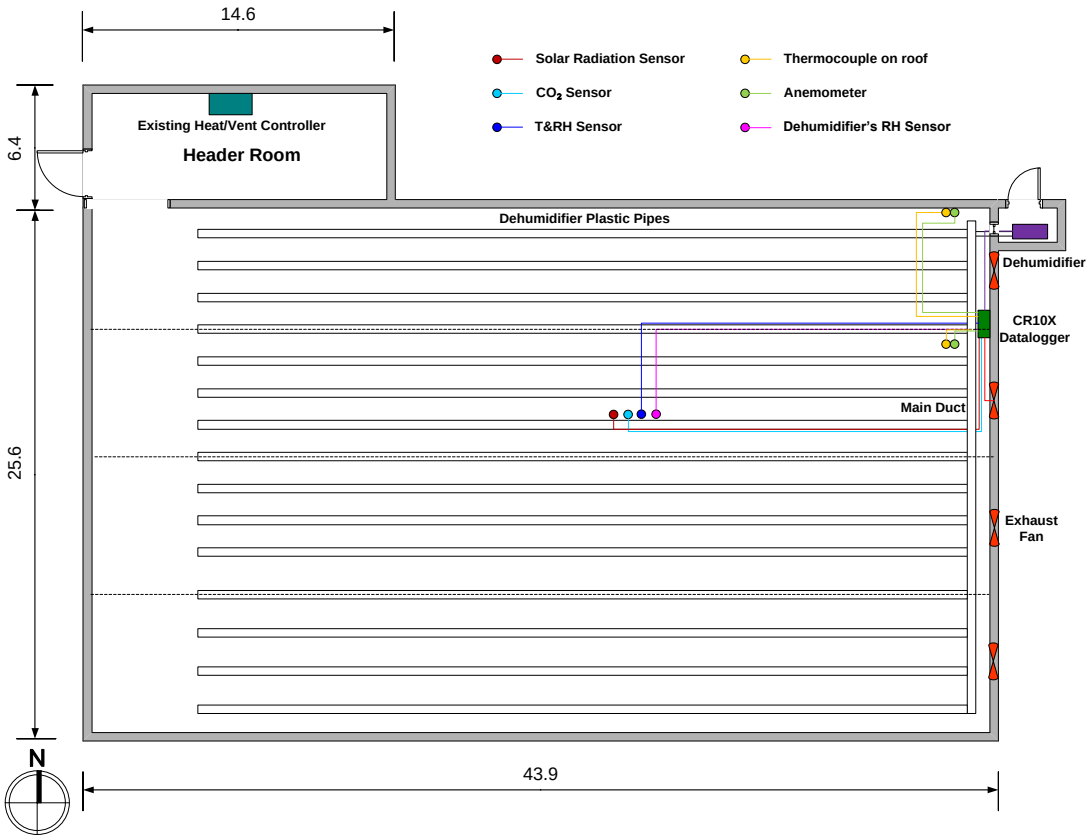


**Figure 7.3. Greenhouse layout and sensor locations (dimensions are in meters).**

A CR10X data logger (Campbell Scientific Inc., Edmonton, AB, Canada) was installed near the east wall of the greenhouse. The indoor air temperature and RH data, solar radiation, air velocity near the roof, thermocouples as well as the currents of the exhaust fans and dehumidifier were all monitored minute by minute, with 10 min averages recorded by the data logger. The other pieces of ventilation and heating equipment were controlled by the greenhouse ventilation control system based on temperature. The temperature sensor was installed in the middle of the greenhouse at a height of 1.5 m.

In addition to the environmental parameters, the dimensional parameters of plant leaves were also measured on three randomly chosen plants in the middle of each month. The measured dimensional parameters included leaf length ($l$), leaf width ($wd$), and leaf numbers. The relationship between plant leaf dimensions and leaf area ($A_l$) was determined from 71 healthy leaves of different sizes from 4 growing plants. The areas of leaves were measured with a leaf area meter (LI-3100C,

LI-COR Inc., Lincoln, NE, USA). Equation 7.19 gives the regression relationship between $A_l$ and the leaf length and width:

$$A_l = 0.68 \times l \times wd + 1.20 \quad (R^2 = 0.97) \qquad (7.19).$$

### 7.5.4 Model performance evaluation criteria

To evaluate the model, the following statistical parameters were used: *MAPE* (mean absolute percentage error), *RMSE* (root mean square error), and coefficient of determination ($R^2$). They are defined as (Taki et al., 2016; Piscia et al., 2012; Yu et al., 2011):

$$MAPE = \frac{1}{n}\sum_{i=1}^{n}\left|\frac{O_i - P_i}{O_i}\right| \times 100 \qquad (7.20),$$

$$RMSE = \left(\frac{\sum_{i=1}^{n}(O_i - P_i)^2}{n}\right)^{1/2} \qquad (7.21),$$

$$R^2 = \left(\frac{\sum_{i=1}^{n}(O_i - \overline{O})(P_i - \overline{P})}{\sqrt{\sum_{i=1}^{n}(O_i - \overline{O})^2}\sqrt{\sum_{i=1}^{n}(P_i - \overline{P})^2}}\right)^2 \qquad (7.22),$$

where $O_i$ is the $i^{th}$ component of the measured value; $\overline{O}$ is the average of the measured value; $P_i$ is the $i^{th}$ component of the predicted value; and $\overline{P}$ is the average of the predicted value.

## 7.6 Results and Discussion

Data collection was conducted from March to November in 2014. The plant size and indoor environmental conditions are usually similar from June until August, therefore, the data collected in July were chosen to represent the summer months. Besides, the dehumidifier did not begin to work until April 18, therefore, the data collected in May, July, October, and November were used to validate the model.

### 7.6.1 Greenhouse internal climatic condition

Figure 7.4 shows the monthly percentages of indoor RH exceeding 75%, 80% and 85%, respectively. The percentages of the total time when the indoor RH were over 75% and 80% were

both the highest in April, which could be due to the high evapotranspiration rate of crops and the less use of the dehumidifier. Even though high RH occurred during spring and summer time, less than 40% of time RH exceeded 80%, except in April. The percentile exceeding 85% RH was low with the maximum 9% in April, June, and August, which was acceptable for the plants. During March, October, and November, the inside RH was much lower than that during other months, which was caused by low crop evapotranspiration rate during March with small plants and high condensation rates on the greenhouse cover surface during October and November. Overall, this dehumidifier could control the indoor RH in acceptable conditions.

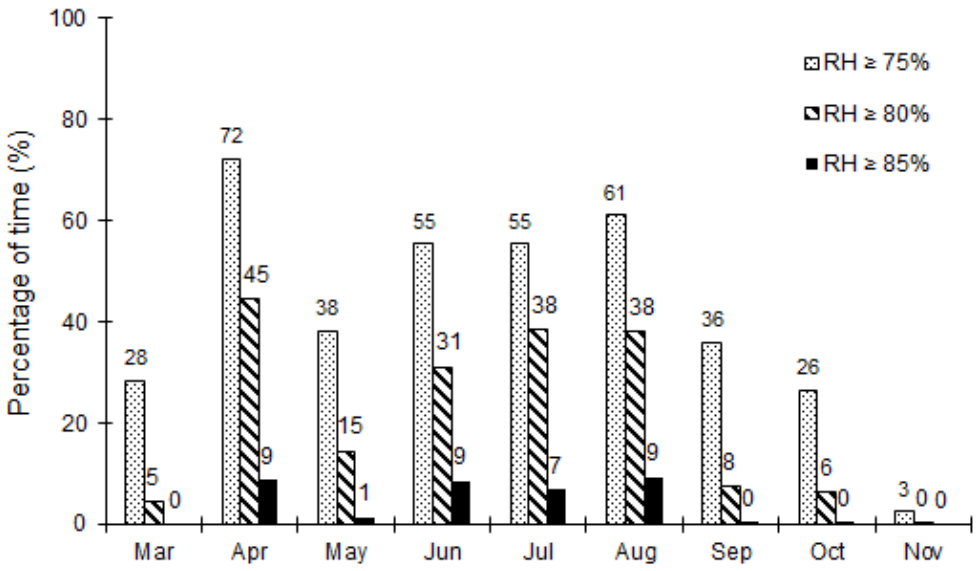


**Figure 7.4. Monthly average indoor high relative humidity (*RH*) occurrence frequencies.**

In general, the RH diurnal profile in the greenhouse was that during the cold season the indoor RH was high during the daytime and low at night, while it was the opposite trend observed under warm and mild weather conditions as low indoor RH during the late morning to the afternoon and high at night and early morning. The reason is that the ventilation during the cold season was minimized to reduce heat loss and the air exchange relied on infiltration. Transpiration and evaporation during the daytime in the greenhouse caused high RH. At night, the low outside temperature caused low inner surface temperatures of the cladding materials leading to condensation; furthermore, the indoor temperature also reduced from 22°C to 19°C, thus reducing the air moisture holding capacity. These two factors caused condensation on the cover interior surface in cold weather, removing moisture from the air. During the mild and warm seasons, the high ventilation rate was required to achieve temperature control brought large volumes of

relatively dry air from outside to replace the moist indoor air during the daytime after the early morning, causing low RH. At night and early morning, the ventilation rate was low due to the relatively low outside temperature, so ventilation was not needed, and little or no condensation occurred, most of the moisture in the air was kept indoor causing the observed high RH.

Figure 7.5 displays the monthly averages of indoor air temperature, RH, and VPD. The VPD had the lowest value of 0.5 kPa in April due to the high indoor RH. The highest VPD value of 1.05 kPa occurred in November due to the lowest indoor RH.

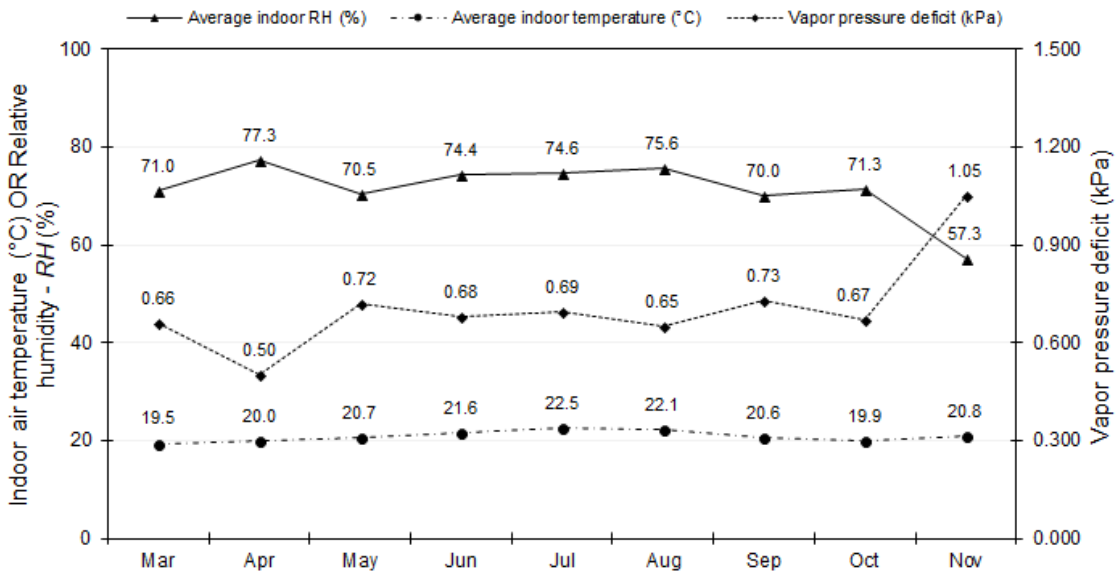


**Figure 7.5. Monthly average indoor temperature (*T*), relative humidity (*RH*), and vapor pressure deficit (*VPD*).**

### 7.6.2 Estimation of air exchange rate

The HumidMod model requires the input of air exchange rate (*AER*) including ventilation and infiltration. Air exchange plays an important role in removing moisture from the greenhouse and it is essential to give an accurate estimation of *AER* if the moisture balance model is used to predict the indoor air RH condition. However, it is difficult to give accurate estimations of *AER* due to the complex operating conditions of the greenhouse. Therefore, a statistical method for *AER* estimation was explored in this study. The first five days of data measured in each month of May, July, October, and November were selected. With the measured evapotranspiration rate, condensation rate, dehumidification rate, as well as the indoor condition, the *AER* was calculated based on the

moisture balance model. The rate was found to have a good exponential relationship with the indoor solar radiation. It is expressed as follows:

$$q_v = c_1 \times \exp(c_2 \times I_s) \quad (7.23),$$

where $c_1$ and $c_2$ are two coefficients. The coefficients of $c_1$ and $c_2$ for the above calculation in each month are listed in Table 7.2. The coefficient of determination ($R^2$) is high for each month and *AER* is highly related to the incoming solar radiation, which is caused by the high correlation between evapotranspiration rate and the incoming solar radiation. However, the relationship exists because during the daytime air exchange rate is mainly determined by the indoor air temperature, which is determined in turn by solar radiation as the greenhouse main heat source caused temperatures to rise in the greenhouse; while during the nighttime, *AER* is solely air infiltration, which is $c_1$ in Equation 7.23. It should be noted that this relationship is obtained from this study greenhouse, further research is needed before it can be applied to other greenhouses.

**Table 7.2. Coefficients of $c_1$ and $c_2$ for air exchange rate (*AER*) estimation.**

| *Month* | *Coefficient* | | | $R^2$ | *Data points* |
|---|---|---|---|---|---|
| | $c_1$ | $c_1^*$ | $c_2$ | | |
| May | 13642 | 12.1 | 0.0046 | 0.92 | 120 |
| Jul | 24580 | 21.9 | 0.0043 | 0.65 | 120 |
| Oct | 9323 | 8.3 | 0.0070 | 0.95 | 120 |
| Nov | 8596 | 7.6 | 0.0055 | 0.92 | 120 |

Note: $c_1^*$ is for the air exchange rate scaled to per square meter of the greenhouse floor area.

Further, the *AER* in each month was estimated using Equation 7.23. The calculated data in each complete month was used for the model validation. According to the calculated results, the air exchange per hour (*ACH*) was 2.2, 4.0, 1.5, and 1.4 $h^{-1}$ during the nighttime in May, July, October, and November, respectively. The maximum *ACH* was 54.1, 79.0, 20.5, and 6.2 $h^{-1}$ during the daytime from May to November, which was reasonable according to Castilla (2012b), who estimated that the greenhouse indoor *ACH* could reach up to 80 $h^{-1}$ during the summer time.

Figure 7.6 displays the predicted average hourly *ACH* from May to November. It was the highest in July, followed by May and then October. The lowest ventilation rate occurred in November when the greenhouse was well sealed to minimize infiltration due to the low ambient temperature.

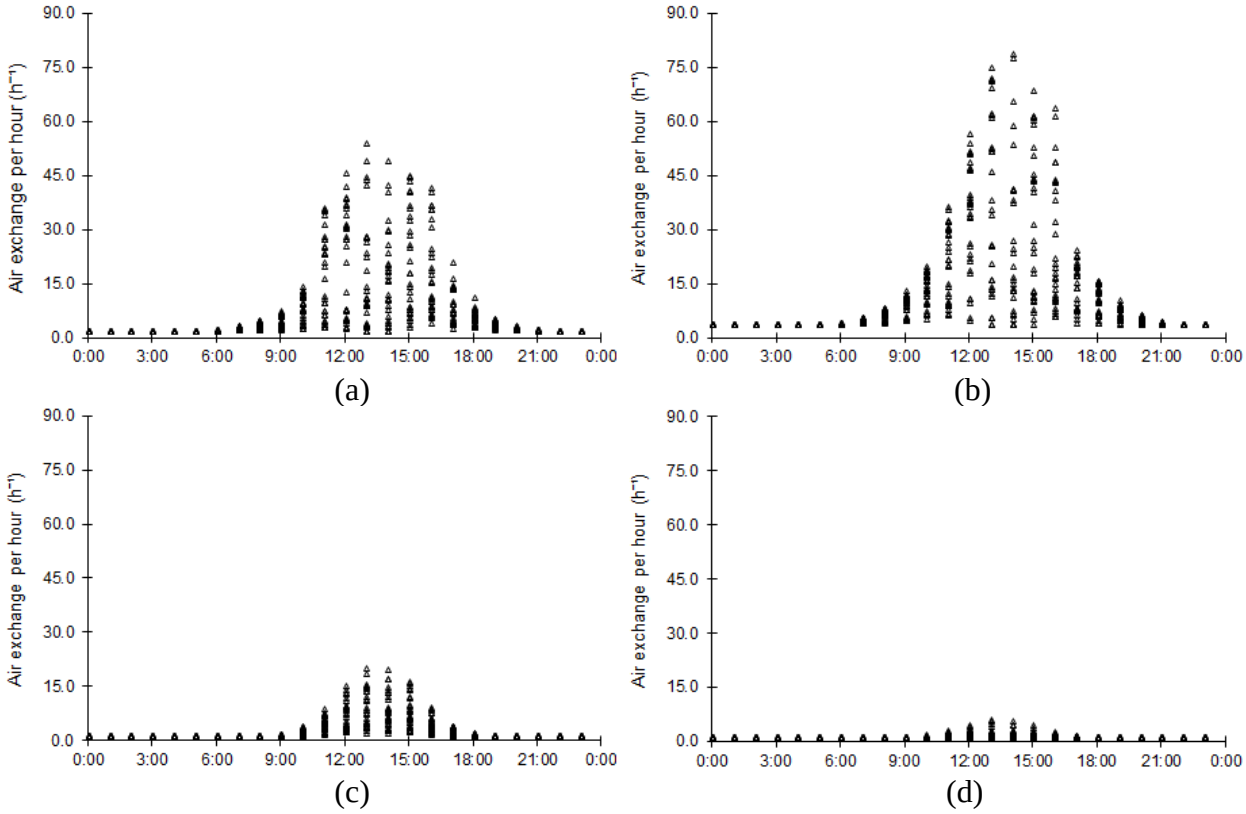


**Figure 7.6. Predicted average diurnal hourly air exchange rate in each month: a. May; b. July; c. October; d. November.**

### 7.6.3 Model prediction of moisture production and removal rates

Figure 7.7 gives the predicted average hourly moisture production or removal rate by evapotranspiration, air exchange, dehumidification and condensation in May, July, October and November, respectively.

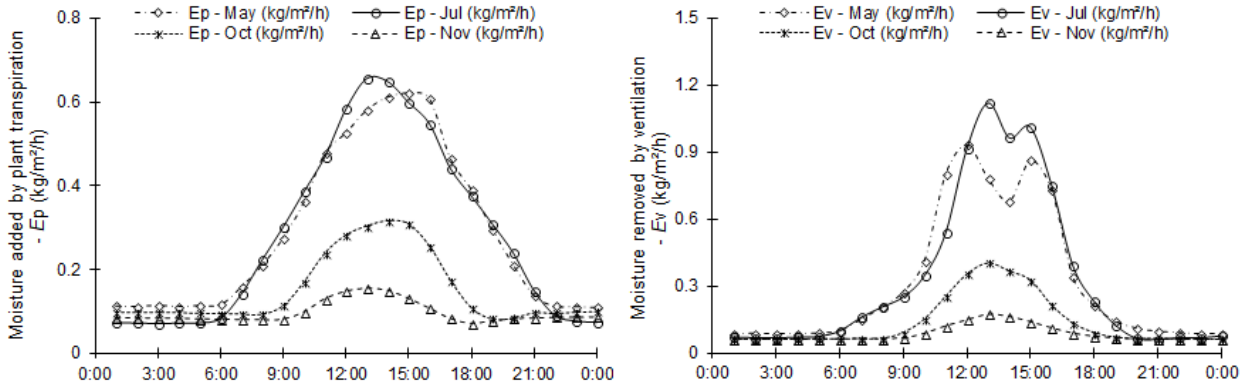

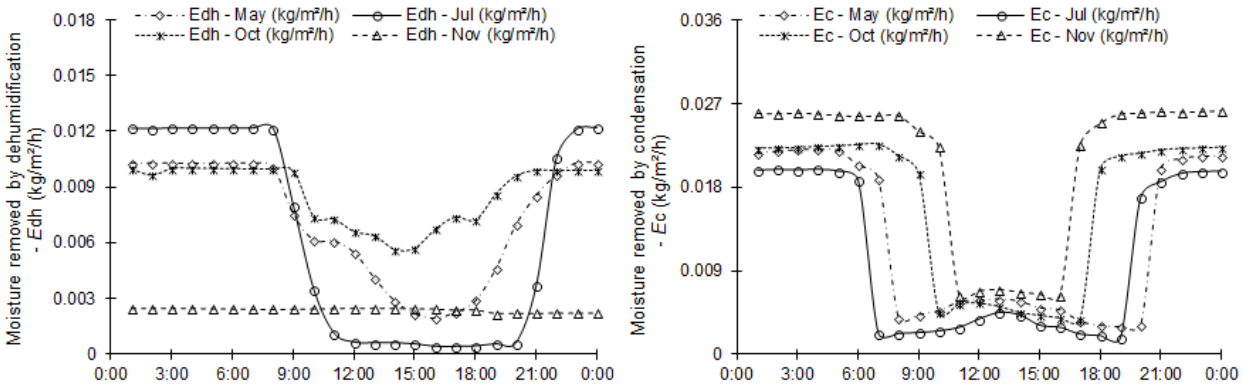


(c) (d)

**Figure 7.7. Comparison of the predicted monthly average moisture production or removal rate by plant transpiration, ventilation, dehumidification, and condensation in May, July, October, and November.**

Figure 7.7 indicates that the evapotranspiration rate in the study greenhouse was similar in May and July. Both were greater than that in October and November. A similar trend was also observed with the moisture removal rate by air exchange. The condensation rate was highest in November due to the cold outside weather conditions, followed by October and May; and it was the lowest in July. The predicted monthly average hourly condensation rate was all positive which means condensation was the sink for most of the time; however, negative hourly values did exist, especially during the early morning in the warm season when the interior cover surface temperature was high enough due to the solar radiation then re-evaporation of the water on the interior surface, if there was any, would occur. During the nighttime, the dehumidifier removed the greatest amount of water from the greenhouse air in July due to the hot and humid indoor air conditions, followed by May and October; while the least water removal occurred in November due to the relatively low indoor RH. However, during the daytime in October and May when the air exchange was low and the RH was high, the dehumidifier was running most of the time and removed more moisture than the other two months. There was none or little water removal from the greenhouse by the dehumidifier in July during the daytime, which was due to the shutdown of the unit by the growers.

Even though the evapotranspiration rate of greenhouse crops was high during the daytime in May and July and there was little or no condensation on the greenhouse cover surface, most of the moisture was discharged from the greenhouse through ventilation. Therefore, the indoor RH was not high during the daytime and there was not much of a need for dehumidification. During the nighttime, little or no condensation on the greenhouse cover surface, the shutdown of the

ventilation system, and low infiltration caused most of the moisture be captured inside the greenhouse, leading to high indoor RH. Therefore, the dehumidifier was kicked in and removed the greatest amount of moisture from the greenhouse at night. On the contrary during the cold months such as in October and November, even though the plants were close to the final stage and the evapotranspiration rate was lower than that in May and July, the ventilation or infiltration rate was low as well due to the cold ambient weather conditions, causing high indoor RH during the daytime and high moisture removal rates by the dehumidifier. At night, the condensation rate on the greenhouse cover was higher compared to that in May and July, causing the decrease of indoor RH, leading no or low dehumidification needs.

To compare the contribution of the four sources or sinks, Figure 7.8 shows the predicted monthly averages of hourly moisture production or removal rate of these sources or sinks during the period with indoor RH exceeding 75%. Evapotranspiration is the only source, all the other three are sinks. The moisture removal rate by dehumidification and condensation was very small as compared to the moisture removal rate by air exchange. The moisture removal by air exchange accounted for 85.3% in July to 91.4% in November of the total amount of moisture removal by all three sinks. The moisture removal by condensation was 1.3 to 1.7 times of that by way of the dehumidifier. Over 91.0% of the moisture was removed by air exchange during the daytime and it was reduced to 70.0% during the nighttime. The average moisture removal by condensation was increased from 3.2% during the daytime to 19.0% at night and early morning. Dehumidifier removed less than 4.9% of the total moisture during the daytime and about 10.5% during the nighttime and early morning.

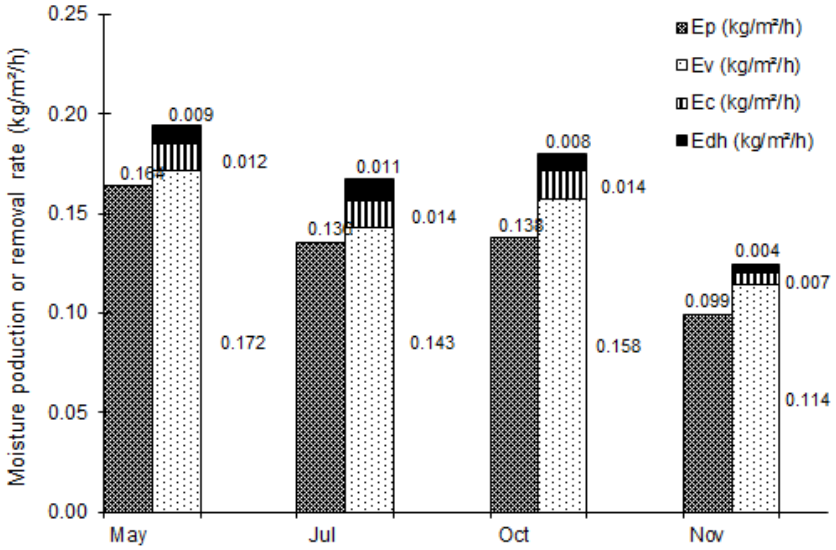


**Figure 7.8. Predicted monthly average of hourly moisture production or removal rate by plant transpiration ($E_p$), ventilation ($E_v$), dehumidification ($E_{dh}$), and condensation ($E_c$).**

Overall, ventilation or infiltration was the main way to remove the moisture from the greenhouse, especially during the daytime. Dehumidification was mostly required during the nighttime in May and July. Due to the limited use of ventilation in the cold months such as in October and November, condensation played an important role in removing the moisture from the greenhouse. However, dehumidification was still necessary, especially during the daytime in winter and nighttime in summer.

### 7.6.4 Validation of HumidMod model

Figure 7.9 shows the comparison of monthly averages of hourly diurnal data between the simulated and the measured indoor RH and $e_i$ in each month from May to November.

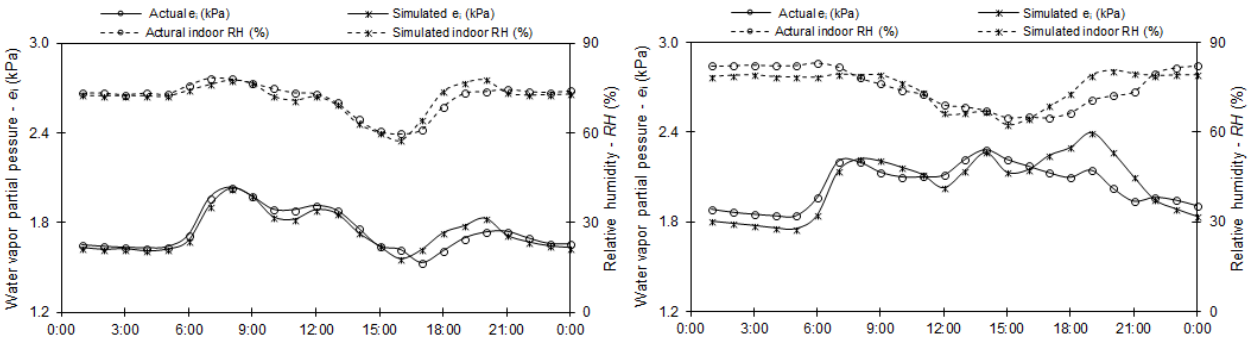


(a) May (b) July

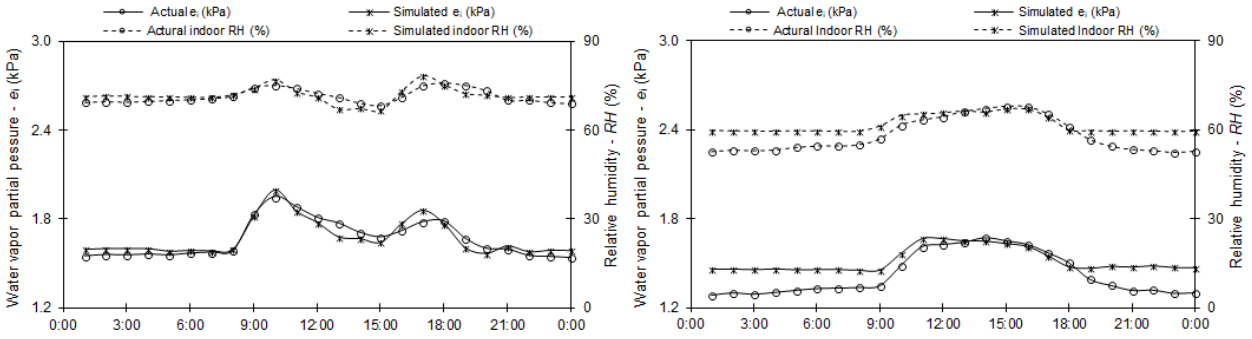


(c) October (d) November

**Figure 7.9. Comparison between the monthly average of diurnal hourly simulated and the measured indoor relative humidity (*RH*) and water vapor partial pressure ($e_i$) in each month.**

The diurnal average predicted data and measured data of RH and air water vapor partial pressure had the same variation pattern. A relatively better agreement between the predicted and the measured data was found in May and October than in July and November. That might be because the predicted condensation rate in May and October had higher accuracy than in July and November compared to the measured data (Chapter 6). Both measured and simulated values had small fluctuation during the night from 22:00 pm until 7:00 am in the early morning; however, in May and July, the simulated values were lower than the measured data while the opposite happened in October and November. During the daytime, both simulated and measured values were very close, and both varied greatly, which means the predicted $E_p$ and $E_v$ were close to the actual values.

Table 7.3 gives some statistical results of comparison between the model predicted results and the experimental results. The percentage of mean absolute error (*MAPE*) for both RH and $e_i$ are between 5.0 and 10.0%. The *RMSE* factor shows that this moisture balance model can estimate the inside $e_i$ with an acceptable accuracy (with about 0.15 kPa difference between predicted and measured values), and the indoor RH with the maximum of 6.4% difference between predicted and measured values. The $R^2$ of RH and $e_i$ in each month were between 0.62 and 0.81, meaning more than 62% of the measured data can be predicted by the moisture balance model, except in October, which was caused by the greater errors between modeled and measured RH values in October.

**Table 7.3. Statistical results of comparison between modeled and measured relative humidity (*RH*) and water vapor partial pressure ($e_i$).**

| *Month* | $R^2$ | | *RMSE* | | *MAPE (%)* | |
|---|---|---|---|---|---|---|
| | *RH* | $e_i$ | *RH (%)* | $e_i$ *(kPa)* | *RH* | $e_i$ |
| May | 0.63 | 0.70 | 5.7 | 0.143 | 6.1 | 6.10 |
| Jul | 0.62 | 0.70 | 5.6 | 0.159 | 6.3 | 6.31 |
| Oct | 0.32 | 0.64 | 4.5 | 0.107 | 5.0 | 5.03 |
| Nov | 0.81 | 0.65 | 6.4 | 0.161 | 10.0 | 9.98 |
| Total | 0.59 | 0.75 | 5.57 | 0.144 | 6.85 | 6.86 |

Figures 7.10 and 7.11 show the scattered plots between predicted and measured values of $e_i$ and RH for the whole four months, respectively. The regression analysis of predicted against measured data gave a gradient of 1.00 for both $e_i$ and RH. The $R^2$ values were 0.75 and 0.59, respectively. The standard error for the simulated $e_i$ and RH were 0.29 kPa and 8.7%, respectively. The errors between the predicted and the measured data would be caused by the uncertainty in estimated moisture removal by condensation and air exchange. However, considering the difficulty of estimating condensation rate and air exchange rate, the accuracy of the model is acceptable.

There may be several applications of this model: (1) the direct estimation of evapotranspiration and condensation rate on the greenhouse inner cover surface; (2) the prediction of the greenhouse indoor air RH and water vapor partial pressure; (3) the estimation of the greenhouse dehumidification requirement for humidity control with the known of greenhouse environmental conditions and plant characteristics.

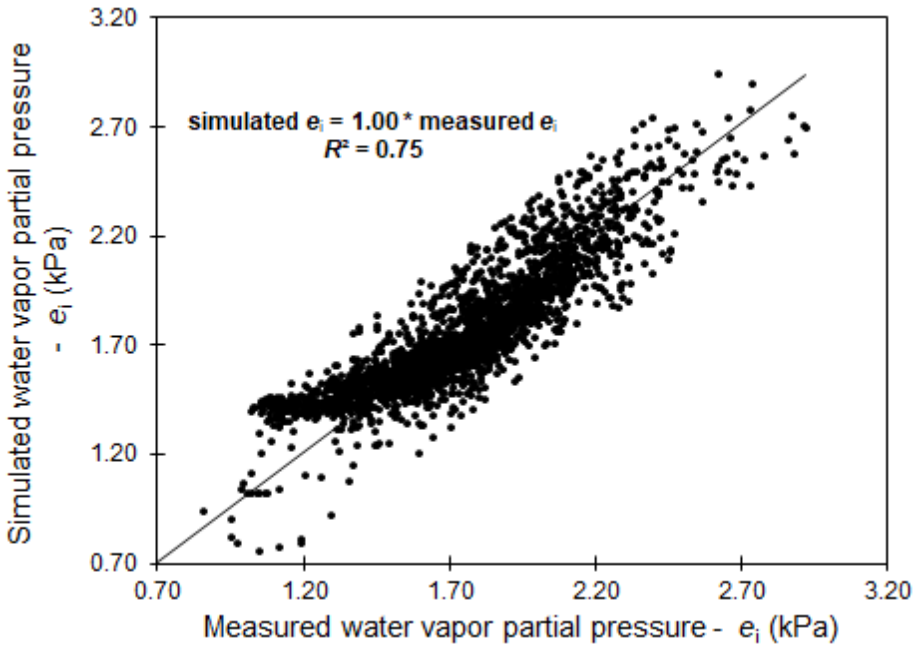


**Figure 7.10. Scatter plot between simulated and measured water vapor partial pressure ($e_i$).**

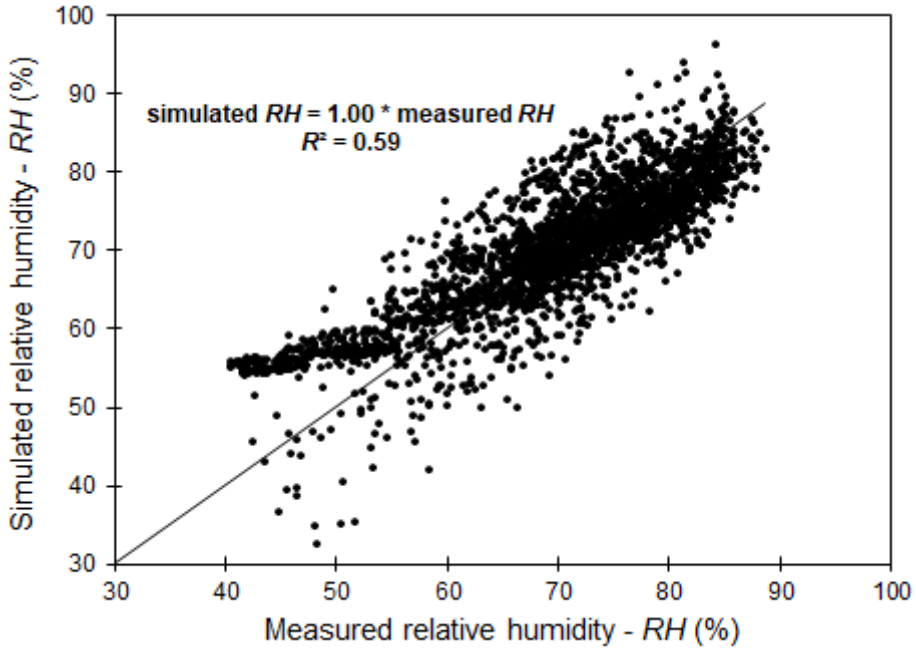


**Figure 7.11. Scatter plot between simulated and measured relative humidity (*RH*).**

## 7.7 Conclusions

A dynamic moisture balance model named HumidMod was developed for predicting the indoor RH and air water vapor partial pressure. MATLAB was used to solve the mathematical

equations. This model can predict the moisture production/removal rate by evapotranspiration, condensation, as well as by air exchange (ventilation/infiltration) based on the indoor and outdoor environmental conditions and the plant and greenhouse characteristics. In this model, the condensation rate on the greenhouse inner cover surface was predicted by using a statistical regression model instead of the complicated theoretical model. Air exchange rate including ventilation and infiltration was also predicted using an exponential relationship with the indoor solar radiation based on the experimental data. The model was validated by comparing the predicted results with experimental measurements in a tomato greenhouse, which had a commercial-grade dehumidifier for humidity control. The mean absolute uncertainty between the predicted and the measured results was about 6.9% for both RH and water vapor partial pressure. The coefficient of determinations were 0.59 and 0.75 for RH and water vapor partial pressure, respectively. A good agreement was found between the predicted and the measured results with root mean square error of 5.6% for RH and 0.144 kPa for water vapor partial pressure. This model can be satisfactorily applied for prediction of indoor RH and air water vapor partial pressure, as well as the evapotranspiration rate and the condensation rate on the greenhouse inner cover surface.

This moisture balance model also could be used to estimate the dehumidification requirement of greenhouses for a given indoor RH and vapor pressure set points. Future work is needed to validate the model for greenhouse dehumidification requirement prediction.

# CHAPTER 8

# SENSITIVITY ANALYSIS OF A GREENHOUSE MOISTURE BALANCE MODEL FOR PREDICTING INDOOR HUMIDITY

(This is a prepared manuscript and will be submitted soon)

Jingjing Han, Mohamed S. Ahamed, Huiqing Guo

## Contribution of this paper to overall study

A moisture balance model (HumidMod) was developed in Chapter 7 to predict the greenhouse indoor RH and water vapor partial pressure conditions. This chapter presents the sensitivity analysis of this model to several important input parameters to explore the impacts of the input parameters on the HumidMod model simulation results. This chapter fulfills objective 7.

The manuscript presented in this chapter will be submitted soon. The first author (PhD student – Ms Jingjing Han) conducted the sensitivity analyses and wrote the manuscript. The second author (supervisor – Prof. Huiqing Guo) and the third author (Dr. Mohamed S. Ahamed) reviewed the manuscript.

## 8.1 Abstract

A moisture balance model was developed to predict the indoor air water vapor partial pressure as well as the indoor relative humidity by considering the greenhouse indoor and outdoor environmental conditions, as well as the greenhouse and plant characteristics. This study is focused on sensitivity analysis of this model to several important input parameters in three different seasons: cold winter (January), mild season (April), and summer season (July). The results showed that under different ambient weather conditions, the sensitivity of the moisture balance model estimates of the indoor air water vapor partial pressure is very dependent on the greenhouse indoor air temperature and the incoming solar radiation, as well as the air exchange rate. The leaf area index also has a significant influence on the model output. The sensitivity analysis results indicate that these input parameters should be decided carefully.

The manuscript presented in this chapter will be submitted soon. The data analyses and manuscript writing were performed by the first author (PhD student – Miss Jingjing Han). The manuscript was reviewed by the second author (D. M.S. Ahamed) and the third author (supervisor – Prof. Huiqing Guo).

## 8.2 Nomenclature

| | |
|---|---|
| $A_g$ | greenhouse floor area, $m^2$ |
| $C_p$ | specific heat of water, J $kg^{-1}$ $K^{-1}$ |
| $E$ | moisture added, extracted, transpired, condensed, exchanged by ventilation or infiltration, kg $m^{-2}$ $h^{-1}$ |
| $e$ | air water vapor partial pressure, kPa |
| $e_i$ | indoor air water vapor partial pressure, kPa |
| $e_s$ | air water vapor pressure at saturation, kPa |
| $IP$ | input parameter of a model |
| $\Delta IP$ | variance of input parameter |
| $I_s$ | incoming shortwave radiation above the canopy, W $m^{-2}$ |
| $LAI$ | leaf area index |
| $OP$ | output of a model |
| $\Delta OP$ | variance of output |
| $P$ | atmospheric pressure, kPa |
| $q$ | air flow rate due to ventilation or infiltration, $m^3$ $h^{-1}$ |
| $R_n$ | net radiation above canopy, W $m^{-2}$ |
| $r_a$ | canopy external, or aerodynamic resistance, s $m^{-1}$ |
| $r_c$ | internal canopy resistance to the transfer of water vapor, s $m^{-1}$ |

| | |
|---|---|
| $SC$ | sensitivity or influence coefficient |
| $T$ | air temperature, °C |
| $t$ | time, s |
| $u$ | mean air speed, m $s^{-1}$ |
| $V_g$ | greenhouse volume, $m^3$ |
| $\gamma$ | psychrometric constant, kPa $K^{-1}$ |
| $\Delta$ | slope of water saturation vapor pressure curve, kPa $K^{-1}$ |
| $\lambda$ | latent heat of water vaporization, kJ $kg^{-1}$ |
| $\rho$ | air density, kg $m^{-3}$ |

***Subscripts***

| | |
|---|---|
| *add* | added to the greenhouse air |
| *base* | base case |
| *c* | condensation or cover |
| *dh* | dehumidification |
| *i* | indoor air |
| *o* | outside air |
| *p* | plant transpiration |
| *v* | ventilation or infiltration |

***Abbreviations***

| | |
|---|---|
| *ACH* | air exchange per hour, $h^{-1}$ |
| *RH* | relative humidity, % |

## 8.3 Introduction

A moisture balance model, named HumidMod, was developed in Chapter 7 to predict a greenhouse indoor air water vapor partial pressure as well as the indoor relative humidity. The model involves numerous related parameters, which can be categorized into four groups: the greenhouse indoor environmental conditions, the greenhouse characteristics, the plant characteristics, as well as the ambient weather conditions. The model performance was evaluated and validated by comparing the simulated results with experimental measurement results conducted in a commercial tomato greenhouse. However, the sensitivity analysis of the model to various parameters has not yet been studied.

There always exists changes and errors in the input parameters and assumptions when developing a model (Pannell, 1997). It is important to explore the relationship between the potential changes and their influence on the conclusions that are drawn from the model (Baird, 1989; Pannell, 1997). Sensitivity analysis (SA) has been shown a very useful and widely used tool to support decision making (Pannell, 1997). If a system does not change greatly to a change in an input variable, it means the system is not sensitive to the parameter; otherwise, the system is sensitive to the input factor.

The objective of this paper was to conduct a study of a sensitivity analysis of the HumidMod model for predicting a greenhouse indoor air water vapor partial pressure. The sensitivity analysis was conducted on several important parameters including the greenhouse indoor air conditions, as well as the plant characteristics in three different ambient weather conditions.

## 8.4 HumidMod Model

First, a brief description of the HumidMod model is introduced here. In the model, it mainly includes four moisture sources or sinks: evapotranspiration, condensation, ventilation/infiltration, and dehumidification. The HumidMod model gives moisture balance of the greenhouse as follows:

$$\frac{0.62\cdot\rho_i\cdot V_g}{A_g\cdot P}\frac{de_i}{dt} = E_P(t) + E_{add}(t) - E_c(t) - E_v(t) - E_{dh}(t) \qquad (8.1),$$

where $\rho_i$ is the indoor air density, in kg $m^{-3}$; $V_g$ is the volume of the greenhouse, in $m^3$; $A_g$ is the greenhouse floor area, in $m^2$; $P$ is the atmospheric pressure, in kPa; $e_i$ is the air water vapor partial pressure, in kPa; $t$ is time, in s; and 0.62 is the ratio of molecular mass of water vapor and air. The term on the left side of Equation 8.1 represents the variation of humidity ratio of the greenhouse air with time $t$. The first term $E_p$(t) on the right side of Equation 8.1 is evapotranspiration. The second term $E_{add}$(t) is the moisture added to or extracted from the greenhouse air. The third term $E_c$(t) is condensation on the greenhouse inner cover surface. The fourth term $E_v$(t) is moisture exchange between the inside and outside air by air exchange (ventilation or infiltration). The last term $E_{dh}$(t) is moisture removed from the greenhouse air by dehumidification. By introducing all the parameters into Equation 8.1, the solution of Equation 8.1 can be given by:

$$e_i = \frac{B}{A} \pm C\cdot e^{-At} \qquad (8.2),$$

where $C$ is a constant value when $t = 0$; and $A$ and $B$ are expressed as follows:

$$A = \frac{A_g\cdot P}{0.62\cdot\rho_i\cdot V_g}\times(b+f), \qquad B = \frac{A_g\cdot P}{0.62\cdot\rho_i\cdot V_g}\times(a + b\cdot e_s + f\cdot e_o - E_c - E_{dh}).$$

The terms of $a$, $b$ and $f$ in the above two equations are determined as:

$$a = \frac{3.6\cdot\Delta\cdot R_n}{\lambda\cdot(\Delta+\gamma\cdot(1+\frac{r_c}{r_a})}, \qquad b = \frac{7.2\cdot LAI\cdot\rho_i\cdot\frac{C_P}{r_a}}{\lambda\cdot(\Delta+\gamma\cdot(1+\frac{r_c}{r_a})}, \qquad f = \frac{0.62\cdot\rho_i\cdot q_v}{A_g\cdot P}.$$

More detailed information about the model can be found in Chapter 7.

## 8.5 Sensitivity Analysis Methodology

Among the numerous input parameters and assumptions of the HumidMod model, it is important to identify which are the key variables that affect the results of the model. Sensitivity analysis compares the changes in output with the changes in input, thus it can also be expressed as an "input-output analysis" (Lam and Hui, 1996). Global and local approaches are two main methods of sensitivity analysis in the field of building performance analysis (Tian, 2013). The global sensitivity analysis is calculated by changing all input factors simultaneously. The disadvantage of this method is that it is very computationally demanding. Compared with the global sensitivity analysis, the local sensitivity analysis is more straightforward, which is calculated with only one input factor changed and all the other input parameters are fixed. The local sensitivity analysis is easier to apply and interpret (Tian, 2013), therefore, it is chosen for this study.

### 8.5.1 Sensitivity coefficient

The sensitivity coefficient, also called an influence coefficient, is often used as a measure of sensitivity. Considering the application for multiple sets of data, the following Equation 8.3 is used for sensitivity coefficient calculation (Lam and Hui, 1996; Yang et al., 2016),

$$SC = \frac{\Delta OP/OP_{\text{base}}}{\Delta IP/IP_{\text{base}}} \qquad (8.3),$$

where $SC$ represents the sensitivity coefficient; $OP_{\text{base}}$ and $IP_{\text{base}}$ are the base case of output and input. $\Delta OP$ and $\Delta IP$ are the variance of output and input. The sensitivity coefficient calculated by Equation 8.3 shows the sensitivity in percentage change (Lam and Hui, 1996). A high value indicates that the model is more sensitive to the input parameter, which needs to be chosen carefully (Yang et al., 2016).

### 8.5.2 Initial input data

The HumidMod model was evaluated and validated by comparing the simulated results with the experimental measurement results conducted in a commercial tomato greenhouse located in Saskatchewan, at 52.09° latitude, -107.03° longitude and 504 m elevation. The sensitivity analysis

of the model was also conducted by using the same greenhouse. The constant values of default parameters in the model were listed in Table 8.1. The sensitivity analysis was conducted for three months: January, April, and July, to represent three different seasons such as cold, mild, and warm seasons, respectively. Typical meteorological year data of Saskatoon from 1953-1995 were used as the outdoor weather conditions. Table 8.2 gives the average outdoor air temperature and relative humidity (*RH*) in each month during the daytime and nighttime respectively. It also gives the base case value of the input parameters in each month, which includes leaf area index (*LAI*), air-exchange rate (*ACH*), and the indoor air speed close to the inner cover surface. The values are assigned based on the measured results in the tomato greenhouse. The designed indoor set point temperature was 20°C for the daytime and 18°C for the nighttime. Besides the default parameters given in Table 8.1, the rest of input parameters that related to the greenhouse moisture balance modeling are selected for the sensitivity study, as listed in Table 8.2.

**Table 8.1. Constant values of default parameters adopted for the greenhouse moisture balance model.**

| *Greenhouse characteristics* | |
|---|---|
| Floor Area $A_g$ ($m^2$) | 1123.8 |
| Volume $V_g$ ($m^3$) | 6182.1 |
| Air thermal properties (at 20°C) | |
| Density $\rho_i$ (kg $m^{-3}$) | 1.205 |
| Pressure $P$ (Pa) | 101.3 |
| Specific heat $C_p$ (J $kg^{-1}$ $K^{-1}$) | 1005 |
| Air velocity $u_i$ (m $s^{-1}$) | 0.15 |
| Other parameters | |
| Slope of water saturation vapor pressure curve $\Delta$ (kPa $K^{-1}$) | 0.145 (at 20°C) |
| Psychrometric constant $\gamma$ (kPa $K^{-1}$) | 0.0668 |
| Latent heat of water vaporization $\lambda$ (kJ $kg^{-1}$) | 2450 |

**Table 8.2. Base case values under different months for the HumidMod model.**

| *Month* | *Period* | *Indoor temperature - T (°C)* | *Outdoor temperature - T (°C)* | *Outdoor relative humidity - RH (%)* | *Incoming solar radiation - $I_s$ (W $m^{-2}$)* | *Indoor air speed - $u_c$ (m $s^{-1}$)* | *Leaf area index - LAI* | *Air exchange per hour - ACH ($h^{-1}$)* |
|---|---|---|---|---|---|---|---|---|
| Jan | day | 20 | -14.9 | 70.0 | 90.7 | 0.1 | 1.5 | 1.0 |
| | night | 18 | -16 | 71.5 | 0 | | | 1.0 |
| Apr | day | 20 | 6.0 | 53 | 210.4 | 0.2 | 3 | 5.5 |
| | night | 18 | 0.79 | 70.4 | 0 | | | 2.2 |
| Jul | day | 20 | 20.8 | 50.0 | 252.6 | 0.2 | 6 | 10.0 |
| | night | 18 | 14.8 | 70.0 | 0 | | | 4.0 |

## 8.6 Results and Discussion

The input parameters can be categorized into several groups: the greenhouse environmental conditions, the greenhouse characteristics, the ambient weather conditions, as well as the plant characteristics. The sensitivity analysis is conducted on the main input variables in three months representing three different outdoor weather conditions: cold (January), mild (April), and warm (July).

### 8.6.1 Model sensitivity to indoor air temperature

The indoor air temperature of the greenhouse could reach as high as 28°C during the daytime in summer and be lower than 14°C at night. Therefore, the sensitivity analysis to the indoor air temperature is conducted with the range of 14 to 28°C during the daytime, and from 14 to 22°C at night.

Figures 8.1 and 8.2 display the simulated $e_i$ and sensitivity coefficients in each month during the daytime and nighttime, respectively. As shown in Figure 8.1, the simulated $e_i$ is positively correlated with the indoor air temperature. No matter during the daytime or at night, the simulated $e_i$ has the highest values in July and the lowest values in January, which is mainly caused by the high evapotranspiration rate in July. In January, the simulated $e_i$ increased by 37% during the daytime and reduced by 24% at night for changing the indoor air temperature from 20 to 28°C during the daytime and from 18 to 14°C at night, respectively. Smaller changes were found in April and July. The sensitivity coefficient shown in Figure 8.2 tells the same story, as the sensitivity coefficient is higher than 1.0 in January during the nighttime, which means the HumidMod model

is more sensitive to the indoor air temperature in January than that in April and July. This is because the base case of $e_i$ values simulated in January, April, and July are very similar. However, the variation of simulated $e_i$ in January was larger than that in April and July, resulting in higher sensitivity coefficients in January. Based on the sensitivity analysis, it could be concluded that the HumidMod model is more sensitive to the indoor air temperature during the cold weather conditions, and less sensitive in the warm season due to the high sensitivity coefficient in January.

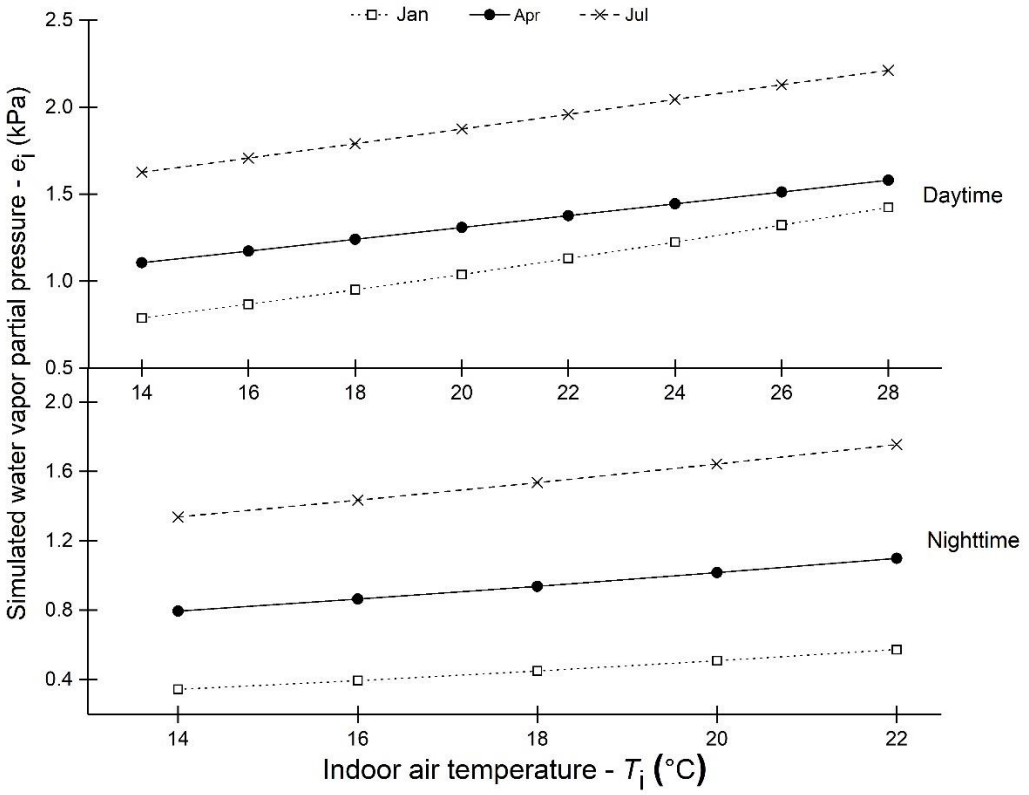


**Figure 8.1. Simulated indoor air water vapor partial pressure under different indoor air temperatures.**

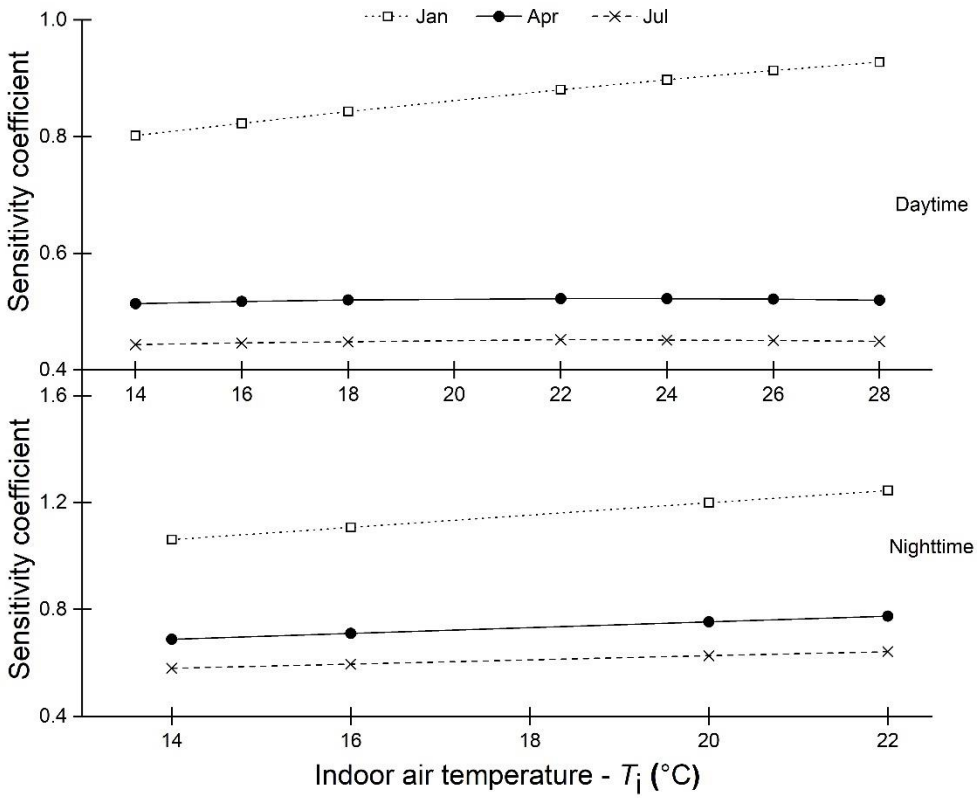


**Figure 8.2. Sensitivity coefficients under different indoor air temperatures.**

### 8.6.2 Model sensitivity to incoming solar radiation

The sensitivity of HumidMod model to the incoming solar radiation is also analyzed, which is mainly conducted for the daytime since no solar radiation at night. The incoming solar radiation could reach up to 700 W $m^{-2}$ in Saskatoon based on the previous field experiment, especially during the summer seasons, therefore the model sensitivity to the incoming solar radiation is analyzed from 50 to 700 W $m^{-2}$ with 50 W $m^{-2}$ as the interval. Figure 8.3 shows the sensitivity of the model to the incoming solar radiation in three months. The simulated $e_i$ does not change very much in January, whereas greater changes are observed both in April and July. The average simulated $e_i$ is increased by 26.9% in April and 13.6% in July, respectively, for changing the incoming solar radiation from 50 to 700 W $m^{-2}$. The sensitivity coefficients reflect the similar outcome as the values are high in April and July, and low in January. That means the HumidMod model is sensitive to solar radiation during the mild and warm seasons, and not very sensitive in the cold months when the plants are very small. That is because in January, the plants are at their early growing stage and very small, only a small portion of solar energy is used for crop evapotranspiration, which

is the main source of moisture production in the greenhouse. Therefore, the model is not sensitive to the incoming solar radiation when the plants are very small.

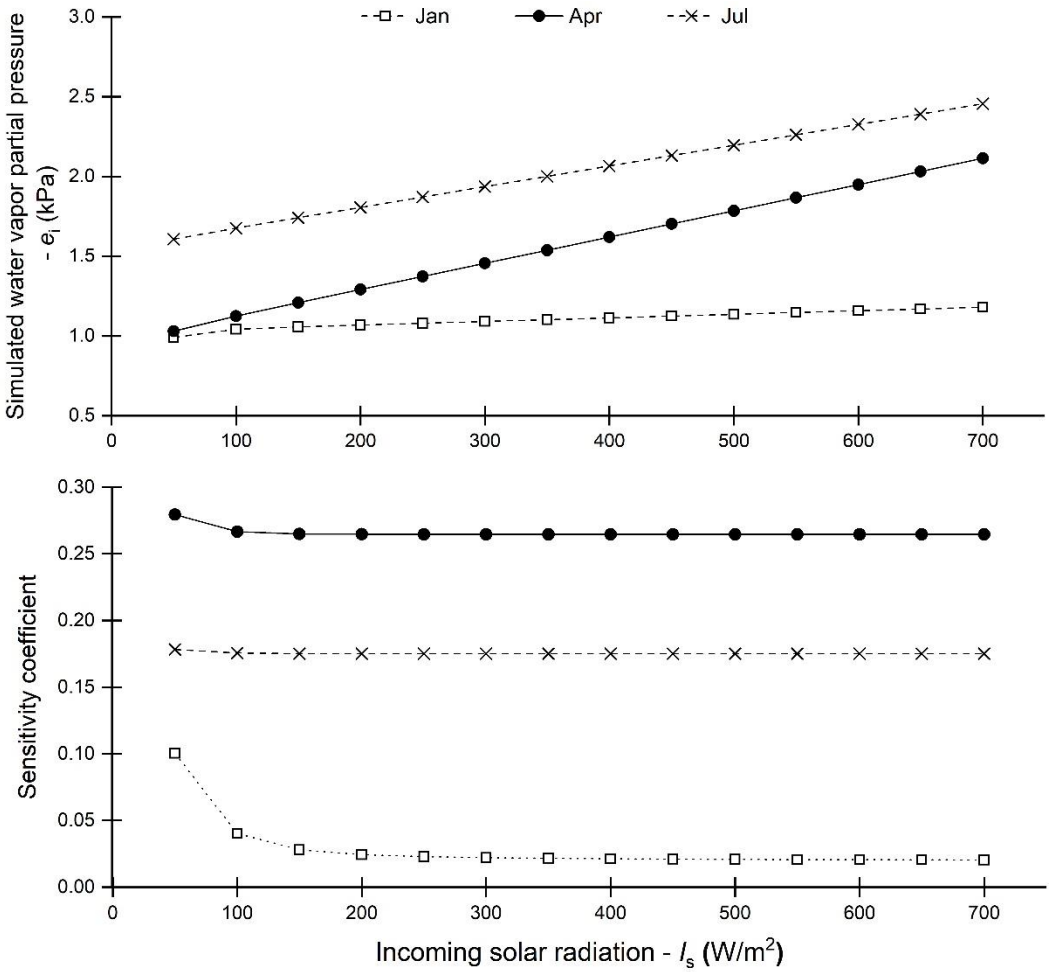


**Figure 8.3. Simulated indoor air water vapor partial pressure under different incoming solar radiation.**

### 8.6.3 Model sensitivity to air exchange rate

The air exchange rate due to ventilation or infiltration varies greatly in different seasons. According to Han et al. (manuscript draft, 2018), the air exchange per hour (*ACH*) during the nighttime could be ranged between 1.4 to 4.0 $h^{-1}$ depending on the ambient weather conditions. The maximum *ACH* during the daytime could reach up to 79 $h^{-1}$ in July. Therefore, the sensitivity analysis was conducted at different levels in each month. Table 8.3 shows the *ACH* ranges in each month. Figures 8.4 and 8.5 display the simulated $e_i$ and sensitivity coefficients during the daytime and nighttime for January, April, and July.

**Table 8.3. Air exchange per hour (*ACH*) under different testing levels.**

| *Month* | *Period* | *Max ACH* ($h^{-1}$) | *Min ACH* ($h^{-1}$) | *Interval* ($h^{-1}$) |
|---|---|---|---|---|
| Jan | day | 6 | 1 | 1 |
| | night | 6 | 1 | 1 |
| Apr | day | 40 | 4 | 4 |
| | night | 10 | 2 | 2 |
| Jul | day | 74 | 2 | 8 |
| | night | 22 | 2 | 2 |

No matter whether it is daytime or night, the simulated $e_i$ decreases along with an increase of air exchange rate. In January, the HumidMod model is sensitive to the air exchange rate with the average simulated $e_i$ is decreasing by 22.3% and 14.5% during the daytime and at night for changing the value from 1 to 6 $h^{-1}$, respectively. In April and July, when the air exchange rate is less than 28 $h^{-1}$, the simulated $e_i$ could be decreasing by more than 50%. When *ACH* is higher than that point, the HumidMod model is not sensitive anymore, which means the indoor RH is reaching a stable state, and the moisture production rate by crop evapotranspiration equals to the moisture removal rate by ventilation and condensation. During the nighttime, the simulated $e_i$ is also reaching a stable point when *ACH* is higher than 3 $h^{-1}$ in January and 8 $h^{-1}$ in both April and July.

Compared to the nighttime in April and July, the sensitivity coefficient is higher during the daytime, especially when *ACH* is lower than 10 $h^{-1}$, which means the HumidMod model is more sensitive to *ACH* during the daytime. This is because at night the moisture production rate by crop evapotranspiration is very low compared to the high rate during the daytime. Ventilation is the main way to discharge a large amount of moisture from the greenhouse during the daytime. In January, similar sensitivity coefficients are found during the daytime and nighttime, respectively. That means the HumidMod model has similar sensitivity to *ACH* during the daytime and at night in January. Hence, *ACH* should be decided very carefully when using HumidMod model to predict the air water vapor partial pressure, especially in April and July.

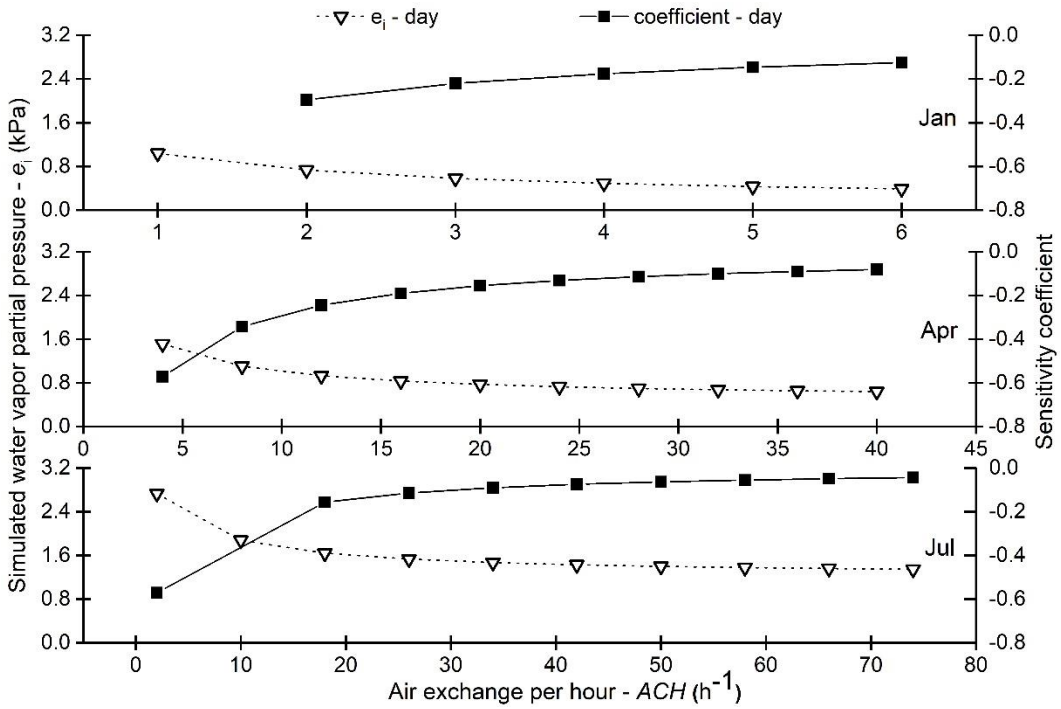


**Figure 8.4. Simulated indoor air water vapor partial pressure and sensitivity coefficients under different air exchanger per hour during the daytime.**

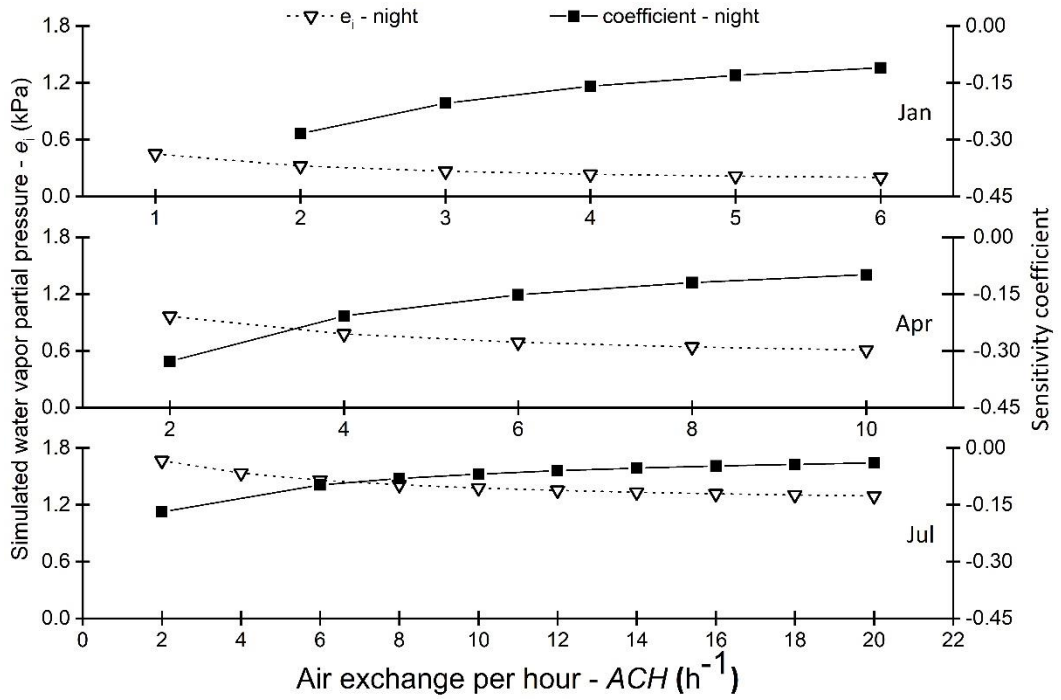


**Figure 8.5. Simulated indoor air water vapor partial pressure and sensitivity coefficients under different air exchange per hour during the nighttime.**

### 8.6.4 Model sensitivity to indoor air speed

Greenhouse indoor air speed could be in the range from 0.05 to 0.3 m $s^{-1}$ (Bailey et al., 1993). To fully understand the influence of indoor air speed on the indoor air water vapor partial pressure simulation, the model sensitivity to the indoor air speed was tested in the range from 0.05 to 1.05 m $s^{-1}$ with an interval of 0.1 m $s^{-1}$.

A positive correlation is found between the simulated $e_i$ and the indoor air speed when all the other input variables are fixed in the HumidMod model. When the indoor air speed is greater than 0.45 m $s^{-1}$, the simulated $e_i$ is only increased by less than 5%, no matter during the daytime or at night. That means the evapotranspiration rate of greenhouse crops increases as the indoor air speed increases, considering it is the only moisture source of the greenhouse. When the indoor air speed gets to 0.45 m $s^{-1}$ or higher, the water moving rate from the surface of leaf cells to the surrounding air gets stable, which leads to a stable indoor air water vapor partial pressure. As a result, the sensitivity coefficients are very small, and the model is not sensitive to air speed when the indoor air speed is exceeding 0.45 m $s^{-1}$. However, when the indoor air speed is less than 0.45 m $s^{-1}$, the sensitivity coefficient could get up to 0.9 at nighttime in January, which means the HumidMod model is sensitive to the low indoor air speed, especially in January than that in April and July.

Overall, the HumidMod model is more sensitive to the indoor air speed in cold weather conditions rather than in the mild and warm weather conditions, especially when the indoor air speed is lower than 0.45 m $s^{-1}$.

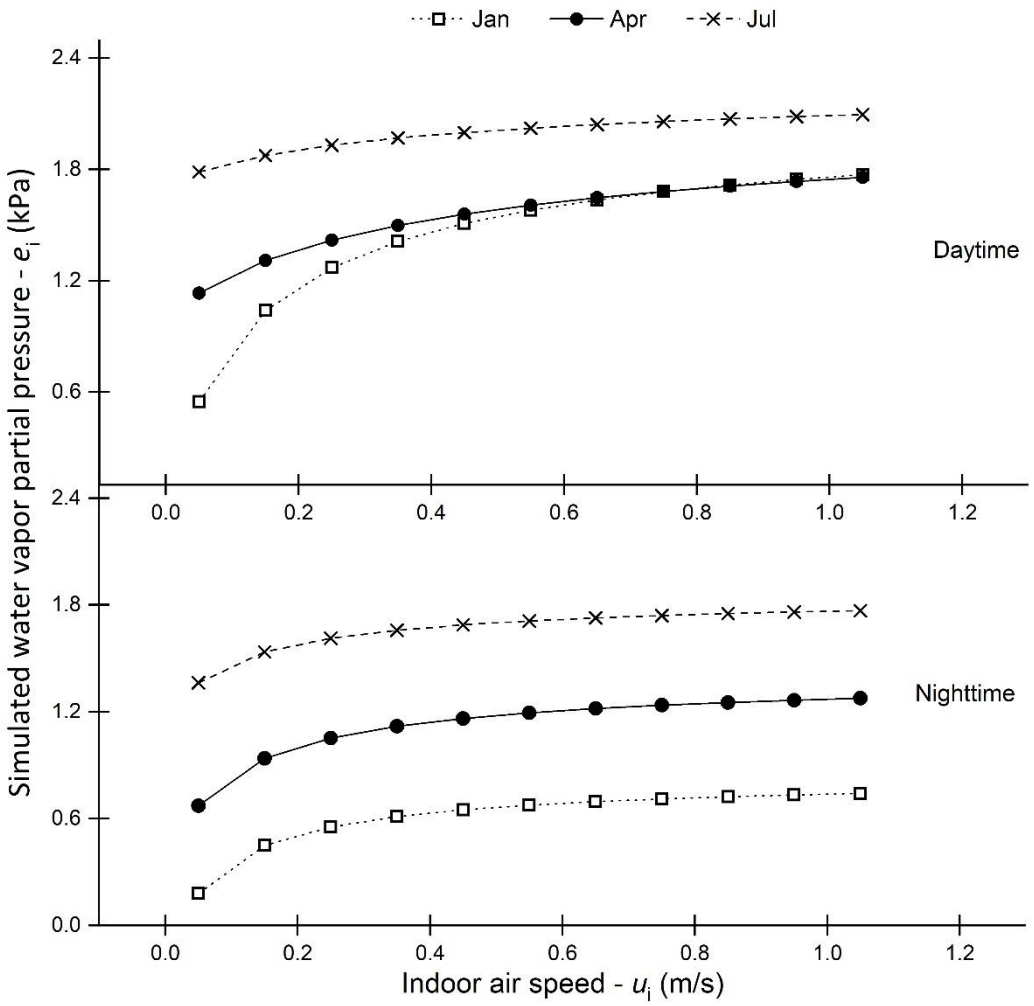


**Figure 8.6. Simulated indoor air water vapor partial pressure under different indoor air speeds.**

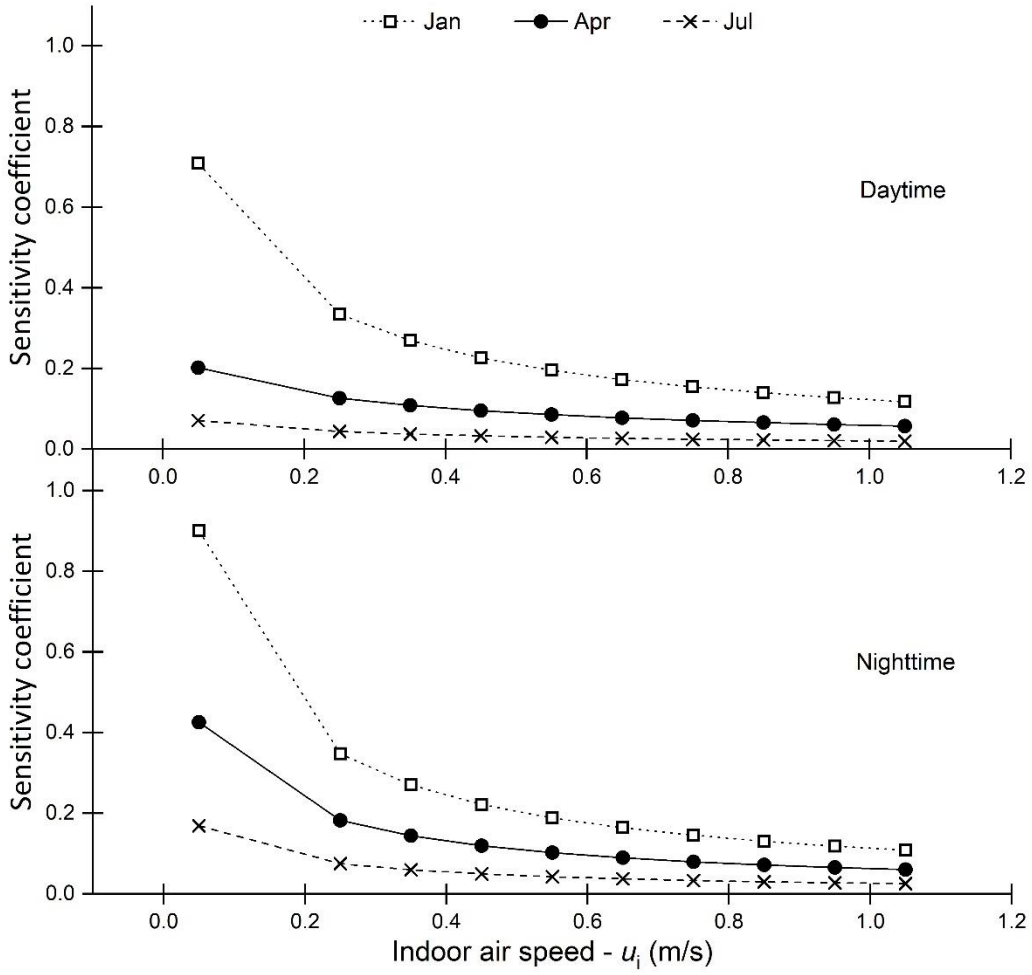


**Figure 8.7. Sensitivity coefficients under different indoor air speeds.**

### 8.6.5 Model sensitivity to air speed near cover surface

The indoor air speed near the cover surface is very small, especially during the nighttime when all the vents are closed, and the exhaust fans are shut down. Based on the experimental data, the air speed close to the cover inner surface is less than 0.3 m $s^{-1}$ for most of the time (Bailey et al., 1993). To explore the sensitivity of the model to the cover inner surface air speed, eight levels of air speed from 0.05 to 0.40 m $s^{-1}$ were tested with an interval of 0.05 m $s^{-1}$. In the HumidMod model, the air speed near the cover is only related to the nighttime condensation rate estimation, so the sensitivity analysis is only conducted for the nighttime. Figure 8.8 gives the simulated $e_i$ and sensitivity coefficients at different air speed near the cover inner surface. The results showed that the simulated $e_i$ is negatively correlated with the indoor air speed near the cover surface, which is because in the HumidMod model the nighttime condensation rate has a positive relationship with the air speed near the cover surface. When all the other input parameters are fixed, the nighttime

condensation rate increases as the air speed near the cover surface increases, which leads to more moisture removed from the greenhouse air, therefore, the simulated $e_i$ decreases. In April and July, the simulated $e_i$ is decreased by 3% and 0.9% for changing the air speed from 0.05 to 0.40 m $s^{-1}$; and the corresponding sensitivity coefficients are also smaller than that in January. The HumidMod model is more sensitive to the air speed near the cover surface in cold season than that in mild and warm seasons due to the high condensation rate occurrence in January.

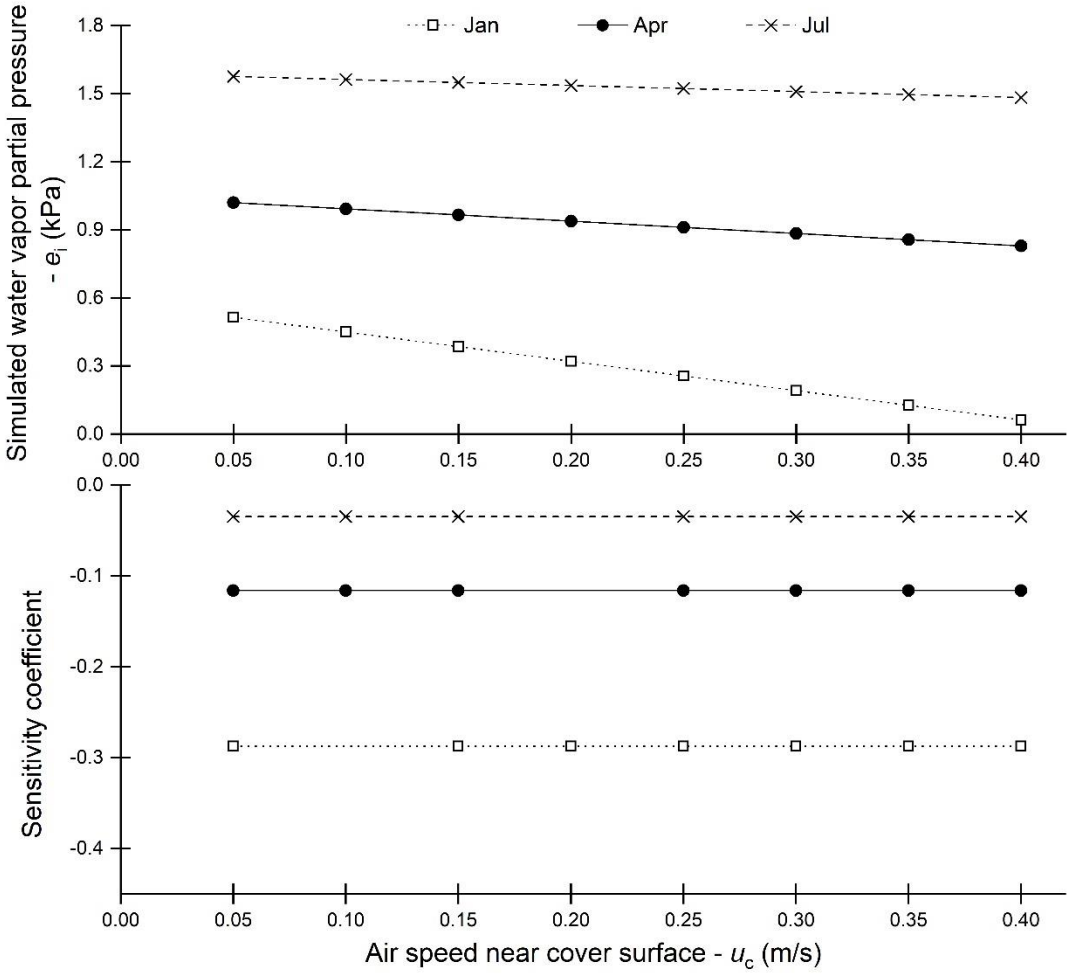


**Figure 8.8. Simulated indoor air water vapor partial pressure and sensitivity coefficients under different air speeds near the cover surface.**

### 8.6.6 Model sensitivity to leaf area index

As measured in the experimental greenhouse, the leaf area index (*LAI*) could reach as high as 7.8 in July. Hence, the sensitivity to *LAI* was analyzed in the range of 1 to 8 with 1 as the interval. Figures 8.9 and 8.10 are showing the simulated $e_i$ and sensitivity coefficients, respectively. There

is a large difference of the simulated $e_i$ between the values when *LAI* increases from 1 to 8. The high sensitivity coefficients illustrate that the HumidMod model is very sensitive to *LAI*, which is because *LAI* directly determines the amount of solar energy using by evapotranspiration. Besides, the influence of *LAI* on the simulated $e_i$ could be significantly different depending on the outdoor weather conditions as well as the initial input values. As shown in Table 8.2, due to the different initial input values in the HumidMod model, the simulated $e_i$ in January is even higher than that in April and July during the daytime. Hence, the model users should also be careful to decide the initial input parameter values of *LAI*.

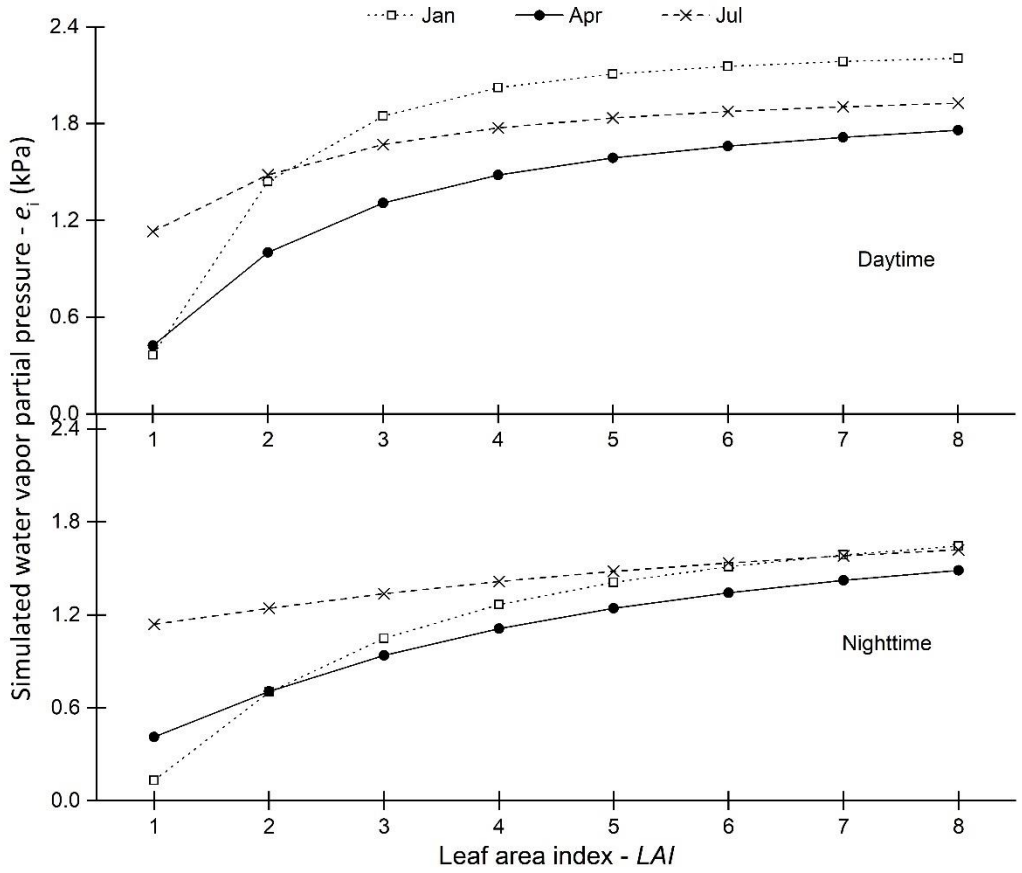


**Figure 8.9. Simulated indoor air water vapor partial pressure under different leaf area index.**

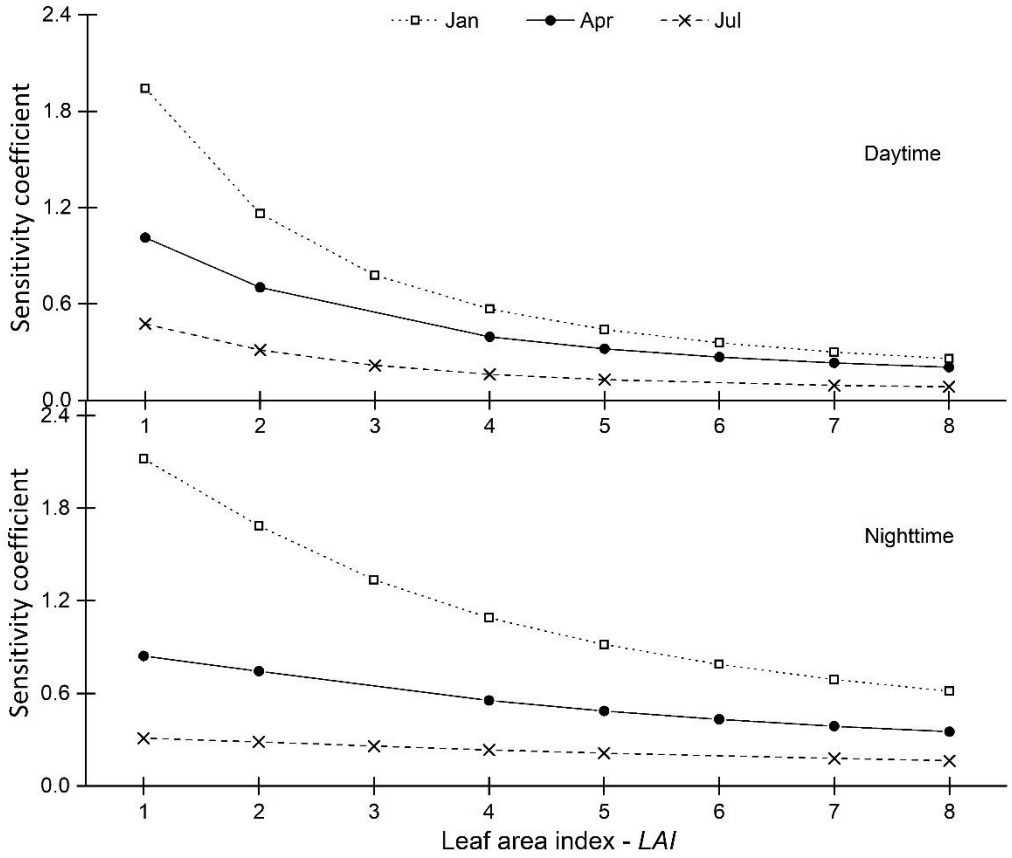


**Figure 8.10. Sensitivity coefficients under different leaf area index.**

## 8.7 Conclusions

Sensitivity analysis is conducted for the HumiMod model which is used to estimate the greenhouse indoor air RH and water vapor partial pressure. Important input parameters are identified and analyzed. Based on the results, it could be concluded that the HumidMod model is very sensitive to the indoor air temperature, especially during the cold weather conditions, whereas less sensitivity to the indoor air temperature for the summer months. The HumidMod model is also very sensitive to the air exchange rate and *LAI* because these two factors determine the moisture discharge rate through ventilation or infiltration, and the total amount of moisture transpired by the plants. As compared to January, the model is more sensitive to the incoming solar radiation in April and July, which is also due to the high crop evapotranspiration rate in mild or warm season. On the contrary, the model is more sensitive to the indoor air speed and the indoor air speed near the cover surface in cold months than that in the mild and warm weather conditions. Hence, the fluctuation of indoor air temperature, *ACH, LAI,* and the incoming solar radiation have significant effects on

the model output. These variables should be selected carefully to reduce the error and uncertainty in model predictions.

# CONCLUSIONS, CONTRIBUTIONS AND RECOMMENDATIONS

## Conclusions

In this research, various humidity control measures including ventilation, air-to-air heat exchanger, and mechanical refrigeration dehumidification have been evaluated for use in greenhouses. Greenhouse RH profiles have been obtained and high RH periods have been identified, and humidity control strategies in cold region were recommended. After the initial evaluation, an air-to-air heat exchanger and a commercial-grade mechanical refrigeration dehumidifier were selected and evaluated in a Venlo-type tomato greenhouse for humidity control. A condensation rate measurement method was developed and used in the same greenhouse for long-term condensation rate measurement. Based on the measured data, two statistical regression models for condensation rate prediction in daytime and nighttime were developed. Finally, a greenhouse moisture balance model was developed aiming at simulating the indoor relative humidity and water vapor partial pressure and predicting dehumidification requirement. The main findings in this thesis are listed as follows:

1) Three dehumidification methods including air-to-air heat exchangers and exhaust ventilation, and mechanical refrigeration (domestic scale) were evaluated in a tomato greenhouse. Both air-to-air heat exchangers and exhaust ventilation system dehumidification were not effective during humid and warm seasons for humidity control. They controlled RH satisfactorily during the cold and mild seasons. Mechanical refrigeration dehumidification was effective for controlling indoor moisture year-round. Mechanical refrigeration dehumidifiers had the lowest total energy consumption, followed by the heat exchangers and the exhaust ventilation system dehumidification. However, regarding total cost, mechanical refrigeration dehumidification was the costliest method due to high electricity consumption, while the exhaust ventilation system dehumidification was the

cheapest way of dehumidifying. The exhaust ventilation system dehumidification is the most economical method due to its low capital and maintenance cost. A combination of the exhaust ventilation system dehumidification and the mechanical refrigeration dehumidification would provide the most effective and economical way of humidity control year-round.

2) Greenhouse RH profiles have been obtained and high RH periods have been identified, and humidity control strategies in cold region were recommended. The general trend of the RH diurnal profile in cold season was the indoor RH being higher during daytime and lower during nighttime, while just the opposite occurred in mild and warm seasons with the inside RH being lower during the daytime and higher during the nighttime. The peak RH periods occurred during late morning to afternoon during the cold season. During the mild and warm seasons, most of the peak RH periods occurred during the night and early morning. During the summer season, mechanical refrigeration dehumidification is recommended for humidity control. A combination of the exhaust ventilation system dehumidification and the mechanical refrigeration dehumidification would provide the most effective and economical way of humidity control year-round.

3) An air-to-air heat exchanger was installed and tested in a Venlo-type greenhouse and was found that the capacity was not sufficient for humidity control, especially during the humid and warm seasons. It is important to give an accurate estimation of the dehumidification needs in a greenhouse. An experimental method of estimating dehumidification needs was proposed. The additional moisture that needed to be removed from the greenhouse to keep the inside RH at or below 75% was calculated by using the measured indoor RH when it was above 75%. Then the dehumidification requirement or the extra moisture removal rate was determined by removing the additional moisture within one hour. Based on the actual moisture removal rates of the heat exchanger and its humidity control performance, the dehumidification requirement was estimated to be 0.018 L $h^{-1}$ per square meter of the greenhouse floor area.

4) A commercial-grade mechanical refrigeration dehumidifier was selected and installed to control RH in a commercial tomato greenhouse. Its performance was evaluated. The unit showed effective control of the indoor RH and could maintain the indoor RH at an acceptable level year-round, especially during summer and fall nights, meeting most of the dehumidification requirement for the greenhouse. Even though the capital cost and annual cost were high, the plant loss rate was

dramatically reduced compared with that in the previous years when there was no dehumidification. The equipment payback was achieved within one year.

5) A condensation rate measurement method was developed in greenhouses or in any other building. A commercially available leaf wetness sensor was calibrated in an environment chamber for the relationship of condensation rate and sensor voltage output under various room temperature and RH conditions. The results indicated that the sensor temperature, angle, and indoor RH had no significant effect on the sensor voltage output. The sensor voltage output was positively correlated to the amount of condensate on the sensor surface and a regression model was obtained to convert the sensor voltage output to the condensation rate ($R^2$ = 0.91).

6) Greenhouse condensation profiles were quantified by applying the condensation measurement method in a tomato greenhouse. The results indicated that condensation mainly occurred during the nighttime and early morning, when the cover surface temperature was low, and RH was high in the greenhouse due to low air exchange. The cover surface acted as a moisture sink of the greenhouse air when condensation occurs. The opposite situation might occur for a short period of time in the morning when cover surface temperature increased to above the dew point temperature of the room air, thus the cover surface acted as a moisture source of the greenhouse air. The average condensation rate during the nighttime in the eight months was around 9.5 g $m^{-2}$ $h^{-1}$ or 88.6 g $m^{-2}$ $d^{-1}$.

7) Based on the condensation measurement data, three different theoretical convective heat transfer coefficient condensation models were evaluated, and the results showed the models' predictions were 7 to 8 times higher than the measured values, thus were not usable in greenhouses. Two statistical models were developed for condensation rate prediction. They can fit the measured data well during May, July, and September, except during November when the greenhouse moisture production rate and the indoor humidity ratio were at much lower levels comparing with the other months.

8) A moisture balance model, named HumidMod, was developed to simulate the greenhouse indoor RH and water vapor partial pressure, it can also be used to calculate dehumidification needs of greenhouses. In the model, the indoor RH and water vapor partial pressure can be directly calculated as a function of the indoor and outdoor air conditions, as well as the plant and greenhouse characteristics. The data collected in a tomato greenhouse was used to validate the model. A good

agreement was found between the predicted and measured results ($R^2$ = 0.59). This model can serve as a reliable tool for the estimation of dehumidification requirement inside a greenhouse to achieve a desired humidity level.

9) Sensitivity analysis of the HumidMod model to several important input variables were conducted to explore their influence on the model simulation results. The results indicate that the input parameters including the indoor air temperature, incoming solar radiation, air exchange rate, as well as plant leaf area index have significant impact on model output so should be decided carefully.

## Contributions

The contributions of this study are summarized as follows.

A comprehensive study has been done on the comparison of three dehumidification methods: air-to-air heat exchangers, mechanical refrigeration dehumidifiers, and exhaust ventilation system dehumidification. Exhaust fan ventilation and air-to-air heat exchangers were effective in cold season but were not effective in warm and mild seasons when ambient air is humid. The comparison results (Chapter 1) showed that dehumidification by the exhaust ventilation system was the most cost-effective method with the lowest capital and maintenance cost during cold and mild seasons. Mechanical refrigeration dehumidification is effective all year-round and has the lowest energy consumption, yet the highest operation cost due to high power consumption. Hence, mechanical refrigeration dehumidification is recommended for summer while exhaust fan can be used in cold season dehumidification, and both methods could be used during different seasons to achieve good moisture control year-round.

An experimental method for predicting a greenhouse dehumidification needs was proposed, which was defined as removing the additional moisture that needed to be removed from the greenhouse to keep the indoor RH at or below 75% within one hour. Based on the performance of an air-to-air heat exchanger, the estimated dehumidification requirement of 0.018 L $h^{-1}$ per square meter of the greenhouse floor area was obtained (Chapter 2).

A commercial-grade mechanical refrigeration dehumidifier was evaluated in the same tomato greenhouse (Chapter 3) and the RH condition was controlled much better by this unit than the previous air-to-air heat exchanger through most of the growing season. Even though the capital

and the annual cost of the dehumidifier were high, the plant loss rate was dramatically reduced from 43.3% prior to 2012 without dehumidification to 0.9% with the mechanical dehumidifier in 2013. The equipment payback period was within one year. It was found to be costly and unnecessary to achieve a dehumidification performance that control the RH at all times, as meeting the peak requirement would require a 60% increase of dehumidification capacity, which means the capital cost of the dehumidification system would almost double, and the power consumption and operating cost would also double, whereas it is also unnecessary to control the RH all the time as the peak RH periods occurred during the night and early morning in warm seasons. Once the ventilation operation starts to cool, the RH would reduce rapidly.

RH profiles and high RH periods were identified. The indoor RH was high during daytime and low during nighttime in cold season, while the opposite occurred in mild and warm seasons with low RH during daytime and high RH during nighttime. Most of the peak RH periods occurred during the night and early morning in the mild and warm seasons. In the cold season, it occurred during the late morning to afternoon.

A condensation rate measurement method using a leaf wetness sensor was developed for use in greenhouses or any other building. A commercially available leaf wetness sensor was calibrated in an environment chamber for the relationship of condensation rate and sensor voltage output under various room temperature and RH conditions (Chapter 4). The results indicated that the sensor angle and room temperature and RH had no significant effect on the sensor voltage output. The sensor voltage output was only positively correlated to the amount of condensate on the sensor surface and a regression model was obtained to convert the sensor voltage output to the condensation rate ($R^2$ = 0.91). This method should be considered as a breakthrough of technology for condensation rate measurement on greenhouse interior surface, or on any other surfaces with condensation.

Condensation profiles on greenhouse cover interior surface were identified and quantified by using the method developed by this study (Chapter 5). It was found that condensation mainly occurred during the nighttime and early morning when the cover surface temperature was low, and RH was high in the greenhouse due to low air exchange. The cover surface mostly acted as a moisture sink of the greenhouse air but could be a source during the short period in the morning.

This is the first study on condensation quantification for greenhouses or any buildings that prone to condensation occurrence.

Three different theoretical convective heat transfer coefficient condensation models were evaluated using the condensation measurement data from this study, and the results showed the models' predictions were too high so were not usable in greenhouses (Chapter 6). Two statistical models were developed for condensation rate prediction in greenhouses, one for the daytime ($R^2$=0.55) and another for the nighttime ($R^2$ = 0.61).

A moisture balance model HumidMod was developed to simulate the greenhouse indoor RH and water vapor partial pressure given indoor and outdoor air conditions as well as the plant and greenhouse characteristics, it can also be used to calculate dehumidification needs of greenhouses (Chapter 7). The model was validated using data collected in a tomato greenhouse ($R^2$=0.59). This model can serve as a reliable tool for the estimation of dehumidification requirement of a greenhouse to achieve a desired humidity level. Sensitivity analysis of the HumidMod model indicated that air temperature, solar radiation, air exchange rate, as well as plant leaf area index have significant impact on model outputs. This is the first model for indoor RH and dehumidification estimation, it provides a reliable tool for researchers and greenhouse industry (Chapter 8).

## Recommendations for Future Work

Although this study conducted great amount of experiment work and theoretical studies, it still could not provide all the answers for greenhouse humidity control. There are still a lot of work that need to be done in the future.

In this study, exhaust ventilation system was proved to be the most cost-effective method for greenhouse humidity control during cold and mild seasons, and not for warm weather conditions when ambient air is humid, thus mechanical refrigeration is recommended for summer dehumidification. A study should be carried out to test the combination of the two dehumidification systems for greenhouse humidity control, especially in cold regions.

An air-to-air heat exchanger was not effective for humidity control in a commercial tomato greenhouse; therefore, a commercial-grade mechanical refrigeration dehumidifier was selected and installed in the same greenhouse, which was shown to have better control on the indoor RH. One

main reason was that the capacity of the air-to-air heat exchanger was lower than that of the dehumidifier. Hence, more research should be conducted to compare the performance of the dehumidifier with an air-to-air heat exchanger, which should have a similar moisture removal capacity as the dehumidifier.

As greenhouses become more profitable, some costly dehumidification technologies such as desiccant dehumidification may become acceptable; therefore, this type of dehumidification technologies should be evaluated for the effectiveness and safety in the greenhouses.

The moisture balance model developed in this study was used to predict the greenhouse indoor RH and water vapor partial pressure. It can also be used to quantify and adjust the dehumidification requirements to maintain a predetermined RH condition within a greenhouse. Hence, further experiment needs to be conducted to validate the model for greenhouse dehumidification requirement determination.

Soil evaporation from the greenhouse floor surface is considered in the evapotranspiration rate in the moisture balance model developed in this study. It is generally considered very small as compared to the plant transpiration. Further research should be carried out to explore the contribution of the soil evaporation to the moisture balance in the greenhouse air space. The irrigation system should also need to be monitored inside the greenhouse. A water balance model should be developed in the future, which could be helpful for the growers to improve the irrigation system together with the moisture balance model.

# REFERENCES


Abdel-Ghany, A. M., Ishigami, Y., Goto, E., & Kozai, T. (2006). A method for measuring greenhouse cover temperature using a thermocouple. *Biosystems Engineering*, Vol. 95(1), pp. 99-109.

Albright, L. D. (1990). *Environment Control for Animals and Plants.* St. Joseph, Michigan: ASAE.

Ali, A., Ishaque, K., Lashin, A., & Al Arifi, N. (2017). Modeling of a liquid desiccant dehumidification system for close type greenhouse cultivation. *Energy,* Vol. 118, pp. 578-589.

ASABE Standards. (2006). *EP406.4: Heating, Ventilating and Cooling Greenhouses*. St. Joseph, Michigan: ASABE.

ASHRAE. (2009). Nonresidential Cooling and Heating Load Calculations. In *ASHRAE Handbook of Fundamentals*. Atlanta, Georgia: ASHRAE.

Axial Fans. (2012). Axial Fans main catalogue FC. Retrieved from http://www.ziehl-abegg.com/ww/fans-product-3-Axial-fan-FC-design.html. Accessed May 09, 2011.

Bailey, B., Montero, J., Biel, C., Wilkinson, D., Anton, A., & Jolliet, O. (1993). Transpiration of *Ficus benjamina*: comparison of measurements with predictions of the Penman-Monteith model and a simplified version. *Agricultural and Forest Meteorology*, Vol. 65, pp. 229-243.

Baird, B. F. (1989). *Managerial Decisions under Uncertainty: an Introduction to the Analysis of Decision Making*. New York: Wiley.

Bakker, J. C. (1991). Analysis of humidity effects on growth and production of glass house fruit vegetables. PhD dissertation, Wageningen Agricultural University: Wageningen, The Netherlands.

Barradas, V. L., & Glez-Medellín, M. G. (1999). Dew and its effect on two heliophile understorey species of a tropical dry deciduous forest in Mexico. *International Journal of Biometeorology*, Vol. 43, pp. 1-7.

Berroug, F., Lakhal, E. K., El Omari, M., Faraji, M., & El Qarnia, H. (2011). Numerical study of greenhouse nocturnal heat losses. *Journal of Thermal Scicence,* Vol. 20(4), pp 377-384.

Boulard, T., Baille, A., Lagier, J., Mermier, M., & Vanderschmitt, E. (1989). Water vapour transfer in

a plastic house equipped with a dehumidification heat pump. *Journal of Agricultural Engineering Research,* Vol. 44, pp. 191-204.

Boulard, T., Baille, A., Mermier, M., & Vilette, F. (1991). Mesureset modélisation de la résistance stomatique foliaire et de la transpiration d'un couvert de tomate de serre (in French). *Agronomie,* Vol. 11, pp. 259-274.

Boulard, T., & Wang, F. (2000). Greenhouse crop transpiration simulation from external climate conditions. *Agricultural and Forest Meteorology,* Vol. 100, pp. 25-34.

Byun, J., Jeon, C. D., Jung, J. H., & Lee, J. (2006). The application of photo-coupler for frost detecting in an air-source heat pump. *Internatinal Journal of Refrigeration,* Vol. 29(2), pp. 191-198.

Campen, J. B. (2009). Dehumidification of greenhouses. PhD dissertation, Wageningen University: Wageningen, the Netherlands.

Campen, J. B., & Bot, G. P. A. (2001). Design of a low energy dehumidifying system for greenhouses. *Journal of Agricultural Engineering Research,* Vol. 78(1), pp. 65-73.

Campen, J. B., Bot, G. P. A., & de Zwart, H. F. (2003). Dehumidification of greenhouses at northern latitudes. *Biosystems Engineering*, Vol. 86(4), pp. 487-493.

Castilla, N. (2012a). *Greenhouse Technology and Management,* 2nd Edition. Chapter 2: The external climate. pp. 11-28. Granada, Spain: CABI.

Castilla, N. (2012b). *Greenhouse Technology and Management,* 2nd Edition. Chapter 8: Management of high temperatures: cooling. pp. 134-152. Granada, Spain: CABI.

Cemek, B., & Demir, Y. (2005). Testing of the condensation characteristics and light transmissions of different plastic film covering materials. *Polymer Testing,* Vol. 24, pp. 284-289.

Chandra, P., Albright, L. D., & Scott, N. R. (1981). A time dependent analysis of greenhouse thermal environment. *Transactions of the ASAE,* Vol. 81, pp. 442-449.

Chasseriaux, G. (1987). Heat pumps for reducing humidity in plastics greenhouses. *Plasticulture,* Vol. 73, pp. 29-40.

CO2Meter. (2012). K-30 sensor datasheet. Retrieved from http://www.co2meters.com/Documentation/Manuals/Manual-SE-0118-K-30-10-pct-

sensor.pdf. Accessed Dec. 05, 2013.

Danby Dehumidifiers. (2014). DDR6510E. Retrieved from file:///C:/Users/Jingjing/Downloads/DDR6510E_spec%20.pdf. Accessed Oct. 02, 2011.

De Freitas, C. R., & Schmekal, A. (2003). Condensation as a microclimate process: measurement, numerical simulation and prediction in the glowworm cave. *International Journal of Climatology*, Vol. 23, pp. 557-575.

De Halleux, D., & Gauthier, L. (1998). Energy consumption due to dehumidification of greenhouses under northern latitudes. *Journal of Agricultural Engineering Research*, Vo. 69, pp. 35-42.

De Zwart, H. F. (1996). Analyzing energy-saving options in greenhouse cultivation using a simulation model. PhD dissertation, Wageningen Agricultural University: Wageningen, the Netherlands.

Delwiche, S. R., & Willits, D. H. (1984). The effect of condensation on heat transfer through polyethylene films. *Transactions of the ASAE,* pp. 1476-1482.

Del-Air Systems. (2014). Heat exchangers. Retrieved from http://www.del-air.com/heatexchangers.html. Accessed Sep. 16, 2011.

Environment Canada. (2011). Daily Data Report for 2011. Retrieved from http://climate.weather.gc.ca/climateData/dailydata_e.html?StationID=47707&timeframe=2&cmdB1=Go&Year=2011&Month=5&cmdB1=Go#. Accessed Dec. 01, 2011.

Environment Canada. (2013). Daily Data reported for 2013. Retrieved from http://climate.weather.gc.ca/climate_data/daily_data_e.html?StationID=47707&timeframe=2&StartYear=1840&EndYear=2018&Day=9&Year=2013&Month=4#. Accessed Dec. 20, 2013.

Environment Canada. (2014). Canadian Climate Normals 1981-2010 Station Data. Retrieved from http://climate.weather.gc.ca/climate_normals/results_1981_2010_e.html?stnID=3328&autofwd=1. Accessed Jun. 09, 2014.

Feuilloley, P., & Guillaume, S. (1990). The heat pump: a tool for humidity excess control in greenhouses (in French). *CEMAGREF BTMEA*, Vol. 54, pp. 9-18.

Feuilloley, P., & Issanchou, G. (1996). Greenhouse covering materials measurement and modelling of thermal properties using the hot box method, and condensation effects. *Journal of Agricultural Engineering Research,* Vol. 65, pp. 129-142.

Gao, Z. (2012). Dehumidification of greenhouses in cold regions. MSc thesis, University of Saskatchewan: Saskatoon, Canada.

Gao, Z., Guo, H., Brad, R., Waterer, D., & VanDuyendyke, R. (2010). Greenhouse dehumidification in cold regions. ASABE Annual International Meeting, Pittsburgh, PA, June 20-23, 2010, Paper No. 1008785.

Garzoli, K. V., & Blackwell, J. (1981). An analysis of the nocturnal heat loss from a single skin plastic greenhouse. *Journal of Agricultural Engineering Research,* Vol. 26, pp. 203-214.

Granados, M. R., Ortega, B., Bonachela, S., Hernández, J., López, J. C., Pérez-Parra, J. J., & Magán, J. J. (2011) Measurement of the condensation flux in a venlo-type glasshouse with a cucumber crop in a Mediterranean area. *Acta Horticulturae,* Vol. 893, pp. 531-538.

Han, J., Gao, Z., Guo, H., Brad, R., & Waterer, D. (2015a). Comparison of greenhouse dehumidification strategies in cold regions. *Applied Engineering in Agriculture,* Vol. 31(1), pp. 133-142.

Han, J., Guo, H., Brad, R., Gao, Z., & Waterer, D. (2015b). Dehumidification requirement for a greenhouse located in a cold region. *Applied Engineering in Agriculture,* Vol. 31(2), pp. 291-300.

Han, J., Guo, H., Brad, R., & Waterer, D. (2016). Mechanical refrigeration dehumidifier performance evaluation in a tomato greenhouse in cold regions. *Transactions of the ASABE,* Vol. 59(4), pp. 933-941.

Han, J., Guo, H., & Gao, Z. (2011). Dehumidification in a tomato greenhouse in cold region. CSBE/SCGAB Annual Conference, Winnipeg, MB, July 10-13, 2011, Paper No. CSBE11-029.

Hao, X., Zheng, J., Celeste, L., Guo, X., & Kholsa, S. (2017). Liquid desiccant dehumidification system for improving microclimate and plant growth in greenhouse cucumber production. *Acta Horticulturae,* Vol. 1170, pp. 861-866.

Hong Kong. (2008). The Hong Kong voluntary energy efficiency labeling scheme for

dehumidifiers. Government of Hong Kong. Retrieved from http://www.emsd.gov.hk/emsd/e_download/pee/veels_photocopier.pdf. Accessed Mar. 18, 2015.

Jolliet, O. (1994). HORTITRANS, a model for predicting and optimizing humidity and transpiration in greenhouses. *Journal of Agricultural Engineering Research,* Vol. 57(1), pp. 23-37.

Jolliet, O., & Bailey, B. J. (1992). The effect of climate on tomato transpiration in greenhouses: measurements and models comparisons. *Agricultural and Forest Meteorology*, Vol. 58, pp. 43-62.

Kittas, C. (1986). Greenhouse cover conductances. *Boundary-Layer Meteorology*, Vol. 36, pp. 213-225.

Kittas, C., & Bartzanas, T. (2007). Greenhouse microclimate and dehumidification effectiveness under different ventilator configurations. *Building and Environment,* Vol. 42(10), pp. 3774-3784.

Körner, O., & Challa, H. (2003). Process-based humidity control regime for greenhouse crops. *Computers and Electronics in Agriculture*, Vol. 39, pp. 173-192.

Lam, C. J., & Hui, S. C. (1996). Sensitivity analysis of energy performance of office buildings. *Building and Environment*, Vol. 31(1), pp. 27-39.

Li-Cor. (2012). Terrestrial radiation sensors instruction manual. Retrieved from https://www.licor.com/documents/8yfdtw1rs27w93vemwp6. Accessed May 07, 2012.

Lindeburg, M. R. (1992). *Engineering-in-training Reference Manual,* 8th Edition. Belmont, California: Professional Publications, Inc.

López-Cruz, I. L., Olivera-López, M., & Herrera-Ruiz, G. (2008). Simulation of greenhouse tomato transpiration by two theoretical models. *Acta Horticulturae*, Vol. 797, pp. 145-150.

López Mosquera, E., & Martínez Cortizas, A. (1993). Water balance in greenhouses under polyethylene cover: first results for Galicia (NW Spain). *Acta Horticulturae,* Vol. 335, pp. 183-190.

McAdams, W. H. (1954). *Heat Transmission,* 3rd Edition. New York: McGraw-Hill Book Company, Inc.

Monteith, J. L. (1965). Evaporation and environment. In: The State and Movement of Water in Living Organisms. *Symposia of the Society for Experimental Biology*, Vol. 19, pp. 205-234.

Montero, J. I., Antón, A., Muñoz, P., & Lorenzo, P. (2001). Transpiration from geranium grown under high temperatures and low humidities in greenhouses. *Agricultural and Forest Meteorology*, Vol. 107, pp. 323-332.

Montgomery, D. C., Peck, E. A., & Vining, G. G. (2012). *Introduction to Linear Regression Analysis*, 5th Edition. New York: Wiley.

Montross, M. D., Duncan, G. A., & Gates, R. S. (2006). Development and testing a low-cost condensation detection system. *Applied Engineering in Agriculture*, Vol. 22(4), pp. 603-608.

Mortensen, L. M. (1986). Effect of relative humidity on growth and flowering of some greenhouse plants. *Scientia Horticulturae,* Vol. 29(4), pp. 301-307.

Munters. (2014a). EM36 exhaust fan. Retrieved from http://www.munters.com/upload/Related%20product%20files/EM36%20English.pdf. Accessed Sep. 19, 2011.

Munters. (2014b). EM50n exhaust fan. Retrieved from http://www.munters.com/upload/Related%20product%20files/EM50n%20English.pdf. Accessed Sep. 19, 2011.

NRC. (2015). Dehumidifers: Energy efficiency regulations. Ottawa, Ontario, Canada: Natural Resources Canada. Retrieved from http://www.nrcan.gc.ca/energy/regulations-codes-standards/products/6889. Accessed Mar. 18, 2015.

Pannell, D. J. (1997). Sensitivity analysis: Strategies, methods, concepts, examples. *Agricultural Economics*, Vol. 16, pp. 139-152.

Papadakis, G., Frangoudakis, A., & Kyttitsis, S. (1992). Mixed, forced and free convection heat transfer at the greenhouse cover. *Journal of Agricultural Engineering Research*, Vol. 51, pp. 191-205.

Pedro, M. J., & Gillespie, T. J. (1981). Estimating dew duration. I. Utilizing micrometeorological data. *Agricultural Meteorology*, Vol. 25, pp. 283-296.

Penman, H. L. (1948). Natural evaporation from open water, bare soil, and grass. *Proceedings of the Royal Society of London (A),* Vol. 193, pp. 120-145.

Pieters, J. G., Deltour, J. M., & Debruyckere, M. J. (1994). Condensation and static heat transfer through greenhouse covers during night. *Transactions of ASAE,* Vol. 37(6), pp. 1965-1972.

Piscia, D., Montero, J. I., Baeza, E., & Bailey, B. J. (2012). A CFD greenhouse night-time condensation model. *Biosystems Engineering,* Vol. 111(2), pp. 141-154.

Pollet, I. V., & Pieters, J. G. (2002). PAR transmittances of dry and condensate covered glass and plastic greenhouse cladding. *Agricultural and Forest Meteorology,* Vol. 110, pp. 285-298.

Prenger, J. J., Fynn, R. P., & Hansen, R. C. (2002). A comparison of four evapotranspiration models in a greenhouse environment. *Transactions of the ASAE,* Vol. 45(6), pp. 1779-1788.

Reiersen, D., & Sebesta, Z. (1981). A comparison of single glass and double acrylic sheeting with respect to heat loss and effects on plants environments. *Acta Horticulturae,* Vol. 115, pp. 409-416.

Richards, K. (1999). Observations and Modelling of Urban Dew. PhD dissertation, University of British Columbia: Vancouver, Canada.

Roberts, W. J, & Mears, R. (1969). Double covering a film greenhouse using air to separate film layers. *Transactions of the ASAE,* Vol. 12(1), pp. 32-33, 38.

Rodríguez, A., Perdigones, A., Valiño, V., & García J. L. (2008). Experimental measurements and prediction of condensation in heated greenhouses. International Conference on Agricultural Engineering, Hersonissos, Greece, June 23-25, 2008, pp. OP-1725 ref.1.

Rosenberg, N. J., Blad, B. L., & Verma, S. B. (1983). *Microclimate - the Biological Environment,* 2nd Eedition. New York: Wiley.

Rouphael, Y., & Colla, G. (2004). Modelling the transpiration of a greenhouse zucchini crop grown under a Mediterranean climate using the Penman-Monteith equation and its simplified version. *Australian Journal of Agricultural Research,* Vol. 55, pp. 931-937.

Rousse, D. R., Martin, D. Y., Theriault, R., Leveillee, F., & Boily, R. (2000). Heat recovery in greenhouses: A practical solution. *Applied Thermal Engineering,* Vol. 20(8), pp. 687-706.

Saskatoon. (2013). Monthly electrical rates. Saskatoon, Saskatchewan, Canada: City of Saskatoon.

SaskEnergy. (2011). SaskEnergy historical rates. Retrieved from www.saskenergy.com/business/comrates_hist.asp. Accessed Dec. 01, 2011.

SaskPower. (2011). Power rates. Retrieved from www.saskpower.com/customer_service/rates/farm. Accessed Dec. 02, 2011.

SaskEnergy. (2013). Historical residential rates. Saskatoon, Saskatchewan, Canada: SaskEnergy. Retrieved from www.saskenergy.com/residential/resrates_hist.asp. Accessed Aug. 22, 2014.

Seemann, S. (2013). Configuration and field testing of a liquid desiccant dehumidification system for greenhouse applications. MSc thesis. Queen's University: Kingston, Canada.

Seginer, I., & Kantz, D. (1986). In situ determination of transfer coefficient for heat and water vapour in a small greenhouse. *Journal of Agricultural Engineering Research*, Vol. 35, pp. 39-54.

Seginer, I., Kantz, D., Levav, N., & Peiper, U. M. (1990). Night-time transpiration in greenhouses. *Scientia Horticulturae*, Vol. 41(3), pp. 265-276.

Seginer, I., & Zlochin, I. (1997). Night-time greenhouse humidity control with a cooled wetness sensor. *Agricultural Forest Meteorology,* Vol. 85(3-4), pp. 269-277.

Shrivastava, P. K., Parikh, M. M., Sawani, N. G., & Raman, S. (1994). Effect of drip irrigation and mulching on tomato yield. *Agricultural Water Management,* Vol. 25(2), pp. 179-184.

Šinkūnas, S., & Kiela, A. (2011). Heat transfer for film condensation of vapour. *Mechanika*, Vol. 17(2), pp. 144-148.

Silveston, P. L., Costigane, W. D., Tiessen, H., & Hudgins, R. R. (1980). Energy conservation through control of greenhouse humidity. I. Condensation heat losses. *Canadian Agricultural Engineering*, Vol. 22(2), pp. 125-132.

Snyder, R. G. (2001). Greenhouse tomato handbook. Mississippi State University Publication 1828. Mississippi State, Mississippi: Mississippi State University.

Stanghellini, C. (1987). Transpiration of greenhouse crops: an aid to climate management. PhD dissertation, Wageningen Agricultural University: Wageningen, the Netherlands.

Stanghellini, C., & De Jong, T. (1995). A model of humidity and its application in a greenhouse. *Agricultural and Forest Meteorology*, Vol. 76, pp. 129-148.

Takakura, T., Takayama, L., Nishina, H., Tamura, K., & Muta, S. (2005). Evapotranspiration estimate by heat balance equation. ASAE Annual International Meeting, Tampa, FL, July 17-20, 2005, Paper No. 054151.

Takakura, T., Kubota, C., Sase, S., Hayashi, M., Ishii, M., Takayama, K., Nishina, H., Kurata, K., & Giacomelli, G. A. (2009). Measurement of evapotranspiration rate in a single-span greenhouse using the energy balance equation. *Biosystems Engineering,* Vol. 102, pp. 298-304.

Taki, M., Ajabshirchi, Y., Ranjbar, S. F., Rohani, A., & Matloobi, M. (2016). Modeling and experimental validation of heat transfer and energy consumption in an innovative greenhouse structure. *Information Processing in Agriculture,* Vol. 3, pp. 157-174.

Tian, W. (2013). A review of sensitivity analysis methods in building energy analysis. *Renewable and sustainable energy reviews,* Vol. 20, pp. 411-419.

Tong, Y., Kozai, T., Nishioka, N., & Ohyama, K. (2010). Greenhouse heating using heat pumps with a high coefficient of performance (COP). *Biosystems Engineering,* Vol. 106(4), pp. 405-411.

Villarreal-Guerrero, F., Kacira, M., Fitz-Rodríguez, E., Kubota, C., Giacomelli, G. A., Linker, R., & Arbel, A. (2012). Comparison of three evapotranspiration models for a greenhouse cooling strategy with natural ventilation and variable high pressure fogging. *Scientia Horticulturae,* Vol. 134, pp. 210-221.

Von Elsner, B., Briassoulis, D., Waaijenberg, D., Mistriotis, A., Von Zabeltitz, C., Gratraud, J., Russo, G., & Suay-Cortes, R. (2000). Review of structural and functional characteristics of greenhouse in European Union countries, part I: design requirements. *Journal of Agricultural Engineering Research,* Vol. 75, pp. 1-16.

Wang, H., & Li, Y. (2008). Research progress in control of air humidity in horticultural greenhouse and measures of dehumidification (in Chinese). *Acta Agriculturae Jiangxi,* Vol. 20(10), pp. 50-54.

Yang, S. H., Son, J. E., Lee, S. D., Cho, S. I., Ashtiani-Araghi, A., & Rhee, J. Y. (2016). Surplus thermal energy model of greenhouses and coefficient analysis for effective utilization. *Spanish Journal of Agricultural Research,* Vol. 14(1), pp. e0202.

Yu, Z., Guo, H., & Laguë, C. (2011). Development of a livestock odor dispersion model: part II.

evaluation and validation. *Journal of the Air & Waste Management Association,* Vol. 61, pp. 277-284.

Ziehl-Abegg. (2012). FC Series axial fans. Künzelsau, Germany: Ziehl-Abegg. Retrieved from www.ziehl-abegg.com/gb/en/product-range/ventilation-systems/axial-fans/fc/. Accessed May 09, 2011.

# APPENDIX COPYRIGHT PERMISSIONS

## 1 Permission for manuscripts used in Chapters 1 to 3

The manuscripts included in Chapter 2, 3, and 4 is accepted and published online by American Society of Agricultural and Biological Engineers. ASABE grants permission to students to include the full text of papers and articles that they have authored in their theses or dissertations. The photograph shown below is copied from the website of ASABE.

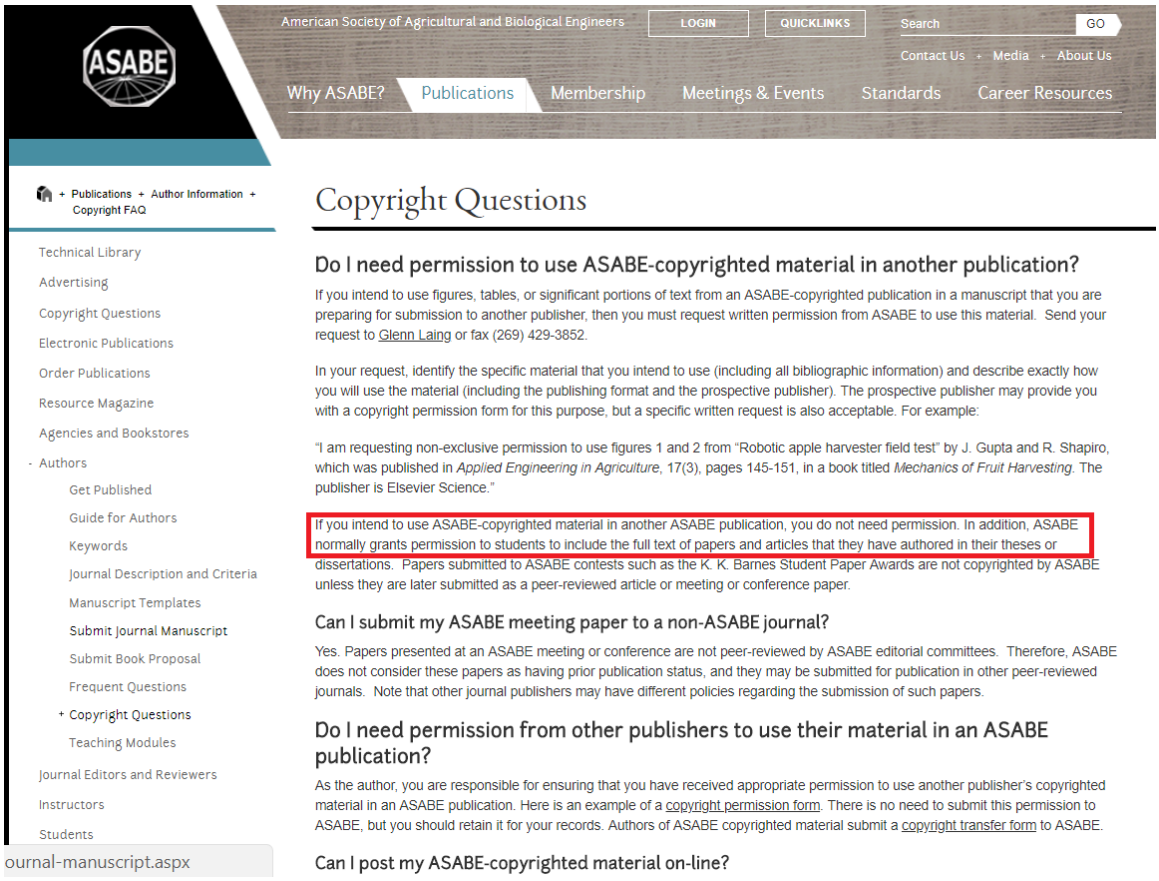


Source: https://www.asabe.org/publications/authors/copyright-questions.aspx

(accessed Apr. 16, 2018)

## 2. Permission for manuscript used in Chapter 4

The manuscript included in Chapter 4 is accepted and will be published online by Information Processing in Agriculture. Elsevier grants permission to students to include the full text of papers and articles that they have authored in their theses or dissertations. The photograph shown below is copied from the website of Elsevier.

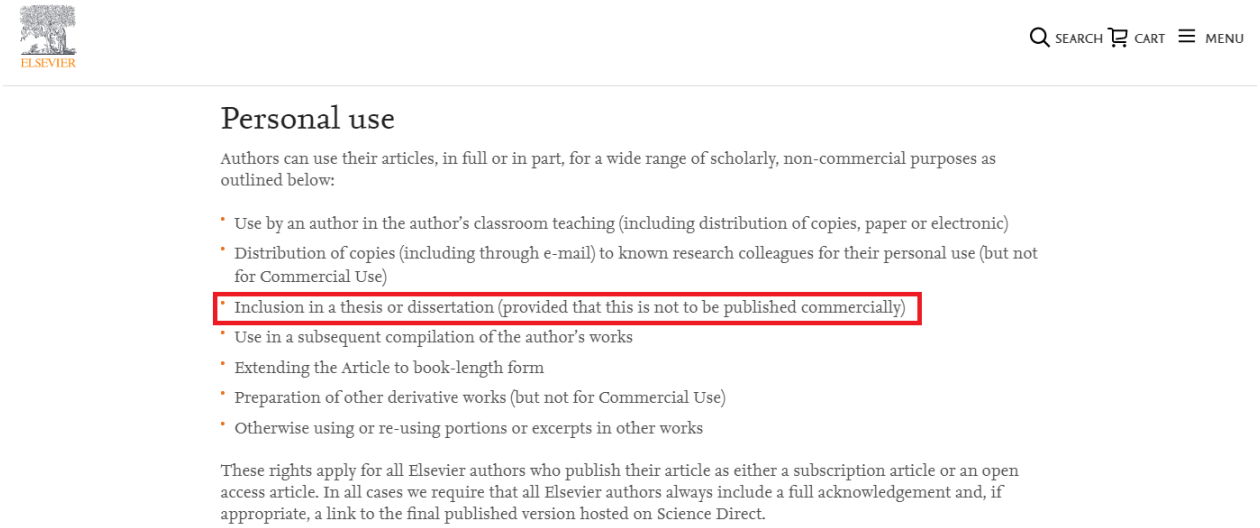


Source: https://www.elsevier.com/about/policies/copyright/personal-use

(accessed Jun. 15, 2018)

## 3 Permission for manuscripts used in Chapters 5 to 8

The manuscripts include in Chapter 5 to Chapter 8 are unpublished; therefore, a copyright permission is requested and obtained from the co-author of the paper (Prof. Huiqing Guo).

**Copyright Permission Requested Form**

I am presently preparing manuscripts titled "Measurement and modelling of condensation on greenhouse cover: part I condensation measurement", "Measurement and modelling of condensation on greenhouse cover: part II theoretical and regression models", "Greenhouse moisture balance modelling for predicting indoor humidity", and "Sensitivity analysis of a greenhouse moisture balance model for predicting indoor humidity" to be published as the fifth, sixth, seventh, and eighth chapter of my Ph.D. thesis and submitted to the Department of Chemical and Biological Engineering at the University of Saskatchewan. The author that contributes towards the finishing of these manuscripts is Huiqing Guo.

I hereby request for permission to use the contents of these manuscripts in my Ph.D. thesis and all successive revisions that may be prepared at the University of Saskatchewan. Please, kindly confirm your agreement by signing below.

Yours faithfully,

Jingjing Han

May 28, 2018

Permission granted by: Huiqing Guo

Signature:

Date: